CRANEOLOGÍA FUNCIONAL Y EVOLUCIÓN HUMANA:

RELACIONES ESTRUCTURALES Y ORGANIZACIÓN ESPACIAL EN LA EVOLUCIÓN DE LAS ÁREAS FRONTO-PARIETALES

TESIS DOCTORAL

ANA SOFIA PEREIRA PEDRO

2019

Dirigida por: Dr. E. Bruner; dr. j.m. bermúdez de castro

UNIVERSIDAD
DE BURGOS

ESCUELA DE DOCTORADO

PROGRAMA DE DOCTORADO EN EVOLUCIÓN HUMANA,
PALEOECOLOGÍA DEL CUATERNARIO Y TÉCNICAS GEOFÍSICAS
APLICADAS A LA INVESTIGACIÓN

CRANEOLOGÍA FUNCIONAL Y EVOLUCIÓN HUMANA: RELACIONES ESTRUCTURALES Y ORGANIZACIÓN ESPACIAL EN LA EVOLUCIÓN DE LAS ÁREAS FRONTO-PARIETALES.

FUNCTIONAL CRANEOLOGY AND HUMAN EVOLUTION: STRUCTURAL RELATIONSHIPS AND SPATIAL ORGANIZATION IN THE FRONTO-PARIETAL EVOLUTION

TESIS DOCTORAL

ANA SOFIA PEREIRA PEDRO

2019

Dirigida por:
Dr. Emiliano Bruner
Dr. José María Bermúdez de Castro Risueño

CENIEH
Centro Nacional de Investigación sobre la Evolución Humana

ESCUELA DE DOCTORADO
Edificio de Administración y Servicios
C/Don Juan de Austria, 1, 1ª planta
09001 Burgos (España)

D. EMILIANO BRUNER, Doctor en Biología Animal y Responsable de Paleoneurobiología de Homínidos del Centro Nacional de Investigación sobre la Evolución Humana; D. JOSÉ MARÍA BERMÚDEZ DE CASTRO RISUEÑO, Doctor en Ciencias Biológicas, Codirector del Proyectos Atapuerca Y Coordinador del Programa de Paleobiología de Homínidos del Centro Nacional de Investigación sobre la Evolución Humana,

HACEN CONSTAR:

Que el presente trabajo de investigación titulado "Craneología funcional y evolución humana: relaciones estructurales y organización espacial en la evolución de las áreas fronto-parietales" y llevado a cabo por Dña. ANA SOFIA PEREIRA PEDRO dentro del Programa de Doctorado de Doctorado en Evolución Humana, Paleoecología del Cuaternario y Técnicas Geofísicas Aplicadas a la Investigación ha sido realizado bajo su dirección en el Centro Nacional de Investigación sobre la Evolución Humana, y cumple todos los requisitos necesarios para ser aprobado como Tesis Doctoral.

Burgos, a 11 de Noviembre de 2019

Dr. Emiliano Bruner

Dr. José María Bermúdez de Castro

RESUMEN

Cerebro y cráneo están funcional y estructuralmente integrados, influenciándose recíprocamente durante la morfogénesis, a través de interacciones entre los tejidos adyacentes. Asimismo, cambios evolutivos en uno de ellos produce cambios en el otro para mantener el equilibrio funcional entre toda la estructura. Comprender las relaciones morfológicas entre cerebro y cráneo es fundamental en el campo de la paleoneurología, que estudia la evolución cerebral con base en el análisis de moldes de la cavidad interna del cráneo. La morfología craneofacial única de los humanos modernos, caracterizada por la forma globular del neurocráneo y por la retracción de la cara, se atribuye generalmente al aumento del tamaño cerebral. Aunque se considera que la bóveda craneal está moldeada en gran medida por el tejido neuronal subyacente, los patrones de integración morfológica difieren entre las regiones frontales y parietales. El hueso frontal forma parte de la bóveda craneal, fosa anterior y techo de las órbitas, estando estructural y funcionalmente vinculado a los lóbulos frontales y a los ojos, dos elementos cuya proximidad anatómica ha aumentado durante la evolución humana. El hueso parietal, que forma la porción más grande de la bóveda, aunque está indirectamente influenciado por la base craneal, está principalmente vinculado al cerebro, y el abultamiento parietal típico de los humanos modernos puede resultar de modificaciones en la corteza parietal. En este contexto, la presente tesis investiga la región frontal principalmente en relación con las interacciones estructurales, mientras que las regiones parietales se evalúan tanto en relación con las interacciones estructurales como en relación con la variación anatómica de los elementos corticales. Los estudios están divididos en tres partes: la primera se enfoca en las relaciones estructurales y espaciales entre las partes del cráneo; la segunda parte evalúa la morfología del lóbulo parietal mediante moldes endocraneales; la ultima parte investiga la variabilidad anatómica del elemento parietal de la superficie sagital del cerebro, el precúneo. La morfología del cerebro y endocráneo se investiga a través de análisis de morfometría geométrica basada en puntos de referencia anatómicos, aplicada, respectivamente, a imágenes de resonancia magnética (MRI) y tomografía computerizada (CT).

En relación a las interacciones estructurales entre ojo y cerebro, los resultados obtenidos indican que la posición del ojo varía, principalmente, en la dirección horizontal en relación a los lóbulos temporales. Este patrón de variación está asociado al tamaño del cerebro ya que con el aumento del volumen frontal y temporal el ojo se encuentra más cerca de los lóbulos temporales. En el caso de la relación espacial entre órbitas y cráneo, el principal patrón de variación en humanos modernos comprendió la orientación de las órbitas, mientras que la variación interespecífica en chimpancés, humanos modernos y homininos del Pleistoceno medio, describió la distancia entre las órbitas y cráneo. Cambios en las dimensiones del hueso parietal están asociados a una rotación de la cara y base del cráneo, lo que sugiere que la morfología parietal puede afectar la orientación de las órbitas en humanos modernos.

Considerando el análisis de moldes endocraneales, los resultados indican que es posible

aislar y cuantificar la morfología del lóbulo parietal mediante la aplicación de morfometría geométrica basada en referencias corticales. En el caso de los cercopitécidos, la claridad de las huellas de los surcos en los moldes endocraneales facilita la definición de los límites del lóbulo parietal. Nuestro modelo geométrico fue capaz de reproducir las proporciones opuestas de los lóbulos parietales y occipitales que distinguen las subfamilias cercopitecinae y colobinae, pero también ha demostrado que *Theropithecus* y *Papio* tienen proporciones similares a las de los colobinos, adquiridas probablemente de modo independiente. En el caso de humanos modernos y neandertales, la baja visibilidad de los elementos corticales en la superficie endocraneal dificulta la definición de los lóbulos parietales, cuyos límites pueden ser solo estimados. No obstante, nuestro modelo geométrico pudo demostrar que los lóbulos parietales en humanos modernos son más grandes en superficie, especialmente en la región dorsal posterior y en la región lateral que se corresponde con el lóbulo parietal inferior situado entre los dos giros y el surco intraparietal.

Con respecto al precúneo, nuestros estudios proporcionan información detallada sobre los patrones de surcos y las dimensiones coronales. Los resultados muestran que las dimensiones verticales del precúneo están asociadas con la morfología del contorno dorsal del parietal, lo que sugiere que la forma del perfil del parietal externo puede ser usado para inferir la dimensión del precúneo en especies fósiles. Además, los resultados apuntan a las porciones anterior y superior del precúneo como el origen de su variabilidad longitudinal en humanos modernos. Por último, un análisis comparativo de la variación medio-sagital en primates no humanos indica que la variación longitudinal del precúneo es un rasgo específico de los humanos.

En definitiva, los resultados sugieren que los procesos de integración craneofacial pueden influir en la orientación de las órbitas, lo que afecta el ojo. Con respecto a la región parietal, esta tesis proporcionó considerable información sobre la variación anatómica de los lóbulos parietales, y especialmente del precúneo. Aún así, el origen de tal variabilidad sigue siendo una cuestión abierta. Estudios futuros deberían centrarse en la relación anatómica y geométrica entre los elementos parietales mediales y laterales con el objetivo de tener una perspectiva general sobre la integración morfológica dentro de este distrito cerebral.

Palabras clave: Paleoneurología; anatomía del cerebro; anatomía comparativa; lóbulos parietales, lóbulos frontales, integración morfológica; *Homo sapiens*; *Homo neanderthalensis*; Hominినos del Pleistoceno medio; Cercopithecidae; moldes endocraneales; precúneo

ABSTRACT

Brain and skull are functionally and structurally integrated due to reciprocal interactions among the adjacent tissues throughout morphogenesis. Similarly, evolutionary changes to one are accompanied by accommodating changes to the other in order to maintain functional balance among the whole structure. Understanding how the morphology of the brain and skull relate to each other is fundamental within paleoneurology, which studies brain evolution based on endocasts, i.e. casts of the endocranial cavity. The unique craniofacial morphology of modern humans, characterized by neurocranial globularity and retraction of the face is usually attributed to encephalization. While the cranial vault is largely molded by the underlying neural tissue, the patterns of morphological integration differ between the frontal and parietal regions. Making part of the cranial vault, anterior cranial floor, and roof of the orbits, the frontal bone is structurally and functionally linked to the frontal lobe and to the eye, two elements which underwent increasing spatial proximity during human evolution. The parietal bone, which forms the largest portion of the vault, although being indirectly influenced by the cranial base, primarily interacts with the brain, and the parietal bulging of modern humans might result from changes to the parietal cortex below. In this context, the present thesis investigates the frontal region mainly in terms of structural interactions while the parietal regions are assessed both in terms of structural interactions and in terms of anatomical variation of the cortical elements. The studies are divided into three parts: the first focuses on the structural and spatial relationships among the skull parts; the second on the morphology of the parietal lobe as assessed through endocasts; the last one investigates the anatomical variability of the medial parietal element, the precuneus. We investigate brain and endocranial morphology through landmark-based geometric morphometrics analysis of magnetic resonance images (MRI) and computed tomography (CT), respectively.

Regarding the structural interactions among the eye and the brain, we found the main pattern of variation to be the horizontal position of the eyeball relative to the temporal poles. This variation is associated with brain size, as the eyeball is closer to the temporal lobe with increasing frontal and temporal volumes. When considering the spatial relationship between orbits and anterior braincase, the main pattern of variation within modern humans comprised the orientation of the orbits while the interspecific variation, among chimpanzees, modern humans, and Middle Pleistocene hominins, described the distance between the orbits and the braincase. Changes in the dimensions of the parietal bone are associated with rotation of the cranial base and face, indicating parietal bone could influence the orientation of the orbits within modern humans.

Considering the analysis of endocasts, our results indicate it is possible to isolate and quantify parietal lobe morphology through the application of geometric morphometrics based on cortical references. In the case of cercopithecid endocasts, the visibility of the sulcal imprints allows for a more reliable definition of the parietal lobe boundaries. Our geometrical model was able to reproduce the opposite proportions of the parietal and occipital lobes distinguishing cercopithecine and colobine conditions, and even demonstrating that *Theropithecus* and *Papio* display colobine-like patterns, probably constituting independent traits. In the case of modern humans and Neanderthals, since few cortical references are visible on the endocast surfaces, the parietal boundaries can only be estimated. Nonetheless, we were able to demonstrate that modern human parietal lobes are larger in surface area, especially on the posterior dorsal region and on the lateral regions corresponding to a region of the inferior parietal lobule between the two main bosses and the intraparietal sulcus.

With respect to the precuneus, our studies provide detailed information on the sulcal patterns and coronal dimensions. We show that the vertical dimensions of the precuneus are associated with the morphology of the dorsal parietal outline, suggesting that the form of the outer parietal profile can be used to infer on precuneus dimension in fossil species. Moreover, our results point to the anterior and superior portions of the precuneus as the origin of the longitudinal variation within modern humans. Lastly, a comparative analysis of the midsagittal brain variation across non-human primates indicated that the longitudinal variation of the precuneus within humans is a species-specific trait.

Overall, our results suggest that processes of craniofacial integration might influence the orientation of the orbits, thus affecting the eye. Regarding the parietal region, this thesis provided much information on the anatomical variation of the parietal lobes, and especially the precuneus. Still, the origin of such variability remains an open question. Future studies should focus on the anatomical and geometrical relationship between the medial and lateral parietal elements in order to have a broader perspective on the morphological integration within this brain district.

Keywords: Paleoneurology; brain anatomy; comparative anatomy; parietal lobes, frontal lobes, morphological integration; *Homo sapiens*; *Homo neanderthalensis*; Middle Pleistocene hominins; Cercopithecidae; endocast; precuneus

“Nothing in biology makes sense
except in the light of evolution”

Theodosius Dobzhansky

Acknowledgments

I want to start by thanking my thesis advisors, Emiliano Bruner and José María Bermúdez de Castro, for giving me the opportunity to do research on this fascinating topic which is human brain evolution. I am grateful to Emiliano for all his teachings on conducting research, image processing, blogging, networking and communicating science, and for always having a simple solution.

I am indebted to Fundación Atapuerca for funding my research, and to the CENIEH for providing me with equipment and a place for developing my work.

Most of the research work within this thesis was accomplished through collaborations with national and international researchers. I want to thank my co-authors in the papers presented here: Michael Masters, Markus Bastir, James K. Rilling, Xu Chen, Todd M. Preuss. In particular, I thank Philipp Gunz and Simon Neubauer, for receiving me in The Max Planck Institute for Evolutionary Anthropology during a short research visit, and Amélie Beaudet, for hosting me in the GAES (University of the Witwatersrand) and teaching me how to use Avizo. The visit to the GAES was supported by a travel fellowship from Universidad de Burgos.

A doctoral thesis is also a personal journey, and I am grateful for everything I've learned and for all the people I've met during the last few years. Thank you, 'seshi people' for teaching me the Spanish 'ways', and making me a bit more sociable. Thank you guys at Wits for welcoming me into your group and making me feel cosy so far from home. And thanks to my colleagues in Atapuerca for the team work and for giving me another perspective on science communication.

And last but not least, I want to thank my family for all of their support and encouragement. I thank my parents for always giving us the freedom to follow our dreams, and for giving their best to support us on everything. Things wouldn't be the same without the long conversations with my sister, sharing all the difficulties and accomplishments from the other side of the world. And definitely things would never be the same without Bruno, who's always been there for me. Thank you for all of your encouragement and patience throughout these years.

À memoria do avô Armando e do tio Jorge.

TABLE OF CONTENTS

Chapter 1

INTRODUCTION

1. INTRODUCTION

The present doctoral thesis focuses on the anatomical and structural analyses of the frontal and parietal lobes and bones within the context of functional craniology and human brain evolution.

Paleoneurology studies fossil evidence for brain evolution, comprising the only line of evidence on evolutionary changes to the brain within a lineage (Holloway et al., 2004). Since neural tissue does not fossilize, changes in the brain can be secondarily inferred from general cranial anatomy or, more precisely, from endocasts, that is, molds of the internal bony table of the cranial bones (Falk, 1980; Bruner, 2003, 2007; Holloway et al., 2004). Endocasts are not casts of the brain itself as these also incorporate other intracranial soft tissues. The amount of information on the brain that the endocast provides depends on whether the cortical features got imprinted onto the endocranial bone surface (Holloway et al., 2009; Neubauer, 2014). Hence, the correct interpretation of the information provided by endocasts requires previous knowledge not only about brain anatomy and variation across species (Holloway et al., 2009), but also on the structural and functional relationships among the neural and cranial elements (Bruner, 2003, 2007). This kind of information is only provided by comparative studies of extant species, i.e. comparative neuroanatomy.

Comparative neuroanatomy refers to the study of similarities and differences in brain organization across living species (Schoenemann, 2006). Although supplying indirect information on brain evolution, since each living species constitutes the final product of their own evolutionary trajectory, this approach represents a particularly rich source of data on brain anatomy (Holloway et al., 2009; Rilling, 2008). In addition, considering structural and functional relationships between cranial and brain elements can inform on the structural limits to evolutionary changes in brain morphology (Moss & Young, 1960; Bruner, 2007).

The study of endocasts and cerebro-cranial anatomy and their structural relationships has been substantially improved by the introduction of medical imaging techniques and multivariate statistics for the quantification of morphological covariation in paleoanthropology.

In this context, this introductory chapter reviews the relevant concepts and literature behind the rationale of the present work. Because the research is focused on brain anatomy, the first section provides a basic overview of the macroanatomical features of the human brain. Then, the concepts of functional craniology and morphological integration are reviewed as well as the tools and methodologies currently used for their analysis. Finally, it describes the specific challenges addressed throughout the research, and lists the main goals of the present thesis.

1.1. HUMAN BRAIN ANATOMY AND GENERAL FUNCTIONAL ORGANIZATION

The brain, or encephalon, comprises the part of the central nervous system that is contained within the cranial cavity. The primary embryonic subdivisions of the brain include, from rostral to caudal, the forebrain or prosencephalon, the midbrain or mesencephalon, and the hindbrain or rhombencephalon. These regions are further subdivided, giving origin to the main components of the adult human brain (Purves et al., 2004; Seeley et al., 2004; **Fig. 1.1**). The forebrain is composed by the cerebrum or telencephalon, and the diencephalon, which includes the thalamus and hypothalamus. The hindbrain includes the pons and the cerebellum, which form the metencephalon, and the medulla oblongata or myelencephalon. The midbrain, the pons, and the medulla collectively form the brainstem, which connects the cerebrum to the spinal cord, the other component of the central nervous system.

1.1.1. General anatomical organization of the human brain

The cerebrum composes most of the human brain, containing the cerebral cortex and the subcortical structures, such as the hippocampus, basal ganglia, and olfactory bulb. The cerebral cortex comprises the outermost portion of the cerebrum, and is separated into left and right hemispheres by a deep median cleft called the longitudinal or interhemispheric fissure. Each cerebral hemisphere is folded into a complex pattern of convolutions or gyri (singular gyrus) and grooves or sulci (singular sulcus). Although the patterns of folding vary among individuals and between hemispheres, there are some consistent sulci which allow the subdivision of the hemispheres into four main lobes (**Fig. 1.2a**). Two main prominent folds are helpful to identify the main brain lobes visible on the dorsolateral cerebral surface. The central sulcus, also known as Rolandic fissure, consists on a vertical fold located about halfway between the rostral and caudal poles of the hemispheres. It separates the frontal lobe, on the anterior portion, from the parietal lobe, posteriorly. The lateral sulcus, or Sylvian fissure, runs horizontally, separating the temporal lobe, below, from the frontal and parietal lobes above. This fissure is only visible on the lateral surface, while the central sulcus extends shortly into the medial surface. The parieto-occipital sulcus, which makes the boundary between the parietal and occipital lobes, forms a deep sulcus on the medial surface but only a small part can be seen on the lateral surface. Separation among the temporal, parietal and occipital lobes on the dorsolateral cortical surface is less clear.

The cerebral cortex consists of tightly packed neurons organized into columns, forming the gray matter of the brain (**Fig. 1.2b**). Underneath the cortical layers, the myelinated axons of the white matter connect neurons from different cortical and subcortical areas. The cerebral cortex includes the paleocortex, i.e. the olfactory cortex, the archicortex (or hippocampus in humans), and the neocortex, characteristic of the mammalian brain (Rilling, 2006; Ribas, 2010). The mammalian neocortex comprises the phylogenetically more recent cortex, and is

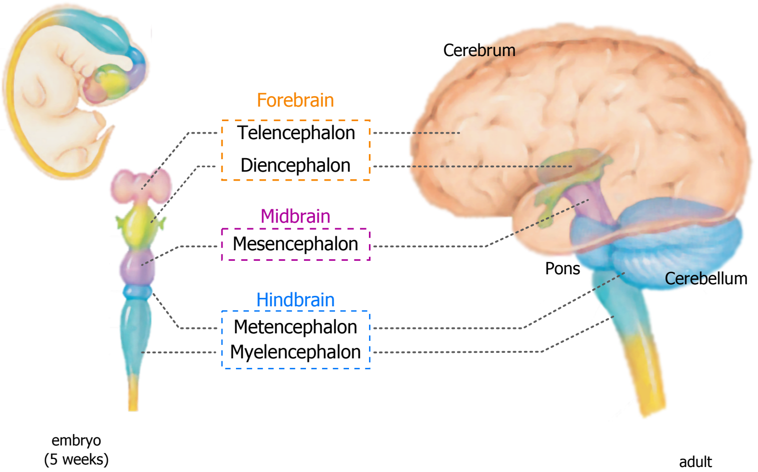

Fig. 1.1. Human brain embryonic origins. Three main embryonic regions originate the different portions of the adult brain [modified from Seeley et al., 2004].

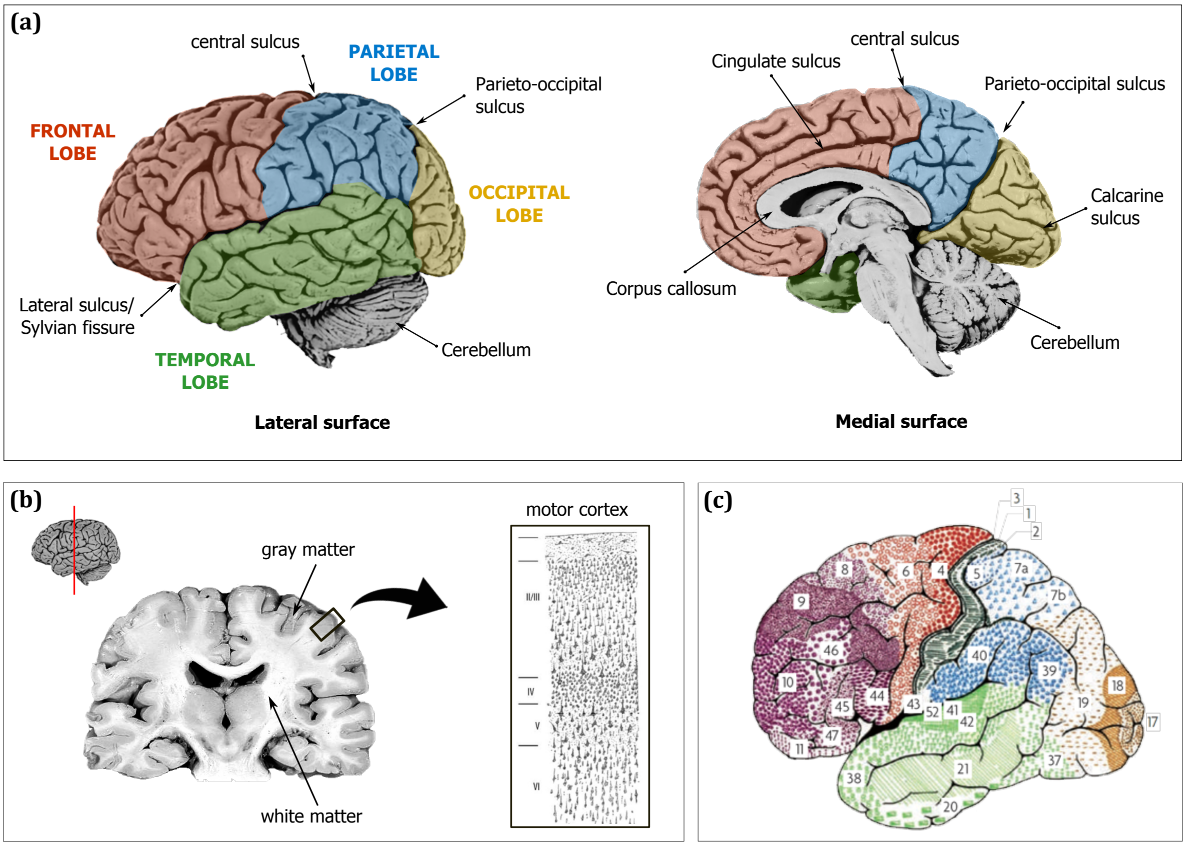

Fig. 1.2. Anatomical organization of the cerebral cortex. (a) Macroscopically, the cerebral cortex is divided into four lobes, separated by the most prominent sulci; (b) Microscopically, the cerebral cortex is composed of neuronal cell bodies, forming the gray matter, and the white matter consist of axonal fibers connecting the neurons; (c) regional variation in cellular composition along the gray matter has been extensively studied, providing cytoarchitectonic maps of the cerebral cortex, such as that of Brodmann. [Image of the motor cortex from Ramon Y Cajal's drawings, available at Wikimedia Commons; Brodmann's map after Zilles & Amunts, 2010].

defined by the presence of four to six laminae, or layers of neurons (Northcutt & Kaas, 1995). Regional variations in neuronal composition and structural features of each of these layers throughout the neocortex have been used to identify discrete cortical territories. In 1909, Korbinian Brodmann published the first parcellation of the cerebral cortex into different cytoarchitectonic areas based on the distribution, organization, and typology of the cells along the gray matter layers (**Fig. 1.2c**; Zilles & Amunts, 2010). Brodmann's map is the most widely known and has been subject to various modifications throughout the years, especially after the introduction of neuroimaging techniques which provide a way to link structure and function (Zilles & Amunts, 2010; Judas et al., 2012). In fact, Brodmann areas (BA) are still used as reference for both structure and function.

1.1.2. General functional organization of the human brain

Understanding the functional organization of the brain is essential to recognize the significance of changes to particular brain subdivisions. The cerebral cortex can be divided into three main types of areas: the primary sensory areas, the association areas and the primary motor areas. The primary sensory areas receive input from the sensory organs of the body via thalamic projections, and include primary somatosensory cortex, primary visual cortex, and primary auditory cortex. The association areas receive and process information from the primary sensory areas, while the primary motor cortex receives projections from the primary sensory and from association areas, and sends output to the motor neurons throughout the body through the thalamus (Purves et al., 2004).

The brain lobes represent conventional subdivisions intended to aid anatomical description, but contain no functional meaning (Campero et al., 2014). In this sense, no direct relationship exists between function and macro anatomical features. However, there seems to be some association between the functional organization of the cortex and the hierarchy and degree of variability of the folds, as more specialized, primary cortical areas are topographically associated with the most prominent and invariant sulci (**Fig. 1.3a**; Chi et al., 1997; Ribas, 2010). For instance, the primary visual cortex, or striate cortex, occupies the walls of the calcarine sulcus, in the medial brain surface. Similarly, the primary auditory areas lie within the lateral sulcus and the superior temporal gyrus of the temporal lobe. The central sulcus separates the primary somatosensory cortex, located along the postcentral sulcus, from the primary motor cortex, located along the precentral gyrus. The primary areas sub serve the basic sensory and motor functions and their neurons are organized in a topographical fashion. The primary somatosensory and motor cortices display a similar somatotopic representation of the body, with adjacent parts of the body surface being represented in neighboring regions of these primary cortices. Surrounding the primary areas, the association areas are less specialized, and also less predictable from macroanatomy, occupying most of the cortical mantle.

Throughout the cortex, the information flows from the primary sensory areas to the association areas, and then to the motor areas (**Fig. 1.3b**). First, the primary sensory areas receive and process input from the sensory organs of the body; then, each modality of sensory information flows to unimodal association areas that surround each of the primary sensory cortices. With increasing distance from the primary areas, the association areas become progressively less specialized, and the processing progressively more complex (Pandya & Seltzer, 1982). The parieto-temporo-occipital association cortex is implicated in the complex processing of sensory information. The frontal association cortex, i.e. prefrontal cortex, integrates complex sensory and emotional information and is mostly involved in executive control functions (Fuster, 2014). The primary motor cortex sends output to the motor organs of the body, mediated by the premotor cortex and sensory areas. Hence, the association cortex is involved in the integration of information from the primary areas, and in the processing of more complex information, being responsible for all the higher cognitive functions in humans and other primates (Kornack & Rakic, 2001). The areas of the association cortex are involved in multiple, distributed networks that are interdigitated with one another, and converge in zones of the parietal and prefrontal association cortices (Yeo et al., 2011). In fact, the prefrontal and parietal cortices are strongly interconnected and seem to make part of multiple brain networks (Goldman-Rakic, 1988; Fox et al., 2005; Cole et al., 2010). It has been suggested that a fronto-parietal network might be the neural basis for consciousness and cognition, underlying the individual differences in general intelligence (Naghavi & Nyberg, 2005; Jung & Haier, 2007).

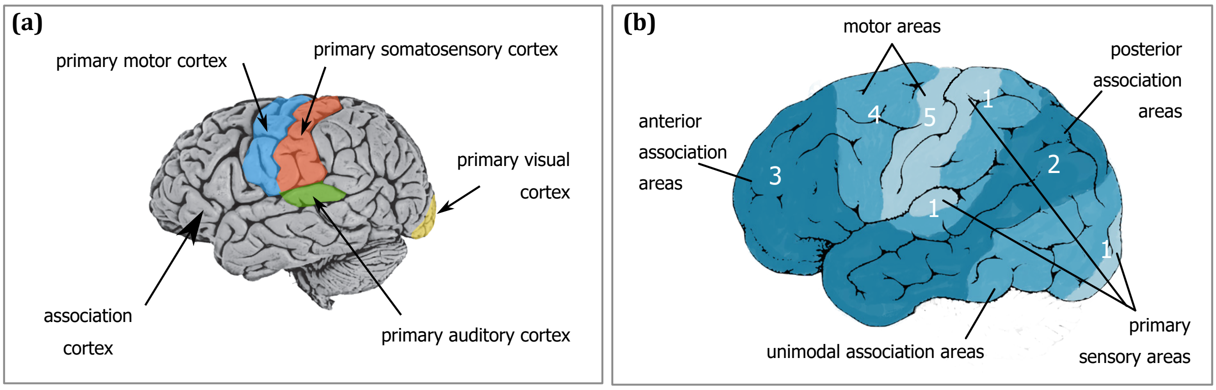

Fig. 1.3. Functional organization of the human brain. (a) The primary sensory and motor areas are located close to the prominent sulci (see Fig. 1.2a); (b) within the cortex information flows from the sensory primary areas (1) to the unimodal and posterior association areas (2), then passing to the anterior association areas, or prefrontal cortex (3), and to the premotor (4) and primary motor (5) areas [after Rilling, 2008].

1.1.3. The human brain among primates

With an average volume of 1300 cm³, three times bigger than those of great apes, which range between 300-400 cm³, the human brain is the largest among living primates, both in absolute and relative terms (Holloway, 2015). Besides differences in brain size, it is important to understand whether the human brain displays the same design or a different organization. Changes in internal brain organization can be indicated by differences in the proportions of particular subdivisions, in the degree of folding, or even by the development of novel areas or structures (Passingham, 1973; Zilles et al., 1988; Semendeferi et al., 2002; Rilling, 2006; Smaers et al., 2011; Barton & Venditti, 2013).

The cerebral cortex, and particularly the neocortex, is usually associated with perception and reasoning, thus considered the source of cognitive and behavioral specializations of primates and humans (Rilling, 2008). Compared to other mammals, primates display a disproportionately enlarged neocortex, being about five times larger than that of an insectivore of the same total brain size (Finlay & Darlington, 1995; Barton & Harvey, 2000). This expansion occurs mainly through an increase in surface area with little changes in cortical thickness (Welker, 1990), which is accomplished through folding of the cortical sheet (Hofman, 2012). Folding allows for a significant expansion of the surface area without proportional increase of the outer dimensions or total volume, so that the brain can still fit inside the skull (Hofman, 2012; Ribas, 2010). As a result, among mammals, large-brained species display more complex folding than small-brained species. And within primates, anthropoids display higher degree of folding with size compared to prosimians (Zilles et al., 1989).

The neocortex of humans is larger than expected for a primate with a human brain size (Passingham, 1973). The increase in white matter volume outpaces that of the gray matter, indicating a greater increase in connectivity rather than neuron numbers (Rilling & Insel, 1999). The relative volumes of the whole lobes seem to be rather homogeneous across great apes, as the frontal lobes and the parieto-occipital sector are as large as expected for an ape with the brain size of a human, while the cerebellum is proportionately smaller and the temporal lobes slightly larger (Semendeferi et al., 2002). The temporal lobes of humans are larger than expected for an ape with a human brain size, in terms of total volume and white matter volume (Rilling & Seligman, 2002). Considering the neocortex, the human frontal cortex as a whole is as large as expected from primate brain scaling (Semendeferi et al., 2002), but the human prefrontal cortex (PFC) seems to have enlarged disproportionately to the rest of the neocortex, while the primary motor and premotor cortices are smaller than expected (Passingham, 1973). A similar trend seems to have occurred on the occipital cortex, with the human primary visual (striate) cortex being smaller than expected relative to neocortex size, and the prestriate cortex being larger than expected relative to occipital cortex (Passingham, 1973).

Regarding the degree of folding, humans and great apes seem to display similar gyrification values and patterns of convolution, which increase within the association areas (Zilles et al., 1988). Among the association areas, humans show more folding on the prefrontal and temporal cortices compared to the great apes, but both humans and great apes display the highest folding values within the parietal cortex (Zilles et al., 1988). Interestingly, the parietal and frontal association cortices seem to have undergone major expansion during human evolution (Eidelberg & Galaburda, 1984; van Essen et al., 2001; Preuss, 2011), stressing the role of a fronto-parietal network in higher cognitive functions (Naghavi & Nyberg, 2005; Jung & Haier, 2007).

1.2. THE BRAIN AND THE BRAINCASE: FUNCTIONAL CRANIOLOGY AND MORPHOLOGICAL INTEGRATION

The morphology of the brain might be primarily determined by internal factors associated with the neural tissue, such as number of neurons and connectivity patterns (Hofman, 2012), but it also depends on external structures, like the surrounding cranial bones that limit the available space. In fact, during morphogenesis, which encompasses changes in shape (development) and size (growth), the anatomical components of the brain and skull interact functionally and structurally to originate a highly integrated and functional whole (Cheverud, 1996; Bruner, 2007).

A thorough description of the structural and functional relationships among anatomical structures has been first applied to cranial anatomy. Moss & Young (1960) emphasized the importance of studying the form of the skull from a functional and biological perspective by considering each cranial bone as part of a functional matrix that includes the adjacent soft tissues. The shape of a particular anatomical element would thus result primarily from the interactions with the neighboring structures, maintaining structural and functional balance (Moss & Young, 1960; Enlow, 1990). These localized interactions are not homogeneous across the cranium, and strongly depend on the functional roles of the different components of the skull (Enlow, 1968; Moss and Young, 1960). In this sense, the three main anatomical subdivisions of the skull – the cranial base, the cranial vault, and the facial skeleton – are involved in different structural and functional interactions. The brain is housed within the braincase, or neurocranium, which is composed of bones from the cranial base and vault (**Fig. 1.4a**). During morphogenesis, the growing brain exerts pressure against the internal walls of the neurocranium, which in turn constitutes a limit to brain expansion. Hence, the morphology of the brain is intimately connected with that of the neurocranium, though the reciprocal influences depend on the structural and functional demands of the cranial components of the braincase.

1.2.1. Reciprocal interactions of the neurocranial components

The cranial vault, or calvaria, grows through intramembranous ossification, surrounding the neural tissues (**Fig. 1.4b**; Sperber, 2001). The growth of the cranial vault is largely influenced by the expanding brain, which pushes the bones outward inducing ossification of the bone front edges, along the membranous joints between the bones, i.e. the sutures (Enlow, 1968; Opperman, 2000). The frontal and parietal bones form most of the cranial vault (**Fig. 1.4a**), and the sutures between them comprise the main growth sites in the human skull (Jiang et al., 2002). These two vault bones differ in embryonic origin, as the frontal bones are derived from the neural crest and the parietal bones from the mesoderm (Jiang et al., 2002). The neural crest- mesoderm interface is found within these bones, and both coronal and sagittal

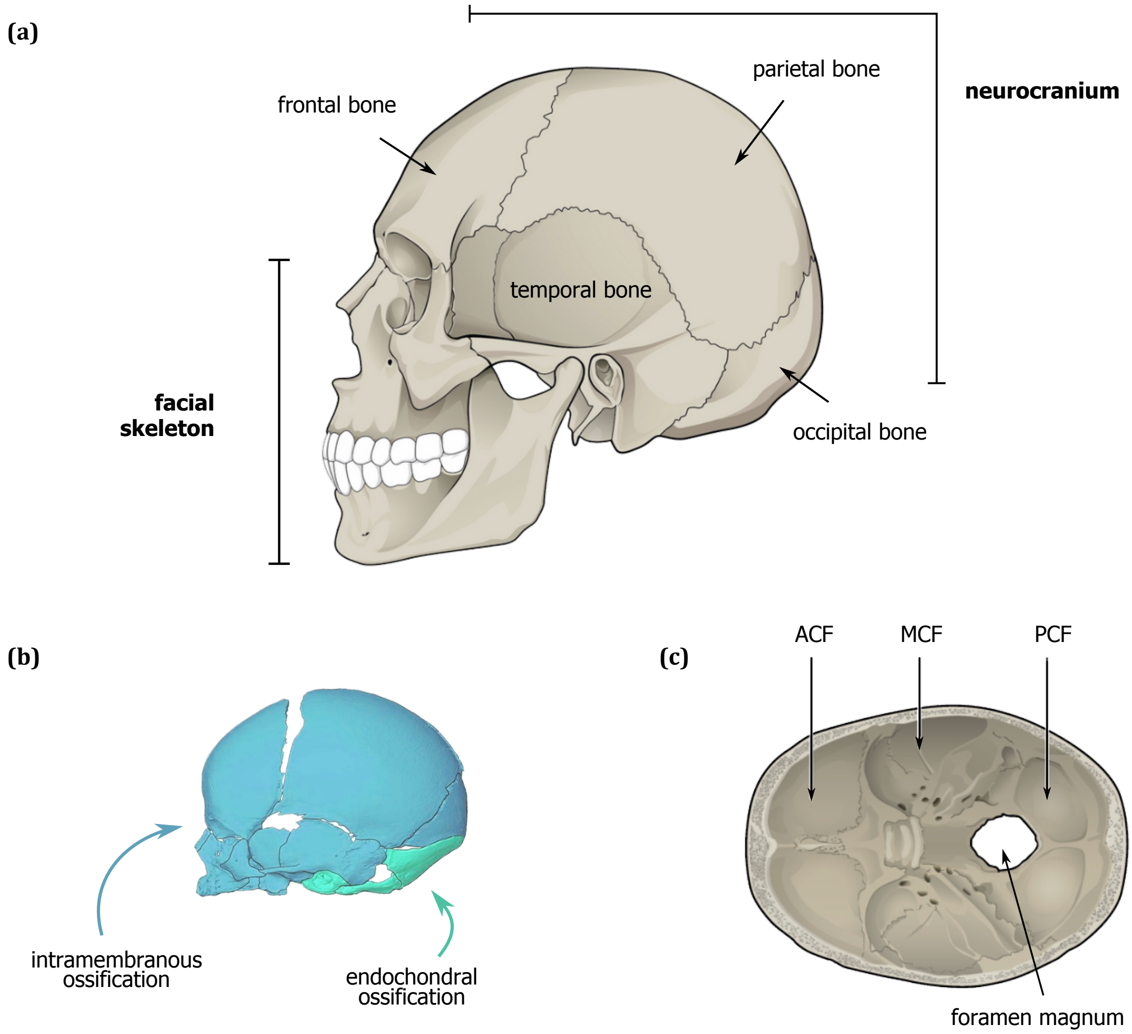

Fig. 1.4. Anatomy of the human skull. (a) The skull can be divided into three main parts: the facial skeleton, and the cranial base and cranial vault, which compose the neurocranium; (b) the bones from the face and the vault grow through intramembranous ossification, and those of the cranial base via endochondral ossification; (c) the floor of the cranial cavity is divided into three depressions, the anterior cranial fossa (ACF), the middle cranial fossa (MCF), and the posterior cranial fossa (PCF). [(b) after Flaherty et al., 2016].

sutures constitute juxtapositions of the two tissues, and the presence of neural crest tissue is thought to be essential for the initiation of signaling required for suture growth (Jiang et al., 2002; Morriss-Kay & Wilkie, 2005). The expansion of the brain is restricted by the location, orientation, and closure timing of the sutures, which determine the direction of bone growth (Morriss-Kay & Wilkie, 2005; Lieberman, 2011). Following growth and development of the brain, the midline vault achieves adult form between the ages of 10 and 13 years (Bastir et al., 2006).

Three protective layers of connective tissue, called the meninges, surround and support the brain (Purves et al., 2004). These are of particular interest, especially the outer layer, the dura mater, due to its structural and functional roles, which contribute to the integration of brain and skull (Friede, 1981). In terms of function, the dura mater participates in the regulation of bone formation and in suture closure within the cranial vault (Opperman, 2000). In terms of structure, it provides support to the neural tissues, connecting the neurocranial vault to the basicranium, by attaching to the cranial base at the *crista galli* of the ethmoid bone, the lesser wings of the sphenoid, and the petrous crests of the temporal bones (Moss & Young, 1960). Its medial in-fold, the *falx cerebri*, develops between the two cerebral hemispheres, conferring a rather flat and vertical shape to the medial brain surface (Friede, 1981; Mancall & Brock, 2010). It also attaches to the *tentorium cerebellum*, pulling it upward and protecting the cerebellum and the foramen magnum from the weight of the cerebrum (Lieberman, 2011). The dural fiber tracts attach to the cranial floor and underlie the sutural system, determining the preferential direction of growth (Moss & Young, 1960). Accordingly, the dura mater might constitute a bridge for structural interaction between the cranial base and the vault (Bruner & Ripani, 2008).

The cranial base, or basicranium, grows via endochondral ossification, from cartilaginous precursors located at the bone joints, the synchondroses, with bone deposition progressing from posterior to anterior, and then to the lateral bones (**Fig. 1.4b**; Sperber, 2001). The cranial base comprises the bridge that connects the head to the body, articulating the skull with the vertebral column while also providing all the necessary foramina for the blood vessels and cranial nerves (Enlow, 1968). Besides, it comprises the central axis of the skull, with the neurocranium growing above, and the face below (Lieberman et al., 2008). In this context, the morphogenesis of the base is rather complex (Lieberman et al., 2000; Bastir et al., 2004; Bruner & Ripani 2008), having to accommodate the development of the surrounding structures. The midline cranial base grows in accordance with the ventral axis of the brain, accommodating the diencephalon and the brainstem, while the lateral floor adjusts for the relatively faster expansion of the cerebral and cerebellar hemispheres, housed within three well defined cranial fossae (**Fig. 1.4c**; Enlow, 1968). The midline and lateral basicranial regions have different patterns of maturation, with the former attaining adult morphology earlier in development. In humans, the midline base reaches adult shape and size at about ages 8 and 13, respectively, while the lateral base reaches mature shape at about age 12, and size at about age 16 (Bastir et al., 2006). As a result, the midline and lateral portions of the cranial base are relatively independent from each other (Bastir & Rosas, 2005). Similarly, the anterior, middle, and posterior cranial fossae are relatively independent from each other in terms of morphology, being more influenced by the adjacent neural elements (Bruner & Ripani, 2008).

Although maturing later than the neurocranium, the facial skeleton can still exert structural influences (Bastir et al., 2006). It can also influence brain development indirectly by limiting growth of the cranial base in the anterior and inferior direction (Hallgrimsson et al., 2007). Interestingly, the dynamics of lateral cranial floor maturation seem to be similar to those of the neurocranium in terms of shape, and to those of the face in terms of size (Bastir et al., 2006), emphasizing its role as a structural interface between the different cranial elements (Bastir et al., 2006; Bastir & Rosas, 2006; Bruner & Ripani, 2008). In fact, basicranial flexion is thought to be an adjustment to brain expansion in primates, as it seems to be associated with large brain size relative to basicranial length (Ross & Ravosa, 1993). In humans, increased relative brain size might have created a 'spatial packing' problem that was solved by bending the cranial base (Gould, 1977; Lieberman et al., 2008). Nonetheless, differences in timing and mode of cranial base angle development between humans and non-human primates might reflect distinct patterns of structural interactions with the brain and the face (Lieberman & McCarthy, 1999; Neaux et al., 2013). Similarly, experiments with rats showed that the basicranium seem to flex to accommodate a large brain relative to the length and width of the basicranial fossae, and to extend to conform to variations in facial length and width relative to the anterior cranial base, indicating that cranial base angle is subjective to epigenetic influences, resulting from assorted combinations of brain size and face length, considering both ontogeny and evolution (Lieberman et al., 2008).

1.2.2. Morphological integration within the skull

Morphological integration refers to the coordinated changes among structurally or functionally related anatomical elements (Olson & Miller, 1958). Evidences of integration among cranial and endocranial components in humans come from artificial cranial modifications as well as from pathological conditions. Artificial cranial deformations, such as fronto-occipital flattening and annular binding, have their origin in cultural practices in which a force is applied to the immature head for permanent reshaping. The resulting shape depends on the method used. The fronto-occipital flattening method restricts antero-posterior growth originating short and wide cranial configurations, while annular binding prevents circumferential expansion producing long vaults and narrow base and face (Cheverud, 1996). The pathological evidence mostly includes cases of developmental anomalies. For instance, in microcephaly the reduced brain growth results in a small skull with fused sutures (Chervenak et al., 1984), and in hydrocephalus increased intracranial volume due to excessive cerebrospinal fluid leads to expanded and thinner vaults (Morimoto et al., 2003). An extensively studied condition is craniosynostosis, i.e. the premature fusion of one or more cranial sutures, which is associated with coordinated deformations of the skull, brain, and meninges (Aldridge et al., 2002; Richtsmeier et al., 2006). Both the artificial cranial deformations and premature suture fusion constrain the direction of growth, resulting in related shape changes throughout the whole structure, especially the cranial base (Moss & young, 1960; Richtsmeier et al., 2006). In the case of craniosynostosis, it has been suggested this condition must be considered in terms of interactions among brain, skull and dural tissues as a system, and its cause could be associated with modifications to the morphogenetic mechanisms regulating within-population variability or evolutionary change (Aldridge et al., 2002; Richtsmeier et al., 2006).

During morphogenesis, as the organism or structure changes in size (growth), its shape must change accordingly in order to maintain functional and structural balance. This relationship between size and shape variation is referred to as allometry, a factor that also provides morphological integration (Gould, 1977; Klingenberg, 1998, 2009, 2013). In this sense, size and shape covary within a fixed structural and functional model (Bruner, 2007). Alterations in timing and rate of morphogenetic events, i.e. heterochrony, might lead to changes in size and shape at the intra- or inter-specific level (Gould, 1977). For example, accelerating, decelerating and/or displacing the beginning or ending of an event can result in a shift, an extension (peramorphosis), or an abbreviation (paedomorphosis) of the ontogenetic trajectory (Klingenberg, 1998). Heterochronic processes might also alter the allometric relationships, originating a new biological model. For instance, neoteny, which is the retention of juvenile characters in the adult, is caused by a delay only in the rate of shape changes, resulting in a different allometric pattern (Bruner, 2007).

Another important factor underlying the morphological variation and evolution is the pattern of morphological integration within and among structures. Groups of elements that are more integrated with each other and more independent from other anatomical elements constitute a modular unit or module (Wagner, 1996; Klingenberg, 2008, 2014). While an integrated structure is characterized by strong covariation among the different components, modularity may be regarded as its opposite or counterpart, as it refers to the differences in degree of covariation among different components of a structure (Klingenberg, 2008, 2014). The human skull has been shown to be formed by two separate modules, the anterior facial module, including the face and the frontal bone, and the posterior cranial module, comprised by the vault and the base (Esteve-Altava et al., 2013). The patterns of bone articulation indicate their structural role, and three bones seem to be essential for the integration among the skull. The ethmoid bone provides an integrative bridge within the facial module, while the frontal and sphenoid bone connect the two modules (Esteve-Altava et al., 2013). The patterns of bone articulation in the facial module seem to be more complex and dependent on the influence from other structures, like the muscular attachments (Esteve-Altava & Rasskin-Gutman, 2014; Esteve-Altava et al., 2015). The patterns of integration and modularity might both constrain and facilitate evolutionary change, promoting coordinated evolution of structures in the same modular unit and mosaic evolution of different modular units (Wagner, 1996; Cheverud, 1996). Hence, knowing the patterns of developmental integration help interpret the patterns of morphological variation, which in turn are essential for understanding morphological evolution (Cheverud, 1996; Klingenberg, 2008).

1.3. THE FOSSIL EVIDENCE

1.3.1. Paleoneurology and endocasts

Paleoneurology studies human brain evolution based on the analysis of endocranial casts from fossil hominids, which comprise the only direct evidence as to how the human brain has changes through time (Bruner, 2003; Holloway et al., 2004). Due to the close proximity and reciprocal interactions during development, the form of the braincase closely resembles that of the brain, and some features of the cortical surface might get imprinted on the internal walls of the neurocranial bones (Holloway et al., 2004; Neubauer, 2014). In this sense, molds of the endocranium, or endocasts, are used as a proxy for brain morphology in the absence of the brain (Falk, 1980; Holloway et al., 2004). Some endocasts occur naturally when the skull of the deceased animal is filled with fine sediments that enter through the cranial foramina. These sediments become compacted and solidified by infiltrating mineral solutions, resulting in a solid sedimentary rock. Others can be made, either manually, by covering the endocranial cavity with molding material such as liquid latex rubber or silicon rubber, or digitally by rendering from computed tomography (CT) data on specialized computer software (Holloway et al., 2004, 2009).

Endocasts are not molds of the brain, since three meningeal layers and cerebrospinal fluid lie between the brain and the endocranial walls. This leads to two main consequences: first, these endocranial tissues along with blood vessels and portions of the venous sinuses will also contribute to the form of the endocast (Neubauer, 2014); and second, the meningeal layers that involve the brain surface prevent a clear impression of all the cortical sulci and gyri on the bones. Modern human endocasts display an outstandingly smooth surface compared to the complex convolutions of their neocortex (**Fig. 1.5**.; Zollikofer & Ponce de León, 2013). Still, the general form of the endocast closely reflects the form of the brain, and it can provide valuable information on size and shape of the whole structure, as well as of brain regions (Bruner et al., 2003; Holloway et al., 2009; Neubauer, 2014). However, more localized changes are only given by imprints of brain features, such as cortical convolutions, which can give insight on the major lobe subdivisions of the brain, thus providing clues about brain organization (Holloway, 1975). This is only possible to discern if these features get imprinted into the internal bony tables, and their identification is rather subjective, requiring thorough knowledge of cortical anatomy (Holloway et al., 2004, 2009).

1.3.2. Some distinctive features and evolutionary changes of the modern human brain

According to the fossil evidence, there seems to be a steady increase in cranial capacity from about 3.5 to 1.5 MYA (million years ago), across Australopithecines (400 - 600 cm^3) and the first *Homo* (600-800 cm^3), which then accelerates from *Homo erectus* to anatomically modern humans (Falk, 2015; Holloway, 2015). During the last million year, the cranial capacity increased from about 800 cm^3 in *H. erectus* to about 1000-1200 cm^3 in Middle Pleistocene specimens (*H. heidelbergensis*), and 1500 cm^3 or more in modern humans and Neanderthals (Holloway et al., 2004).

Changes in brain organization seem to have preceded increase in size (Holloway et al., 2004). For example, a reduction of the primary visual cortex, and relative increase of the parietal cortex is suggested for *Australopithecus* (3.5-2 MYA), based on the position of the lunate sulcus. Moreover, early *Homo* endocasts display some reorganization of the frontal

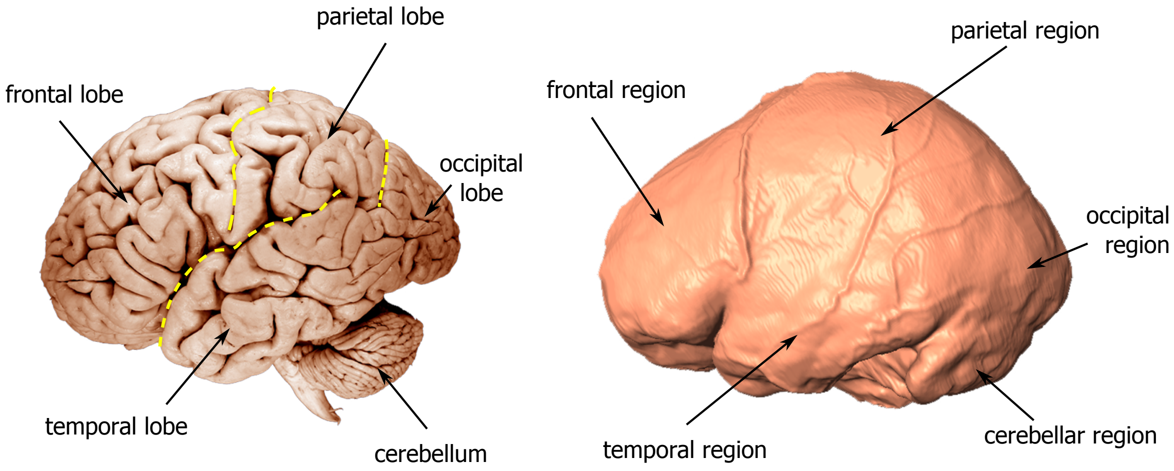

Fig. 1.5. Comparison of the lateral surfaces of the human brain and endocast [human brain modified from brainmuseum.org].

region, which become slightly rounder and wider, and cerebral asymmetries about 2-1.8 MYA (Holloway et al., 2004). From early *Homo* to Neanderthals and modern *H. sapiens*, increase in size was accompanied by related changes in general shape, such as a slight development of the vertical dimensions, relative widening of the frontal and parietal regions, and a relative reduction of the occipital regions (Bruner et al., 2003; Bruner, 2004, 2010). Neanderthals and archaic humans share a common endocranial model based on the same allometric trajectory, while modern humans deviate from allometry, having undergone a more prominent dilation of the parietal region (Bruner et al., 2003). Both Neanderthals and modern humans display developed parietal regions, but the former mostly displays widening of the lower region with the upper parietal vault remaining short and flat, while the latter display a dilation of the whole parietal, including lateral, vertical, and longitudinal expansion (Bruner, 2010; Bruner et al., 2011). Hence, Neanderthals and modern humans seem to correspond to two distinct morphotypes resulting from separate evolutionary trajectories, with the Neanderthals maintaining a plesiomorphic endocranial design and modern humans developing derived neurocranial architecture (Bruner et al., 2003, 2004). In fact, the modern parietal bulging has been deemed responsible for the unique modern human globular braincase (Bruner et al., 2003) which is an autapomorphy, i.e. a distinctive feature, of modern *H. sapiens* (Lieberman et al., 2002) distinguishing them from other living apes (Bienvenu et al., 2011; Aldridge, 2011). The globular shape of the neurocranium is established early in postnatal ontogeny in a developmental stage that occurs only in modern humans, being absent in Neanderthals, chimpanzees and other living great apes (Neubauer et al., 2009, 2010; Gunz et al., 2010, 2012; Neubauer & Hublin, 2012; Scott et al., 2014).

Overall, evolutionary changes to the modern human neurocranium involved a general bulging of the fronto-parietal profile with particular development of the posterior district (Bruner et al., 2004). Since the cranial vault is mostly molded by the expanding brain (Moss & Young, 1960), the bulging of upper braincase could indicate changes to the underlying neural tissues.

1.4. DIGITAL IMAGING TECHNIQUES AND GEOMETRIC MORPHOMETRICS IN PALEOANTHROPOLOGY

The study and quantification of morphological variation has been given a boost in the last few decades with the introduction and improvement of digital techniques and specialized software (Bruner, 2007). One important advance within the fields of physical anthropology and human paleontology was the incorporation of biomedical imaging techniques into the analysis of anatomy (Zollikofer et al., 1998; Weber, 2015). These include computed tomography, which enables imaging the skeletal tissue, and magnetic resonance imaging, which captures the soft tissue, such as the brain. The noninvasive nature of these methods, which allows creating collections from living, functional organisms, on the one hand, and of fossil specimens, on the other brought a significant advantage, since the virtual copies can be handled and manipulated without modifying or damaging the original organisms or specimens.

1.4.1. Medical imaging techniques for visualizing brain and cranial structures

Computed tomography (CT) was the first medical imaging technique to emerge. This technique consists in the use of a computer (computed) to obtain images (graph) from a series of slices or cuts (*tomo*) of biological tissues (Caldemeyer & Buckwalter, 1999). The CT scanner includes an X-ray source and an array of receptors located on opposite sides of the specimen to be scanned. Both the source and the detectors rotate around the specimen producing multiple projections from different angles, which are then integrated to form a cross-sectional image (**Fig. 1.6a**.; Zollikofer et al., 1998; Spoor et al., 2000). The cross-sectional images display the anatomical structures in a gray scale, which reflects the attenuation coefficients of single volumetric units of the different tissues to the X-rays beams passing through the specimen. Air, and low-density tissues, such as fat and water, cause lower attenuation, and thus appear darker in the CT images, while high-density tissues, like bone, cause higher attenuation and will appear brighter on the CT images (Caldemeyer & Buckwalter, 1999). The degree of attenuation and the white color in which bone tissue appears makes the CT scanning excellent for studying skeletal morphology (Caldemeyer & Buckwalter, 1999). By changing some parameters, namely regarding the resolution, CT scanners can be adapted to the density range of fossils specimens (Spoor et al., 2000).

Magnetic resonance imaging (MRI) is based on the magnetization properties of the

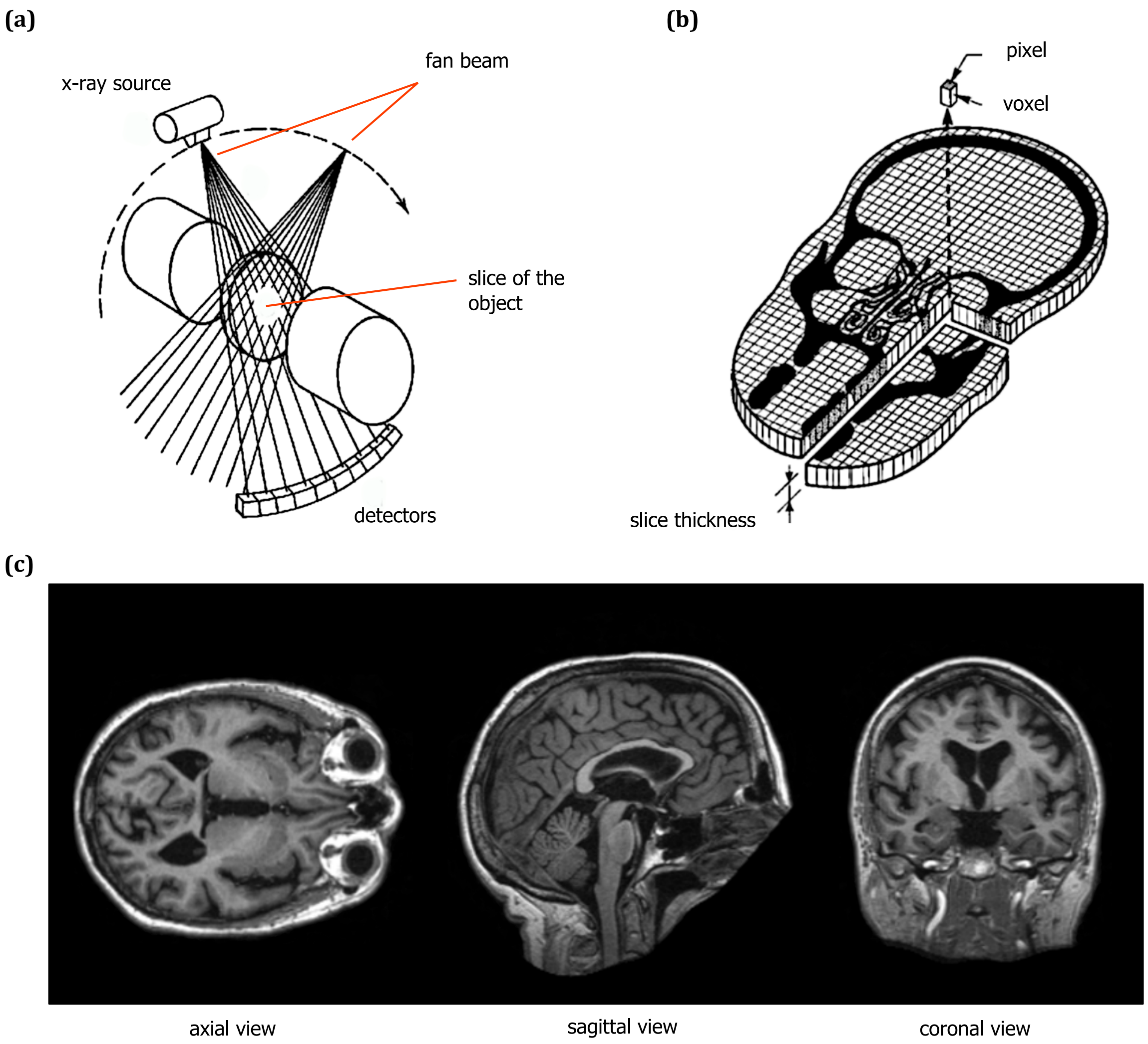

Fig. 1.6. Medical imaging techniques. (a) During data acquisition in CT, an x-ray source and an array of detectors rotate about the object or specimen measuring the attenuation of the slice volumes in many directions, using a fan beam; (b) the scans that result from CT or MRI are characterized by the slice thickness, and the pixel and voxel sizes; (c) example of the orthogonal views of an MRI scan. [(a) and (b) after Spoor et al., 2000].

hydrogen nuclei protons of the tissues (Caldemeyer & Buckwalter, 1999). First, the tissue is exposed to an external magnetic field that aligns the protons into a state of equilibrium. Then, this magnetization is disrupted by radiofrequency pulses to excite the protons into a higher energy state (Spoor et al., 2000). After the pulses, the protons go back to their initial state, emitting radiofrequency energy. The intensity of the emitted radiofrequency signal, which depends on the tissue fat and water composition, is converted into corresponding shades of gray in the final images. In this sense, MRI is very effective in discriminating between the gray and white matter of the brain, respectively representing neurons and connecting axons (Rilling, 2008). Usually, two types of images are generated by varying the sequence of radiofrequency pulses that are emitted and detected. T1-weighted images are produced by using short times between successive pulses and between the pulses and the received signal; T2-weighted images are produced by using longer times. The produced images show differences in the intensities of the tissues, as on T1-weighted images the cerebrospinal fluid is darkest, followed by gray matter and then white matter, while on T2-weighted images the cerebrospinal fluid is brightest, followed by gray matter and white matter (Caldemeyer & Buckwalter, 1999). The low intensity signal of air and bone result in their black coloration in the images (Spoor et al., 2000). MRI constitutes the best tool for non-invasive imaging of brain anatomy in living specimens, and the easy accessibility allows generating large databases that can be used for further analyses (Rilling, 2008).

The products of both CT and MRI comprise series of two-dimensional (2D) images, each representing the values from a single slice of the anatomical structures. The observable details will depend on the resolution, or size of the imaging voxels (volumetric elements; **Fig. 1.6b**). Each voxel has a surface dimension in the plane of the emission and a depth dimension on the perpendicular plane. The first depends on the power of the machine and on the filed-of-view, which is the area covered by the emission, and the latter on the slice thickness, which is the space between each slice. The resulting slices can then be assembled together to reconstruct the different scan planes and orthogonal projections, or even the entire three-dimensional (3D) volume of the scanned structure (**Fig. 1.6c**; Bruner, 2003). By using appropriate software, it is possible not only to assess the internal structures, such as the inner ear (Spoor & Zonneveld, 1995) in the case of CT, or the subcortical brain elements in the case of MRI, but also segment and create 3D models of isolated structures. Importantly, digital tools simplify the reconstruction of endocasts.

1.4.2. Landmark-based geometric morphometrics

The use of digital samples and tools enhanced the application of quantitative multivariate statistics for morphological analyses that capture the geometry of the anatomical structure (Zollikofer et al., 1998; Weber, 2015). In this sense, geometric morphometrics is the culmination of the advances in both imaging techniques and computational power and multivariate statistical approaches (Bookstein, 1997). Geometric morphometrics is based on landmarks, which consist in discrete anatomical loci defined by Cartesian coordinates, in two or three dimensions. Within a study, each specimen or anatomical structure will be represented by a set of landmarks called the landmark configuration, whichconstitutes the datum for statistical analysis (Zelditch et al., 2004). Because the spatial relationship between the landmarks is preserved, the geometry of the anatomical structure is incorporated into the analysis. The landmark configuration thus constitutes the geometric model of the structure under study, which makes the selection of landmarks a decisive step. Overall, three main criteria must be fulfilled: the landmarks must (1) represent discrete anatomical loci that are corresponding across all specimens under study, (2) effectively cover the structures under study in order to obtain an adequate model, and (3) be as reliable and repeatable as possible to reduce measurement error and allow for replication (Zelditch et al., 2004). In cases such as the skull vault or the surface of endocasts, curves and surfaces that provide important information lack reliable references that can be used to define landmarks. These regions can be sampled by placing semilandmarks along them (Gunz & Mitteroecker, 2013). These represent the structure as a group, and the correspondence is between the curves (2D), or surfaces (3D), and not between each point (Bookstein, 1997; Gunz et al., 2005). Semilandmarks must be in rough geometrical correspondence, being similarly and evenly spaced (Gunz et al., 2005). In order to be comparable, whether using anatomical landmarks or semilandmarks, the sequence and number of point coordinates has to be the same across the sample.

Comprising a coordinate system, the landmark configuration contains information about size, shape, position, and orientation of the structure it represents. Shape is mathematically defined as the attributes of an object that are not size, position, and orientation (**Fig. 1.7a**; Kendall, 1977). Hence, in order to obtain only information on shape, the non-shape attributes must be removed. The most widely used method to extract shape information is the General Procrustes Analysis (GPA; Gower, 1975), or simply Procrustes superimposition, as it superimposes the configurations so that the distance between corresponding landmarks

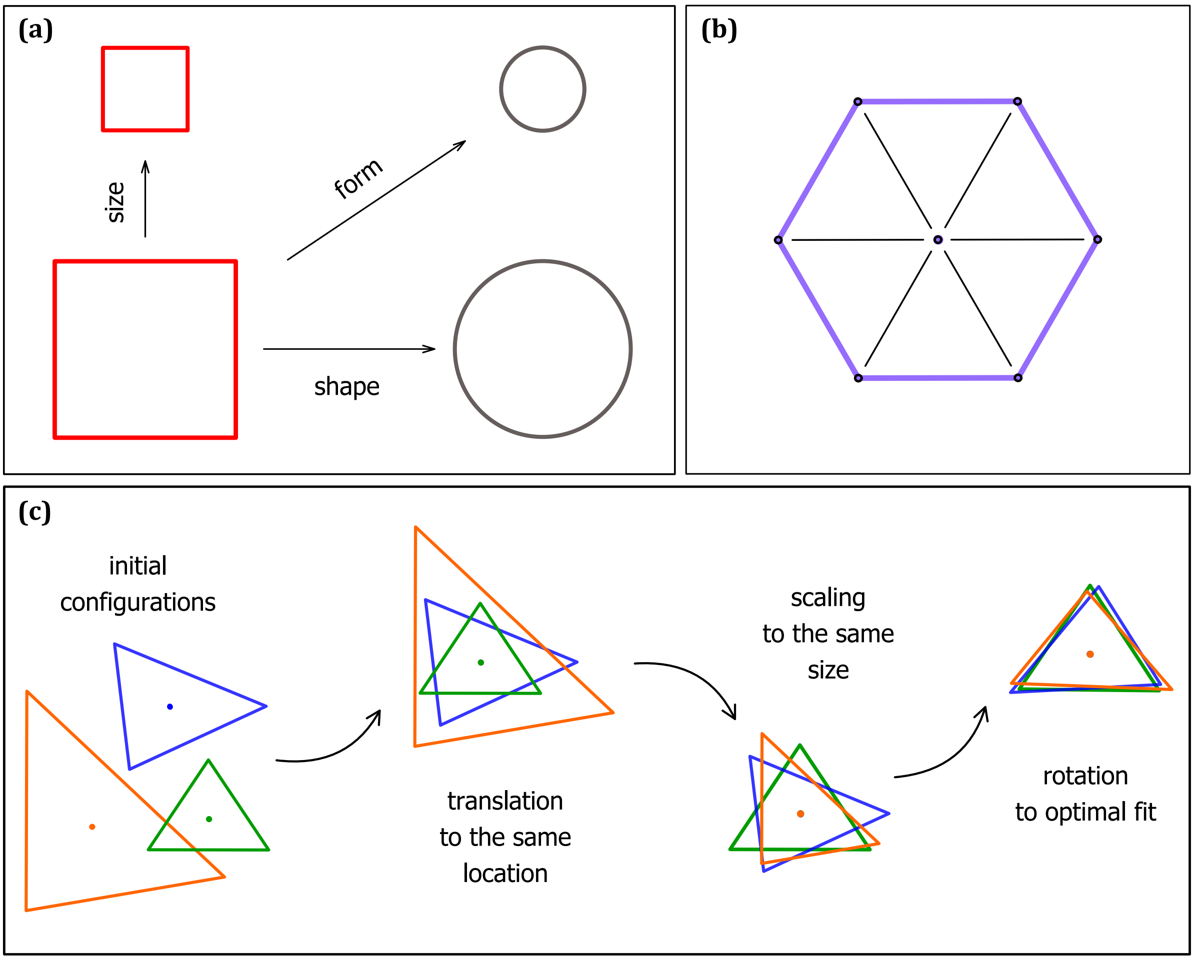

Fig. 1.7. Geometric morphometrics. (a) form contains information about shape and size; (b) the centroid corresponds to the centre of gravity of a landmark configuration; (c) Procrustes superimposition eliminates the differences in location, size, and orientation, so that the variation in shape can be analyzed.

will indicate the differences in shape (Rohlf & Slice, 1990). In sum, non-shape information is eliminated by translating the configurations to the same location, scaling to the same size, and rotating to the same orientation. The location of a configuration corresponds to the coordinates of its centroid (center of gravity; **Fig. 1.7b**), which is computed as the average of all landmark coordinates (Zelditch et al., 2004). Information on position is eliminated by setting all the centroids to zero so that the configurations are all centered to the origin of the coordinate system (Rohlf, 1999). Differences in size are eliminated by scaling all the configurations to unit centroid size. Centroid size is calculated as the square root of the sum of squared distances of the landmarks to the centroid (Bookstein, 1996), and it is scaled to one by dividing the landmark coordinates of each configuration by the respective centroid size (Rohlf & Slice, 1990). Differences in orientation are removed by rotating the configurations until optimal alignment, minimizing the squared distances between corresponding landmarks (**Fig. 1.7c**; Rohlf & Slice, 1990; Zelditch et al., 2004). The residuals of the Procrustes superimposition, i.e. the remaining spatial differences among the configurations, constitute the shape variables, and can be subsequently used in multivariate statistical analysis.

A first step into the analysis of shape variation and comparison is to use ordination techniques that reveal the main patterns of covariance (Bruner, 2007), such as Principal Component Analysis (PCA). The PCA transforms the original variables into a new set of uncorrelated variables, the principal components (PCs), which are linear combinations of the original variables (Jolliffe, 2002). The criterion is to maximize the variance described by the first axis or component, such that successive axes will describe sequentially less variation (Jolliffe, 2002; Zelditch et al., 2004). In this sense, the first principal component (PC1) describes the direction of the largest proportion of variance, while PC2 describes the second largest direction, etc; usually most of the variance is described by the first few axes. The distribution of the specimens along each PC gives insight on the differences and similarities in shape among the individuals in the sample. The main patterns of shape change along each PC can also be easily visualized through wireframe diagrams and deformation grids. The former illustrates shape variation as differences in location of corresponding landmarks between a reference and a target, while the latter as deformation of the reference into the target. The graphical output of the results constitutes one great advantage of geometric morphometrics, facilitating the visualization and interpretation of shape changes (Rohlf & Marcus, 1993; Adams et al., 2004). Another convenient attribute of geometric morphometrics is that size information can be recovered to use in the statistical analysis, since a measure of size is preserved as the Centroid size. This is a linearized measure of size that is geometrically and statistically independent from shape, and thus is only expected to correlate with shape if there is allometry (Zelditch et al., 2004). In this sense, Centroid size is the most suitable to investigate shape changes associated with size.

The combination of digital imaging and geometric morphometrics tools has thus significantly improved the analysis of shape and morphological variation in terms of covariation among multiple traits and in terms of spatial relationships among the different anatomical elements. In this sense, the phenotype is currently viewed as the ensemble of structurally and functionally integrated systems (Bruner, 2007).

1.5. ON THE EVOLUTION OF THE FRONTAL AND PARIETAL REGIONS: STRUCTURAL ORGANIZATION AND ANATOMICAL VARIATION

The frontal and parietal cortices are tightly interconnected through multiple brain networks that underlie higher-order cognitive functions, such as working-memory, executive control, language, and tool use (Naghavi & Nyberg, 2005; Jung & Haier, 2007; Meunier et al., 2009; Cole et al., 2010). Interestingly, vertical and lateral dilation of the frontal and parietal regions seem to characterize the evolution of the modern human braincase (Bruner et al., 2003, 2004). Nonetheless, it seems that evolutionary changes to the frontal region follow the allometric pattern across *Homo*, while parietal changes deviate from allometry (Bruner et al., 2003). Besides, the frontal and parietal bones, although adjacent, are integrated into different structural and functional contexts, which must be taken into account when interpreting evolutionary changes (Bruner, 2007).

Regarding the brain districts, the frontal lobes of humans seem to be as large as expected according to great ape scaling patterns (Semendeferi et al., 1997, 2002), though some organizational changes seem to have occurred (Schoeneman et al., 2005; Aldridge, 2011; Smaers et al., 2011; Smaers & Soligo, 2013). In the case of the parietal lobes, due to the difficulty in defining homologous boundaries, volumetric studies have considered the parietal and occipital lobes together, determining this parieto-occipital block to be as large as expected in human (Semendeferi & Damasio, 2000). However, the relative reduction of the primary visual cortex of the occipital lobes in humans compared to other primates (de Sousa et al., 2010), could indirectly point to a relative increase of the human parietal cortex. Additionally, both cytoarchitectonic and morphometric data point to expansion and reorganization of the parietal cortex in modern humans (Simon et al., 2004; Husain & Nachev, 2007; Peeters et al., 2009; Caminiti et al., 2010; Aldridge, 2011; Bruner et al., 2017).

Regarding the cranial elements, the frontal bones are involved in a more complex structural and functional environment than the parietal bones. The frontal bone is functionally and structurally linked both to the frontal lobe and to the ocular contents as it composes the anterior portion of the vault and most of the anterior cranial floor, and contributes to the roofs of the orbits (Friede, 1981; Moss & Young, 1960). The positioning of the orbit below the frontal lobes in modern humans, as well as in Neanderthals, might create a structural limit for the vertical development of this brain region, as well as for the development of the orbito-ocular structures (Bruner, 2004; Bruner et al., 2010, 2014a). In contrast, the parietal bones only contribute to the cranial vault, being less influenced by the dynamics of the cranial base. Since the cranial vault is thought to be mostly shaped by the expansion of the underlying neural tissues (Moss & Young, 1960), the apparent bulging of the parietal profile in modern humans could result from a reorganization of the underlying parietal cortex - either due to functional changes in the parietal itself or due to adjustment to biomechanical changes in neural wiring - which might have involved cognitive effects (Bruner, 2004, 2010). Nonetheless, there is still structural limitation to growth of the parietal bones, mediated by the cranial base, via the dural and sutural systems (Enlow, 1968; Opperman, 2000).

In sum, the evolution of the frontal region seems to be mostly affected by the structural relationships among the hard and soft tissues of the face and neurocranium, while the evolution of the parietal region could result mainly from changes to the underlying neural tissues, although indirect influence from changes to the cranial base cannot be ruled out. Taking this into account, the present thesis considers the frontal regions in the context of the structural interactions among the neurocranial and facial hard and soft tissues, while the parietal regions are considered mainly in terms of neural anatomy, though also considering the spatial relationship with the cranial base.

1.5.1. Structural organization of the frontal bones: on the spatial conflict between the brain and the oculo-orbital elements

The frontal bone composes, simultaneously, the endocranial base and the roof of the orbits, and thus must respond to the functional and structural needs of both the frontal lobes and the orbital contents (Moss & Young, 1960). Besides, the frontal bone seems to constitute an interface between the facial and the neurocranial modules of the human skull (Esteve-Altava et al., 2013). In this sense, the form of the frontal bones results from the spatial relationships between the orbit and the braincase (Moss & Young, 1960). Facial prognathism and increased separation between the orbit and the anterior braincase, such as in some extant apes and archaic human species, results in the formation of a browridge to make part of the orbital roof. By contrast, in modern humans, with the increased proximity between craniofacial and neural elements, the browridge disappears (Moss & Young, 1960; Ravosa, 1991).

Increase in brain size and in basicranial flexion in anthropoids has been suggested to relocate the orbits into a more inferior and medial position relative to the anterior and middle cranial fossae, when compared to prosimians (Ravosa, 1991; Ross & Ravosa, 1993). The orbits become closer together, more frontated and convergent (vertically and forward oriented orbital rims), and the orbital cavities decrease in relative size (Cartmill, 1980; Ravosa, 1991; Ross & Ravosa, 1993; Ross, 1995). These modifications in the craniofacial configuration of anthropoids changed the structural interactions between neurocranium and orbit (Ravosa, 1991). Further craniofacial changes have emerged in modern humans, since encephalization was accompanied by a reduction of the facial skeleton, which becomes narrower, flatter, and anteroposteriorly and vertically shorter (Bookstein et al., 2003; Bastir & Rosas, 2009, 2016; Bastir et al., 2010). As an outcome of these opposite evolutionary trends, the orbits of modern humans are completely tucked under the frontal lobes (Lieberman et al., 2000, 2002; Bruner

2007). The anterior cranial fossae constitute the only portion of bone separating the ocular and neural tissues, and its thinnest portion corresponds to the portion that sits directly above the eye (Lang, 2012). This spatial proximity probably conveyed structural constraints to the development of the adjacent organs. The position of the orbits below the frontal lobes might have imposed a biomechanical limit for their vertical expansion, resulting in frontal widening (Bruner & Holloway, 2010). In turn, the anterior and lateral expansion of the frontal lobes above the orbits might exert spatial constraints to the growth of the orbit, which could affect the development of the eye as well as its function (Masters, 2012; Bruner et al., 2014a). In a similar way, posterior constraints might have been exerted by expansion of the temporal lobes (Rilling & Seligman, 2002) and anterior projection of the middle cranial fossa (Bastir et al., 2008). It is interesting to notice though that, when compared to less encephalized humans, Neanderthals and modern humans both display a marked widening of the prefrontal regions (Bruner & Holloway, 2010), and exhibit a closer proximity of the orbits to the anterior cranial fossa as well as to the middle cranial fossa (**Fig. 1.8**; Bruner et al., 2014a).

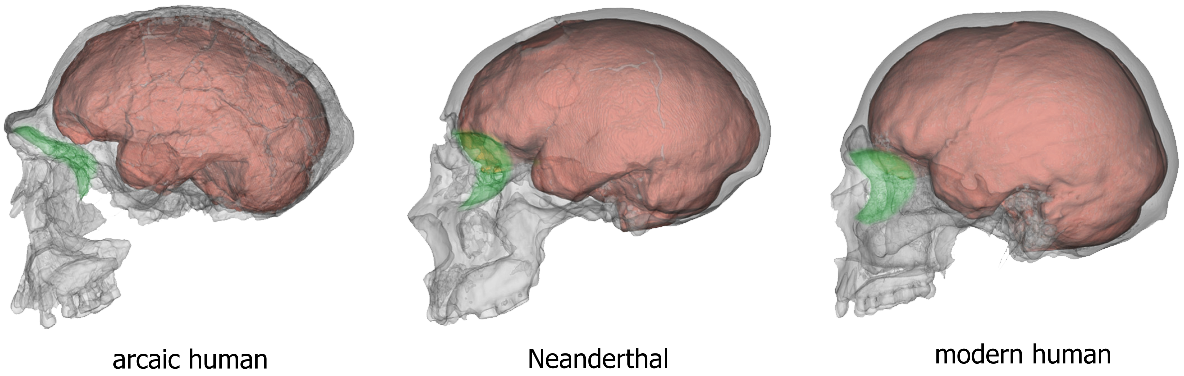

Fig. 1.8. Compared to more arcaic humans (KNM-ER3733), the orbits of Neanderthals (Saccopastore 1) and modern humans are closer to the frontal and temporal regions.[modified from Bruner et al., 2014a].

The eye and the orbit undergo different developmental pathways. The morphogenesis of the eye follows the neural growth trajectory (Scammon & Armstrong, 1925; Todd et al., 1940), while the orbits, composed of several facial and basicranial bones, undergo a rather complex pattern of development (Enlow, 1968). Though initially the growth of the orbit responds to the development of the eyeballs and other soft tissue contents, as part of the facial skeleton, it is mainly influenced by other facial structures (Enlow, 1968; Waitzman et al., 1992). Among primates, the volumes of the eye and orbit are both dependent on body weight, regardless of sex or age, with larger primates having relatively smaller eyeballs and orbit capacities (Schultz, 1940). However, as the relative orbit size decreases more rapidly with body size than relative eye volume, the percentage of the orbit occupied by the eye is widely variable, not only across species but also within species, and thus the size of the orbit is only slightly related to the size of the eye (Schultz, 1940). Among adult humans, although there is a positive correlation between the sizes of the two structures, variation in size of the orbit explain less than 20% of the variation in eye size (Pearce & Bridge, 2013; Masters et al., 2015).

Given this rather general association between eye and orbit, it stands to reason that further (abnormal) increase in eyeball dimensions would have no corresponding increase in the orbit capacity. In fact, vision impairment seems to be associated with the relative size of the eye within the orbit, as individuals with larger eyes in smaller orbits display higher degree of refractive error, at least in a Chinese population (Masters, 2012). This could indicate that development of juvenile-onset myopia could result from spatial constraints, and thus human craniofacial architecture should be considered when analyzing the causes and correlates of myopia (Masters, 2012). For example, prevalence of myopia is much higher in Asia (70-90%), than in Europe or the United States (20-30%), and Africa (10-20%; Fredrick, 2002). This could be explained by craniofacial changes to East Asian populations, which orbits became rounder and smaller during the Holocene, about 30 thousand years ago (Brown & Maeda, 2004; Wu et al., 2007), while no apparent decrease in orbital size has been documented among Western Europeans (Masters, 2009). In this sense, prevalence of myopia could be associated with the form of the orbit affecting the form of the eye (Masters, 2012). Myopia, or nearsightedness, occurs when the eye focuses the image (parallel light rays) in front of the retina, instead of focusing on the retina as in normal vision, or emmetropia (Fredrick, 2002). This can result from a strong curvature of the cornea or lens, or from an abnormally elongated eyeball (Saw et al., 1996; Fredrick, 2002). In contrast to the normal eye, which grows to become emmetropic about the ages of 5 to 8 years (Fredrick, 2002), the myopic eye continues to grow becoming larger in all dimensions, but especially in axial length (Goss et al., 1990; Atchison et al., 2004). Myopia is usually associated with an elongated eye form (Goss et al., 1990; Goldschmidt & Fledelius, 2011).

Hence, based on the fact that myopia is associated with an elongation of the eyeball, which can result from limited space within the orbit, Masters (2012) proposed that the prevalence of myopia in humans, and especially in Asian populations, could be associated with the modern human craniofacial architecture characterized by increased proximity between the ocular and neural structures. Currently, the extent to which the anterior brain regions might constrain the orbital and ocular structures is still unknown. Within the present thesis we investigate the spatial conflict between the frontal and temporal regions of the brain and the ocular and orbital structures of the upper face within *Homo sapiens*, and compared to chimpanzees and fossil human species.

1.5.2. On the parietal bulging and endocranial architecture in modern humans

Facial reduction and cranial globularity are distinctive of modern humans, and have been suggested to result from basicranial flexion and increase of frontal and temporal lobes (Lieberman et al., 2000). Modern humans also display a unique dilation of the parietal region, characterized by vertical bulging and greater curvature and extension of the parietal bone, which could affect the whole endocranial architecture (Bruner et al., 2003, 2011). In contrast to the frontal, temporal, and occipital bones, which also contribute to the cranial base, the parietal bones are only part of the cranial vault, thus being less affected by the base dynamics. Clearly, structural interactions with the other vault bones might still influence the parietal bone, which has been demonstrated to be firmly integrated with the occipital bones (Gunz & Harvati, 2007). Besides, structural integration between the vault and the cranial base has been demonstrated in craniosynostosis (Richtsmeier et al., 2006). Interestingly, an anterior projection of the middle cranial fossae seems to also distinguish modern humans from other *Homo* species and from chimpanzees (Bastir et al., 2008). Given that the middle cranial fossa is structurally related with neurocranium and face, this anterior projection could be associated with enlargement of the parietal volumes and consequent change in the functional axis of the head (Bruner, 2003). The specific association between middle cranial floor and parietal bone morphology is explicitly evaluated within the present thesis.

Brain globularity could also be associated with intrinsic factors, such as optimal wiring, a principle for improving neuronal communication and decreasing energy costs that might be behind the organization of the mammalian neural system (Kaas, 2000; Karbowski, 2001, 2009; Hofman, 2014). With a larger relative brain size, humans allocate a greater proportion of their resting metabolic rate to brain metabolism – 20-25% compared to 8-10% in other primates (Leonard et al., 2007). Increased metabolism also increases temperature, and variation in patterns of heat distribution seem to be influenced by both brain size and geometry (Bruner et al., 2012). Interestingly, the parietal surface of modern humans exhibits lower heat loadings and is associated with increased branching complexity of both the middle meningeal and diploic vessels, compared to non-modern humans (Bruner et al., 2005, 2012; Rangel de Lázaro et al., 2016). Nonetheless, neither the role of the vascular system in thermoregulation nor the relationship between branching complexity and endocranial geometry have been proved yet (Bruner & Sherkat, 2008; Bruner et al., 2009, 2011; Rangel de Lázaro et al., 2016). Still, it is important to note that the two most encephalized humans, modern *H. sapiens* and Neanderthals also exhibit such differences in endocranial shape and vascular complexity on the parietal region.

1.5.3. Parietal bulging as an expansion of the parietal cortex: lateral and medial elements

Since the bones of the cranial vault are generally shaped by the underlying brain, both in terms of ontogeny and evolution (Young, 1957; Moss & Young, 1960), the dilation of the parietal region could represent changes to the neural elements (Bruner, 2004). Both Neanderthals and modern humans seem to have evolved larger parietal regions, though only the latter displays parietal vault elevation, or vertical bulging (Bruner, 2004). Evaluating whether these differences in parietal shape involve differences in cortical features is only possible through the comparison of cortical features imprinted in endocasts, which are rather infrequent. As a consequence, morphological analyses based on endocasts usually consider the structure as a whole. Nonetheless, the relative position of some cortical elements, such as the central and the lateral sulci can be estimated on the endocast surface, allowing for the detection of differences in cortical arrangement. A preliminary study comparing the parietal region among three endocasts representing *H. erectus*, Neanderthals, and modern humans, indicated that parietal bulging in modern humans could have involved elements of the superior and inferior parietal lobules, including the intraparietal sulcus and the supramarginal and angular gyri (Bruner, 2010). Hence, it is important to further explore the viability of defining main cortical regions on the surface of endocasts in order to infer on evolutionary changes to the different brain districts.

The parietal association cortex, or posterior parietal cortex (PPC), is the region of the cerebral cortex posterior to the primary somatosensory cortex, that is, to the postcentral sulcus, and anterior to the occipital lobe (**Fig. 1.9a**). On the lateral surface, it is subdivided by an oblique sulcus, the intraparietal sulcus, into the superior and inferior parietal lobules. The superior parietal lobule corresponds to Brodman Area 7 (BA 7), and comprises most of the dorsal parietal surface, also extending into the medial wall, where it comprises the precuneus. The inferior parietal lobule displays two main gyri, the supramarginal gyrus and angular gyrus, which respectively correspond to BA 40 and BA 39. While the boundary between the parietal and the temporal and occipital lobes are difficult to define on the dorsolateral brain surface, due to complexity and variability in the pattern of convolutions, the definition of the parietal lobe on the medial brain surface is more straightforward.

The precuneus, which constitutes the medial aspect the superior parietal lobule (BA 7) is macroscopically limited by the marginal branch of the cingulate sulcus, anteriorly, the parieto-occipital sulcus posteriorly, and by the subparietal or postlimbic sulcus, inferiorly (Cavanna & Trimble, 2006). The longitudinal extension of the precuneus constitutes the main source of midsagittal brain variation in adult humans (**Fig. 1.9b**; Bruner et al., 2014b). This variation involves changes in the cortical surface area of the precuneus, such that more extended precuneus display absolutely larger surface areas (Bruner et al., 2015a). The dilation of the precuneus also constitutes the main variation on the midsagittal brain surface distinguishing humans from chimpanzees (Bruner et al., 2017). The changes in precuneus proportions are greater on the upper and anterior portions, towards the marginal ramus of the cingulate sulcus, both in terms of intra-specific and inter-specific variation (Bruner et al., 2015a, 2017). Currently, we ignore whether the expansion of the precuneus results from allometric trends across primates or constitutes a species-specific trait of modern humans (Bruner et al., 2017).

Understanding the parietal brain features distinguishing modern humans from other extant and extinct species, as well as the origin of within-human variability, is fundamental since the parietal association cortex is involved in several higher cognitive functions. Indeed, the functions of the PPC are essential for effective interaction with the environment, as it is

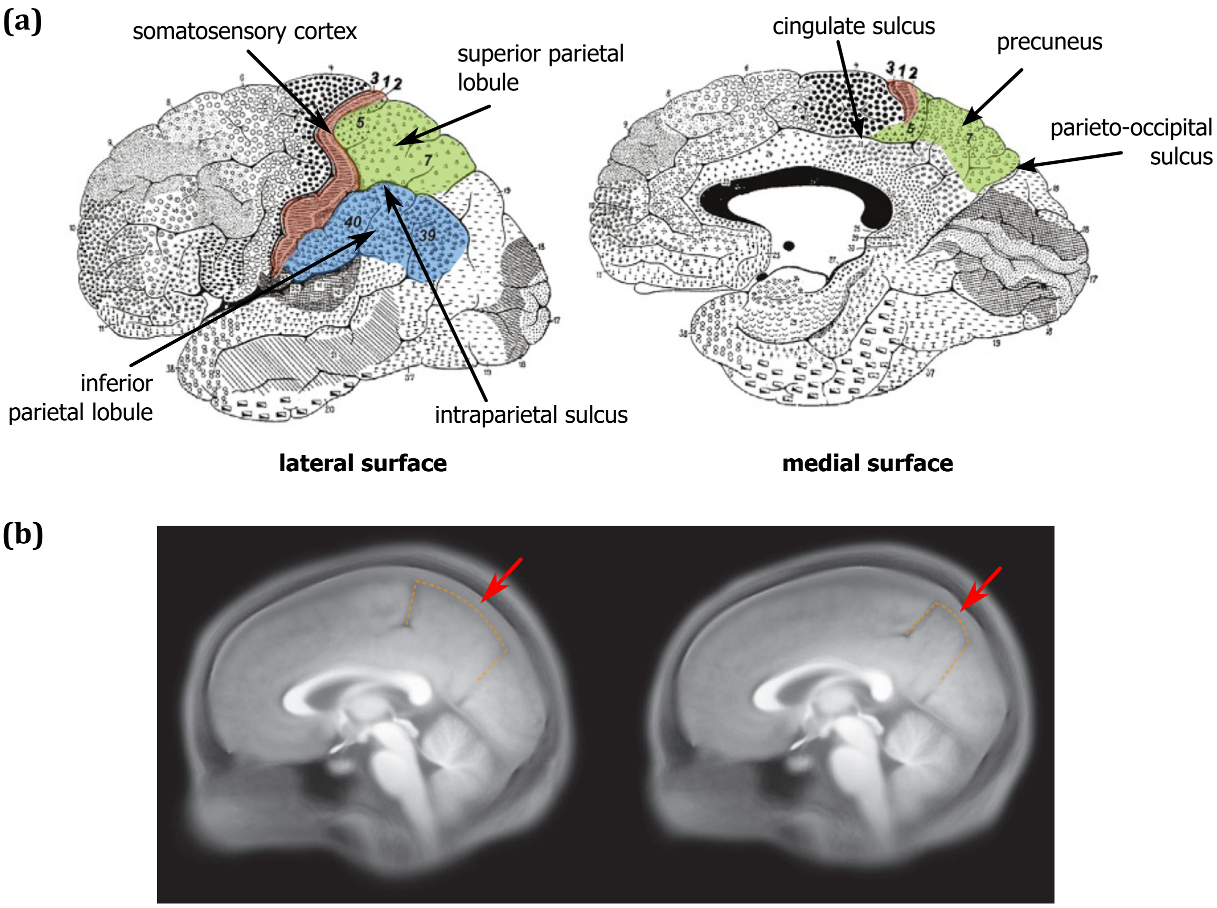

Fig. 1.9. The parietal cortex. (a) on the lateral surface, the intraparietal sulcus divides the parietal lobe into the superior and inferior lobules; the inferior parietal lobule contains the supramarginal and angular gyri, which respectively correspond to BA 40 and 39, and the superior parietal lobule forms the precuneus on the medial surface, corresponding to BA 7; (b) the precuneus is the most variable structure in the medial brain surface in adult humans. [(a) modified from Caspers & Zilles, 2018; (b) modified from Bruner et al., 2014b].

involved in object manipulation, eye-hand coordination, and control of attention (intraparietal sulcus; Grefkes & Fink, 2005), tool use and phonological processing (supramarginal gyrus; Caspers et al., 2010; Deschamps et al., 2014; Nejad et al., 2015), social cognition, semantic and numerical processing (angular gyrus; Price, 2000; Vigneau et al., 2006; Seghier, 2013; Studer et al., 2014), and visual imagery, working-memory, and self-awareness (precuneus; Cavanna & Trimble, 2006; Wallentin et al., 2008; Phillips et al., 2012). The parietal functions seem to be essential for the integration of information from the inner and outer environments, referred to as visuospatial integration, which includes eye-hand coordination, body and space integration, visual imagery and simulation (Bruner & Iriki, 2016). Evolution of the parietal cortex and visuospatial functions in modern humans has been hypothesized to have enhanced the capacity for embodiment, as for instance experience the tools as part of the body (Iriki, 2006; Bruner & Iriki, 2016). Despite the outstanding anatomical variability of the precuneus within humans, and its involvement in diverse cognitive functions (Cavanna & Trimble, 2006), no correlation between the morphological variation of the precuneus and cognitive differences has been detected, at least regarding performance on psychometric test (Bruner et al., 2015a). Nonetheless, the precuneus constitutes one of the main centers of integration in terms of functional and structural processes (Hagmann et al., 2008; Meunier et al., 2009). In fact, its role as a connectivity and functional hub, being involved in brain intrinsic function and maintaining continuously high metabolism might increase the vulnerability of the precuneus to metabolic impairment and pathological conditions such as Alzheimer's disease (Buckner et al., 2009; Bruner & Jacobs, 2013).

The involvement of the parietal cortex in a variety of higher cognitive function, and the outstanding anatomical variation observed in this cortical region, especially the precuneus, suggest the lateral and medial parietal cortices might contribute to modern human cognitive specializations. Currently, the causes and consequences of precuneus variability, as well as the macroscopic features distinguishing human parietal lobes are still largely unknown. The present thesis further explores parietal and precuneus anatomical variation within humans and in a comparative perspective.

1.6. AIMS AND RATIONALE OF THE THESIS

The only direct evidence for the evolutionary changes to the brain on the course of human evolution is provided by the analysis of endocasts of our fossil relatives (Holloway et al., 2004). However, since these provide limited information on cortical features, it is essential to also investigate actual brain anatomy, both in the context of within-human variability and in a comparative framework, considering differences and similarities across extant primate species. The frontal and parietal cortices are structurally and functionally connected, forming a frontoparietal network involved in higher cognitive functions (Jung & Haier, 2007), but development and evolution of the frontal and parietal lobes are differently constrained by the surrounding hard and soft tissues (Moss & Young, 1960). While the evolution of the frontal region might have involved a spatial conflict with the underlying orbital and ocular structures, the evolution of the parietal regions might have occurred through interactions with the cranial base or due to an expansion or reorganization of the underlying neural elements. Among these neural elements, the precuneus is of particular interest as it represents a region of great connectivity and variability among adult modern humans.

The present thesis aims to provide further information on structural relationships that might have influenced the evolution the frontal and parietal bones and lobes, as well as on the evolutionary changes and within-human variability of the parietal cortex. In this sense, the research work focused on three main goals:

i. To analyse the structural interactions of the frontal and parietal regions in the context of functional craniology;
ii. To explore the analysis of parietal lobe morphology as assessed on endocasts;

iii. To provide more detailed information on the anatomical variation of the precuneus within humans and across primates.

The next three chapters contain the research articles that represent the result of the empirical work. These are organized according to the general goals of the thesis.

Chapter 2 is grounded on the importance of studying shape from a functional point of view, considering the structural relationships among adjacent anatomical elements. Given the different structural contexts of the frontal and parietal regions, these are addressed separately, although we intend to contribute to the knowledge of the general patterns of craniofacial integration. Due to the anatomical proximity between the face and the anterior neurocranium in modern humans, our first study (chapter 2.1.) investigates the spatial relationships between the eye and the brain (frontal and temporal lobes) and between the orbit and the anterior braincase, in order to detect possible constraints to eye and orbit position and morphology. In exploring the possible interaction between the cranial vault and base, the second paper (chapter 2.2.) investigates the morphological integration between the parietal bone and the middle cranial fossa (temporal region).

Chapter 3 explores the possibility of investigating parietal lobe morphology on endocasts through the application of geometric morphometrics analysis based on landmarks representing features of the brain cortical surface. A first study (chapter 3.1.) comprised a comparative analysis across a sample of Old World monkeys (Cercopithecidae), which diversity in ecological strategies could provide a platform to test whether macroscopic changes to the parietal lobe could be associated with ecological factors. In the second study (chapter 3.2.) we compared the parietal lobe regions of modern humans and Neanderthals as to shed some light on the differences in shape and size of this brain region between the two human species.

Chapter 4 seeks to add to the knowledge on precuneus anatomy, with two studies focusing on the human intra-specific variability, and a third exploring the variation among non-human primates. In the first study (chapter 4.1.) we explored the coronal section of the precuneus, describing its dimension and the patterns of folding, and investigating the correlation among these variables and the correspondence between the precuneus and the dorsal parietal profile. The second study on intra-specific variation (chapter 4.2.) reassessed the variation in precuneus proportions on the midsagittal brain surface in a larger, racially diverse human sample. The third paper (chapter 4.3.) investigated the midsagittal brain shape variation across non-human primates, including apes and New and Old world monkeys, in order to evaluate whether the precuneus enlargement observed in humans compared to chimpanzees could be explained by allometric factors.

Chapter 2

STRUCTURAL RELATIONSHIPS OF THE FRONTAL AND PARIETAL REGIONS

2. STRUCTURAL RELATIONSHIPS OF THE FRONTAL AND PARIETAL REGIONS

In the context of functional craniology, we investigate the spatial relationships between the upper face and anterior neurocranium and between the endocranial parietal bone and middle cranial base in two separate works. The analyses are based on geometric morphometrics analysis of 2D scout views, which display sagittal (midsagittal profile) and parasagittal (orbits/eye and temporal tip) elements after the projection of the gray scale values of the different (MRI or CT) stacks onto the same plane.

In 2.1, we focus on the structural surroundings of the frontal region, specifically regarding the spatial proximity between the neurocranium and brain to the orbit and ocular elements. The eye-brain relationship is investigated in an MRI sample of adult modern humans to test whether the size and position of the frontal and temporal lobes affect size, shape, and position of the eyeball. The orbit-braincase relationship was investigated in a CT sample composed of modern humans, chimpanzees and Middle Pleistocene hominids (Bodo, Broken Hill 1, and Gibraltar 1) in order to include information on modern human variation as well as on the evolutionary trends regarding human fronto-orbital spatial organization.

In 2.2, we address the structural relationship and morphological integration between the parietal bones and the cranial base concerning the endocranial surface. A sample of modern human CT is used to test whether changes in parietal proportions can influence the spatial arrangement of the middle cranial fossa, especially considering the anterior projection of the temporal tip.

2.1. SHAPE ANALYSIS OF SPATIAL RELATIONSHIPS BETWEEN ORBITO-OCULAR AND ENDOCRANIAL STRUCTURES IN MODERN HUMANS AND FOSSIL HOMINIDS

Authors: Ana Sofia Pereira Pedro, Michael Masters, Emiliano Bruner

Journal: Journal of Anatomy, 231: 947-960

Status: Published in 2017

Journal of Anatomy

J. Anat. (2017) doi: 10.1111/joa.12693

Shape analysis of spatial relationships between orbito-ocular and endocranial structures in modern humans and fossil hominids

Ana Sofia Pereira-Pedro,[1] Michael Masters[2] and Emiliano Bruner[1]

[1]*Centro Nacional de Investigación sobre la Evolución Humana, Burgos, Spain*
[2]*Montana Tech, Butte, MT, USA*

Abstract

The orbits and eyes of modern humans are situated directly below the frontal lobes and anterior to the temporal lobes. Contiguity between these orbital and cerebral elements could generate spatial constraints, and potentially lead to deformation of the eye and reduced visual acuity during development. In this shape analysis we evaluate whether and to what extent covariation exists between ocular morphology and the size and spatial position of the frontal and temporal areas in adult modern humans. Magnetic resonance imaging (MRI) was used to investigate patterns of variation among the brain and eyes, while computed tomography (CT) was used to compare cranial morphology in this anatomical region among modern humans, extinct hominids and chimpanzees. Seventeen landmarks and semi-landmarks that capture the outline of the eye, frontal lobe, anterior fossa/orbital roof and the position of the temporal tips were sampled using lateral scout views in two dimensions, after projection of the average grayscale values of each hemisphere, with midsagittal and parasagittal elements overlapped onto the same plane. MRI results demonstrated that eye position in adult humans varies most with regard to its horizontal distance from the temporal lobes and, secondly, in its vertical distance from the frontal lobes. Size was mainly found to covary with the distance between the eye and temporal lobes. Proximity to these cerebral lobes may generate spatial constraints, as some ocular deformation was observed. Considering the CT analysis, modern humans vary most with regard to the orientation of the orbits, while interspecific variation is mainly associated with separation between the orbits and endocranial elements. These findings suggest that size and position of the frontal and temporal lobes can affect eye and orbit morphology, though potential effects on eye shape require further study. In particular, possible effects of these spatial and allometric relationships on the eye and vision should be examined using ontogenetic samples, vision parameters such as refractive error in diopters, and three-dimensional approaches that include measures of extraocular soft tissues within the orbit.

Key words: eyeball; frontal lobes; functional craniology; geometric morphometrics; orbits; temporal lobes.

Introduction

The unique craniofacial configuration of modern humans with a globular vault and reduced facial block (Lieberman et al. 2002) places the orbits directly below and anterior to the frontal and temporal lobes, respectively. This anatomical proximity involves structural and functional interactions between facial and neurocranial elements during developmental and evolutionary morphogenesis (Moss & Young, 1960; Bruner, 2007). In other words, spatial and volumetric reorganization of the frontal and temporal lobes may induce changes in the orbital region, given that integration between the brain and face is mediated by the lateral cranial base (Lieberman et al. 2000; Bastir & Rosas, 2006; Bruner & Ripani, 2008; Neaux et al. 2013a), and because changes in facial morphology are associated with basicranial variation. Furthermore, the anterior cranial base and the orbits are structurally aligned with the mandibular ramus, and rotate as an entire anatomical block during growth and development (Lieberman et al. 2000; McCarthy & Lieberman, 2001). According to Bastir & Rosas (2016), facial rotation is associated with an elongation of lateral cranial base structures and a change in their overall orientation, while facial reduction and retraction are related to the position of the sphenoid wings relative to that of the sphenoid body.

Correspondence
Ana Sofia Pereira-Pedro, Centro Nacional de Investigación sobre la Evolución Humana, Paseo Sierra de Atapuerca 3, 09002, Burgos, Spain. E: sofia.aspp@gmail.com

Accepted for publication *13 August 2017*

Compared with Neanderthals and Middle Pleistocene humans, modern humans have smaller, narrower and vertically shorter faces that are flatter and more retracted (Bastir & Rosas, 2016). It remains to be established whether modern human facial morphology is derived, or rather, is a primitive condition (Arsuaga et al. 1999; Bermúdez de Castro et al. 2010; Freidline et al. 2013; Lacruz et al. 2015; Stringer, 2016). Nonetheless, this unique morphological configuration, characterized by reduced facial block and expanded braincase, is highly specific to our species.

The frontal lobes of modern humans underwent an enlargement, which is proportional to the general increase in brain size according to the scaling rules of apes (Semendeferi et al. 1997; Semendeferi & Damasio, 2000). However, at least in modern humans and Neanderthals, there was a change in frontal proportions, in which the frontal lobes became wider relative to more archaic hominids (Bruner & Holloway, 2010). Such lateral redistribution of the cortical mass can be a morphogenetic consequence of vertical constraints imposed by the superposition of the brain and orbits (Bruner, 2004).

Considering the temporal lobes, these are larger than expected in humans, both in terms of absolute and relative volume (Rilling & Seligman, 2002). The middle cranial fossae that house the temporal lobes are also wider (Lieberman et al. 2002) and more axially elongated (Bastir et al. 2008) in modern humans compared with other human species. This antero-posterior elongation has displaced the temporal poles into a more anterior position relative to the optic canal (Bastir et al. 2008), which taken together, may have influenced the rotation and positioning of facial structures (Lieberman et al. 2000, 2002).

As a developmentally connected part of the facial skeleton (Waitzman et al. 1992), the orbits follow the same evolutionary trends as the face. Though by contrast, the eye is dimensionally (Scammon & Armstrong, 1925) and genetically (Mak et al. 2006) associated with the brain. Nonetheless, there is a strong correlation between the size of the orbital aperture and the transverse diameter of the eye among primates. However, this relationship differs between suborders, as there is a greater disparity between the two measures in haplorhines, where larger-sized anthropoids exhibit larger eye diameters relative to orbital aperture size (Kirk, 2006). Orbital aperture size is also related to activity pattern in primates, in which nocturnal species generally have larger orbital apertures, despite similar eye sizes between diurnal and nocturnal primates (Kirk, 2006). Instead, orbital aperture size might be more associated with variation in eye shape, i.e. size of the cornea relative to size of the eye (Kirk, 2006; Ross & Kirk, 2007). For instance, nocturnal primates have larger corneal diameters relative to the transverse diameter of the eye and its focal length, while diurnal primates, and especially anthropoids, have smaller corneas relative to eye size (Kirk, 2004; Ross & Kirk, 2007), indicating that the relationship between eye and orbit size depends on both primate phylogeny and activity pattern.

In terms of volume, according to Schultz (1940), size of the eye does not directly determine size of the orbit, as both have different but somewhat complimentary patterns of morphogenesis during ontogeny. Additionally, both the eye and orbit have an opposite allometric relationship to body size, in which larger-bodied primates have proportionately small eyes in relatively large orbits, while smaller primates have eyes that occupy a larger proportion of the orbital cavity by comparison. In spite of this general allometric pattern, humans have a larger eye to orbit ratio than what would be expected of a primate of our body size. For example, the eye occupies about 32% of orbital volume in adult male humans, but only about 21% of orbital volume in adult male chimpanzees; and this dichotomy exists in light of the fact that chimp eye volume can occasionally reach values similar to that of humans (Schultz, 1940).

Thus, the structural relationship between the eye and adjacent anatomical elements must be different in humans and chimpanzees, which is particularly evident from looking at the spatial relationship among the orbit, ocular tissues, facial, neurocranial and cerebral structures in the sagittal profile of these two species (Fig. 1). Compared with modern humans, chimps exhibit more separation between ocular and neural tissues, with eyes that occupy a smaller proportion of orbital volume, and which reside in a far more anterior and superior position relative to the brain, and to the frontal lobes in particular. Moreover, in chimps and gorillas the orbital roof is primarily made up of the browridge, and its antero-posterior development is negatively correlated with the neuro-orbital angle, or the angle between the orbital axis and the anterior cranial vault (Ravosa, 1991). By contrast, in modern humans this feature has largely disappeared (Moss & Young, 1960), and the orbital roof consists of only a thin sliver of bone separating highly adjacent ocular and cerebral tissues. In fact, the thinnest portion of the anterior cranial fossa – averaging between 0.66 and 1.13 mm in adult humans – resides in this area of the orbital roof directly above the eyes (Lang, 2012). This extremely thin portion of the anterior cranial base, which occasionally shows patches of rarefaction and entire gaps in the bone, must now provide support for both intraorbital soft tissues and the wider and more anteriorly located frontal lobes of modern humans. By comparison, archaic humans such as *H. ergaster/erectus* maintained a more ape-like configuration, with greater separation between facial structures and the braincase. However, because the orbits have become situated directly beneath the anterior cranial fossae in modern humans and Neanderthals, we might expect a more direct interaction between the neural and ocular tissues in these two species (Bruner et al. 2014).

Masters (2012) hypothesized that the location of the prefrontal cortex directly above, and the reduced and retracted facial anatomy directly below the orbits in modern humans

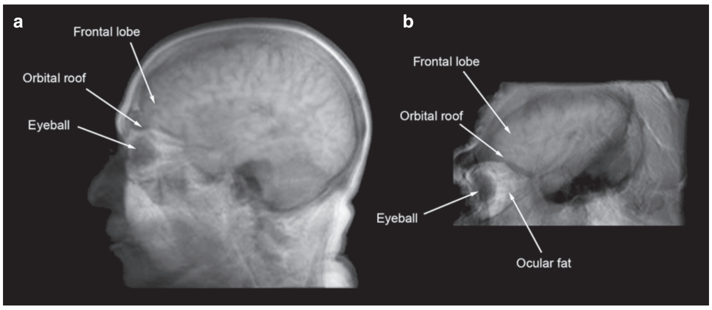

Fig. 1 Comparison between modern human (a) and chimpanzee (b), regarding the anatomical relationship between the eyeball and the frontal and temporal lobes, as seen in the lateral scout view of the sagittal and parasagittal scans (see Materials and methods).

could result in spatial conflicts among cerebral, ocular and craniofacial structures. In this way, the coalescence of neuro and viscerocranial components during recent hominid evolution may act to constrain development of the orbit and internal ocular tissues during ontogeny, and potentially lead to deformation of the eye, and consequent visual defects such as juvenile-onset myopia. Supero-inferior pressure resulting from structural constraints imposed by the frontal lobes above, and a more anterior projection of the temporal lobes behind the orbits (Bastir et al. 2008), would be expected to cause ocular distortion, and specifically axial elongation of the eye, as it shifts more toward the narrowing concave rim of the anterior orbital margins in recent human evolution (Bruner et al. 2014). The disparate impact of these changes would also be expected to vary with population-specific craniofacial variation, and particularly among certain Far East populations, where the orbits have increased in height, but have decreased in width and overall volume since the Holocene in this region (Brown & Maeda, 2004; Wu et al. 2007).

Masters et al. (2015) analyzed the relationship among eye, orbit, and frontal and occipital lobe volumes, and found that ocular and orbital volumes are slightly more associated with frontal lobe volumes than with those of the visual cortex of the occipital lobes. This indicates that ocular and orbital sizes might be more reflective of the structural constraints imposed by the frontal lobe than of the functional demands of the visual system. The study also showed that the correlation between ocular and orbital volume is low, which corroborates the results of previous research demonstrating independent ontogenetic growth trajectories in these structures (Schultz, 1940; Todd et al. 1940; Weale, 1982; Waitzman et al. 1992; Hoyte, 1997), and that orbital size is largely independent of eye size in humans, regardless of how large the myopic eye grows within it (Chau et al. 2004; Masters, 2012).

Ocular growth can induce morphological changes on immature osseous aspects of the orbit during prenatal and early postnatal ontogeny (Wagner et al. 2000). However, recent research shows that following the first year of postnatal life, and as the various anatomical components comprising the orbit begin to ossify, no significant change is observable in size or shape of the orbital aperture (Barbeito-Andrés et al. 2016). In fact, during later stages of postnatal development, when the eye continues to grow rapidly but after the orbit has already ossified, the effects of added ocular growth on orbital size are negligible (Washburn & Detwiler, 1943; Hoyte, 1997). This is further indicated by research showing that a 15% reduction in size of the orbital aperture occurs in children enucleated prior to the age of 5 years, but that enucleation produces no appreciable change in this feature at 9 years of age and older (Taylor, 1939).

As a result of this disconnect between ocular and orbital size following the early stages of postnatal life, a disproportionate enlargement of the eyeball – rather than increasing orbital size – may result in its compression against adjacent soft-tissues circumscribed by the orbital walls. Additionally, because of the shape of the orbit and constraints imposed by cerebral, neurocranial and viscerocranial structures around it, added ocular growth would be expected to result in distortion toward the same eye form common among myopes (Masters et al. 2015), which is generally an overly large and axially elongated eye with a steeper cornea and, subsequently, a higher axial length/corneal radius of curvature ratio relative to emmetropes (Grosvenor & Goss, 1998; Lam et al. 1999, 2008; Atchison et al. 2004; Llorente et al. 2004; Stone & Flitcroft, 2004; Dirani et al. 2006; Ip et al. 2007; Foo et al. 2016).

In the current study, we use geometric morphometrics analysis to investigate the relationship among these cerebral, neurocranial and visual components of the skull, examining variation in orbital and ocular anatomy relative to the size and spatial position of the anterior frontal and temporal areas. This research consists of two parts; firstly we assess the spatial relationship between the eye and brain in a sample of magnetic resonance imaging (MRI) taken from adult modern humans and, secondly, we examine the relationship between the orbit and braincase using computed tomography (CT) of adult modern humans and fossil hominid specimens. The principal aim of this research is to evaluate whether spatial variation of the frontal and temporal lobes may constrain the orbital area and, in the case of modern humans, if these patterns of cerebral and craniofacial variation are associated with size and anatomical position of the eye.

Materials and methods

MRI sample

The adult modern human MRI sample comprises 63 individuals (36 female, 27 male), with ages ranging from 19 to 80 years (mean age 45 ± 15 years). The voxel size for each image is isometric and measures 1.0 × 1.0 × 1.0 mm. These MR images were obtained as part of the International Consortium for Brain Mapping (ICBM) (Mazziotta et al. 2001), and were provided by the Laboratory of Neuro Imaging (LONI) at the University of Southern California.

Using this MRI sample, relationships among orbital, ocular and fronto-temporal profiles were examined in two-dimensions (2D) as seen in the sagittal plane. Sagittal spatial organization is relevant to evaluate interactions between vertical (frontal lobes/orbits) and longitudinal (temporal lobes/orbits) features. Lateral scout views were created by overlapping the midsagittal and parasagittal elements through projection of the average intensity of the whole-stack grayscale values onto the same 2D plane. Two images representing each cerebral hemisphere were generated for each subject and were used to sample a set of 17 landmarks and semi-landmarks (Fig. 2a), which capture the outline of the eye, frontal lobe, anterior fossa (AF)/orbital roof and the position of the temporal tips (anterior-most point of the temporal lobes, *sensu* Bastir et al. 2008).

The landmark configuration was then analyzed using geometric morphometrics (Bookstein, 1991; Zelditch et al. 2004), carried out by first superimposing this landmark configuration to the same location, scale and orientation by Procrustes registration, which minimizes the distance between corresponding landmarks. The resulting shape coordinates were then analyzed using principal component analysis (PCA) in order to examine patterns of shape variation. Independent PCA on right and left sides were strongly correlated ($R = 0.88$, 0.85, 0.90 for PC1, PC2 and PC3, respectively), so the two sides were averaged and the final PCA was computed on the individual mean shape.

To investigate the correlation between shape and size, total shape and each significant PC were regressed against cortical volume of the frontal and temporal lobes, the ratio of frontal and temporal lobe volumes (F/T) and centroid size (CS). Results were considered significant at the 5% level. These cerebral lobe volumes had been previously generated (Masters et al. 2015) with LONI Brain Parser 56 ROI (Tu et al. 2008), which uses a pipeline workflow with automatic segmentation based on standard parcellation schemes (Dinov et al. 2009).

CT sample

The CT sample consists of 30 scans of adult modern humans of both sexes (15 females and 15 males) and distinct geographical origins (resolution between 0.214 and 0.700 mm), three adult chimpanzee specimens (voxel size 0.488 × 0.488 × 0.625 mm), and fossil specimens, which include Bodo [estimated age 600 thousand years (ka); Middle Awash, Ethiopia; voxel size 0.49023 × 0.49023 × 1.0 mm], Broken Hill 1 (estimated age 300–125 ka; Kabwe, Zambia; isometric voxel 0.7 × 0.7 × 0.7 mm) and Gibraltar 1 (estimated age 70–45 ka; Forbes Quarry, Gibraltar; isometric voxel 1.0 × 1.0 × 1.0 mm). Bodo and Broken Hill 1 are generally attributed to *H. heidelbergensis/rhodesiensis*, and Gibraltar 1 to *H. neanderthalensis*. With the exception of Bodo, which was acquired from the University of Vienna, the remaining specimens were obtained from the NESPOS database (Neanderthal Museum, Mettmann, Germany).

The CT sample was analyzed with the same procedure used for the MRI sample, which involved using lateral scout views in 2D, after projection of the average grayscale values of each hemisphere. The landmark set was comparable to that of the MRI sample, and comprised 11 landmarks capturing the lateral profile of the orbits, the frontal pole of the endocranial cavity and the anterior-most point of the temporal tips (Fig. 2b). Left and right sides for each individual were sampled separately (with the exception of Bodo, which retained only one complete orbit), and the two hemispheres were averaged together for the final analysis.

A first PCA was conducted on the modern human sample to assess within-species variation, and a second PCA was computed, which included the chimpanzee and fossil human specimens, in order to evaluate principal phylogenetic differences among them. Because the frontal bone of Gibraltar 1 is broken it could not be included in this broader analysis. However, given that its orbits are complete it was possible to carry out a thin-plate spline comparison using only landmarks on the orbital region. This analysis allows for visualization of major shape changes through a pairwise comparison in cases of reduced sample size. The average shape of each species was also contrasted with the average of modern humans using pairwise comparisons, and Gibraltar 1 was further examined in a pairwise comparison with the average shape of *H. heidelbergensis*, a phylogenetically closer species. For both the MRI and CT samples, 2D images were generated with IMAGEJ 1.48v (Schneider et al. 2012), the landmarks were digitized on tpsDig2 (Rohlf, 2013), and the geometric morphometrics analysis was performed on MORPHOJ (Klingenberg, 2011) and PAST 2.17c (Hammer et al. 2001).

Results

MRI shape analysis

According to the PCA (Fig. 3a–f), the first four components explain 77% of the total variance, while the subsequent PCs are below the threshold for random variation. PC1 (Fig. 3c) accounts for 30% of the variance and is associated with a retraction/projection of the eye relative to the temporal pole. PC2 (19% of variation; Fig. 3d) describes vertical separation/proximity of the eye and the AF. In PC1 and PC2, increased ocular protrusion is apparently associated with a rounder eyeball, while eyes that are closer to the temporal pole (PC1) or to the AF (PC2) are somewhat shorter horizontally and more vertically elongated. PC3 (18%; Fig. 3e) describes the dimensions and spatial relationship between the eye and AF, in which an antero-posteriorly elongated AF is associated with larger eyes, that are also closer to the orbital roof. PC4 (10%; Fig. 3f) illustrates dolichocephaly-brachycephaly neurocranial proportions, with the former

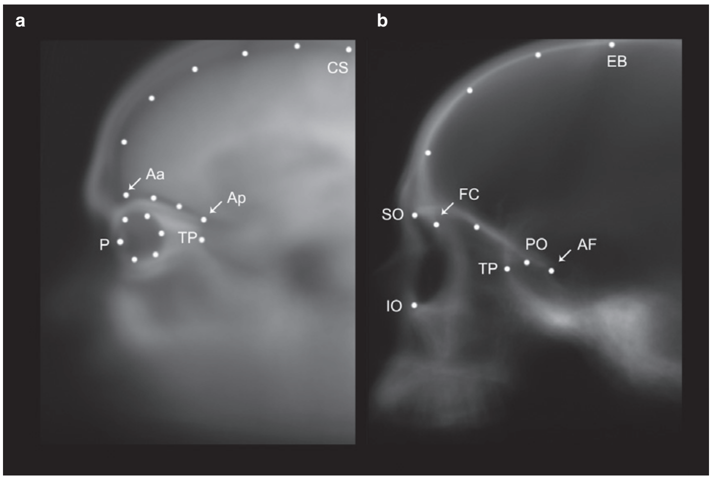

Fig. 2 Landmark set chosen to sample fronto-orbital morphology on the magnetic resonance imaging (MRI) sample (a), and on the computed tomography (CT) sample (b). On the MRI sample landmarks are: central sulcus (CS); anterior point of the anterior fossa (Aa); posterior point of the anterior fossa (Ap); pupil (P); temporal pole (TP); and 12 equidistant semi-landmarks sampling the curvature of the frontal profile, anterior fossa and eye. The landmarks on the CT sample are: endobregma (EB); foramen caecum (FC); posterior end of the anterior fossa (AF); temporal pole (TP); superior (SO) and inferior (IO) orbit aperture; posterior orbital (PO) point on the aperture of the optic nerve canal; and 3 and 1 equidistant semi-landmarks sampling the curvature of the frontal profile and orbital roof, respectively.

morphotype associated with a larger eyeball, and increased distance between the eye and temporal pole. PC1 and PC4, despite describing distinct shape changes, mainly denote the horizontal distance between the eye and temporal lobes, while PC2 and PC3 describe similar changes related to the vertical distance between the eye and the AF/orbital roof. A discriminant analysis reveals that no significant differences exist between males and females with regard to shape variation.

Cortical volume of the frontal and temporal lobes are correlated (Pearson's $R = 0.78$, $P < 0.001$), and both lobe volumes are positively correlated with CS (frontal: $R = 0.76$; $P < 0.001$; temporal: $R = 0.66$; $P < 0.001$), though the relationship with the frontal lobe is stronger, as this region is more represented in the landmark set. Additionally, males are larger than females across all metrics considered in this analysis (*t*-test, $P < 0.001$). Table 1 shows results from the regression of shape variables with CS and cortical volumes, and indicates that the three size measures are significantly correlated with whole shape changes, but that they explain a rather low percentage of the total variation (CS: 8%; frontal volume: 8%; temporal volume: 7%). Considering the correlation between size and shape, it can be seen that CS is associated with a bulging frontal profile, and a smaller, vertically shorter eyeball that is more separated from the anterior part of the AF (Fig. 3g). Regarding each of the principal components individually, CS is correlated with PC2 ($R^2 = 0.14$) and PC3 ($R^2 = 0.11$), denoting further separation of the eye from the AF in larger individuals. An increase in cortical volume of the frontal and temporal lobes is associated with a bulging of the frontal profile, as well as smaller eyes that reside closer to the temporal poles (Fig. 3h,i). These shape changes are reflected in the correlation of both lobes with PC1 (frontal: $R^2 = 0.19$; temporal: $R^2 = 0.15$) and in the correlation of frontal volume with PC2 ($R^2 = 0.08$). The ratio frontal/temporal (Fig. 3j) explains only 3% of whole shape variation, and is mostly associated with a dolichocephalic morphology in individuals with much larger frontals relative to their temporal lobe volumes. The ratio of F/T is not significantly correlated with any PC.

CT shape analysis

When considering modern humans only, the first four PCs are above the threshold of random variation, and together they explain 75% of the total variance (Fig. 4). PC1 (34% of the total variance; Fig. 4c) distinctively characterizes the morphospace, describing the orientation/inclination of the orbits relative to the frontal profile; PC2 (17%; Fig. 4d) regards the antero-posterior size of the orbit, which is shorter in individuals with a bulging superior portion of the frontal profile; PC3 (14%; Fig. 4e) deals with alignment between the orbital margins and the bulging of the anterior portion of the frontal profile; and PC4 (10%; Fig. 4f) with supero-inferior (vertical) proportions of the orbital aperture.

After including chimpanzees and the two *H. heidelbergensis* specimens in the sample, PC1 (70%), which clearly

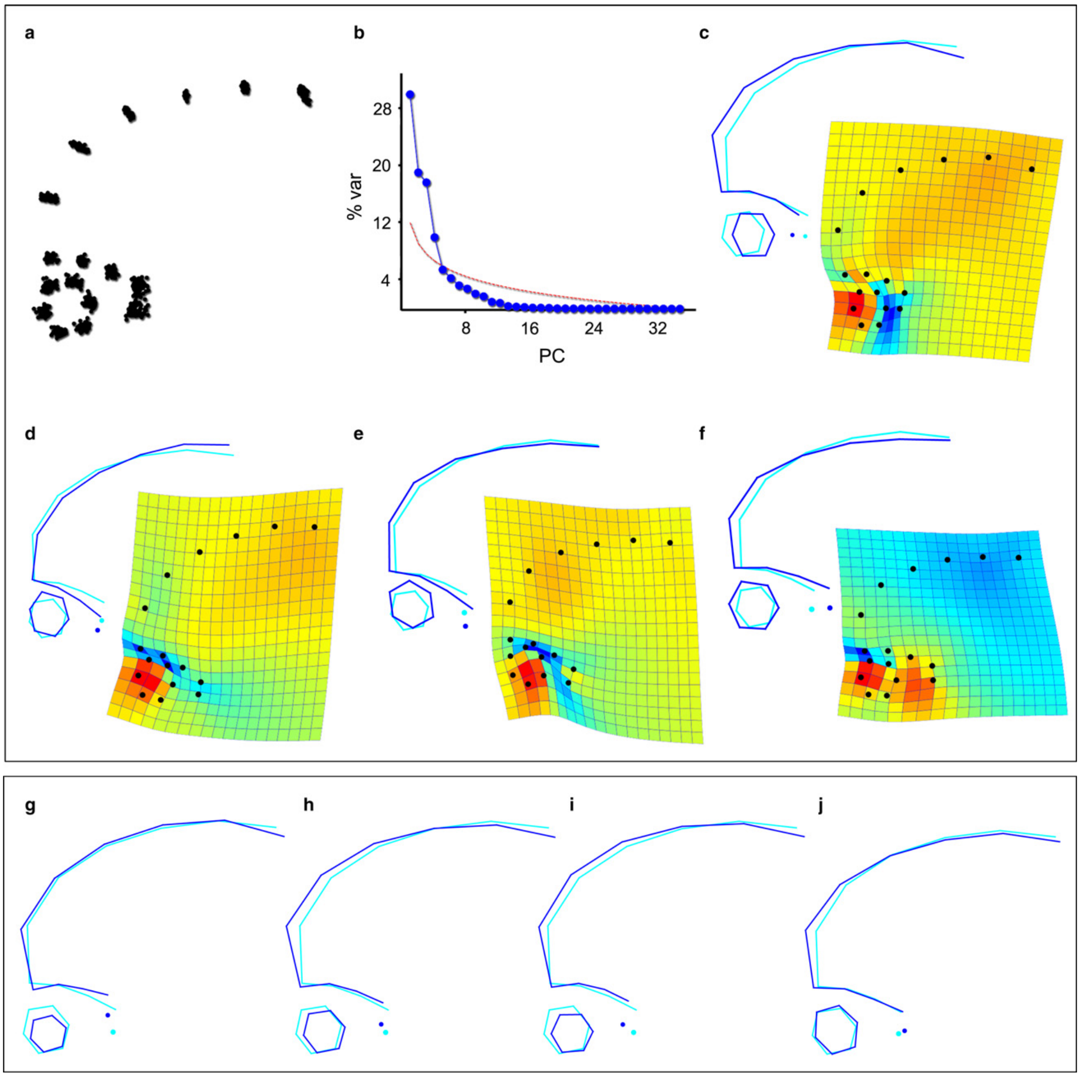

Fig. 3 Shape variation within modern humans according to the magnetic resonance imaging (MRI) sample (a–f) and regression with size variables (g–j). After Procrustes superimposition, the distance between correspondent landmarks is the difference in shape (a), and the principal component analysis (PCA) (b–f) shows the main vectors of shape changes. The first four principal components (PCs) are above the standard threshold of statistical significance (b, red line), while the subsequent PCs account for < 6% of variance. PC1 (c: 30%) is associated with the spatial relationship between the eye and the temporal pole; PC2 (d: 19%) and PC3 (e: 18%) describe the distance between the eye and the fossa; and PC4 (f: 10%) deals with the antero-posterior dimensions of the entire structure. Increasing CS (g) is associated with greater separation between the AF and eye, and a decrease in eye size. Increasing cortical volume of the frontal (h) and temporal (i) lobes is associated with a bulging frontal and a slight decrease in eye size, separation from the anterior fossa (AF), but closer proximity to the temporal pole. Lastly, an increase in the F/T ratio (j) is primarily associated with a bulging of the frontal profile.

separates the three species based on length and height of the orbits, is the only vector representing significant shape changes (Fig. 5). Most notably, chimpanzees have far more protruding orbits that are located anterior and superior to the temporal tips. By contrast, the temporal poles of modern humans are closer to the orbits, and are situated in a more superior position relative to the optic canal, while the orbits themselves are antero-posteriorly shorter and are tucked up under the frontal region. The two *H. heidelbergensis* specimens exhibit a morphology that falls halfway between that of modern humans and the chimpanzee. Shape variation described by PC2 (10%) is similar to that of

Table 1 Correlation of the whole shape and significant PCs (1–4) with Centroid size, frontal and temporal volumes, and the ratio of frontal to temporal volume.

	Centroid size		Frontal volume		Temporal volume		Ratio F/T	
	% predicted	*P*-value	% predicted	*P*-value	% predicted	*P*-value	% predicted	*P*-value
Whole shape	7.83	*< 0.0001*	8.19	*0.0002*	6.52	*0.0005*	3.31	0.052
PC1	5.07	0.080	19.2	*0.0006*	14.94	*0.002*	1.73	0.306
PC2	13.95	*0.003*	8.16	*0.025*	2.41	0.221	4.48	0.094
PC3	10.54	*0.010*	0.73	0.511	5.77	0.058	4.58	0.093
PC4	5.25	0.078	0.15	0.766	0.55	0.560	3.55	0.140

P-values in italics indicate statistical significance (*P*<0.05).

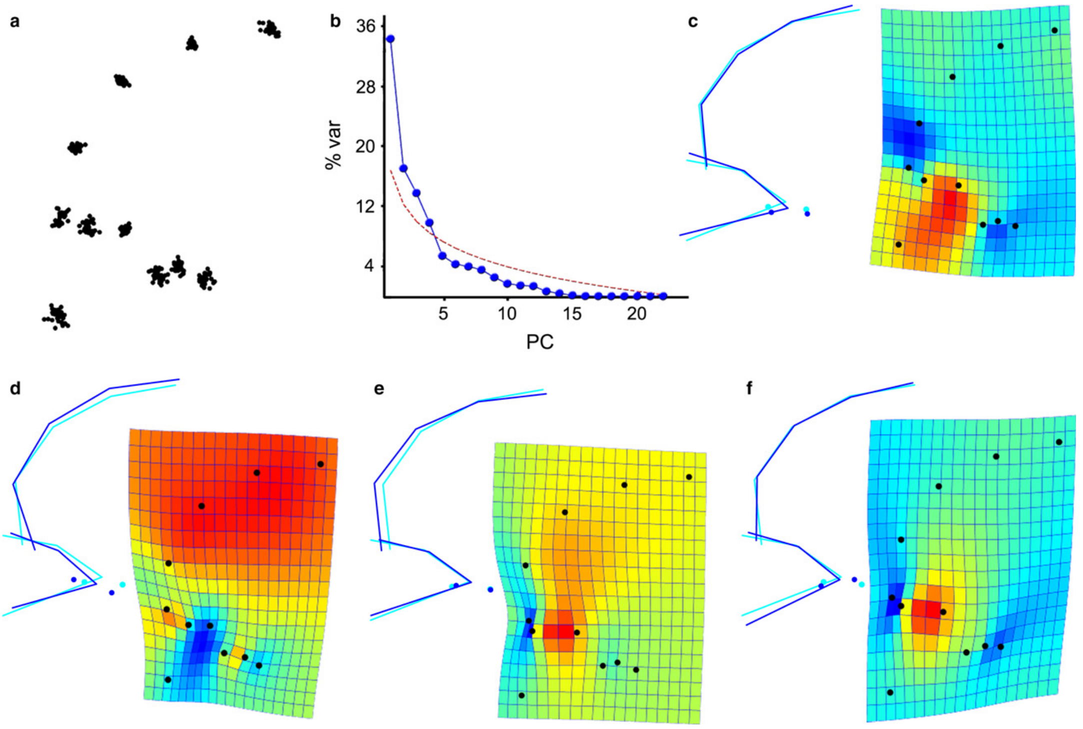

Fig. 4 Shape variation within modern humans according to the landmark configuration applied to the computed tomography (CT) sample (a). The majority of variation is explained by the first four vectors (b). Principal component (PC)1 (c: 34%) is associated with orientation of the orbit relative to the frontal profile; PC2 (d: 17%) describes anteroposterior size of the orbit and bulging of the frontal profile; PC3 (e: 14%) is associated with alignment of the superior orbital margin with the frontal profile; and PC4 (f: 10%) deals with alignment of the orbit with the frontal, and the vertical and horizontal proportions of the orbit.

PC1 in modern humans, in that it is mainly associated with orientation of the orbits. It primarily describes variation within modern humans, with chimps falling close to the mean modern human shape. However, the fossils (and especially Broken Hill 1) can be seen to display more inferiorly oriented orbits by comparison.

Pairwise comparisons of average orbital shape between these species demonstrate differences similar to the variation described by PC1 (Fig. 6). For instance, compared with chimpanzees and *H. heidelbergensis*, modern humans have anteroposteriorly shorter orbits, with superior margins closer to the *foramen caecum*, and a temporal pole that

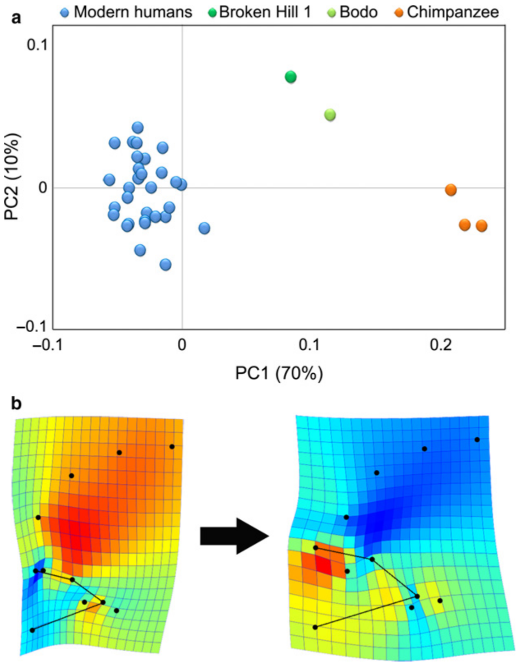

Fig. 5 Shape variation within the whole computed tomography (CT) sample. When introducing the fossil human and chimpanzee specimens, two principal components (PCs) explain the largest percentage of variation (a). PC1 is the main vector of variation, describing the dimensions of the orbit and its alignment with the frontal profile (b).

projects more forward relative to the posterior orbit. As expected, these shape changes are more overt between modern humans and chimpanzees. However, the same general shape pattern is also observable when comparing modern humans with Gibraltar 1, albeit to a somewhat lesser extent. In turn, Gibraltar 1 differs from the average of Bodo and Broken Hill 1 by having a more anteriorly situated temporal pole and a *foramen caecum* in a different position relative to the orbital roof, suggesting that Neanderthal orbital morphology may be intermediate between that of modern humans and *H. heidelbergensis*.

Discussion

The orbits and eyes of modern humans are located directly below the frontal lobes and anterior to the temporal lobes, which together with facial reduction and retraction, has been suggested as a factor contributing to improper ocular development and the potential generation or amplification of vision problems, as a result of competition among structural and functional features in this confined region of the human skull (Masters, 2012). In the present study, we describe variation in the orbit and eye relative to the spatial position of the frontal and temporal lobes among adult modern humans as seen in the sagittal scout view, using both MRI and CT data. The MRI sample allows the inclusion of the eye in this morphological analysis, while the CT analysis allows for the inclusion of human fossils and chimpanzees, which can aid in inferring evolutionary trends with regard to human fronto-orbital spatial organization.

Brain-eye spatial relationship

The main pattern of morphological variation in adult humans is associated with the antero-posterior (horizontal) position of the eye relative to the temporal lobes. Individuals with a greater distance between the eyes and temporal tips tend to have apparently rounder eyes, which are more anteriorly projected beyond the frontal profile (protrusion). Conversely, in individuals with more posteriorly located eyes, the space between the eye and temporal poles is reduced, and the frontal outline is more curved. In this case, a possible constraint is associated with spatial reduction between the eye and middle cranial fossa, which may actually involve an antero-posterior compression of the eye, as it appears taller and shorter when positioned nearer to the temporal tips.

The successive component of variation is due to the supero-inferior (vertical) position of the eye relatively to the frontal lobes. This vertical change is associated with the second and third PCs, which are rather similar in terms of variance explained, involving changes in eye shape and size, respectively. Also in this case, the distance between the eye and the frontal lobes matches minor changes in ocular form. Thus, this analysis has succeeded in separating the two main morphological factors, namely the distance between the eye and the middle fossa, and the distance between the eye and the anterior fossa, and suggests that both patterns of variation are associated with minor changes in the geometry of the eye. The fact that the distance from the temporal lobes represents the main morphological axis of variation may be the result of less stringent constraints in this direction, given that the orbital margins represent the only opening of the orbital cavity. In fact, in terms of structure and development, horizontal changes in the position of the eye are mainly restricted by the posterior limit with the temporal lobes, while vertical changes are limited by the frontal lobes above, and the middle face below.

Frontal and temporal lobe volumes are correlated, which is in agreement with Allen et al. (2002), who found a significant high correlation between the volumes of these districts (left: 0.8; right: 0.7). Indeed, our results show that the regression of both lobe volumes against shape gives the same outcome, explaining about 7–8% of the variation (15–19% when considering only the first PC). With increased 'fronto-temporal' size, the eye is positioned more posteriorly, nearer to the temporal lobe, which could involve some spatial conflicts. In this case, the position of the eye, but not

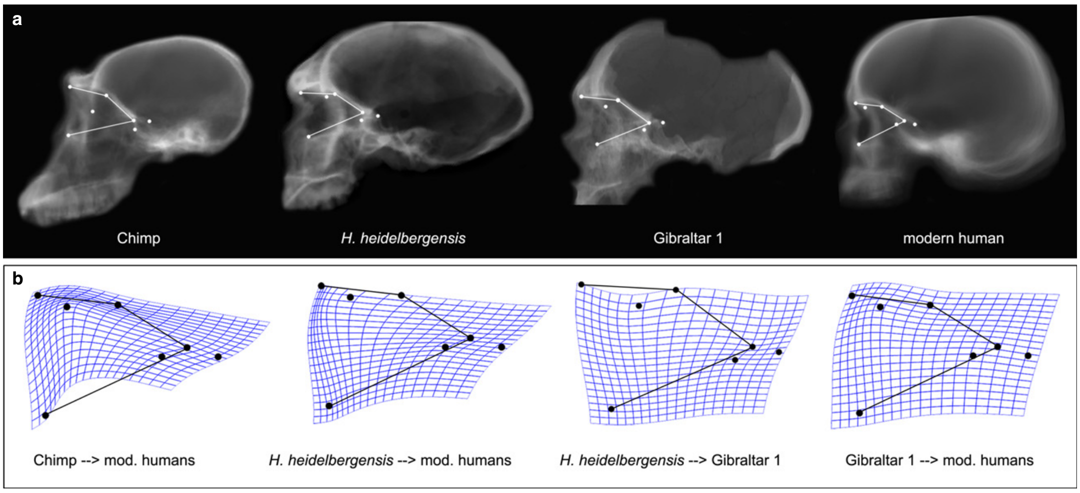

Fig. 6 Between-species comparisons of average orbital shape. Upper row (a), from left to right: average orbital contour of chimpanzees, *H. heidelbergensis*, Gibraltar 1 representing *H. neanderthalensis*, and modern humans. Lower row (b): thin-plate spline deformation grids of the species average deformed into modern humans (the first three) and of modern humans' average deformed into Gibraltar 1.

its general shape, seems to vary with size of the fronto-temporal lobes. These results only partially support Masters' (2012) hypothesis, in that size and position of the frontal and temporal lobes may restrain size and position of the eye in modern humans, eventually leading to certain visual defects.

Myopic eyes tend to be larger and more axially elongated than emmetropic eyes (Atchison et al. 2004; Stone & Flitcroft, 2004; Goldschmidt & Fledelius, 2011), and it is well-established that loss of vision occurs as a result of these changes to ocular size and shape in association with the development of myopic refractive error in humans (Holladay et al. 1991; Zhao et al. 2000; He et al. 2004; Remón et al. 2006). In the current study, we found that the distance between the eye and these cerebral lobes is associated with changes in eye form, but the size of the lobes is only associated with ocular proximity/distance, and does not involve any deformation of the eye outline. Hence, although brain size has an effect on eye position, it is not sufficient in and of itself to induce ocular deformation. We must also assume that the distance between the eye and brain depends upon additional factors other than brain size, which can induce antero-posterior flattening of the eyeball when it approaches the braincase. Even so, it must be taken into account that myopic eyes are neither exclusively nor always elongated (Chau et al. 2004; Stone & Flitcroft, 2004; Guo et al. 2017) and, even when they are, this axial elongation may not always be detectable, and particularly in individuals with lower levels of refractive error (Cheng et al. 1992; Palmowski-Wolfe et al. 2009).

Eye form is likely more associated with cranial architecture than with brain size. For example, our data suggest that antero-posterior elongation and outward projection of the eyeball may be associated with flatter frontal curvature, that is, with a more dolichocephalic cranial morphology. The normal range of ocular protrusion can vary with multiple factors, such as the depth of the orbital floor (Migliori & Gladstone, 1984), or the proportion of extraocular fat within the orbit (Peyster et al. 1986). Moreover, ocular protrusion is inversely correlated with orbital capacity, i.e. volume of the orbit minus volume of the eye (Detorakis et al. 2010), meaning that relative to eye size, reduced space within smaller orbits contributes to greater ocular protrusion. Considering that variation in frontal and temporal cortical volume explains $<$ 20% of the variation in eye size and position, one might expect that variation in size, shape and relative position of the orbital contents are also important to consider.

There are further factors that could have influenced our results, such as intra-individual variation and age for example. Various studies have shown that ocular dimensions conform to a regular diurnal rhythm synchronized to the external light/dark cycle (Read et al. 2008; Chakraborty et al. 2011; Nickla, 2013; Stone et al. 2013) and, as such, images might display distinct peaks of axial eye length depending upon the time of the day the images were recorded. Also, our sample includes a broad range of age groups, introducing senescence as a further factor (i.e. orbicularis muscle laxity, changes in fat position, atrophy, etc.) that may perhaps influence certain morphological variables (Berger & Kahn, 2012). Although our results showed no significant correlation between shape changes and age, further analyses on specific age ranges may add to subsequent studies. In addition, it is recommended that future research examining cerebral/craniofacial anatomy and the form and function of the eye also include individuals with high myopia, use Standard Error of Refraction as a measure of reduced visual acuity, and investigate spatial and volumetric relationships using a three-dimensional approach that also includes measures of extraocular soft tissues within the orbit.

Braincase-orbit spatial relationship

The orbital and fronto-temporal morphology of modern humans as captured in the CT sample mainly varies with regard to the orientation of the orbits. Subsequent shape changes concern the position of the orbit relative to the frontal profile, orbital axial proportions, and changes in size of the orbital aperture. Although we attempted to sample corresponding regions in both the MRI and CT samples, the landmark sets are inherently different, and thus describe different shape changes. More specifically, the MRI sample primarily describes changes in the relationship among soft tissue components of the upper skull, while results from the CT analysis mostly describe changes in craniofacial-braincase morphology. For instance, the frontal profile is more posteriorly extended in the MRI sample than in the CT sample, as its posterior limit is marked by the central sulcus in the former, and by endobregma in the latter, which are two landmarks that have previously been shown to deviate from each other by about 57.9 ± 6.8 mm (Bruner et al. 2015). Similarly, the roof of the orbit differs in the two samples, with the antero-posterior extension of the orbital roof being captured only on the CT sample. Hence, variation in modern humans is mostly determined by the position of the eye in the MR images, and by the orientation of the orbits in the CT scans. Nonetheless, some comparable changes are observable. For instance, it is possible that shape changes describing the spatial relationship between the eye and the orbital roof in the MRI analysis also depict variation in orbital orientation as observed in the CT analysis. Moreover, variation in the space between the eye and frontal lobe may be related to height of the orbit, although it must be taken into account that this is a secondary variation in the CT sample.

Differences in the orientation of the orbits might be associated with dolichocephalic/brachycephalic proportions. Analyzing integration between the face and lateral basicranium in the sagittal view, Bastir & Rosas (2006) separated two main patterns related to height of the face. More specifically, they discriminated between vertically longer (taller) and antero-posteriorly shorter faces with shallower cranial bases (middle cranial fossae), from vertically shorter but antero-posteriorly stretched faces associated with deeper cranial bases. This study revealed that in individuals with taller faces, the orbital roof also appeared antero-posteriorly shorter, and the authors attributed this retraction of the orbits to an upward rotation of the anterior cranial base (Bastir & Rosas, 2006). Orientation of the orbits is strongly associated with orientation of the anterior cranial base and, together, these form an angle with the posterior maxillary plane that is close to 90° (McCarthy & Lieberman, 2001). In turn, the mandibular ramus is vertically aligned with the middle cranial fossae (Bastir et al. 2004; Bastir & Rosas, 2005), and integration among each of these structures – which in our study is indicated by somewhat coordinated variation among the orbital landmarks, the temporal pole and the posterior limit of the AF– causes the face to rotate as an entire block relative to the posterior cranial base, which acts to influence overall craniofacial shape (McCarthy & Lieberman, 2001; Neaux et al. 2013b).

Within adult modern humans, size of the parietal bones is a major source of variability, and larger parietal bones are associated with a forward rotation of the cranial base and facial block (Bruner et al. 2017), which influences the functional axis of the head. This is in agreement with our main morphological vector of variation concerning orientation of the orbits. If these two studies are referring to the same process, they suggest that when the parietal bones are larger the facial block is more ventrally flexed, and the orbits undergo a corresponding adjustment. On the other hand, the frontal profile was found to be rather invariable in its shape, and variation observed in its lower limit might be due to variability in the morphology of *crista galli*, influencing the location of the *foramen caecum* (Moss, 1963).

Regarding the inter-specific analysis, differences between modern humans and the other species considered did not follow the main pattern of intra-specific variation seen in the former, but rather, it largely centered on separation between the orbits and braincase. For instance, when compared with more archaic humans and chimpanzees, modern humans display a specific cranial architecture, in which the orbits are positioned directly below the frontal lobes (Bruner & Holloway, 2010) and in close proximity to the temporal lobes, which are positioned directly behind the orbits (Bastir et al. 2008). On the other extreme, chimpanzees exhibit larger and more anteriorly projected orbits, which remain highly separated from the frontal and temporal areas.

The fossil hominids in this analysis display a morphology that is intermediate between modern humans and chimpanzees, as their faces and orbits are larger and more detached from the braincase when compared with modern humans, but less so relative to the chimps in this study. Moreover, the temporal poles of these fossil humans are situated in a lower position than that of the orbits, which is more characteristic of chimpanzees; however, the position of their *foramen caecum* was found to be more like that of modern humans by comparison. Interestingly, although the main spatial relationship separating these species involves both the frontal and temporal areas, it is the proximity with the latter that could generate spatial conflicts in modern humans. Indeed, in our species the temporal tip is more anteriorly projected than in chimpanzees or fossil humans, and this close proximity with the middle cranial fossa could constrain the orbit in terms of antero-posterior development. On the other hand, the anterior portion of the temporal lobe in modern humans is flexed against the anterior wall of the middle cranial fossa, twisting toward the midline (Bruner et al. 2017), which could be a direct consequence of spatial constraints between the temporal pole and orbits as evidenced in this study.

Although we could not include Neanderthals in this analysis due to a lack of specimens with cranial anatomy complete enough to sample all required landmarks, it was possible to compare the orbital morphology of Gibraltar 1 with that of modern humans and *H. heidelbergensis*. This assessment revealed that with a more anteriorly located temporal pole and less separation between the orbits and frontal areas, this specimen appears to have an orbital morphology between that of *H. heidelbergensis* and modern humans. Naturally, with only one Neanderthal specimen, broader generalizations cannot be made in terms of species-wide variation. Nonetheless, Gibraltar 1 is a good representative of the Neanderthals, a species with a limited degree of variation (when compared with other hominid taxa), and with characteristic facial traits (Schwartz & Tattersal, 2003). More generally, a scarcity of complete human fossils available for this type of analysis is a limitation of the study, as orbits and frontal bones are often broken, missing or deformed in fossil specimens. However, Bodo and Broken Hill 1 retained intact frontal bones and at least one complete orbit, and thus were the only specimens complete enough to be included. Notwithstanding this inherent limitation, the specimens representing each species grouped together, and were well-separated in shape space from specimens of the other species considered. Furthermore, Bodo and Broken Hill 1 adequately represent the morphotype associated with archaic human species preceding the differentiation towards modern humans and Neanderthals (Stringer, 2012). Therefore, considering that they share a similar morphology according to the geometrical model used in this study, we can assume that inter-specific differences are sufficiently marked to be generally detected in this analysis. However, future surveys using larger fossil samples could be used to investigate the degree of variation of extinct species, and their specific patterns of variability.

According to Bastir & Rosas (2016), the flatter faces of modern humans are associated with retraction of the midline anterior cranial fossae and sphenoid body, and relative projection of the sphenoid wings. This pattern seems to be corroborated by our results showing anterior projection of the temporal pole and antero-posterior retraction of the orbits in modern humans. As in the modern human sample, change in the frontal profile of the different species was negligible, confirming the unvarying outline of the internal frontal table during human evolution (Bookstein et al. 1999). However, the frontal squama is more curved in modern humans when compared with non-modern human species, which is likely a spatial consequence of reduction in the facial block, positioned below the braincase (Bruner et al. 2013). Also, a surface analysis of archaic and modern frontal lobes suggests that the degree of frontal bulging is proportional to the proximity between the frontal lobes and orbits, with extinct human species showing an intermediate morphotype between modern humans and living apes (Beaudet & Bruner, 2017). While variation explained by the second PC in the current study was not significant, it is noteworthy that chimps fall within the same range of variation as modern humans, which could indicate a similar mechanism for orientation of the orbits between the two species (Neaux et al. 2013b, 2015). Patterns of covariation between the cranial base and face are undoubtedly complex, and a complete understanding of the spatial relationship between these structures requires a three-dimensional approach that includes both hard and soft tissue morphology, as this could detect patterns of integration that are indistinguishable in a two-dimensional study.

The dimensionality of the geometrical model represents a limitation of this study. However, both frontal and temporal lobes interact with the orbital space through longitudinal variations and sagittal changes, which is why only morphological variation in this anatomical plane was considered. Nonetheless, we cannot exclude that factors along the coronal plane can also elicit some structural effects. For instance, Moriyama et al. (2011) found that myopia is associated with a temporally distorted eyeball, with asymmetric posterior elongation of the temporal portion of the eye. Also, in a recent study Takada et al. (2015), associated pathogenic exophthalmos with lateral expansion of the ethmoidal sinus and consequent inflation of the medial orbital walls, which acts to constrict the contents of the orbit and shift the eye anteriorly. Beyond the sagittal and axial relationships revealed here, a three-dimensional approach incorporating coronal dimensions could add relevant information to aid in evaluating other potential constraints associated with the spatial relationship among these cranial districts.

Although it is impossible to know how the eyes were positioned within the orbits of fossil specimens, comparing modern humans and chimpanzees can provide some clues. For instance, in both species the eye assumes a rather anterior position within the orbit (Fig. 1), though in modern humans it is closer to the frontal lobe, but is located below the browridge in chimpanzees. Moreover, chimpanzees can be seen to have a much larger amount of extraocular fat within the orbit, which might contribute to a more forward projection of the eye, or it may simply exist to fill the extraocular space within what is proportionately a much larger orbit in chimps. According to Denion et al. (2015a,b), modern humans have more protruding eyes and more rearward lateral orbital margins relative to other hominoids, which are hypothesized to help increase lateral vision in our species. By comparison, Neanderthals and *H. heidelbergensis* have large and projecting browridges, and their eyes may also have been positioned below these structures, more separated from the neural tissues than what is characteristic of modern humans. Still, having a larger brain than chimpanzees, their eyes could also have been larger (Scammon & Armstrong, 1925), which would be expected to change their relative spatial position among circumscribing hard and soft tissues in this anatomical region of the skull. Furthermore, because of observed variation in ocular protrusion and relative position of the lateral orbital margins, analyzing the morphology of the lateral orbital walls in fossil crania could potentially provide insight regarding the lateral angle of vision, and relative protrusion of the eye in fossil specimens.

It is worth noting that certain structural constraints might not necessarily be the target of negative selection in terms of evolutionary processes. Many characters that involve suboptimal conditions, or even negative effects, can be positively selected if associated with more beneficial traits (antagonistic pleiotropy), or if their effects do not influence general reproductive success (such as in the case of detrimental conditions that occur during later life stages). Therefore, the localization of possible spatial conflicts in terms of morphogenesis is crucial to understand in the context of the rules behind evolutionary schemes and limitations, and potentially in considering eventual clinical consequences, though they should not be interpreted individually in terms of evolutionary fitness.

Conclusion

According to the MRI analysis, variation within adult modern humans is primarily related to the horizontal position of the eye relative to the temporal lobes and, secondly, to the vertical position of the eye relative to the base of the frontal lobes. Both cases involve an apparent deformation of the eye, and possible constraints associated with proximity to the temporal and frontal lobes, respectively. The size of the frontal and temporal lobes seems to have the same effect on the eye, which in larger individuals, appears smaller and closer to the temporal lobe, suggestive of a possible posterior constraint. On the one hand, these results support Masters' (2012) hypothesis, as a slight deformation of the eye, coupled with possible spatial constraints with the temporal and frontal lobes were identified. On the other hand, it was not possible to verify a clear association between cortical size and eye shape.

According to the CT analysis, shape variation within adult modern humans is primarily determined by the orientation of the orbits. Though by contrast, an interspecific comparison with other human species and chimpanzees shows that the main change is a shift of the whole orbit from a position anterior to the braincase (apes), to one inferior to the braincase (modern humans), with fossil humans representing an intermediate position between the two. In our species this change involves more direct contact between the temporal and orbital spaces. Taken together, these results suggest that the specific hypothesis of competition among the eye, extraocular soft tissues, the orbit, brain and broader craniofacial anatomy should be further examined using a 3D morphometric approach, which can extend the analysis to include the entire orbital and frontal surfaces. Moreover, an ontogenetic study of patterns of variation among these anatomical components during different stages of growth, and particularly prior to and following age 9 years (Taylor, 1939), could elucidate more about the development of vision problems, and to what extent they may arise in association with spatial constraints among adjacent hard and soft tissue features in this confined region of the modern human skull.

Acknowledgements

Ana Sofia Pereira-Pedro is funded by Fundación Atapuerca, Spain. Michael Masters was supported by the National Institute of General Medical Sciences of the National Institutes of Health, award number 8 P20 GM103474-12. Emiliano Bruner is funded by the Spanish Government (Proyecto Atapuerca – CGL2015-65387-C3-3-P).

Conflict of interest

The authors declare no conflict of interest.

References

Allen JS, Damasio H, Grabowski TJ (2002) Normal neuroanatomical variation in the human brain: an MRI-volumetric study. *Am J Phys Anthropol* **118**, 341–358.

Arsuaga J-L, Martínez I, Lorenzo C, et al. (1999) The human cranial remains from Gran Dolina Lower Pleistocene site (Sierra de Atapuerca, Spain). *J Hum Evol* **37**, 431–457.

Atchison DA, Jones CE, Schmid KL, et al. (2004) Eye shape in emmetropia and myopia. *Invest Ophthalmol Vis Sci* **45**, 3380.

Barbeito-Andrés J, Anzelmo M, Ventrice F, et al. (2016) Morphological integration of the orbital region in a human ontogenetic sample. *Anat Rec* **299**, 70–80.

Bastir M, Rosas A (2005) Hierarchical nature of morphological integration and modularity in the human posterior face. *Am J Phys Anthropol* **128**, 26–34.

Bastir M, Rosas A (2006) Correlated variation between the lateral basicranium and the face: a geometric morphometric study in different human groups. *Arch Oral Biol* **51**, 814–824.

Bastir M, Rosas A (2016) Cranial base topology and basic trends in the facial evolution of Homo. *J Hum Evol* **91**, 26–35.

Bastir M, Rosas A, Kuroe K (2004) Petrosal orientation and mandibular ramus breadth: evidence for an integrated petroso-mandibular developmental unit. *Am J Phys Anthropol* **123**, 340–350.

Bastir M, Rosas A, Lieberman DE, et al. (2008) Middle cranial fossa anatomy and the origin of modern humans. *Anat Rec* **291**, 130–140.

Beaudet A, Bruner E (2017) A frontal lobe surface analysis in three African human fossils: OH 9, Buia, and Bodo. *C R Palevol* **16**, 499–507.

Berger AJ, Kahn D (2012) Growth and development of the orbit. *Oral Maxillofac Surg Clin North Am* **24**, 545–555.

Bermúdez de Castro JM, Martinón-Torres M, Prado L, et al. (2010) New immature hominin fossil from European Lower Pleistocene shows the earliest evidence of a modern human dental development pattern. *PNAS* **107**, 11 739–11 744.

Bookstein FL (1991) *Morphometric Tools for Landmark Data: Geometry and Biology*. Cambridge: Cambridge University Press.

Bookstein F, Schäfer K, Prossinger H, et al. (1999) Comparing frontal cranial profiles in archaic and modern Homo by morphometric analysis. *Anat Rec* **257**, 217–224.

Brown P, Maeda T (2004) Post-Pleistocene diachronic change in East Asian facial skeletons: the size, shape and volume of the orbits. *Anthropol Sci* **112**, 29–40.

Bruner E (2004) Geometric morphometrics and paleoneurology: brain shape evolution in the genus Homo. *J Hum Evol* **47**, 279–303.

Bruner E (2007) Cranial shape and size variation in human evolution: structural and functional perspectives. *Childs Nerv Syst* **23**, 1357–1365.

Bruner E, Holloway RL (2010) A bivariate approach to the widening of the frontal lobes in the genus Homo. *J Hum Evol* **58**, 138–146.

Bruner E, Ripani M (2008) A quantitative and descriptive approach to morphological variation of the endocranial base in modern humans. *Am J Phys Anthropol* **137**, 30–40.

Bruner E, Athreya S, de la Cuétara JM, et al. (2013) Geometric variation of the frontal squama in the genus homo: frontal bulging and the origin of modern human morphology. *Am J Phys Anthropol* **150**, 313–323.

Bruner E, De la Cuétara JM, Masters M, et al. (2014) Functional craniology and brain evolution: from paleontology to biomedicine. *Front Neuroanat* **8**, 19.

Bruner E, Amano H, de la Cuétara JM, et al. (2015) The brain and the braincase: a spatial analysis on the midsagittal profile in adult humans. *J Anat* **227**, 268–276.

Bruner E, Pereira-Pedro AS, Bastir M (2017) Patterns of morphological integration between parietal and temporal áreas in the human skull. *J Morphol* **278**(10), 1312–1320.

Chakraborty R, Read SA, Collins MJ (2011) Diurnal variations in axial length, choroidal thickness, intraocular pressure, and ocular biometrics. *Invest Ophthalmol Vis Sci* **52**, 5121–5129.

Chau A, Fung K, Pak K, et al. (2004) Is eye size related to orbit size in human subjects? *Ophthalmic Physiol Opt* **24**, 35–40.

Cheng HM, Singh OS, Kwong KK, et al. (1992) Shape of the myopic eye as seen with high-resolution magnetic resonance imaging. *Optom Vis Sci* **69**, 698–701.

Denion E, Hitier M, Guyader V, et al. (2015a) Unique human orbital morphology compared with that of apes. *Sci Rep* **5**, 11 528.

Denion E, Hitier M, Levieil E, et al. (2015b) Human rather than ape-like orbital morphology allows much greater lateral visual field expansion with eye abduction. *Sci Rep* **5**, 12 437.

Detorakis ET, Drakonaki E, Papadaki E, et al. (2010) Effective orbital volume and eyeball position: an MRI study. *Orbit* **29**, 244–249.

Dinov ID, Van Horn JD, Lozev KM, et al. (2009) Efficient, distributed and interactive neuroimaging data analysis using the LONI Pipeline. *Front Neuroinform* **3**, 22.

Dirani M, Chamberlain M, Shekar SN, et al. (2006) Heritability of refractive error and ocular biometrics: the genes in myopia (GEM) twin study. *Invest Ophthalmol Vis Sci* **47**, 4756–4761.

Foo VHX, Verkicharla PK, Ikram MK, et al. (2016) Axial length/corneal radius of curvature ratio and myopia in 3-year-old children. *Transl Vis Sci Technol* **5**, 5.

Freidline SE, Gunz P, Harvati K, et al. (2013) Evaluating developmental shape changes in *Homo antecessor* subadult facial morphology. *J Hum Evol* **65**, 404–423.

Goldschmidt E, Fledelius HC (2011) Clinical features in high myopia. A Danish cohort study of high myopia cases followed from age 14 to age 60. *Acta Ophthalmol* **89**, 97–98.

Grosvenor T, Goss DA (1998) Role of the cornea in emmetropia and myopia. *Optom Vis Sci* **75**, 132–145.

Guo X, Xiao O, Chen Y, et al. (2017) Three-dimensional eye shape, myopic maculopathy, and visual acuity: the Zhongshan Ophthalmic Center – Brien Holden Vision Institute high myopia cohort study. *Ophthalmology* **124**, 679–687.

Hammer Ø, Ryan P, Harper D (2001) PAST: Paleontological Statistics software package for education and data analysis. *Palaeontol Electronica* **4**, 9.

He M, Zeng J, Liu Y, et al. (2004) Refractive error and visual impairment in urban children in southern China. *Invest Ophthalmol Vis Sci* **45**, 793–799.

Holladay JT, Lynn M, Waring G III, et al. (1991) The relationship of visual acuity, refractive error, and pupil size after radial keratotomy. *Arch Ophthalmol* **109**, 70–76.

Hoyte D (1997) Growth of the orbit. In: *Fundamentals of Craniofacial Growth*. (eds Dixon AD, Hoyte D, Rönning O), pp. 225–255. New York: CRC Press.

Ip JM, Huynh SC, Kifley A, et al. (2007) Variation of the contribution from axial length and other oculometric parameters to refraction by age and ethnicity. *Invest Ophthalmol Vis Sci* **48**, 4846–4853.

Kirk EC (2004) Comparative morphology of the eye in primates. *Anat Rec* **281A**, 1095–1103.

Kirk EC (2006) Effects of activity pattern on eye size and orbital aperture size in primates. *J Hum Evol* **51**, 159–170.

Klingenberg CP (2011) MorphoJ: an integrated software package for geometric morphometrics. *Mol Ecol Resour* **11**, 353–357.

Lacruz RS, Bromage TG, O'Higgins P, et al. (2015) Ontogeny of the maxilla in Neanderthals and their ancestors. *Nat Commun* **6**, 8996.

Lam CS, Edwards M, Millodot M, et al. (1999) A 2-year longitudinal study of myopia progression and optical component changes among Hong Kong schoolchildren. *Optom Vis Sci* **76**, 370–380.

Lam DSC, Fan DSP, Lam RF, et al. (2008) The effect of parental history of myopia on children's eye size and growth: results of a longitudinal study. *Invest Ophthalmol Vis Sci* **49**, 873–876.

Lang J (2012) *Clinical Anatomy of the Head: Neurocranium, Orbit, Craniocervical Regions*. New York: Springer Science & Business Media.

Lieberman DE, Pearson OM, Mowbray KM (2000) Basicranial influence on overall cranial shape. *J Hum Evol* **38**, 291–315.

Lieberman DE, McBratney BM, Krovitz G (2002) The evolution and development of cranial form in Homo sapiens. *PNAS* **99**, 1134–1139.

Llorente L, Barbero S, Cano D, et al. (2004) Myopic versus hyperopic eyes: axial length, corneal shape and optical aberrations. *J Vis* **4**, 288–298.

Mak W, Kwan MWM, Cheng TS, et al. (2006) Myopia as a latent phenotype of a pleiotropic gene positively selected for facilitating neurocognitive development, and the effects of environmental factors in its expression. *Med Hypotheses* **66**, 1209–1215.

Masters MP (2012) Relative size of the eye and orbit: an evolutionary and craniofacial constraint model for examining the etiology and disparate incidence of juvenile-onset myopia in humans. *Med Hypotheses* **78**, 649–656.

Masters MP, Bruner E, Queer S, et al. (2015) Analysis of the volumetric relationship among human ocular, orbital and fronto-occipital cortical morphology. *J Anat* **227**, 460–473.

Mazziotta J, Toga A, Evans A, et al. (2001) A probabilistic atlas and reference system for the human brain: International Consortium for Brain Mapping (ICBM). *Philos Trans R Soc Lond B Biol Sci* **356**, 1293–1322.

McCarthy RC, Lieberman DE (2001) Posterior maxillary (PM) plane and anterior cranial architecture in primates. *Anat Rec* **264**, 247–260.

Migliori ME, Gladstone GJ (1984) Determination of the normal range of exophthalmometric values for black and white adults. *Am J Ophthalmol* **98**, 438–442.

Moriyama M, Ohno-Matsui K, Hayashi K, et al. (2011) Topographic analyses of shape of eyes with pathologic myopia by high-resolution three-dimensional magnetic resonance imaging. *Ophthalmology* **118**, 1626–1637.

Moss ML (1963) Morphological variations of the crista galli and medial orbital margin. *Am J Phys Anthropol* **21**, 159–164.

Moss ML, Young RW (1960) A functional approach to craniology. *Am J Phys Anthropol* **18**, 281–292.

Neaux D, Guy F, Gilissen E, et al. (2013a) Covariation between midline cranial base, lateral basicranium, and face in modern humans and chimpanzees: a 3D geometric morphometric analysis: basicranium and face integration. *Anat Rec* **296**, 568–579.

Neaux D, Guy F, Gilissen E, et al. (2013b) Facial orientation and facial shape in extant great apes: a geometric morphometric analysis of covariation. *PLoS One* **8**, e57026.

Neaux D, Gilissen E, Coudyzer W, et al. (2015) Implications of the relationship between basicranial flexion and facial orientation for the evolution of hominid craniofacial structures. *Int J Primatol* **36**, 1120–1131.

Nickla DL (2013) Ocular diurnal rhythms and eye growth regulation: where we are 50 years after Lauber. *Exp Eye Res* **114**, 25–34.

Palmowski-Wolfe AM, Kober C, Berg I, et al. (2009) Globe restriction in a severely myopic patient visualized through oculodynamic magnetic resonance imaging (od-MRI). *J AAPOS* **13**, 322–324.

Peyster R, Ginsberg F, Silber J, et al. (1986) Exophthalmos caused by excessive fat: CT volumetric analysis and differential diagnosis. *Am J Roentgenol* **146**, 459–464.

Ravosa MJ (1991) Interspecific perspective on mechanical and nonmechanical models of primate circumorbital morphology. *Am J Phys Anthropol* **86**, 369–396.

Read SA, Collins MJ, Iskander DR (2008) Diurnal variation of axial length, intraocular pressure, and anterior eye biometrics. *Invest Ophthalmol Vis Sci* **49**, 2911–2918.

Remón L, Tornel M, Furlan WD (2006) Visual acuity in simple myopic astigmatism: influence of cylinder axis. *Optom Vis Sci* **83**, 311–315.

Rilling JK, Seligman RA (2002) A quantitative morphometric comparative analysis of the primate temporal lobe. *J Hum Evol* **42**, 505–533.

Rohlf FJ (2013) tpsDig version 2.17, Department of Ecology and Evolution, State University of New York at Stony Brook.

Ross CF, Kirk EC (2007) Evolution of eye size and shape in primates. *J Hum Evol* **52**, 294–313.

Scammon RE, Armstrong EL (1925) On the growth of the human eyeball and optic nerve. *J Comp Neurol* **38**, 165–219.

Schneider CA, Rasband WS, Eliceiri KW (2012) NIH Image to ImageJ: 25 years of image analysis. *Nat Methods* **9**, 671–675.

Schultz AH (1940) The size of the orbit and of the eye in primates. *Am J Phys Anthropol* **26**, 389–408.

Schwartz JH, Tattersal I (2003) *The Human Fossil Record, Volume Two: Craniodental Morphology of Genus Homo* (Africa and Asia). New York: John Wiley & Sons.

Semendeferi K, Damasio H (2000) The brain and its main anatomical subdivisions in living hominoids using magnetic resonance imaging. *J Hum Evol* **38**, 317–332.

Semendeferi K, Damasio H, Frank R, et al. (1997) The evolution of the frontal lobes: a volumetric analysis based on three-dimensional reconstructions of magnetic resonance scans of human and ape brains. *J Hum Evol* **32**, 375–388.

Stone RA, Flitcroft DI (2004) Ocular shape and myopia. *Ann Acad Med Singapore* **33**, 7–15.

Stone RA, Pardue MT, Iuvone PM, et al. (2013) Pharmacology of myopia and potential role for intrinsic retinal circadian rhythms. *Exp Eye Res* **114**, 35–47.

Stringer C (2012) The status of *Homo heidelbergensis* (Schoetensack 1908). *Evol Anthropol* **21**, 101–107.

Stringer C (2016) The origin and evolution of *Homo sapiens*. *Philos Trans R Soc Lond B Biol Sci* **371**, 20150237.

Takada K, Sakamoto Y, Shimizu Y, et al. (2015) A hypothesis for the pathologic mechanism of idiopathic exophthalmos based on computed tomographic evaluations. *J Craniofac Surg* **26**, 1639–1642.

Taylor W (1939) The effect of enucleation of one eye in childhood upon the subsequent development of the face. *Trans Ophthalmol Soc UK* **59**, 361–371.

Todd TW, Beecher H, Williams GH, et al. (1940) The weight and growth of the human eyeball. *Hum Biol* **12**, 1–20.

Tu Z, Narr KL, Dollár P, et al. (2008) Brain anatomical structure segmentation by hybrid discriminative/generative models. *IEEE Trans Med Imaging* **27**, 495–508.

Wagner A, Schneider C, Lagogiannis G, et al. (2000) Pulsatile expansion therapy for orbital enlargement. *Int J Oral Maxillofac Surg* **29**, 91–95.

Waitzman AA, Posnick JC, Armstrong DC, et al. (1992) Craniofacial skeletal measurements based on computed tomography: Part II. Normal values and growth trends. *Cleft Palate Craniofac J* **29**, 118–128.

Washburn SL, Detwiler SB (1943) An experiment bearing on the problems of physical anthropology. *Am J Phys Anthropol* **1**, 171–190.

Weale RA (1982) *A Biography of the Eye: Development, Growth, Age*. London: H. K. Lewis.

Wu X, Liu W, Zhang Q, et al. (2007) Craniofacial morphological microevolution of Holocene populations in northern China. *Chin Sci Bull* **52**, 1661–1668.

Zelditch ML, Swiderski DL, Sheets HD, et al. (2004) *Geometric Morphometrics for Biologists*: A Primer. New York; London: Elsevier Academic Press.

Zhao J, Pan X, Sui R, et al. (2000) Refractive error study in children: results from Shunyi District, China. *Am J Ophthalmol* **129**, 427–435.

2.2. PATTERNS OF MORPHOLOGICAL INTEGRATION BETWEEN PARIETAL AND TEMPORAL AREAS IN THE HUMAN SKULL

Authors: Emiliano Bruner, Ana Sofia Pereira Pedro, Markus Bastir
Journal: Journal of Morphology, 278: 1312-1320
Status: Published in 2017

Received: 28 February 2017 | Revised: 28 April 2017 | Accepted: 9 May 2017
DOI: 10.1002/jmor.20714

RESEARCH ARTICLE

Patterns of morphological integration between parietal and temporal areas in the human skull

Emiliano Bruner[1] | **Ana Sofia Pereira-Pedro**[1] | **Markus Bastir**[2]

[1]Grupo de Paleobiología, Centro Nacional de Investigación sobre la Evolución Humana, Burgos, Spain

[2]Departamento de Paleobiología, Museo Nacional de Ciencias Naturales, Madrid, Spain

Correspondence
Emiliano Bruner, Centro Nacional de Investigación sobre la Evolución Humana, Paseo Sierra de Atapuerca 3, 09002 Burgos, Spain.
Email: emiliano.bruner@cenieh.es

Funding information
Emiliano Bruner and Markus Bastir are funded by the Ministerio de Economía y Competitividad, Spain (EB: CGL2015-65387-C3-3-P; MB: CGL2012-37279, CGL2015-63648-P) and by the Italian Institute of Anthropology (Isita). ASPP is funded by the Atapuerca Foundation, Spain. The authors declare no conflict of interest.

Abstract

Modern humans have evolved bulging parietal areas and large, projecting temporal lobes. Both changes, largely due to a longitudinal expansion of these cranial and cerebral elements, were hypothesized to be the result of brain evolution and cognitive variations. Nonetheless, the independence of these two morphological characters has not been evaluated. Because of structural and functional integration among cranial elements, changes in the position of the temporal poles can be a secondary consequence of parietal bulging and reorientation of the head axis. In this study, we use geometric morphometrics to test the correlation between parietal shape and the morphology of the endocranial base in a sample of adult modern humans. Our results suggest that parietal proportions show no correlation with the relative position of the temporal poles within the spatial organization of the endocranial base. The vault and endocranial base are likely to be involved in distinct morphogenetic processes, with scarce or no integration between these two districts. Therefore, the current evidence rejects the hypothesis of reciprocal morphological influences between parietal and temporal morphology, suggesting that evolutionary spatial changes in these two areas may have been independent. However, parietal bulging exerts a visible effect on the rotation of the cranial base, influencing head position and orientation. This change can have had a major relevance in the reorganization of the head functional axis.

KEYWORDS
cranial base, functional craniology, head orientation, parietal lobes, temporal lobes

1 | INTRODUCTION

Brain and braincase are part of an integrated system, in which functional and structural relationships may channel and constrain ontogeny and evolution (Enlow, 1990; Moss & Young, 1960; Richtsmeier et al., 2006). Selection does not act on single cranial traits, but instead on the whole phenotype, which is based on functional and developmental interactions shaping the facial and neurocranial morphology (Cheverud, 1982). Many general patterns of cranial integration are conserved among hominoids (Singh, Harvati, Hublin, & Klingenberg, 2012), although some localized differences can be detected when comparing extant and extinct humans (Roseman, Weaver, & Stringer, 2011). However, the multiple factors involved in craniofacial morphogenesis make these relationships scarcely linear, and sensitive to local effects more than to long-range global schemes. Endocranial ontogenetic changes are associated with distinct stages which involve different local growth rates (Jeffery, 2002; Neubauer, Gunz, & Hublin, 2009). In adult humans, the three endocranial fossae are influenced by independent bone and brain factors (Bruner & Ripani, 2008), and the midsagittal skull morphology is relatively independent by the morphological variations of the lateral areas (Bastir & Rosas, 2006; Gkantidis & Halazonetis, 2011; Neaux, Guy, Gilissen, Coudyzer, & Ducrocq, 2013). Even when considering the form of the brain, the available information suggests that integration is mostly based on spatial proximity, and not on overall distributed patterns (Bruner, Martin-Loeches, & Colom, 2010; Gómez-Robles, Hopkins, & Sherwood, 2014).

Despite the influence of growth and development in ontogeny and phylogeny (Gould, 1966, 1977), morphogenetic and evolutionary variations are also sensitive to distinct kinds of mechanisms. In evolutionary terms, hard elements with biomechanical constraints (like bones) probably have a relevant morphological effect on soft tissues which functions are less dependent on form (like cerebral lobes and gyri). This is particularly evident for example taking into account the influence of the facial block and mandibular elements on the anterior and middle fossae respectively (Bastir & Rosas, 2005, 2006). Soft tissues usually mold bones only when there are no spatial conflicts or antagonist effects, like for example in the vault (Moss & Young, 1960). In contrast, during ontogeny the sequence of maturation may be more relevant, because those components maturing earlier exert an influence on those components maturing later (Bastir, Rosas, & O'higgins, 2006). In this case, the neurocranium and brain are supposed to constrain the successive maturation of the endocranial base and facial block. Nonetheless, facial variation may induce some secondary minor brain changes due to later adjustments (Bastir et al., 2006; Neubauer et al., 2009).

During human evolution two cerebral areas have been hypothesized to have undergone major morphological changes: the temporal and parietal lobes. Humans have relatively larger temporal lobes than non-human primates (Rilling & Seligman, 2002), and endocranial analyses showed that modern humans have also a forward displacement of the temporal poles, when compared with non-modern human species (Bastir et al., 2011). At the same time, modern humans display a unique sagittal (longitudinal) bulging of the parietal bones and lobes (Bruner, Manzi, & Arsuaga, 2003; Bruner, De La Cuétara, & Holloway, 2011), hypothesized to be associated with an increase in the size and proportions of the medial parietal cortex (Bruner, Rangel de Lázaro, et al., 2014; Bruner, Amano, de la Cuétara, & Ogihara, 2015; Bruner, Preuss, Chen, & Rilling, 2017). Despite the fact that the vault and the base are supposed to be scarcely integrated, it can be hypothesized that the change of the position of the temporal poles can be a secondary effect of the parietal bulging, displacing these elements forward. Both parietal and temporal characters deal with variations involving antero-posterior enlargements and displacements, and we currently ignore to what extent these two morphological patterns may be related through reciprocal spatial influences.

In this study, we analyze the sagittal spatial correlation between parietal morphology and the position of the temporal poles relatively to the cranial base in a sample of modern human skulls. We consider the covariation structure and the association among these elements, following the null hypothesis of independent morphological changes.

2 | MATERIALS AND METHODS

The tomographic scans of 48 modern human skulls (28 males and 20 females) available from the NESPOS database (Neanderthal Museum, Mettmann, Germany) have been used to sample coordinate data. All specimens are adult (age > 20 yrs) from different geographic origins (Europe, $N = 16$; Africa $N = 15$; Asia and Inuit, $N = 7$; South America $N = 10$). Voxel size averages .33 mm. The two characters we want to evaluate, parietal bulging and temporal displacement, both involve changes through the sagittal plane, the former being characterized by midsagittal longitudinal enlargement/reduction, the latter by parasagittal antero-posterior shift of the temporal poles relative to the basicranial and facial areas. Please note that parietal bulging described in modern humans deals with a longitudinal expansion of the midsagittal profile, increasing the parietal length and curvature (e.g., Bruner, 2004; Bruner et al., 2011; Bruner, De la Cuétara, Masters, Amano, & Ogihara, 2014). This feature must not be confounded with "parietal bossing," which deals with a lateral expansion of the parietal squama, and which is described also in Neandertals, a species that does not display a parietal longitudinal expansion. Therefore, to focus on these specific patterns associated with antero-posterior displacements and proportions, we limited the study to the sagittal spatial variation, excluding other factors associated with cranial widths and lateral proportions. Specimens have been therefore projected on a lateral view, and 2D landmarks have been sampled after correspondence between 2D-slices from the full original stack and its 2D-projection, with ImageJ 1.49g (Schindelin et al., 2012; Schneider, Rasband, & Eliceiri, 2012). The geometrical model includes 10 landmarks (Figure 1a). The morphology of the parietal bone was sampled from endobregma to endolambda, with three additional equally distant points along the outline. The cranial base is represented by the most anterior point of the anterior fossa (anterior limit of the crista galli), the posterior edge of the anterior fossa, the lower point of the sella, and the endobasion. The position of the two temporal poles has been averaged, the coordinate of this point being the mean value of the left and right most anterior point of the medial fossa. This configuration allows evaluating possible spatial variations of the temporal poles relatively to the cranial base angle and to the anterior cranial fossa. Data were sampled by one single observer (ASPP). Intra-observer error (sampling uncertainty associated with spatial placement of the landmarks) was estimated by resampling four specimens three times each, and then calculated as mean standard deviation and mean difference at each landmark for both x and y coordinate. Coordinates were superimposed by Procrustes registration, normalizing size, translating the coordinate systems to a common centroid, and rotating so as to minimize the distance between corresponding landmarks (Bookstein, 1991). Multivariate analyses were computed according to the principles of geometric morphometrics (Zelditch, Swiderski, Sheets, & Fink, 2004), through Principal Component Analysis of shape variables and multiple correlation with parietal chord and arc. Correlation between shape and parietal measures was tested through permutation.

We tested the influence of parietal size to consider whether this can be a factor inducing antero-posterior displacement of the temporal tips. The effect of overall brain size was not considered in this study, because global brain dimensions do not influence parietal proportions at evolutionary or intraspecific level. In fact, Neandertals and modern humans shared a similar cranial capacity but a distinct parietal size (Bruner et al., 2003), brain size is not correlated to the proportions of the medial parietal cortex (Bruner, Pereira-Pedro, Chen, & Rilling, 2017), and non-human primates with different brain size show similar proportions of the medial parietal cortex (Pereira-Pedro, Rilling, Chen, Preuss, & Bruner, 2017).

A Partial Least Square correlation between the parietal and basal landmarks was used to test the overall integration between the parietal and basicranial blocks. Analyses were computed with PAST 2.17c (Hammer, Ryan, & Harper, 2001), tpsRelw 1.54 (Rohlf, 2014), and MorphoJ 1.06a (Klingenberg, 2011).

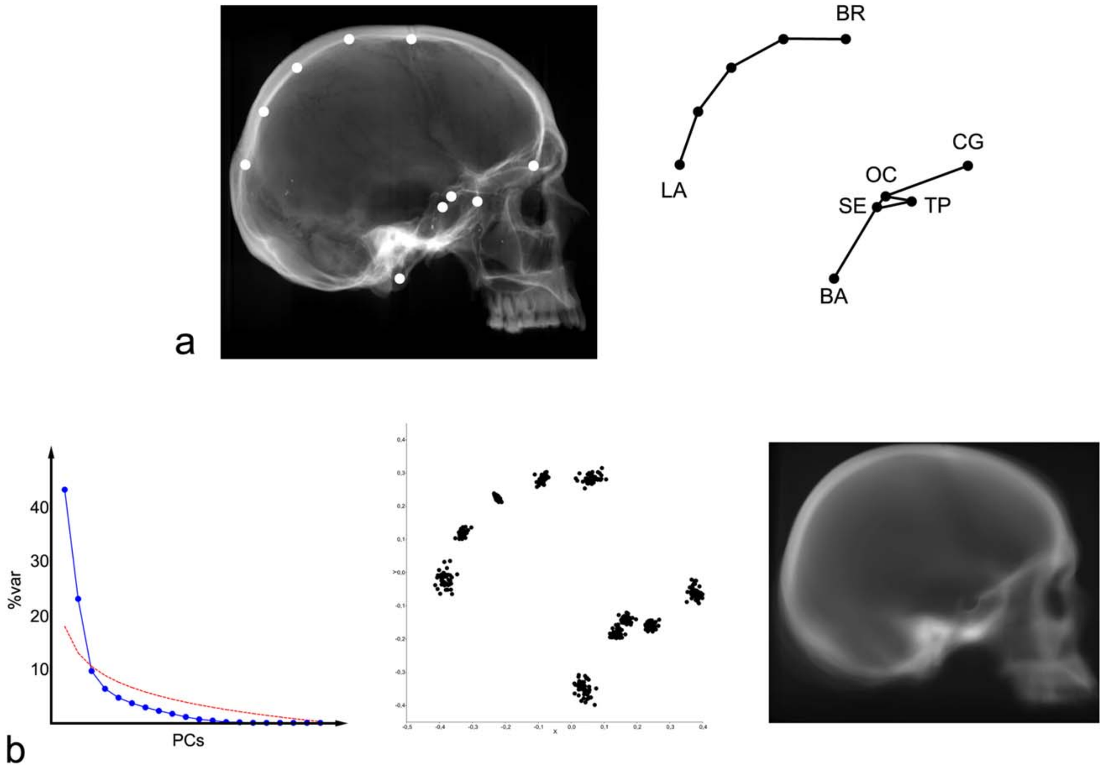

FIGURE 1 (a) Lateral scout view of an adult male skull computed on standard deviation values (left), showing the landmarks used in this study (right). Landmarks were localized on 2D slices, and then sampled onto the 3D lateral scout projection. Landmarks: ba: endobasion; br: endobregma; cg: crista galli (anterior limit); la: endolambda; oc: optic chiasm (posterior edge of the anterior fossa); se: sella (lowest point); tp: temporal poles (averaged sides); (b) scree plot of the Principal Component Analysis (left), showing two main vectors above the random value (broken stick threshold: red curve), scatterplot of the whole sample after Procrustes Superimposition (center) and average image of the whole sample (right) after superimposition (tpsSuper 2.00, Rohlf, 2013)

3 | RESULTS

Table 1 shows the descriptive statistics for parietal chord and arc. Correlation between these two variables is high ($R = .96$, $p = .0001$) and, although females show smaller dimensions than males, analysis of covariance does not evidence different allometric pattern between sexes ($p_{\text{mean}} = .39$, $p_{\text{slope}} = .98$). Values and distributions of these two variables as reported in this survey are largely comparable with the figures obtained from a larger sample on endocranial casts (Bruner et al., 2011). Mean intra-observer error for the ten landmarks was 2.2 mm when calculated in terms of standard deviation, and 2.8 mm in terms of difference between landmarks coordinates. Both values are acceptable when dealing with neurocranial anatomy.

Principal component analysis of shape variation shows a morphological space characterized by two significant patterns of covariance (Figure 1b – see also motion images in supporting information). First component (43% of the variance) is associated with parietal expansion and cranial base rotation: the more the parietal bone enlarges, the more the cranial base undergoes a forward rotation (Figure 2a–d). The spatial relationships within the cranial base, including the position of the temporal poles relatively to the cranial base and to the anterior fossa, remain the same. The second component (23% of the variance) is associated with a vertical stretching of the cranial base, (Figure 2e,f). This second pattern is not associated with any patent variation of the parietal outline, except a change of its orientation due to the vertical lengthening of the cranial dimensions. Successive components are below a threshold of random variation, and will not be hence interpreted in terms of stable covariance patterns.

Interestingly, if nasion and prosthion are added to the configuration, PC1 (41% of the variance) display the same patterns, but showing that parietal bulging and cranial base rotation are also associated with changes of the facial angle, through a spatial scheme in which

TABLE 1 Descriptive statistics for parietal chord and arc

	N	Mean	SD	Min	25th	Med	75th	Max	CV
Parietal chord	48	105	9	87	100	106	111	126	8,1
Parietal arc	48	119	10	92	114	118	124	147	8,7

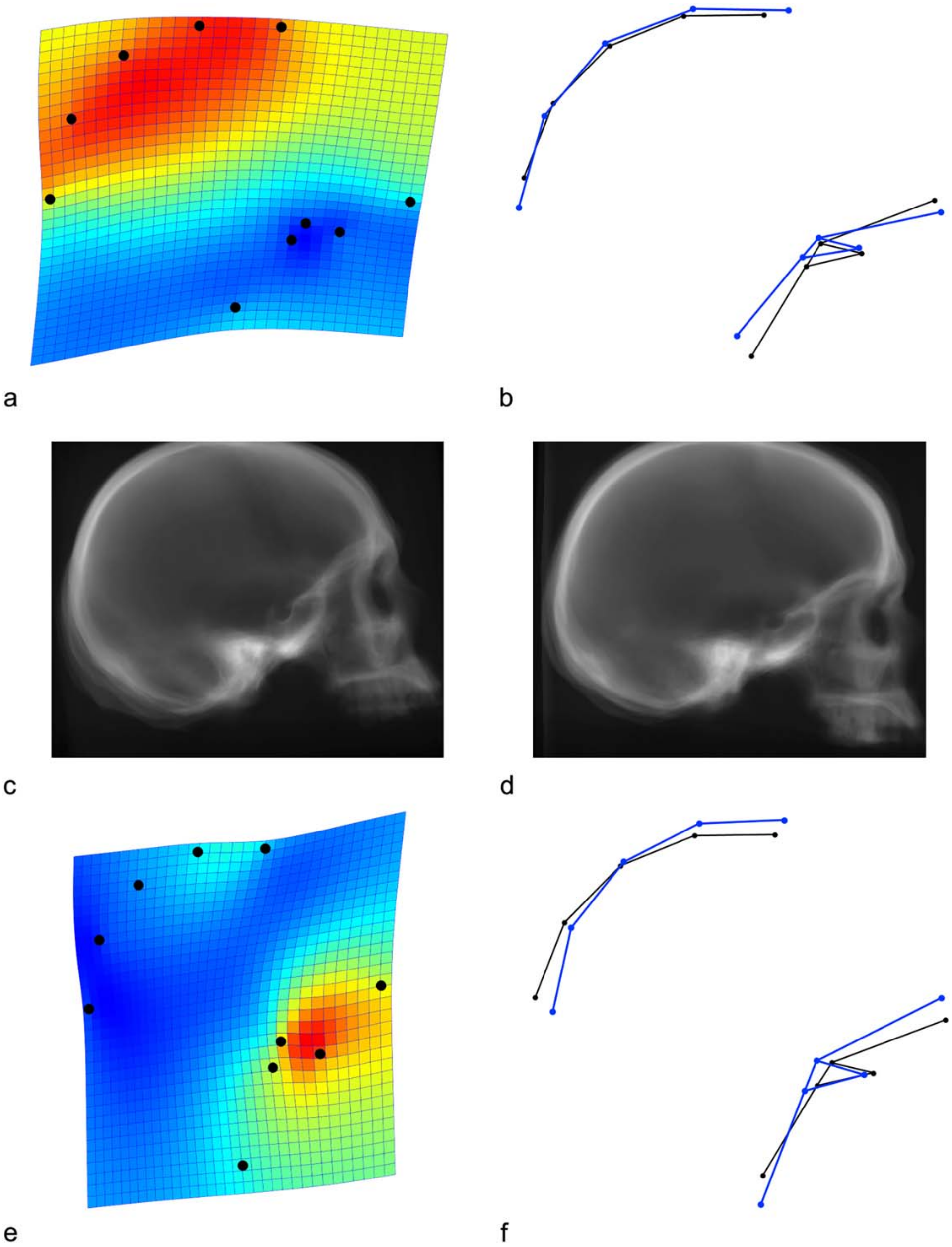

FIGURE 2 PC1 showed through deformation grids and maps (a; red: dilation; blues: compression) and wireframes (b), associated with parietal bulging and cranial base rotation. Overall differences on the whole skull is showed by averaging the ten individuals at the extremes of the vector (c, d). PC2 (e,f) is associated with cranial base vertical stretching and parietal rotation. See also supporting information

parietal reduction is related to prognathism and facial inclination (Figure 3).

A moderate correlation between shape coordinates and parietal chord is significant ($R^2 = .27$, $p < .0001$), and the associated shape changes are the same described for PC1 (Figure 4a). PC1 is actually correlated to both parietal chord ($R^2 = .59$, $p < .0001$) and arc ($R^2 = .69$, $p < .0001$), while PC2 is not correlated to parietal size. Therefore, parietal bulging expressed in PC1 does not only represent a change of shape, but it further involves a change of form: as the parietal gets absolutely or relatively larger, the cranial base undergoes a forward rotation of its axis, without changes in its spatial proportions or relative positions. This allometric pattern, when compared with PC1, is

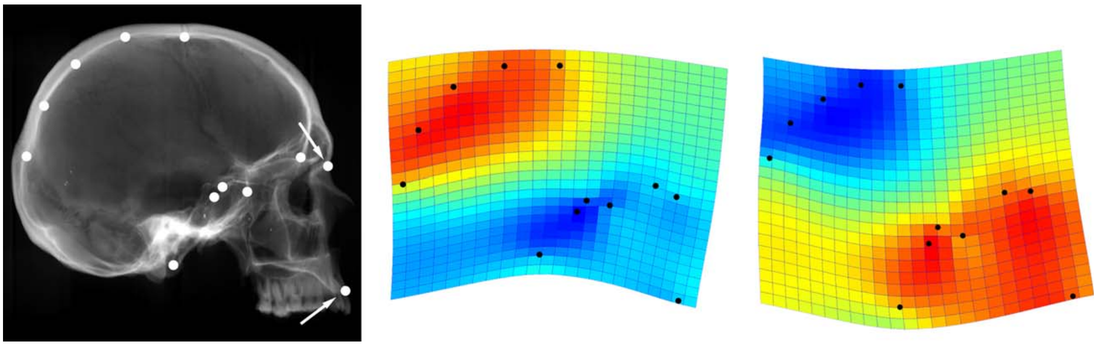

FIGURE 3 Adding nasion and prosthion to the configuration, PC1 displays the same pattern, showing that parietal bulging and cranial base rotation are also associated with the rotation of the facial block

additionally characterized by a minor flattening of the middle fossa. The correlation between shape and parietal dimension is slightly higher when using the parietal arc instead of the parietal chord ($p < .0001$, $R^2 = .30$; Figure 4b). A Partial Least Square correlation between parietal and basal subsets of landmarks is not able to evidence any significant association between these two blocks ($p = .76$).

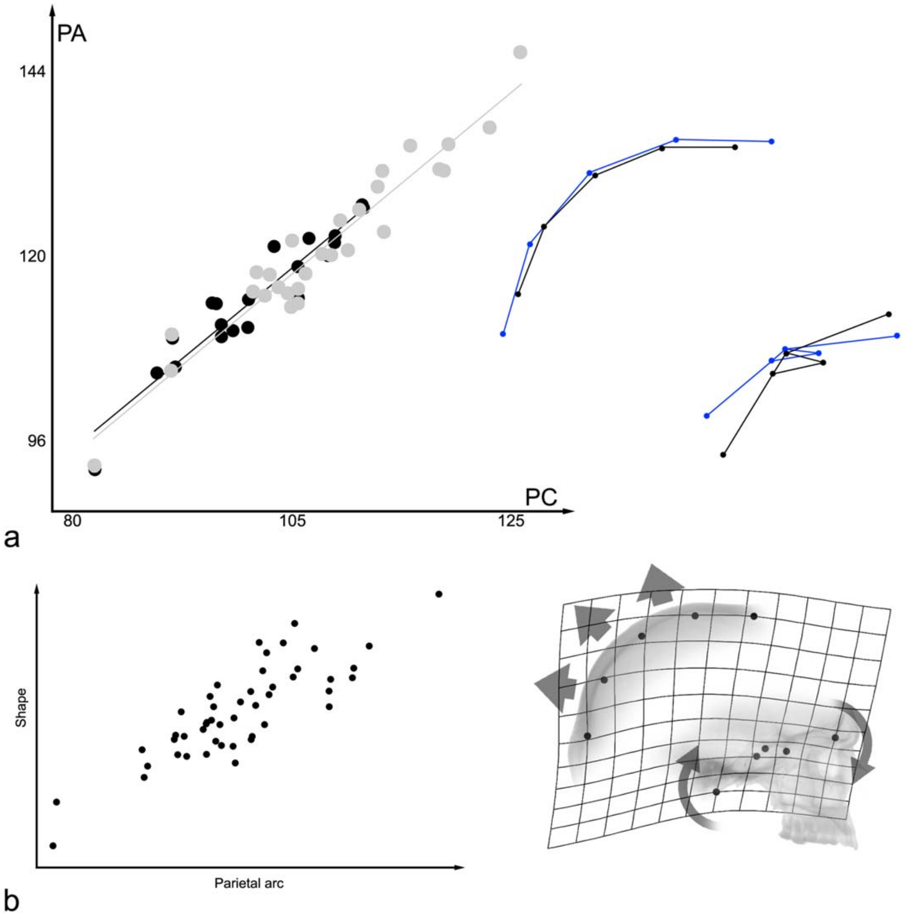

FIGURE 4 (a) Correlation between parietal cord (PC) and arc (PA) in males (gray dots) and females (black dots, and shape variations associated with parietal chord increase (blue wireframe). (b) Correlation between parietal arc and shape scores, and shape changes associated with parietal arc increase (deformation grid). The shape change is similar to PC1: as parietal bone gets larger and more bulging, the cranial base undergoes a rotation, without major changes in its internal proportions

4 | DISCUSSION

One of the most patent changes associated with modern human neurocranial shape is the longitudinal bulging and expansion of the parietal bones and lobes (Bruner, 2004; Bruner et al., 2003, 2011). An enlargement of the parietal cortex cannot be passively generated by mechanical spatial stretching, and it requires a physical increase of some biological components at histological level (size, number, or density of neurons, astrocytes, vessels, etc.; Herculano-Houzel & Lent, 2005). This suggests that modern human parietal changes are not likely to be the consequences of a geometric adjustment of the skull, but else an actual change of the cortical proportions. In fact, these dorsal parietal districts spatially match cortical areas that display a remarkable surface variation (Bruner, Rangel de Lázaro, et al., 2014; Burner, Pereira-Pedro, et al., 2017; Bruner, Román, de la Cuétara, Martin-Loeches, & Colom, 2015) and that are much larger in our species when compared with chimpanzees (Bruner, Preuss, et al., 2017). At the same time, modern humans display larger temporal lobes when compared with living apes (Rilling, 2006; Rilling & Seligman, 2002), and more projecting temporal poles (Bastir et al., 2011; Bastir & Rosas, 2016). Modern humans possibly display also a more pronounced cranial base flexion than living apes (Bastir & Rosas, 2016; Lieberman, Hallgrímsson, Liu, Parsons, & Jamniczky, 2008), combined with a retracted midline base relative to lateral areas and a different orientation of the overall base relative to the face (Bastir & Rosas, 2016).

The changes in the parietal proportions necessarily influence the general spatial arrangement of the other cranial and endocranial elements (Neubauer et al., 2009). Accordingly, anterior displacement of the temporal poles, described in modern humans when compared with extinct human species (Bastir et al., 2011; Bastir & Rosas, 2016), could either reflect volumetric enlargement of the temporal lobes described in *Homo sapiens* (Rilling & Seligman, 2002), or a secondary spatial displacement of the temporal poles due to parietal spatial influence, forcing the temporal lobes in a forward position.

This question is relevant for the study of cranial integration and brain-braincase relationships, but it also represents a crucial issue in paleoneurology. In fact, the middle cranial fossa is part of a complex morphogenetic system influenced by multiple independent factors, and houses only a part of the temporal lobes. Accordingly, it may be difficult to evidence what morphological changes of the middle fossa are due to cranial architecture, and what changes can be due to factors associated with brain morphology. Our study suggests, at the intraspecific level, that parietal longitudinal proportions are unrelated to variations in temporal pole projection.

When dealing with the parietal outline and the cranial base in lateral view, the morphological variability among adults is described by two main patterns of covariance. The first is associated with changes of the parietal form, the second with changes of the cranial base. In both cases, when one of these areas changes, the other one undergoes a reorientation but not any noticeable intrinsic shape variation. Hence, it seems that the two districts account for the two separated and independent effects. Parietal size and shape is once more confirmed as a principal source of variability, but apparently it does not influence the basicranial longitudinal proportions. Actually, quantitative and experimental evidence suggests that major cranial constraints are due to lateral growth and proportions of the cranial base, because of a structural integration among cranial breadths, and not to anterior-posterior or sagittal factors (Hallgrimsson, Lieberman, Liu, Ford-Hutchinson, & Jirik, 2007; Lieberman, Pearson, & Mowbray, 2000). Parietal bulging and temporal displacement concerns longitudinal proportions which, in addition, act on different sagittal planes, the independence of which was previously described even within the basicranial structure (Bastir & Rosas, 2006; Neaux et al., 2013). Nonetheless, it is worth noting that parietal enlargement influences the general orientation of the base, involving the rotation of the whole block, and this is relevant for issues associated with head posture and orientation. In fact, the parietal bulging in modern humans is so apparent that it can modify the functional axis of the head and orbits (Bruner, 2003). Head orientation is a relevant factor in human evolution, dealing with posture and locomotion (Lieberman, 2008; Madsen, Sampson, & Townsend, 2008). This, in turn, may be also relevant for more general somatic factors such as body size or for the functional morphology of cranial airways (Bastir & Rosas, 2016). Taking into account the effect of the cranial base on facial morphology (Bastir & Rosas, 2006; Bastir et al., 2006; Neaux et al., 2013; Neaux, Gilissen, Coudyzer, & Guy, 2015), it could be hence hypothesized that both base and braincase can influence the position of the facial system, through independent factors.

The second component of variation, instead, is largely associated with a vertical stretching of the cranial base, and it influences the parietal bone only in terms of its general orientation: tall skulls must have the parietal bones more rotated backward. Beyond such spatial adjustment, basicranial vertical stretching is apparently not associated with general parietal proportions. This vertical variation can be probably a sexual component previously described in other shape and form analyses (Bruner & Ripani, 2008; Rosas & Bastir, 2002). Also these vertical changes have been hypothesized to be associated with facial morphology, nasal cavity, cranial airway size, and possible energetic differences (Bastir & Rosas, 2016; Bastir et al., 2011; Hall, 2005) bridging structural and functional and evolutionary cranial patterns (Bastir & Rosas 2016; Biegert, 1957; Enlow, 1990; Lieberman, 2011). The morphogenesis of the vault bones is generally more linear, while the cranial base is sensitive to distinct factors. It is not by chance that the imprints of the brain sulcal patterns are more marked on the floor of the anterior and middle fossa, that is where the structural conflict between brain and skull is more patent, because of spatial constraints with orbits and mandible, for the frontal and temporal cortex respectively (Bruner, 2015).

Interestingly, although we do not find evidence of spatial correlation between parietal and temporal cranial districts in adult humans, their relative cortical volumes are inversely correlated, and larger parietal lobes are associated with smaller temporal lobes (Allen, Damasio, & Grabowski, 2002). An opposite situation can be described for the occipital districts, that do not display volumetric correlation of the lobes (Allen et al., 2002) but an inverse shape of the bones (Gunz & Harvati, 2007). Such dissociation stresses further the importance of local factors in shaping the head phenotype, and the absence of global patterns of integration.

5 | CONCLUSIONS

The hypothesis of independence between parietal shape and endocranial base cannot be rejected by the current data, at least when dealing with intra-specific adult variation. These two districts interact in terms of their spatial orientation, but not in terms of their morphological proportions. Independence between sagittal and lateral cranial areas has been already hypothesized (Bastir & Rosas, 2006; Neaux et al., 2013), and this study extends this result to the braincase: parietal proportions, mostly influencing the sagittal skull morphology, have no apparent local effect on the position of the temporal tips, that is on the lateral basicranium. Parietal size and shape variation is confirmed to be a major determinant of adult head phenotype (Bruner, Rangel de Lázaro, et al., 2014; Bruner, Amano, et al., 2015; Bruner, Román, et al., 2015; Bruner, Preuss, et al., 2017; Bruner, Pereira-Pedro, et al., 2017), but the anterior displacement of the temporal poles relatively to the endocranial base is not likely to be a consequence of the parietal enlargement among adult modern humans. This absence of association between parietal and basicranial morphology may suggest minor or negligible constraints in this sense also at evolutionary level. Of course intra-specific and inter-specific patterns of variation can be based on different rules and distinct channeling schemes (Martin & Barbour, 1989). This can be only evaluated using large fossil samples to investigate basicranial and parietal morphological covariation. Unfortunately, because of the fragile nature of the basicranial bones, the available fossil samples are often insufficient to provide reliable statistical inferences. It is worth noting that modern humans are also characterized by a specific position of the cerebellum, which is in a very anterior location when compared with non-modern human species (Grimaud-Hervé, 1997). In this sense, although there is a clear evidence for endocranial basicranial retraction of facial attachment sites (which is part of facial shortening; Bastir & Rosas, 2016) future studies must consider the relationships between temporal morphology, facial shortening, and the whole displacement of the basicranial cerebral and cerebellar elements. This necessarily involves the study of hard and soft tissue relations in the craniofacial system. In fact in modern humans, particularly in dolicho-cephalic head form pattern (Enlow, 1990, Bastir & Rosas, 2006), the temporal lobe is bent against the anterior surface of the middle fossa, remarking potentially a spatial conflict with the facial block, and twisting the anterior portions of the lateral temporal gyri toward the midline and onto the base of the fossa. This spatial arrangement needs further investigation, in terms of ontogeny and of morphological correspondence between cortical and bone surfaces.

At present, we cannot discard that such different position of the temporal tips can be a direct consequence of the increased size of the temporal lobes as described in modern humans when compared with living apes (Rilling, 2006). Temporal morphology should be further investigated in terms of sulcal patterns, to evidence whether spatial changes during human evolution were also associated with changes of the folding schemes (Rosas, Peña-Melián, García-Tabernero, Bastir, & De La Rasilla, 2014). Finally, the analysis of the anatomical correspondence between temporal lobes and middle endocranial fossa will be mandatory to evaluate the possibility of more detailed and indirect quantification of the temporal variations in paleoneurology.

ACKNOWLEDGMENTS

Emiliano Bruner and Markus Bastir are funded by the Ministerio de Economía y Competitividad, Spain (EB: CGL2015-65387-C3-3-P; MB: CGL2012-37279, CGL2015-63648-P) and by the Italian Institute of Anthropology (Isita). ASPP is funded by the Atapuerca Foundation, Spain. The authors declare no conflict of interest.

REFERENCES

Allen, J. S., Damasio, H., & Grabowski, T. J. (2002). Normal neuroanatomical variation in the human brain: An MRI-volumetric study. *American Journal of Physical Anthropology*, *118*(4), 341–358.

Bastir, M., & Rosas, A. (2005). Hierarchical nature of morphological integration and modularity in the human posterior face. *American Journal of Physical Anthropology*, *128*(1), 26–34.

Bastir, M., & Rosas, A. (2006). Correlated variation between the lateral basicranium and the face: A geometric morphometric study in different human groups. *Archives of Oral Biology*, *51*(9), 814–824.

Bastir, M., & Rosas, A. (2016). Cranial base topology and basic trends in the facial evolution of Homo. *Journal of Human Evolution*, *91*, 26–35.

Bastir, M., Rosas, A., Gunz, P., Peña-Melian, A., Manzi, G., Harvati, K., . . . Hublin, J.-J. (2011). Evolution of the base of the brain in highly encephalized human species. *Nature Communications*, *2*, 588.

Bastir, M., Rosas, A., & O'higgins, P. (2006). Craniofacial levels and the morphological maturation of the human skull: Spatiotemporal pattern of cranial ontogeny, M. Bastir et al. *Journal of Anatomy*, *209*(5), 637–654.

Biegert, J. (1957). Der Formwandel des Primatenschädels und seine Beziehungen zur ontogenetischen Entwicklung und den phylogenetischen Spezialisationen der Kopforgane. *Gegenbaurs Morphol Jahrb*, *98*, 77–199.

Bookstein, F. L. (1991). *Morphometric Tools for Landmark Data: Geometry and Biology*. Cambridge, UK: Cambridge University Press.

Bruner, E. (2003). Fossil traces of the human thought: Paleoneurology and the evolution of the genus *Homo*. *Journal of Anthropological Sciences*, *81*, 29–56.

Bruner, E. (2004). Geometric morphometrics and paleoneurology: Brain shape evolution in the genus *Homo*. *Journal of Human Evolution*, *47* (5), 279–303.

Bruner, E. (2015). Functional craniology and brain evolution. In E. Bruner (Ed.), *Human Paleoneurology* (pp. 57–93). Switzerland: Springer.

Bruner, E., Amano, H., de la Cuétara, J. M., & Ogihara, N. (2015). The brain and the braincase: A spatial analysis on the midsagittal profile in adult humans. *Journal of Anatomy*, *227*(3), 268–276.

Bruner, E., De La Cuétara, J. M., & Holloway, R. (2011). A bivariate approach to the variation of the parietal curvature in the genus *Homo*. *Anatomical Record*, *294*(9), 1548–1556.

Bruner, E., De la Cuétara, J. M., Masters, M., Amano, H., & Ogihara, N. (2014). Functional craniology and brain evolution: From paleontology to biomedicine. *Frontiers in Neuroanatomy*, *8*, 19.

Bruner, E., Manzi, G., & Arsuaga, J. L. (2003). Encephalization and allometric trajectories in the genus Homo: Evidence from the Neandertal and modern lineages. *Proceedings of the National Academy of Sciences*, *100*(26), 15335–15340.

Bruner, E., Martin-Loeches, M., & Colom, R. (2010). Human midsagittal brain shape variation: Patterns, allometry and integration. *Journal of Anatomy*, *216*(5), 589–599.

Bruner, E., Pereira-Pedro, A. S., Chen, X., & Rilling, J. K. (2017). Precuneus proportions and cortical folding: A morphometric evaluation on a racially diverse human sample. *Annals of Anatomy*, *211*, 120–128.

Bruner, E., Preuss, T. M., Chen, X., & Rilling, J. K. (2017). Evidence for expansion of the precuneus in human evolution. *Brain Structure and Function*, *222*, 1053–1060.

Bruner, E., Rangel de Lázaro, G., de la Cuétara, J. M., Martín-Loeches, M., Colom, R., & Jacobs, H. I. L. (2014). Midsagittal brain variation and MRI shape analysis of the precuneus in adult individuals. *Journal of Anatomy*, *224*(4), 367–376.

Bruner, E., & Ripani, M. (2008). A quantitative and descriptive approach to morphological variation of the endocranial base in modern humans. *American Journal of Physical Anthropology*, *137*(1), 30–40.

Bruner, E., Román, F. J., de la Cuétara, J. M., Martin-Loeches, M., & Colom, R. (2015). Cortical surface area and cortical thickness in the precuneus of adult humans. *Neuroscience*, *286*, 345–352.

Cheverud, J. M. (1982). Relationships among ontogenetic, static, and evolutionary allometry. *American Journal of Physical Anthropology*, *59* (2), 139–149.

Enlow, D. H. (1990). *Facial growth*. Philadelphia: Sounders.

Gkantidis, N., & Halazonetis, D. J. (2011). Morphological integration between the cranial base and the face in children and adults. *Journal of Anatomy*, *218*(4), 426–438.

Gómez-Robles, A., Hopkins, W. D., & Sherwood, C. C. (2014). Modular structure facilitates mosaic evolution of the brain in chimpanzees and humans. *Nature Communications*, *5*, 4469.

Gould, S. J. (1966). Allometry and Size in Ontogeny and Phylogeny. *Biological Reviews*, *41*(4), 587–638.

Gould, S. J. (1977). *Ontogeny and Phylogeny*. Cambridge, MA: The Belknap Press of Harvard University Press.

Grimaud-Hervé, D. (1997). *L'évolution de l'encéphale chez l'Homo erectus et l'Homo sapiens*. Paris: CNRS.

Gunz, P., & Harvati, K. (2007). The Neanderthal "chignon": Variation, integration, and homology. *Journal of Human Evolution*, *52*(3), 262–274.

Hall, R. L. (2005). Energetics of nose and mouth breathing, body size, body composition, and nose volume in young adult males and females. *American Journal of Human Biology*, *17*(3), 321–330.

Hallgrimsson, B., Lieberman, D. E., Liu, W., Ford-Hutchinson, A. F., & Jirik, F. R. (2007). Epigenetic interactions and the structure of phenotypic variation in the cranium. *Evolution & Development*, *9*, 76–91.

Hammer, Ø., Ryan, P., & Harper, D. (2001). PAST: Paleontological Statistics software package for education and data analysis. *Palaeontologia Electronica*, *4*(1), 9.

Herculano-Houzel, S., & Lent, R. (2005). Isotropic fractionator: A simple, rapid method for the quantification of total cell and neuron numbers in the brain. *The Journal of Neuroscience*, *25*(10), 2518–2521.

Jeffery, N. (2002). Differential regional brain growth and rotation of the prenatal human tentorium cerebelli. *Journal of Anatomy*, *200*(2), 135–144.

Klingenberg, C. P. (2011). MorphoJ: An integrated software package for geometric morphometrics. *Molecular Ecology Resources*, *11*(2), 353–357.

Lieberman, D. E. (2008). Speculations about the selective basis for modern human craniofacial form. *Evolutionary Anthropology: Issues, News, and Reviews*, *17*(1), 55–68.

Lieberman, D. E., Hallgrímsson, B., Liu, W., Parsons, T. E., & Jamniczky, H. A. (2008). Spatial packing, cranial base angulation, and craniofacial shape variation in the mammalian skull: Testing a new model using mice. *Journal of Anatomy*, *212*(6), 720–735.

Lieberman, D. E., Pearson, O. M., & Mowbray, K. M. (2000). Basicranial influence on overall cranial shape. *Journal of Human Evolution*, *38*(2), 291–315.

Madsen, D. P., Sampson, W. J., & Townsend, G. C. (2008). Craniofacial reference plane variation and natural head position. *The European Journal of Orthodontics*, *30*(5), 532–540.

Martin, R. D., & Barbour, A. D. (1989). Aspects of line-fitting in bivariate allometric analyses. *Folia Primatologica*, *53*(1–4), 65–81.

Moss, M. L., & Young, R. W. (1960). A functional approach to craniology. *American Journal of Physical Anthropology*, *18*(4), 281–292.

Neaux, D., Gilissen, E., Coudyzer, W., & Guy, F. (2015). Implications of the relationship between basicranial flexion and facial orientation for the evolution of hominid craniofacial structures. *International Journal of Primatology*, *36*(6), 1120–1131.

Neaux, D., Guy, F., Gilissen, E., Coudyzer, W., & Ducrocq, S. (2013). Covariation between midline cranial base, lateral basicranium, and face in modern humans and chimpanzees: A 3D geometric morphometric analysis: Basicranium and face integration. *The Anatomical Record*, *296*(4), 568–579.

Neubauer, S., Gunz, P., & Hublin, J.-J. (2009). The pattern of endocranial ontogenetic shape changes in humans. *Journal of Anatomy*, *215*(3), 240–255.

Pereira-Pedro, A. S., Rilling, J. K., Chen, X., Preuss, T. M., & Bruner, E. (2017). Midsagittal brain variation among non-human primates: Insights into evolutionary expansion of the human precuneus. Unpublished.

Richtsmeier, J. T., Aldridge, K., DeLeon, V. B., Panchal, J., Kane, A. A., Marsh, J. L., … Cole, T. M. (2006). Phenotypic integration of neurocranium and brain. *Journal of Experimental Zoology Part B: Molecular and Developmental Evolution*, *306B*(4), 360–378.

Rilling, J. K. (2006). Human and nonhuman primate brains: Are they allometrically scaled versions of the same design?. *Evolutionary Anthropology: Issues, News, and Reviews*, *15*, 65–77.

Rilling, J. K., & Seligman, R. A. (2002). A quantitative morphometric comparative analysis of the primate temporal lobe. *Journal of Human Evolution*, *42*(5), 505–533.

Rohlf, F. J. (2013). tpsSuper 2.99. Retrieved from http://life.bio.sunysb.edu/morph/

Rohlf, F. J. (2014). tpsRelw 1.54. Retrieved fromhttp://life.bio.sunysb.edu/morph/

Rosas, A., & Bastir, M. (2002). Thin-plate spline analysis of allometry and sexual dimorphism in the human craniofacial complex. *American Journal of Physical Anthropology*, *117*(3), 236–245.

Rosas, A., Peña-Melián, A., García-Tabernero, A., Bastir, M., & De La Rasilla, M. (2014). Temporal lobe sulcal pattern and the bony impressions in the middle cranial fossa: The case of the El Sidrón (Spain) Neandertal Sample. *The Anatomical Record*, *297*(12), 2331–2341.

Roseman, C. C., Weaver, T. D., & Stringer, C. B. (2011). Do modern humans and Neandertals have different patterns of cranial integration? *Journal of Human Evolution*, *60*, 684–693.

Schindelin, J., Arganda-Carreras, I., Frise, E., Kaynig, V., Longair, M., Pietzsch, T., . . . Cardona, A. (2012). Fiji: An open-source platform for biological-image analysis. *Nature Methods*, *9*(7), 676–682.

Schneider, C. A., Rasband, W. S., & Eliceiri, K. W. (2012). NIH Image to ImageJ: 25 years of image analysis. *Nature Methods*, *9*(7), 671–675.

Singh, N., Harvati, K., Hublin, J.-J., & Klingenberg, C. P. (2012). Morphological evolution through integration: A quantitative study of cranial integration in *Homo*, *Pan*, *Gorilla*, and *Pongo*. *Journal of Human Evolution*, *62*, 155–164.

Zelditch, M. L., Swiderski, D. L., Sheets, H. D., & Fink, W. L. (2004). *Geometric Morphometrics for Biologists*. New York and London: Elsevier Academic Press.

SUPPORTING INFORMATION

Additional Supporting Information may be found in the online version of this article.

Supplementary Video 1: Spatial changes associated with PC1.
Supplementary Video 2: Spatial changes associated with PC2.

How to cite this article: Bruner E, Pereira-Pedro AS, Bastir M. Patterns of morphological integration between parietal and temporal areas in the human skull. *Journal of Morphology*. 2017;00:1–9. https://doi.org/10.1002/jmor.20714

Chapter 3

PARIETAL LOBE MORPHOLOGY: VARIATION OF THE LATERAL SURFACE THROUGH THE ANALYSIS OF ENDOCASTS

3. PARIETAL LOBE MORPHOLOGY: VARIATION IN THE LATERAL SURFACE THROUGH THE ANALYSIS OF ENDOCASTS

Endocasts comprise the only direct evidence on changes to the brain across an evolutionary lineage. However, inferences on brain anatomy depend on the clear imprint of the cortical features on the inner bony tables. Here we evaluate the assessment of parietal lobe morphology on endocasts. We use geometric morphometric models based on landmarks representing parietal lobe boundaries located on 3D reconstructions of endocasts.

In 3.1, we performed a comparative analysis of the parietal lobes variation across a sample of Old World monkeys (Cercopithecidae), which comprise a diversified primate group spanning a variety of ecological strategies. This study explores whether macroscopic changes to the parietal lobe could be associated with ecological factors. We also included topographic analysis of the parietal lobe surface through deformation-based methods.

In 3.2, we investigate the differences between Neanderthal and modern human parietal regions. This study incorporates landmarks representing parietal lobe boundaries into a dense endocranial landmark and semilandmark configuration in order to identify localized morphological differences to the parietal regions between these two human species.

3.1. PARIETAL LOBE VARIATION IN CERCOPITHECID ENDOCASTS

Authors: Ana Sofia Pereira Pedro, Amélie Beaudet, Emiliano Bruner
Journal: American Journal of Primatology - 81(7):e23025
Status: published in 2019

This study resulted from a research visit to the School of Geography, Archaeology and Environmental Studies (GAES), University of the Witwatersrand funded by the University of Burgos

Received: 5 January 2019 | Revised: 10 April 2019 | Accepted: 2 June 2019
DOI: 10.1002/ajp.23025

RESEARCH ARTICLE

AMERICAN JOURNAL OF PRIMATOLOGY WILEY

Parietal lobe variation in cercopithecid endocasts

Ana Sofia Pereira-Pedro[1] | Amélie Beaudet[2,3] | Emiliano Bruner[1]

[1]Programa de Paleobiología, Centro Nacional de Investigación sobre la Evolución Humana, Burgos, Spain
[2]School of Geography, Archaeology and Environmental Studies, University of the Witwatersrand, Johannesburg, South Africa
[3]Department of Anatomy, University of Pretoria, Pretoria, South Africa

Correspondence
Ana Sofia Pereira-Pedro, Centro Nacional de Investigación sobre la Evolución Humana, Paseo Sierra de Atapuerca 3, 09002 Burgos, Spain.
Email: sofia.aspp@gmail.com

Funding information
Fundación Atapuerca; Centre of Excellence in Palaeosciences; Italian Institute of Anthropology; Universidad de Burgos; Ministerio de Economía y Competitividad, Grant/Award Number: CGL2015-65387-C3-3-P; Claude Leon Foundation; Ministerio de Ciencia, Innovación y Universidades, Grant/Award Number: PGC2018-093925-B-C31

Abstract

In extant primates, the posterior parietal cortex is involved in visuospatial integration, attention, and eye-hand coordination, which are crucial functions for foraging and feeding behaviors. Paleoneurology studies brain evolution through the analysis of endocasts, that is molds of the inner surface of the braincase. These may preserve imprints of cortical structures, such as sulci, which might be of interest for locating the boundaries of major cortical regions. Old World monkeys (Cercopithecidae) represent an interesting zoological group for evolutionary studies, because of their diverse ecologies and locomotor behaviors. In this study, we quantify parietal lobe variation within the cercopithecid family, in a sample of 30 endocasts including 11 genera and 17 species, by combining landmark-based and landmark-free geometric morphometric analyses. More specifically, we quantitatively assess variation of the parietal proportions based on landmarks placed on reliable anatomical references and of parietal lobe surface morphology through deformation-based methods. The main feature associated with the cercopithecid endocranial variation regards the inverse proportions of parietal and occipital lobes, with colobines, *Theropithecus*, and *Papio* displaying relatively larger parietal lobes and smaller occipital lobes compared with cercopithecins. The parietal surface is anteroposteriorly longer and mediolaterally flatter in colobines, while longitudinally shorter but laterally bulging in baboons. Large parietal lobes in colobines and baboons are likely to be independent evolutionary traits, and not necessarily associated with analogous functions or morphogenetic mechanisms.

KEYWORDS
geometric morphometrics, Old World monkeys, parietal cortex, sulcal patterns, surface-based analysis

1 | INTRODUCTION

In primates, parietal lobes generally include the anterior parietal cortex, which mainly deals with somatosensory functions, and the posterior parietal cortex (PPC), which is a major associative region of the mammalian brain (Whitlock, 2017). The PPC receives multiple stimuli from sensorimotor, visual, and auditory systems, including information on spatial properties, motion, location, and orientation of objects, and integrate proprioceptive feedbacks for planning actions, such as eye saccades and visual fixation, or hand movements for reaching (reviewed in Grefkes & Fink, 2005). Furthermore, the PPC is also involved in attention, spatial navigation, and memory, and it has been suggested that its evolution in primates is influenced by explorative and feeding behaviors (Goldring & Krubitzer, 2017). In primates, the eyes and the hands are the main interfaces between brain and environment, and the processes of visuospatial integration that include body cognition and spatial perception, visual imagery and simulation, and eye-hand coordination, are directly involved in the evolution of the PPC (Bruner & Iriki, 2016). Eye-hand coordination is particularly important in the sense that reaching, grasping, and bringing food items to the mouth could have been the major selective force acting on the evolution of the PPC, a region that has increased in terms of size and complexity in primates, especially in humans (Goldring & Krubitzer, 2017). Indeed, the parietal lobes of modern humans are larger when compared with other living apes and to extinct human species, suggesting that regions within the PPC underwent expansion and reorganization in association with human-specific cognitive functions, such as tool use (Bruner, 2018; Catani et al., 2017; Kastner, Chen, Jeong, & Mruczek, 2017). However, in neurosciences, parietal cortical anatomy in primates has been mainly investigated in terms of cytoarchitecture, and data available mainly concern humans and macaques. Accordingly, despite the pivotal role of the parietal lobe in the evolution of primate brain and behavior, evidence documenting the cortical anatomy of the parietal region is relatively scarce or even absent for most of the primate taxa.

The Old World monkeys (superfamily Cercopithecoidea, family Cercopithecidae) represent a large primate group encompassing African and Asian species and spanning a variety of habitats, diets, body sizes, and social organizations. Connolly (1950), in his monograph, observed that their sulcal patterns were fairly uniform, though the two subfamilies differed regarding the relative location of the lunate sulcus, so Colobinae have larger parietal lobes while Cercopithecinae have larger occipital lobes. The description of fossil endocasts, i.e., molds of the inner surface of the braincase, provides additional evidence for discussing brain evolution in the different cercopithecoid lineages. In particular, Radinsky (1974) suggested that the cercopithecine sulcal pattern is derived as compared with that of the colobines, as the latter display some of the features of the prosimian pattern (i.e., smaller occipital lobes, and a similar course of the intraparietal sulcus to its prosimian homolog; Radinsky, 1974). Falk (1978) further described the differences in the sulcal patterns of cercopithecines and colobines, analyzing the endocasts of extant genera. For instance, cercopithecines display convergent Sylvian fissure and superior temporal sulcus, and relatively straight intraparietal and lunate sulci, while in colobines the first two sulci are parallel and the latter two are relatively arched (see Falk, 1978). The cited studies emphasize the endocasts' value for localizing boundaries and cortical proportions of the main cerebral regions through the examination of the sulcal references. Besides the description of sulcal patterns, the observed sulcal imprints could be useful for quantitative analysis through geometric morphometrics. Nonetheless, as endocasts only display partial information of the anatomical details, the use of landmarks based on brain structures is scarcely used (Neubauer, 2014; Pereira-Pedro & Bruner, 2018). On the other hand, it has been shown that sulcal patterns are easier to recognize on smaller endocasts, such as those of macaques because imprints are more marked and probably also because the sulcal schemes are simpler (Kobayashi et al., 2014; Van Minh & Hamada, 2017). In this context, Old World monkeys could be useful for analyses of lobe proportions, as sulcal imprints not only can be identified on their endocasts but have also been extensively studied and described.

More recently, new methods based on surface deformation are emerging in the effort to overcome problems associated with correspondence and localization of landmarks (Dupej et al., 2018; Durrleman, Pennec, Trouvé, Ayache, & Braga, 2012). Beaudet et al. (2016) applied landmark-free surface deformation methods, coupled with automatic detection of sulcal patterns, for quantifying the shape variation in cercopithecoid endocasts. They analyzed South African cercopithecoid fossil endocasts comparatively to the extant taxa, with a particular interest in *Theropithecus* subspecies and *Cercopithecoides williamsi*. The deformation methods subdivided the extant sample into groups corresponding to the main cercopithecid tribes—papionini, cercopithecini, and colobini. Regarding the cercopithecoid fossils, they observed that the fossil colobine *C. williamsi* displayed relative endocranial volume and sulcal pattern similar to papionins and that the sulcal pattern of fossil *Theropithecus* varies across subspecies and differs between the extinct and extant species (Beaudet et al., 2016).

In this study, we quantitatively describe the variation of the parietal lobe in extant cercopithecid endocasts through the use of imaging techniques and geometrical models. First, we use landmark-based geometric morphometric analysis to describe variation in the relative proportions of the parietal lobe, as previously reported by Radinsky (1974) and Falk (1978) based on visual inspection of endocasts. Second, we apply deformation-based models to the endocast's parietal lobe surface to further characterize parietal-only morphological variation. Considering the previously reported differences in the relative position of the lunate sulcus between the two subfamilies (Connolly, 1950; Falk, 1978; Radinsky, 1974), we expect the parietal lobes to be proportionally larger in colobines than in cercopithecines. Regarding morphological variation, we compare the parietal morphology in colobines and cercopithecines under the null hypothesis of no shape differences. By combining the two methods, we aim to provide a complementary analysis of the parietal morphology both in terms of overall form and localized variation.

2 | METHODS

This study was performed on virtual endocasts from previous studies and online collections (see below). The research complies with the American Society of Primatologists Principles for the Ethical Treatment of Nonhuman Primates, protocols of the appropriate Institutional Animal Care Committee, and legal requirements of each country housing collections.

2.1 | Sample

We follow the taxonomy adopted by Grubb et al. (2003). Our sample includes 30 cercopithecid endocasts spanning 11 genera and 17 species (Table 1). The specimens are all considered adult, according to teeth eruption. Sex differences are not considered in this study. The endocasts from most specimens have been reconstructed and analyzed previously in Beaudet et al. (2016). For the present work, we added three more specimens downloaded from the online platform MorphoSource (www.morphosource.org). These include two *Cercocebus torquatus* housed at the Museum of

TABLE 1 Cercopithecoid taxa and repositories

Genus	Species	N	Repository
Colobinae (colobines)			
Colobus	*C. guereza*	6	MRAC; AMNH; MNHN
Piliocolobus	*P. foai*	1	MRAC
Cercopithecinae (cercopithecines)			
Cercopithecini (cercopithecins)			
Cercopithecus	*C. cephus*	2	MHNT
Chlorocebus	*C. aethiops*	2	MHNT
	C. pygerythrus	2	MRAC
Erythrocebus	*E. patas*	1	MHNT
Papionini (papionins)			
Cercocebus	*C. atys*	1	MRAC
	C. turquatus	2	MCZ
Lophocebus	*L. albigena*	2	MRAC; MNHN
Macaca	*M. mulatta*	1	MHNT
	M. sylvanus	1	MHNT
Mandrillus	*M. leucophaeus*	2	MRAC
Papio	*P. anubis*	1	MNHN
	P. cynocephalus kindae	1	MRAC
	P. hamadryas	1	MNHN
	P. ursinus	1	MNHN
Theropithecus	*T. gelada*	3	AMNH; MNHN

Note: Taxonomy based on Grubb et al. (2003).
Abbreviations: AMNH, American Museum of Natural History, New York; MCZ, Museum of Comparative Zoology, Harvard University; MNHN, Muséum National d'Histoire Naturelle, Paris; MHNT, Muséum d'Histoire Naturelle de Toulouse; MRAC, Musée royal de l'Afrique centrale, Tervuren.

Comparative Zoology, Harvard University (Cambridge, MA), and digitized by Copes, Lucas, Thostenson, Hoekstra, and Boyer (2016) and one *Theropithecus gelada* from the Delson Primate Scans Project and the American Museum of Natural History (New York, NY). The virtual endocasts of these three specimens were digitally reconstructed by using the Endex software (Subsol, Gesquière, Braga, & Thackeray, 2010).

2.2 | Landmark analysis

We chose a set of 25 anatomical landmarks largely based on the cortical sulci that can be observed in the cercopithecoid endocasts (Figure 1 and Table 2). On the midsagittal contour, we placed three landmarks defining the boundaries between the parietal, occipital, and cerebellar regions (CS$_{\text{(mid)}}$, POB, and IOP). The other 22 landmarks were located on both hemispheres (11 each), and are either outmost points of the endocast (FP, OP, TP, CP, and BC) or limits or midpoints of the main sulci (IPS, CS$_{\text{(lat)}}$, SF, LU, AS, and PCS).

Landmarks were digitized in three dimensions using Landmark Editor (IDAV), and geometric morphometric analysis was performed with PAST v2.17c (Hammer, Ryan, & Harper, 2001) and MorphoJ v1.6b (Klingenberg, 2011). Landmarks were registered by Procrustes superimposition, which normalizes the information on size, position, and orientation (Zelditch, Swiderski, Sheets, & Fink, 2004). Configurations were symmetrized, averaging right and left hemispheres (Klingenberg, Barluenga, & Meyer, 2002). The number of individuals for each species does not allow a proper survey of the specific or intraspecific variation and, accordingly, we performed the analysis averaging the values for each genus. After registering the coordinates, the main patterns of variation were analyzed through Principal Component Analysis (PCA; Jolliffe, 2002; Zelditch et al., 2004) to identify the main shape differences among the genera. Allometry was tested by the correlation between shape coordinates and endocranial volumes. We used a two-tailed significance level of 0.05. In addition, we computed a cluster analysis by unweighted pair-group average (UPGMA) on the registered coordinates, to quantify the degree of morphological affinity between genera.

2.3 | Extraction of the parietal surface

To analyze the variation of the parietal surface only, we first had to define its limits on the endocasts for subsequent virtual separation from the rest of the endocranial surface (as in Beaudet & Bruner, 2017 for the frontal lobes). Based on previous works (Falk, 1978; Radinsky, 1974), we used the central sulcus as the anterior limit of the parietal lobe, and the lunate sulcus as its posterior limit. For the inferior limit, we used the Sylvian fissure, which roughly separates the parietal lobe from the temporal lobe, at least in its anterior region. However, as these anatomical references are not always visible on endocasts, we tentatively defined the parietal limits in terms of general geometric references. The inferior parietal limits

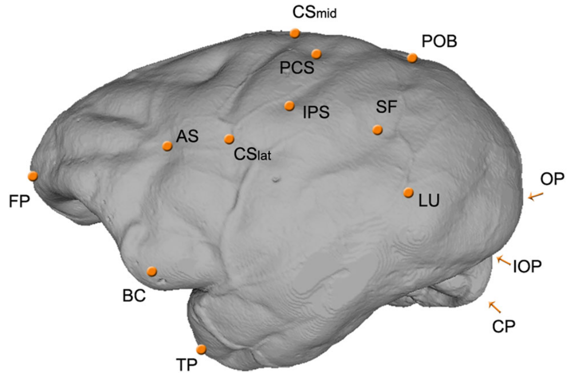

FIGURE 1 Anatomical landmarks used for the geometric morphometrics analysis: AS, arcuate sulcus; BC, Broca's cap; CP, cerebellar pole; CS$_{\text{(lat)}}$, central sulcus (lateral); CS$_{\text{(mid)}}$, central sulcus (midsagittal); FP, frontal pole; IOP, internal occipital protuberance; IPS, intraparietal sulcus; LU, lunate sulcus; OP, occipital pole; PCS, postcentral notch; POB, parietooccipital boundary; SF, Sylvian fissure; TP, temporal pole. See Table 2 for the definition of the landmarks. Specimen: *Chlorocebus aethiops*, Cercopithecini, Cercopithecinae

TABLE 2 Anatomical landmarks and definitions

Landmark	Meaning	Location
$CS_{(mid)}$	Central sulcus (midsagittal)	Point of intersection of the central sulcus with the midline
POB	Parieto-occipital boundary	Point of intersection of the lunate sulcus with the midline
IOP	Internal occipital protuberance	Point of intersection of the four divisions of the cruciform eminence
FP	Frontal pole	Anterior most point; point of maximum curvature
OP	Occipital pole	Posterior most point; point of maximum curvature
TP	Temporal pole	Anterior end of temporal lobe; point of maximum curvature
CP	Cerebellar pole	Outmost point; point of maximum curvature
BC	Broca's cap	Point of maximal width on the frontal region homologous to human Broca's area
AS	Arcuate sulcus	Point of maximal bending, following the length of the frontal sulcus
$CS_{(lat)}$	Central sulcus (lateral)	Inferior limit of the central sulcus
PCS	Postcentral notch	A point of depression anterior and superior to the Intraparietal sulcus
IPS	Intraparietal sulcus	Inferior limit of the intraparietal sulcus
SF	Sylvian fissure	Posterior limit of the Sylvian fissure/lateral sulcus
LU	Lunate sulcus	Inferior limit of the lunate sulcus

correspond to a plane defined by two landmarks placed on the inferior point of the central sulcus and on the posterior point of the Sylvian fissure of both hemispheres. The posterior limits correspond to a plane defined by four landmarks located on the left and right lunate sulci, two of them intersecting the previous plane. The anterior and superior borders correspond to the central sulcus and interhemispheric scissure, respectively. The definition of the parietal limits and subsequent extraction of the parietal surfaces was

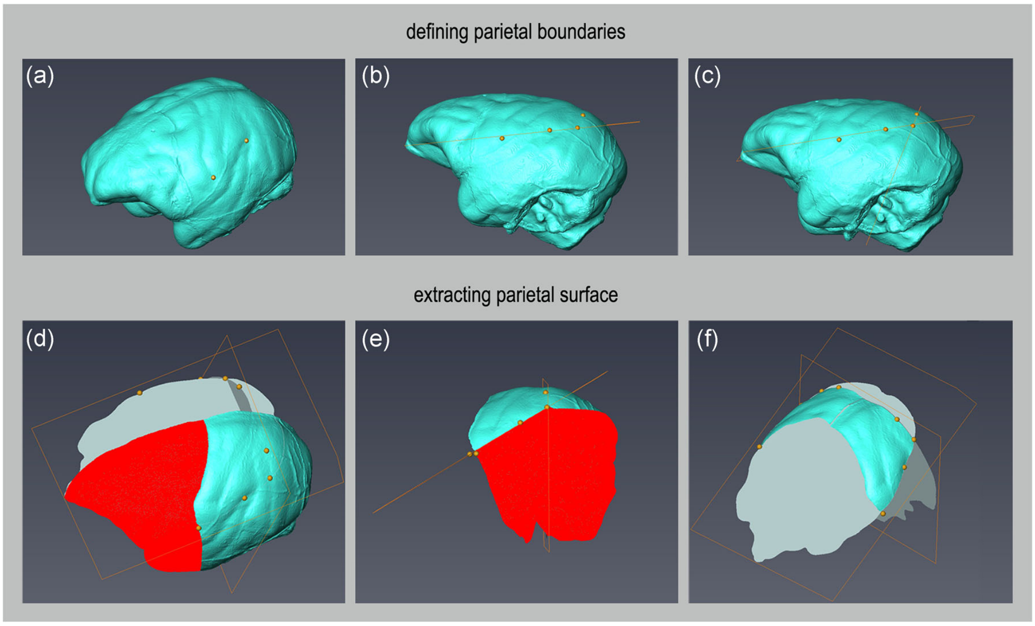

FIGURE 2 Steps for separating the parietal surfaces from the rest of the endocast: the parietal boundaries are delimited by cross-sections defined by four landmarks placed on both hemispheres (upper panel), and the parietal surface on each hemisphere is extracted by deleting the extra-parietal regions (red areas, lower panel). (a) Location of landmarks on the central sulcus and Sylvian fissure; (b) cross-section defined by the landmarks on (a) and location of the landmarks on the lunate sulcus, which define the cross-section for the posterior border of the parietal (c). After deleting one of the hemispheres, the portion anterior to the central sulcus (red area in d), the portion inferior to the first cross-section (red area in e) and the portion posterior to the second cross-section (not shown) are selected and deleted. This is repeated on the other hemisphere, resulting in two separate parietal surfaces—left and right—for each specimen (f). Note that although shown together, each parietal surface was isolated separately. Specimen: *Macaca mulatta*, Papionini, Cercopithecinae

performed with the software Avizo v9.0. (Visualization Sciences Group Inc.), following the steps illustrated in Figure 2. Two separated parietal surfaces left and right were generated for each specimen.

2.4 | Surface deformation methods

The deformation-based models are based on the metric of currents (i.e., a nonparametric representation of shapes as vector fields), which does not assume point-to-point correspondence, allowing for direct comparison of surfaces, measuring the distance between the surfaces as well as the difference between their local orientations (Beaudet & Bruner, 2017; Beaudet et al., 2016; 2018; Durrleman et al., 2012). Following the protocol detailed in Beaudet et al. (2016), endocasts were rigidly aligned in position, orientation, and scale with respect to a reference surface (randomly selected) using the iterative closest point algorithm. A global mean shape (group average) was computed from the set of aligned surfaces and then deformed into each specimen (for further details see Beaudet et al., 2016; 2018; Durrleman et al., 2014). The deformation fields integrating local orientation and the amplitude of the deformations from the global mean shape into each specimen were statistically analyzed through PCA. We consider only the parietal surfaces, analyzing left and right separately. The magnitudes are illustrated by a color code which ranges from dark blue (lowest displacement values) to red (highest displacement values). The computation was performed with the free software Deformetrica (www.deformetrica.org) by using the supercomputer available at the Centre for High-Performance Computing of Cape Town (https://www.chpc.ac.za/).

3 | RESULTS

3.1 | Landmark analysis

Considering the PCA computed on the genus averages, only the first and second PCs were found to be above the threshold for random variation, explaining 66.5% of the variance. Subsequent PCs were below the threshold of random variation, and will not be considered here (Jolliffe, 2002). The distribution of genera and variation in the endocranial shape described by each component is shown in Figure 3. PC1 accounts for 46.4% of the variance, describing the longitudinal (antero-posterior) proportions of the parietal and occipital lobes. Along with this component, colobines, *Papio*, and *Theropithecus* are distributed toward the positive values, displaying larger parietals and reduced occipitals, while cercopithecines plot toward the negative values and show the opposite proportions. The remaining papionins are distributed in between the cercopithecines and the colobines. PC2 explains 20.2% of the variation in shape, and it is associated with variation in height of the vault, especially on the parieto-occipital region. Colobines are characterized by low and flat braincases while cercopithecines, and particularly the baboons, display comparatively taller vaults.

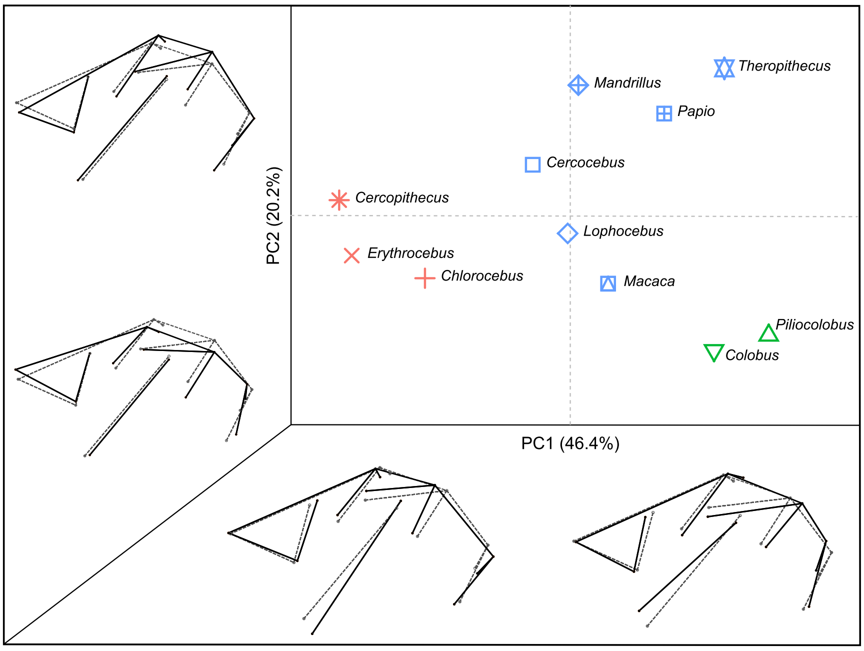

FIGURE 3 Results from the PCA of the endocast shape according to the landmark analysis. Distribution of specimens on the PC1 vs. PC2 plot and wireframes illustrating the shape changes along each axis. The colors on the PCA plot represent the tribes: red, Cercopithecini; blue, Papionini; and green, Colobini. Wireframes show the mean shape (dashed lines), and the shape variation (continuous lines) towards the negative and positive scores along each PC

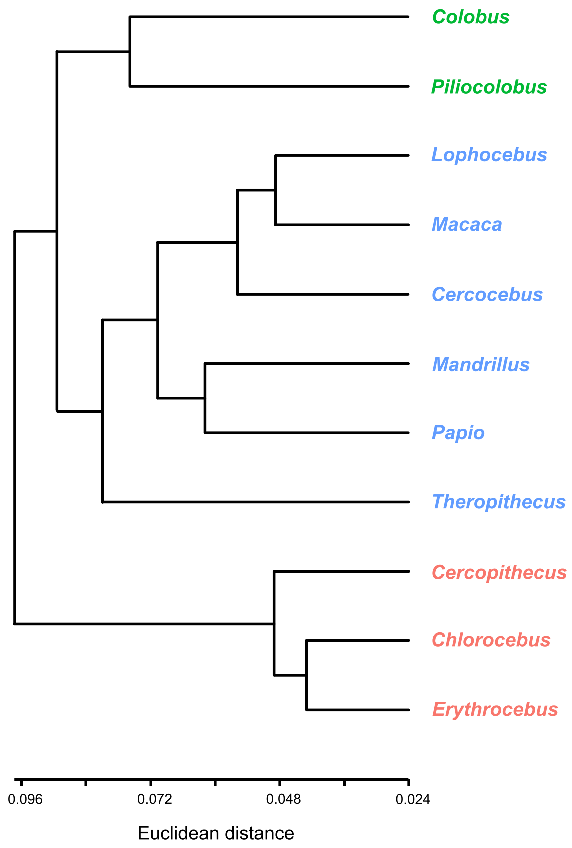

FIGURE 4 Unweighted pair-group averages computed on the registered (Procrustes) coordinates, showing the shape distances between the genera (Cercopithecini in red, Papionini in blue, and Colobini in green). Cophenetic correlation coefficient = 0.705

To further explore the morphological affinity between the genera, we computed a cluster analysis (UPGMA). The results show that the landmark set used is sufficient to separate the three tribes and group the different genera (Figure 4). According to the average shapes, Colobini and Papionini are more similar to each other than to Cercopithecini. The three cercopithecini genera display very similar mean shapes. In contrast, the two colobini genera are more distant to each other in terms of morphology. Within the papionins, *Theropithecus* shows the most distinct figure, *Mandrillus* is closer to *Papio*, and *Macaca* groups with the mangabeys.

The regression of the whole shape with endocranial volume indicates that the variation in the latter explains about 22% ($p \leq .05$) of total shape variation, with the allometric pattern associated with vault height (Figure 5). Endocranial volume is actually correlated with PC2 (68%; $p \leq .05$) but not with PC1 ($p = .23$). In the regression analysis, the colobines and *Theropithecus* depart from the apparent linear trend of the remaining genera.

3.2 | Surface deformation analysis

Figure 6 shows the plots of principal component analyses computed for the left and right parietal surfaces. In both analyses, variation along PC1 is associated with changes in the anteroposterior width of the parietal surface and the shape of the posteroinferior (i.e., the intersection between the lateral and the lunate sulci) and of the anteroinferior (i.e., intersection between the lateral and central sulci) angles. Variation along PC2 is related with changes in anteroposterior width, the shape of the anteroinferior angle, and the degree of inflation of the parietal surface. The distribution of specimens is similar on both PCAs. PC1 mainly separates cercopithecin genera, and *Macaca* and *Cercocebus*, from colobines, *Mandrillus*, *Papio*, and *Theropithecus*. The former group displays a relatively opened posteroinferior angle and a downward projection of the anteroinferior

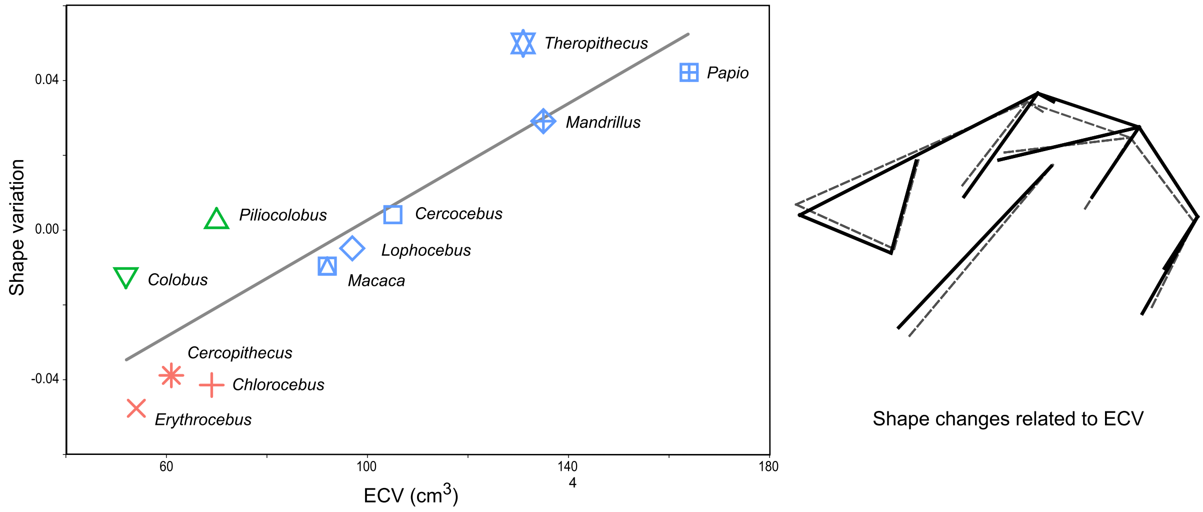

FIGURE 5 Regression of the whole shape variation on total endocranial volume (ECV): scatter plot (left) and associated shape variation (right). Cercopithecini in red, Papionini in blue, and Colobini in green

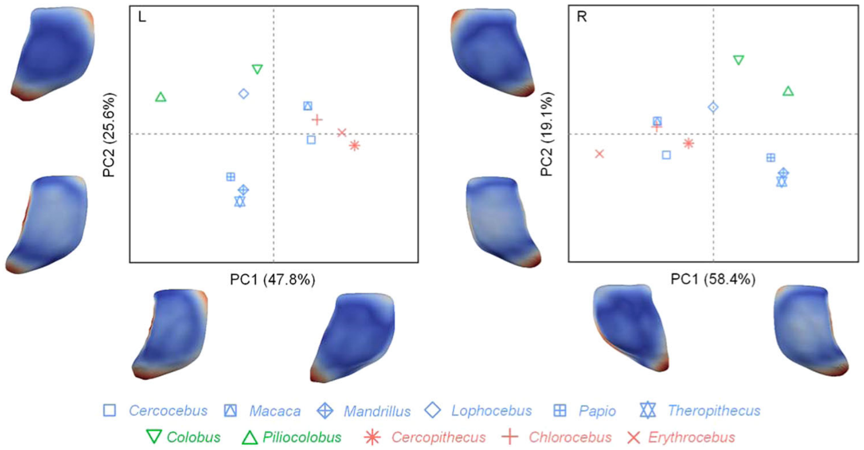

FIGURE 6 Results from PCA of the isolated left (L) and right (R) parietal surfaces according to the deformation methods. Plots of PC1 vs. PC2 are separated per hemisphere, with the PCA and respective color maps of the left parietal on the left panel, and those of the right parietal on the right panel. The colors on the PCA plot represent the tribes: red, Cercopithecini; blue, Papionini; and green, Colobini. The color maps display the morphological deformations of the parietal surfaces from the grand mean shape to the negative and positive scores of each axis, with the colors indicating the magnitude of displacement (blue: small; red: large)

angle, this later being somewhat forwardly projected in colobines and baboons. *Lophocebus* is intermediate between these two groups. PC2 mainly separates colobines and baboons. Colobines plot in the positive space of PC2 separately from the other groups of cercopithecids due to their anteroposteriorly wide and mediolaterally flattened parietal regions, combined with a relatively open anteroinferior angle. *Mandrillus*, *Papio*, and *Theropithecus* are to be found in the negative values of PC2 because of their anteroposteriorly narrow and mediolaterally inflated parietal areas.

4 | DISCUSSION

Despite the critical role of the parietal lobes in primate evolution and behavior, studies assessing variation in parietal morphology and proportions in the endocasts (and brains) of most primate taxa are still lacking. This might be due to inherent difficulties in locating major anatomical boundaries for digitizing landmarks. Nonetheless, reliable identification of the main sulcal patterns in monkey brains and endocasts is a feasible target (Beaudet et al., 2016; Falk, 1978; Kobayashi et al., 2014; Radinsky, 1974). This is particularly important as endocasts are the only direct evidence of brain anatomy in extinct primate species, and are therefore of prime interest for reconstructing the timing and mode of their cortical evolution. In this study, we compute a comparative neuroanatomical investigation of the cercopithecid parietal lobe shape by quantifying its proportions relative to the whole endocranium, and then compute a specific surface analysis on the parietal region, as to evidence local morphological variations.

4.1 | Variation in parietal proportions and shape

One of the purposes of this study was to test whether anatomical differences previously evidenced with descriptive approaches can also be supported through quantitative analysis and to provide quantification of the features involved. By including landmarks located on the main sulci that define the lobes, we attempt to reproduce the previously reported colobine and cercopithecine differences in cortical morphology. According to our landmark set, cercopithecid endocasts vary mostly on the anteroposterior proportions of the parietal and occipital lobes, with colobini exhibiting proportionately larger parietals and cercopithecini larger occipitals. These results are in line with previous descriptive findings on cercopithecid brains (Connolly, 1950) and endocasts (Falk, 1978; Radinsky, 1974), as we found differences between cercopithecinae and colobinae subfamilies. Moreover, our results further evidence that this difference in proportions is mostly between colobin and cercopithecin tribes since papionins display a larger range of variation in the parietal versus occipital proportions. Indeed, among papionins, *Papio*, and *Theropithecus* display proportions similar to colobins, while the remaining taxa have intermediate values. In addition, our geometric model reveals the second component of variation associated with the height of the parieto-occipital region that might indicate variation in the height of the braincase. Taking into account these two main features (parieto-occipital proportions and braincase height), colobines are characterized by larger parietal lobes and flat endocranial vaults; baboons have larger parietal lobes and tall vaults; cercopithecins display larger occipital lobes and intermediate heights; while *Macaca* and mangabeys tend to exhibit average cercopithecid brain proportions.

The other objective of the present study was to further examine parietal variation by considering the left and right parietal lobe surfaces separately through deformation methods. The results show that the main variation of the parietal surface is associated with the anteroposterior width and mediolateral inflation of the parietal surface, as well as with the configurations of the anteroinferior and posteroinferior angles. The null hypothesis of no morphological differences is hence falsified. These differences in morphology further confirm the larger anteroposterior dimensions of colobine parietals (Connolly, 1950; Falk, 1978; Radinsky, 1974), and indicate mediolateral expansion of the baboon parietal lobes. This latter variation could be due to the larger endocrania of the baboons. In addition, parietal-only variation is also driven by differences in the morphology of sulcal intersections, more specifically, on the junctions between the central sulcus and the lunate sulcus with the inferior parietal limit (Sylvian fissure). The variation on the anteroinferior angle could be explained by a variation on the curvature of the lower portion of the central sulcus, which might be more or less bent among cercopithecids (Connolly, 1950). The variation on the posteroinferior angle, given our methodology for defining the inferior parietal border, i.e., a plane passing through the central sulcus, Sylvian fissure, and lunate sulcus, could be influenced by variation in the extension and patterns of these three sulci. The pattern of the Sylvian fissure and lunate sulcus differ between the two subfamilies. In cercopithecines, the Sylvian fissure is bent and converges with the superior temporal sulcus, and the lunate sulcus is relatively straight, while in colobines, the Sylvian fissure is parallel to the superior temporal sulcus and the lunate sulcus is relatively curved (Falk, 1978). Moreover, baboons seem to display greater variability in their sulcal patterns in general and differ from other cercopithecines in the joint of the intraparietal sulcus with the lunate sulcus, which display a rather right angle (Connolly, 1950).

The variation in parietal versus occipital proportions was generally interpreted as a "displacement" of the lunate sulcus, either anteriorly, increasing the occipital cortex in cercopithecines (Falk, 1978; Radinsky, 1974), or posteriorly, increasing the parietal cortex in colobines (Connolly, 1950). This could indicate changes in the PPC, or more specifically in the superior parietal lobule (SPL; Gonzales, Benefit, McCrossin, & Spoor, 2015). In a study on the midsagittal brain variation among primates, the proportions of the precuneus—the midsagittal portion of the SPL—were found to be fairly preserved across monkeys and apes, though varying intra-specifically to the same extent in both chimpanzees and rhesus macaques (Pereira-Pedro, Rilling, Chen, Preuss, & Bruner, 2017). However, as the cited study included only one of the cercopithecid tribes, Papionini, it would be interesting to perform an additional study on the midsagittal brain variation together with Cercopithecini and Colobini to verify what region of the colobine brain is responsible for those differences.

Variation associated with height probably involves general changes on the braincase rather than localized changes to specific brain lobes, as this variation is only observed in the analysis of relative parietal proportion but not in the parietal-only morphology. Furthermore, changes in height correlate with size. Therefore, it is likely that this component of brain form variation is due to the general cranial architecture, rather than to regional brain cortical differences. Cranial shape variation among papionins seems to be largely influenced by allometry (e.g., Singleton, 2002). The characteristic high vaults of baboons have been reported previously. In a study of the midsagittal brain variation, baboons displayed higher vaults relative to other Papionini (Pereira-Pedro et al., 2017). Moreover, the elevation of the parietal surface was also detected in *Theropithecus* through deformation methods (see the Supporting Information material in Beaudet et al., 2016). Interestingly, the allometric analysis with overall endocranial shape variation indicates a clear deviation of the *Theropithecus*, *Colobus*, and *Piliocolobus*. This is probably due to their smaller relative brain sizes compared with similar-sized taxa, which in turn has been associated with their herbivorous diet (Clutton-Brock & Harvey, 1980; Gonzales et al., 2015).

4.2 | Limitations and methodological considerations

The main limit of this study regards the reduced sample size. Our sample is composed of 30 specimens spanning 11 genera, which results in some genera including only a few individuals. Further analyses on endocranial anatomy should be based on larger samples, and include a larger number of specimens within each genus. Other authors have recommended avoiding mixing males and females, for instance, in analyses of volume variation (Isler et al., 2008) and sulcal length asymmetry (Imai, Sawada, Fukunishi, Sakata-Haga, & Fukui, 2011). However, in the case of sulcal patterns, mixing males and females should have no influence on the results, as sex differences do not exceed individual variability (Connolly, 1950).

In general, the distribution of the genera in the shape space is similar in both methods, with the genera being roughly separated by the main tribes predominantly driven by the dimensions of the parietal lobe. However, it is important to note that the two methodological approaches are intrinsically distinct as they are based on different types of data (landmarks vs. surface) and target different information, and thus should be regarded as complementary. The landmark analysis is meant to provide information on parietal variation relative to the whole brain (endocast), i.e., in terms of proportional changes, while the surface deformation analysis was used to gain further insight into the local variation that cannot be captured by landmarks. This study constitutes the first attempt to isolate the parietal surface from endocasts. Results suggest that our approach to extract the parietal region can be useful to investigate the parietal variation, and can also give some insights into variation of sulcal patterns. Nonetheless, it must be taken into account that this is only possible when using specimens in which the traces of the cortical sulci can be distinguished on the endocast, which would be difficult in larger primate species with smoother sulcal imprints.

4.3 | Implications for cercopithecid parietal evolution

The differences in parietal and occipital lobe proportions among cercopithecoids could result from the evolutionary expansion of either the occipital cortex in cercopithecini or the parietal cortex in colobini and baboons. Previous research has focused on the evolution of the occipital cortex, given the contribution of vision to primate brain evolution (Kirk, 2006). For instance, it has been shown that specific visual mechanisms have increased with encephalization in primates, particularly those associated with the analysis of fine detail and color, processed by the parvocellular system of the lateral geniculate nucleus (Barton, 1998). Cercopithecines display six parvocellular layers, while some colobines have fewer, which might be associated with differences in visual processing (de Sousa, Sherwood, Hof, & Zilles, 2013). In macaques, about 55% of the neocortex is visual in function (Felleman & Van Essen, 1991), and the volume of the primary visual cortex increases rapidly with brain size (de Sousa et al., 2010). Larger primary visual cortex can process more information and represent the visual field with more detail, thus increasing visual acuity (de Sousa & Proulx, 2014). However, the visual areas are not only restricted to the occipital lobes (Felleman & Van Essen, 1991), and the larger primary visual cortex might also indicate an increase in connectivity (de Sousa & Proulx, 2014). Moreover, the relatively smaller colobine occipital lobes do not explain why their parietal lobes are larger.

According to Strasser and Delson (1987), most of the anatomical characters distinguishing colobines and cercopithecines are associated with either dietary specializations or locomotor behavior. Visuospatial integration and eye-hand coordination, functions that are essential both for locomotion and feeding behaviors, are processed within the parietal cortex. For instance, the posterior parietal cortex is undoubtedly involved in various forms of visuospatial processing (Kravitz, Saleem, Baker, & Mishkin, 2011), and is part of the dorsal visual stream, integrating identification and spatial location of objects and information on the movement type and part of the body performing it (Freud, Plaut, & Behrmann, 2016). It ultimately has a role in manual dexterity, a distinctive feature of primates (Ross & Martin, 2007).

Gonzales et al. (2015) associated the expansion of colobine SPL to their specialized folivorous diet, specifically to reaching and grasping functions (Bakola, Gamberini, Passarelli, Fattori, & Galletti, 2010; Hadjidimitrakis, Breveglieri, Bosco, & Fattori, 2012) needed for picking up leaves. However, all cercopithecids use their hands to reach and grasp their food, and, as our results show, *Papio* also tend to have proportionately larger parietals, on average, despite being omnivores.

According to van Schaik, Deaner, and Merrill (1999), most of the highly-dexterous genera show tool to use for feeding. Considering only the genera within our study, they observed complex manipulation and use of tools for feeding (mostly in captivity) among *Cercopithecus*, *Erythrocebus*, *Macaca*, *Cercocebus*, *Papio*, and *Mandrillus*. *Theropithecus*, in spite of showing complex manipulation, does not use feeding tools. *Colobus* shows neither hand dexterity nor use of tools. Colobines have a particular hand morphology, characterized by evolutionary reduction, or loss, in the case of *Colobus*, of the thumb (Frost, Gilbert, Pugh, Guthrie, & Delson, 2015; Strasser & Delson, 1987), which is regarded as an adaptation to arboreal life (e.g., Nakatsukasa et al., 2010). In contrast, *Theropithecus* and *Cebus* convergently evolved hand proportions similar to those of humans, with short lateral digits and longer thumbs relative to digits (Almécija, Smaers, & Jungers, 2015). This hand morphology, typical of terrestrial quadruped primates, is compatible with opposable thumbs, and enhances complex manipulation, as in baboons and geladas (Heldstab et al., 2016). Besides substrate use, the evolution of hand dexterity and complex manipulation in primates required changes within the brain (Heldstab et al., 2016), which might have involved an extension of the PPC and somatosensory cortex (Almécija & Sherwood, 2017). It would be interesting to investigate the cortical differences in somatosensory representations between colobines and cercopithecines.

Interestingly, among the New World monkeys, the genus *Cebus* seems to have independently evolved some cercopithecid traits, namely, a similar sulcal pattern (Connolly, 1950; Gonzales et al., 2015), and an opposable thumb, coupled with the ability to use tools for feeding (Goldring & Krubitzer, 2017; Padberg et al., 2007). Padberg et al. (2007) suggested that the emergence of parietal cortical areas involved in skilled hand use in New and Old World monkeys is an outcome of the development of similar hand morphology and use in both families. Including *Cebus* specimens in our analysis would add invaluable information concerning the variation of the parietal lobe anatomy and proportions.

Larger parietal proportions are displayed by Colobines, *Theropithecus*, and *Papio*, which have distinct ecological niches, diets, and locomotion. Therefore, gross morphological brain variations are likely to be due to distinct aspects, and not only influenced by shared ecological factors. In this context, the evolution of large parietal independently in colobines and baboons cannot be ruled out. Aristide et al. (2016) observed significant convergence in overall endocranial shape in different platyrrhine families. Moreover, factors other than ecology could have played a role in parietal evolution. For instance, Falk (1981) associated the anterior displacement of the arcuate sulcus in geladas to an expansion of the somato-motor face representation due to their ability to retract the lip. Additional studies should consider variation in cytoarchitecture and functional parcellation within the parietal cortex to fully understand which roles contributed the most to the variation in the proportion of this lobe within cercopithecids. For instance, it would be interesting to investigate the cytoarchitectonic and functional changes within the parietal cortex in species with rudimentary thumbs in contrast to species with opposable thumbs, especially considering the areas containing a topographic map of the body parts (Padberg et al., 2007).

ACKNOWLEDGMENTS

For their technical and/or scientific discussion/collaboration, we are grateful to J. Braga (Toulouse), S. Durrleman (Paris), J. Dumoncel (Toulouse), D. Stratford (Johannesburg), G. Subsol (Montpellier). We are indebted to J. Cuisin (Paris), G. Fleury (Toulouse), E. Gilissen and W. Wendelen (Tervuren) for having granted access to material under their care. We also thank C. Tenailleau and B. Duployer (Toulouse), G. Clément, and M. Garcia-Sanz (Paris) for the microtomographic acquisitions. This study was supported by the Italian Institute of Anthropology, and by a travel fellowship approved by Universidad de

Burgos (Spain). ASPP is funded by Fundación Atapuerca. AB is funded by the Claude Leon Foundation and by the Centre of Excellence in Palaeosciences. EB is funded by Ministerio de Ciencia, Innovación y Universidades PGC2018-093925-B-C31). The authors would like to thank the Centre for High-Performance Computing (CHPC) in South Africa for granting access to the computational resources used in this work.

CONFLICT OF INTERESTS

The authors declared that there is no conflict of interests.

ORCID

Ana Sofia Pereira-Pedro http://orcid.org/0000-0002-8724-255X
Amélie Beaudet http://orcid.org/0000-0002-9363-5966
Emiliano Bruner http://orcid.org/0000-0002-6686-4616

REFERENCES

Almécija, S., & Sherwood, C. C. (2017). Hands, brains, and precision grips: Origins of tool use behaviors. In L. Krubitzer, & J. H. Kaas (Eds.), *Evolution of Nervous Systems, Volume 3: The Nervous System of Non-Human Primates* (pp. 299–315). Elsevier Academic Press.

Almécija, S., Smaers, J. B., & Jungers, W. L. (2015). The evolution of human and ape hand proportions. *Nature Communications*, *6*, 7717. https://doi.org/10.1038/ncomms8717

Aristide, L., dos Reis, S. F., Machado, A. C., Lima, I., Lopes, R. T., & Perez, S. I. (2016). Brain shape convergence in the adaptive radiation of New World monkeys. *Proceedings of the National Academy of Sciences*, *113*(8), 2158–2163. https://doi.org/10.1073/pnas.1514473113

Bakola, S., Gamberini, M., Passarelli, L., Fattori, P., & Galletti, C. (2010). Cortical connections of parietal field PEc in the macaque: Linking vision and somatic sensation for the control of limb action. *Cerebral Cortex*, *20*(11), 2592–2604. https://doi.org/10.1093/cercor/bhq007

Barton, R. A. (1998). Visual specialization and brain evolution in primates. *Proceedings of the Royal Society of London. Series B: Biological Sciences*, *265*, 1933–1937. https://doi.org/10.1098/rspb.1998.0523

Beaudet, A., & Bruner, E. (2017). A frontal lobe surface analysis in three African human fossils: OH 9, Buia, and Bodo. *Comptes Rendus Palevol*, *16*, 499–507. https://doi.org/10.1016/j.crpv.2016.12.002

Beaudet, A., Dumoncel, J., deBeer, F., Duployer, B., Durrleman, S., Gilissen, E., … Braga, J. (2016). Morphoarchitectural variation in South African fossil cercopithecoid endocasts. *Journal of Human Evolution*, *101*, 65–78. https://doi.org/10.1016/j.jhevol.2016.09.003

Beaudet, A., Dumoncel, J., deBeer, F., Durrleman, S., Gilissen, E., Oettlé, A., … Braga, J. (2018). The endocranial shape of *Australopithecus africanus*: Surface analysis of the endocasts of Sts 5 and Sts 60. *Journal of Anatomy*, *232*(2), 296–303. https://doi.org/10.1111/joa.12745

Bruner, E. (2018). The brain, the braincase, and the morphospace. In E. Bruner, N. Ogihara, & H. C. Tanabe (Eds.), *Digital Endocasts: from skulls to brains* (pp. 93–114). Japan: Springer.

Bruner, E., & Iriki, A. (2016). Extending mind, visuospatial integration, and the evolution of the parietal lobes in the human genus. *Quaternary International*, *405*(A), 98–110. https://doi.org/10.1016/j.quaint.2015.05.019

Catani, M., Robertsson, N., Beyh, A., Huynh, V., deSantiago Requejo, F., Howells, H., … Dell'Acqua, F. (2017). Short parietal lobe connections of the human and monkey brain. *Cortex*, *97*, 339–357. https://doi.org/10.1016/j.cortex.2017.10.022

Clutton-Brock, T. H., & Harvey, P. H. (1980). Primates, brains, and ecology. *Journal of Zoology*, *190*(3), 309–323. https://doi.org/10.1111/j.1469-7998.1980.tb01430.x

Connolly, C. J. (1950). *External morphology of the primate brain*. Springfield Illinois: Charles C. Thomas.

Copes, L. E., Lucas, L. M., Thostenson, J. O., Hoekstra, H. E., & Boyer, D. M. (2016). A collection of nonhuman primate computed tomography scans housed in MorphoSource, a repository for 3D data. *Scientific Data*, *3*, 160001. https://doi.org/10.1038/sdata.2016.1

Dupej, J., Rangel de Lázaro, G., Pereira-Pedro, A. S., Pisová, H., Pelikán, J., & Bruner, E. (2018). Comparing endocranial surfaces: Mesh superimposition and coherent point drift registration. In E. Bruner, N. Ogihara, & H. C. Tanabe (Eds.), *Digital Endocasts: From skulls to brains* (pp. 143–152). Japan: Springer.

Durrleman, S., Pennec, X., Trouvé, A., Ayache, N., & Braga, J. (2012). Comparison of the endocranial ontogenies between chimpanzees and bonobos via temporal regression and spatiotemporal registration. *Journal of Human Evolution*, *62*(1), 74–88. https://doi.org/10.1016/j.jhevol.2011.10.004

Durrleman, S., Prastawa, M., Charon, N., Korenberg, J. R., Joshi, S., Gerig, G., … Trouvé, A. (2014). Morphometry of anatomical shape complexes with dense deformations and sparse parameters. *NeuroImage*, *101*, 35–49. https://doi.org/10.1016/j.neuroimage.2014.06.043

Falk, D. (1978). Brain evolution in old World monkeys. *American Journal of Physical Anthropology*, *48*(3), 315–319. https://doi.org/10.1002/ajpa.1330480307

Falk, D. (1981). Sulcal patterns of fossil *Theropithecus* baboons: Phylogenetic and functional implications. *International Journal of Primatology*, *2*(1), 57–69. https://doi.org/10.1007/BF02692300

Felleman, D. J., & VanEssen, D. C. (1991). Distributed hierarchical processing in the primate cerebral cortex. *Cerebral Cortex*, *1*, 1–47. https://doi.org/10.1093/cercor/1.1.1

Freud, E., Plaut, D. C., & Behrmann, M. (2016). 'What' is happening in the dorsal visual pathway. *Trends in Cognitive Sciences*, *20*(10), 773–784. https://doi.org/10.1016/j.tics.2016.08.003

Frost, S. R., Gilbert, C. C., Pugh, K. D., Guthrie, E. H., & Delson, E. (2015). The hand of *Cercopithecoides williamsi* (Mammalia, Primates): Earliest evidence for thumb reduction among colobine monkeys. *PLoS One*, *10*(5), e0125030. https://doi.org/10.1371/journal.pone.0125030

Goldring, A. B., & Krubitzer, L. A. (2017). Evolution of parietal cortex in mammals: From manipulation to tool use. In L. Krubitzer, & J. H. Kaas (Eds.), *Evolution of Nervous Systems, Volume 3: The Nervous System of Non-Human Primates* (pp. 259–286). Elsevier.

Gonzales, L. A., Benefit, B. R., McCrossin, M. L., & Spoor, F. (2015). Cerebral complexity preceded enlarged brain size and reduced olfactory bulbs in Old World monkeys. *Nature Communications*, *6*, 7580. https://doi.org/10.1038/ncomms8580

Grefkes, C., & Fink, G. R. (2005). The functional organization of the intraparietal sulcus in humans and monkeys. *Journal of Anatomy*, *207*(1), 3–17. https://doi.org/10.1111/j.1469-7580.2005.00426.x

Grubb, P., Butynski, T. M., Oates, J. F., Bearder, S. K., Disotell, T. R., Groves, C. P., … Struhsaker, T. T. (2003). Assessment of the diversity of African primates. *International Journal of Primatology*, *24*(6), 1301–1357. https://doi.org/10.1023/B:IJOP.0000005994.86792.b9

Hadjidimitrakis, K., Breveglieri, R., Bosco, A., & Fattori, P. (2012). Three-dimensional eye position signals shape both peripersonal space and arm movement activity in the medial posterior parietal cortex. *Frontiers in Integrative Neuroscience*, *6*, 37. https://doi.org/10.3389/fnint.2012.00037

Hammer, Ø., Ryan, P., & Harper, D. (2001). PAST: Paleontological statistics software package for education and data analysis. *Palaeontologia Electronica*, *4*(1), 1–9. https://doi.org/10.1.1.459.1289

Heldstab, S. A., Kosonen, Z. K., Koski, S. E., Burkart, J. M., vanSchaik, C. P., & Isler, K. (2016). Manipulation complexity in primates coevolved with brain size and terrestriality. *Scientific Reports*, *6*, 24528. https://doi.org/10.1038/srep24528

Imai, N., Sawada, K., Fukunishi, K., Sakata-Haga, H., & Fukui, Y. (2011). Sexual dimorphism of sulcal length asymmetry in the cerebrum of adult cynomolgus monkeys (*Macaca fascicularis*). *Congenital Anomalies*, *51*(4), 161–166. https://doi.org/10.1111/j.1741-4520.2011.00330.x

Isler, K., Christopher Kirk, E., Miller, J. M. A., Albrecht, G. A., Gelvin, B. R., & Martin, R. D. (2008). Endocranial volumes of primate species: Scaling analyses using a comprehensive and reliable data set. *Journal of Human Evolution*, *55*(6), 967–978. https://doi.org/10.1016/j.jhevol.2008.08.004

Jolliffe, I. T. (2002). *Principal Component Analysis* (2nd ed.). New York, NY: Springer.

Kastner, S., Chen, Q., Jeong, S. K., & Mruczek, R. E. B. (2017). A brief comparative review of primate posterior parietal cortex: A novel hypothesis on the human toolmaker. *Neuropsychologia*, *105*, 123–134DOI: 0.1016/j.neuropsychologia.2017.01.034

Kirk, E. C. (2006). Visual influences on primate encephalization. *Journal of Human Evolution*, *51*, 76–90. https://doi.org/10.1016/j.jhevol.2006.01.005

Klingenberg, C. P. (2011). MorphoJ: An integrated software package for geometric morphometrics. *Molecular Ecology Resources*, *11*(2), 353–357. https://doi.org/10.1111/j.1755-0998.2010.02924.x

Klingenberg, C. P., Barluenga, M., & Meyer, A. (2002). Shape analysis of symmetric structures: Quantifying variation among individuals and asymmetry. *Evolution; International Journal of Organic Evolution*, *56*(10), 1909–1920. https://doi.org/10.1111/j.0014-3820.2002.tb00117

Kobayashi, Y., Matsui, T., Haizuka, Y., Ogihara, N., Hirai, N., & Matsumura, G. (2014). Cerebral sulci and gyri observed on macaque endocasts. In T. Akazawa, N. Ogihara, H. C. Tanabe, & H. Terashima (Eds.), *Dynamics of Learning in Neanderthals and Modern Humans, Volume 2: Cognitive and Physical Perspectives* (pp. 131–137). Japan: Springer.

Kravitz, D. J., Saleem, K. S., Baker, C. I., & Mishkin, M. (2011). A new neural framework for visuospatial processing. *Nature Reviews Neuroscience*, *12*(4), 217–230. https://doi.org/10.1038/nrn3008

VanMinh, N., & Hamada, Y. (2017). Age-related changes of sulcal imprints on the endocranium in the Japanese macaque (*Macaca fuscata*). *American Journal of Physical Anthropology*, *163*(2), 285–294. https://doi.org/10.1002/ajpa.23205

Nakatsukasa, M., Mbua, E., Sawada, Y., Sakai, T., Nakaya, H., Yano, W., … Kunimatsu, Y. (2010). Earliest colobine skeletons from Nakali, Kenya. *American Journal of Physical Anthropology*, *143*(3), 365–382. https://doi.org/10.1002/ajpa.21327

Neubauer, S. (2014). Endocasts: Possibilities and limitations for the interpretation of human brain evolution. *Brain, Behavior, and Evolution*, *84*(2), 117–134. https://doi.org/10.1159/000365276

Padberg, J., Franca, J. G., Cooke, D. F., Soares, J. G. M., Rosa, M. G. P., Fiorani, M., … Krubitzer, L. (2007). Parallel evolution of cortical areas involved in skilled hand use. *Journal of Neuroscience*, *27*(38), 10106–10115. https://doi.org/10.1523/JNEUROSCI.2632-07.2007

Pereira-Pedro, A. S., & Bruner, E. (2018). Landmarking endocasts. In E. Bruner, N. Ogihara, & H. C. Tanabe (Eds.), *Digital Endocasts: From skulls to brains* (pp. 127–142). Japan: Springer.

Pereira-Pedro, A. S., Rilling, J. K., Chen, X., Preuss, T. M., & Bruner, E. (2017). Midsagittal brain variation among nonfuman primates: Insights into evolutionary expansion of the human precuneus. *Brain, Behavior, and Evolution*, *90*(3), 255–263. https://doi.org/10.1159/000481085

Radinsky, L. (1974). The fossil evidence of anthropoid brain evolution. *American Journal of Physical Anthropology*, *41*(1), 15–27. https://doi.org/10.1002/ajpa.1330410104

Ross, C. F., & Martin, R. D. (2007). The role of vision in the origin and evolution of primates. In T. M. Preuss (Ed.), *The Evolution of Nervous Systems, Volume 4: Primates* (pp. 59–78). Oxford: Elsevier.

vanSchaik, C. P., Deaner, R. O., & Merrill, M. Y. (1999). The conditions for tool use in primates: Implications for the evolution of material culture. *Journal of Human Evolution*, *36*(6), 719–741. https://doi.org/10.1006/jhev.1999.0304

Singleton, M. (2002). Patterns of cranial shape variation in the Papionini (Primates: Cercopithecinae). *Journal of Human Evolution*, *42*(5), 547–578. https://doi.org/10.1006/jhev.2001.0539

deSousa, A. A., & Proulx, M. J. (2014). What can volumes reveal about human brain evolution? A framework for bridging behavioral, histometric, and volumetric perspectives. *Frontiers in Neuroanatomy*, *8*, 51. https://doi.org/10.3389/fnana.2014.00051

deSousa, A. A., Sherwood, C. C., Hof, P. R., & Zilles, K. (2013). Lamination of the lateral geniculate nucleus of catarrhine primates. *Brain, Behavior, and Evolution*, *81*, 93–108. https://doi.org/10.1159/000346495

deSousa, A. A., Sherwood, C. C., Mohlberg, H., Amunts, K., Schleicher, A., MacLeod, C. E., … Zilles, K. (2010). Hominoid visual brain structure volumes and the position of the lunate sulcus. *Journal of Human Evolution*, *58*, 281–292. https://doi.org/10.1016/j.jhevol.2009.11.011

Strasser, E., & Delson, E. (1987). Cladistic analysis of cercopithecid relationships. *Journal of Human Evolution*, *16*(1), 81–99. https://doi.org/10.1016/0047-2484(87)90061-3

Subsol, G., Gesquière, G., Braga, J., & Thackeray, F. (2010). 3D automatic methods to segment 'virtual' endocasts: State of the art and future directions. *American Journal of Physical Anthropology*, *141*(Suppl. 50), 226–227.

Whitlock, J. R. (2017). Posterior parietal cortex. *Current Biology*, *27*(14), R691–R695. https://doi.org/10.1016/j.cub.2017.06.007

Zelditch, M. L., Swiderski, D. L., Sheets, H. D., & Fink, W. L. (2004). *Geometric Morphometrics for Biologists*. New York and London: Elsevier Academic Press.

How to cite this article: Pereira-Pedro AS, Beaudet A, Bruner E. Parietal lobe variation in cercopithecid endocasts. *Am J Primatol*. 2019;81:e23025. https://doi.org/10.1002/ajp.23025

3.2. A MORPHOMETRIC COMPARISON OF THE PARIETAL LOBE IN MODERN HUMANS AND NEANDERTHALS

Authors: Ana Sofia Pereira Pedro, Emiliano Bruner, Philipp Gunz, Simon Neubauer

Status: unpublished

This study resulted from a research visit to the Max Planck Institute for Evolutionary Anthropology funded by the Max Planck Institute for Evolutionary Anthropology

3.2. A MORPHOMETRIC COMPARISON OF THE PARIETAL LOBE IN MODERN HUMANS AND NEANDERTHALS

Abstract

The modern human brain and braincase have a characteristic globular shape including parietal and cerebellar bulging. In contrast, Neanderthals, though having similar brain size, displayed more elongated endocrania with flatter parietal and cerebellar regions. Here, we focus on the morphology of parietal lobes that are central to several cognitive functions including tool use or visual imaging. In paleoneurology, endocast shape analyses are either based on restricted landmarks that represent endocranial surface features homologous to cortical convolutions (impressions of brain gyri and sulci) or on dense meshes of semilandmarks that capture overall endocranial shape. Previous analyses using the former suggested that modern humans have relatively longer and taller parietal lobes than extinct human species while the latter emphasized parietal bulging without a significant size difference of parietal regions. In the present study, we combine both data types to investigate the morphological differences of the parietal cortex between modern humans and Neanderthals, as inferred based on endocasts. Our analyses were able to detect and confirm different parietal shapes, with modern humans displaying taller and anteroposteriorly extended parietal lobes. We also show size differences between these human groups, with modern humans having on average larger parietal lobes. Increase in surface area was located on the dorsal posterior district, as well as on the inferior parietal lobule, around the sulcus of Jensen, between the supramarginal gyrus, angular gyrus, and intraparietal sulcus. Despite the average morphological difference in parietal size and shape between modern humans and Neanderthals, their ranges of distribution are nonetheless overlapping. Further analyses on intra-specific variation in parietal lobe morphology within modern human brains should help understand the differences between globular and elongated endocrania. This is crucial since changes to the parietal cortex might affect associative and integrative functions between somatic and visual primary inputs.

Keywords: Paleoneurology; Parietal cortex; Shape analysis; Brain evolution; Endocasts

Introduction

The cognitive capacity of *Homo sapiens* is associated with specializations in brain size, cortical proportions, histology, connection patterns, and metabolic functions (Preuss, 2017). Comparative neuroanatomy and paleoneurology are therefore necessary to supply hypotheses on brain evolution in the human genus, integrating information from extinct and extant species (Bruner, 2019). Previous research has extensively focused on the frontal and temporal cortices due to their involvement in language production and understanding, as well as on the occipital cortex, implicated in visual processing. It has been shown that the frontal lobes of modern human are as large as expected for an ape with a similar brain size, although the prefrontal cortex displays a noticeable increase in connectivity (Schoenemann et al., 2005; Smaers et al., 2010; Donahue et al., 2018; Ardesch et al., 2019). Also the temporal lobes are larger than predicted for an ape with a human-sized brain (Rilling and Seligman, 2002), and may be larger in modern humans than in extinct human species (Bastir et al., 2008). The occipital lobes of modern *H. sapiens* are estimated to be smaller than in Neanderthals (Pearce et al., 2013), while the cerebellum seems to have expanded (Kochiyama et al. 2018; Neubauer et al. 2018; Gunz et al., 2019).

The parietal cortex occupies a central position within the brain, receiving input from the primary somatosensory and visual areas, and integrating these types of information in order to interpret the physical world. More specifically, the precuneus, which comprises the medial and dorsolateral parietal cortex, is involved in visually-guided behavior, mental imagery, and self-awareness (Cavanna and Trimble, 2006). It has been shown to be longitudinally expanded in humans compared to chimpanzees (Bruner et al., 2017a). On the lateral parietal cortex, the intraparietal sulcus, involved in visuomotor and attentional processes, seems to display more functional areas in humans, and with a different arrangement when compared to macaques (Grefkes and Fink, 2005). The left inferior parietal lobe is also specialized in humans, involved in social cognition and language processing (Bzdok et al., 2016), with the angular gyrus displaying increased connectivity (Catani et al., 2017). These regions represent crucial parts of the association cortex (Krienen and Buckner, 2017; Mars et al., 2017), and parietal changes in primates—especially in humans—have been hypothesized to be involved in tool use and technological extension (Bruner and Iriki, 2016; Goldring and Krubitzer, 2017; Valyear et al., 2017). Overall, compared to other primates, the parietal cortex of modern humans seems to have enlarged and become more diversified. These changes might have involved multiple factors, such as the size of specific cortical areas, or the evolution of new cortical elements, as well as changes in connectivity (Bruner, 2019).

When investigating evolutionary changes within the human lineage, in the absence of brains, endocasts, i.e. casts of the endocranial cavity, are the only source of information to approximate size and shape of the brain (Holloway et al., 2004; Neubauer, 2014; Bruner, 2017). One of the most apparent macroscopic differences in the braincase of modern humans concerns the parietal region (Bruner, 2018a). The characteristic round head is highly affected by large and bulging parietal bones (Bruner et al., 2011). Attempts to localize the boundaries of the cortical districts suggested that this change may be actually due to larger parietal lobes which, in modern humans, could be absolutely and relatively taller and longer than in any other human species (Bruner et al., 2003; Bruner, 2004). Such spatial change is mostly apparent on the dorsal parietal regions (Bruner, 2010). Comparing Neanderthals and modern humans is particularly appealing, because these two human groups shared a similar brain size but a different brain shape (Bruner et al., 2003; Gunz et al., 2010). Neanderthals apparently retained a plesiomorphic parietal length, but displayed wider dorsal parietal regions, while modern humans evolved both wider and longer parietal lobes (Bruner et al., 2003). Interestingly, the two lineages may have shared a more similar brain form around 200–300 ka (Bruner and Pearson, 2013), with *Homo sapiens* subsequently undergoing a globularization of the braincase in their later evolutionary stages (Hublin et al., 2017; Bruner et al., 2018; Neubauer et al., 2018). This globular endocranial shape develops early in ontogeny and is unique to modern humans (Neubauer et al., 2009; Gunz et al. 2010, 2012; Ponce de León et al., 2016; Neubauer and Gunz, 2018).

It is important to take into account that morphological variation of endocasts can be due to spatial adjustments of neurocranial bones (e.g., curvature or size of bones) or to changes in the neural tissue (Flaherty and Richtsmeier, 2013). Hence, the challenge in paleoneurology is to extract relevant information about brain morphology without overinterpreting endocranial variation actually related to overall cranial shape (Zollikofer et al., 2017; Scott et al., 2018). The identification of anatomical brain regions in endocasts is only possible through bosses and grooves that represent impressions of brain convolutions, or through neighboring spatial references (Bruner, 2018b). But since endocasts supply only a few neuroanatomical indications in this sense, and these impressions are often blurred, the localization of particular cortical boundaries is difficult and influenced by high uncertainty. One means to overcome these difficulties is considering endocranial shape as a whole by using endocranial landmarks and surface semilandmarks (e.g., Neubauer et al., 2009, 2010; Gunz et al., 2010). Although this approach reduces uncertainty associated with the location of anatomical landmarks, it captures brain shape more holistically, hence not capturing important information about how specific brain regions contribute to overall brain shape changes. In order to capture and investigate the contribution of a given brain region, such as the parietal lobe, the use of anatomical landmarks representing cortical structures or boundaries is essential. Combining landmarks corresponding to cortical references with landmarks representing surface topography might provide a finer model to investigate morphological variation in localized cortical regions.

In this sense, the present study incorporates landmarks that represent parietal lobe elements and boundaries in a dense landmark and semilandmark set in order to obtain a more comprehensive analysis of differences in parietal morphology between modern humans and Neanderthals. We compare these two human species because the parietal regions largely contribute to the general endocranial shape differences between them. Moreover, by considering boundaries within the parietal region, we expect to identify specific local regions responsible for the major variations. Namely, spatial variation of the whole parietal form might be related to changes in size or organization of the intraparietal sulcus (Pereira-Pedro and Bruner, 2016), as well as in proportions of the components of the inferior parietal lobule (supramarginal and angular gyri). More specifically, our main goal is to clarify (1) whether modern humans and Neanderthals differ in shape and size of the parietal lobe, and, in case we observe statistically significant group differences, (2) what parietal lobe regions are involved.

Materials and methods

Sample

Our sample was composed of digital endocasts generated from CT scans, including 52 cranially diverse modern *H. sapiens* from Europe (n=21), Africa (n=15), the Americas (n=9), Asia (n=6), and Australia (n=1), and 6 *Homo neanderthalensis*. The modern sample was part of the collection housed at the Institute for Anatomy, University of Leipzig, Germany, and is available from the NESPOS database (Neanderthal Museum, Mettmann, Germany). The Neanderthal specimens were Amud 1 (Israel), Feldhofer 1 (Germany), Guattari 1 (Italy), La Chapelle-aux-Saints 1 (France), La Ferrassie 1 (France), and Saccopastore 1 (Italy).

Landmark configurations

For the parietal set we sampled 3D coordinates of anatomical cortical brain landmarks defined by morphological features that represent major parietal lobe subdivisions (supramarginal gyrus, angular gurys, intraparietal groove, superior parietal lobule). These points represent gyral and sulcal features as inferred from the endocranial surface, and they are therefore estimations of the corresponding brain regions, based on surface relief and their surrounding elements (Pereira-Pedro and Bruner, 2018). The protocol for locating these landmark points is based on the general organization of the main sulci and gyri and on their relative locations as observed in 3D brain reconstructions (Wild et al., 2017). The lateral and central sulci comprise two of the most distinctive features of the lateral brain surface (Ribas, 2010), and are common to all anthropoids (Connolly, 1950; Radinsky, 1974). On endocasts, these can be recognized as grooves left by cortical impressions (Bruner, 2018b). For the present study, the anterior and posterior limits of the parietal lobe were defined by points located where the projections of the central sulcus (CS) and the parieto-occipital sulcus (POB), respectively, meet the midsagittal plane. Locating these landmarks was aided by using the endobregma and endolambda as reference, since the central sulcus is usually located posterior to the bregma and the parieto-occipital sulcus anterior to the lambda (Bruner et al., 2015). The inferior limit of the parietal region was defined by a landmark positioned on the posterior end of the groove of the lateral sulcus (LS). Within the parietal surface, two landmarks located on the central points of the supramarginal (SMG) and angular (AG) bosses represented the main references of the inferior parietal lobule. As boundary between the superior and inferior parietal lobules, we sampled the point along the intraparietal sulcus/groove (IPS) midway between the angular and supramarginal bosses namely were the primary intermediate sulcus of Jensen is located (Wild et al., 2017). The intermediate sulcus of Jensen is a vertical branch of the intraparietal sulcus and it separates the gyri of the inferior parietal lobule, the supramarginal gyrus, anteriorly, which surrounds the distal portion of the lateral sulcus, and the angular gyrus, posteriorly, which surrounds the distal portion of the superior temporal sulcus (Ribas, 2010). In total, we measured ten anatomical landmarks for each individual (two midsagittal and four bilateral landmarks).

These parietal landmarks defined according to the configuration of the cortical features of the brain were combined with a dense endocranial landmark set composed of 935 landmarks and semilandmarks which captures global endocranial shape (for more details see Neubauer et al., 2009, 2018; Neubauer and Gunz, 2018). To do so, we replaced ten of the sliding surface semilandmarks of the latter landmark set by the ten non-sliding, anatomical landmarks that have been measured as described above. Then semilandmarks were allowed to slide to gain point-to-point correspondence within the sample (Bookstein, 1997; Gunz et al., 2005; Gunz and Mitteroecker, 2013). The sliding of surface semilandmarks in the parietal regions was constrained and affected by the non-sliding, fixed cortical landmarks. After sliding, these surface semilandmarks were informative about shape features within the parietal region while a landmark set not using the parietal anatomical landmarks would be informative on global endocranial shape or global brain shape but not the local configuration of gyri and sulci within the parietal lobe. Figure **3.1** illustrates the combined landmark set.

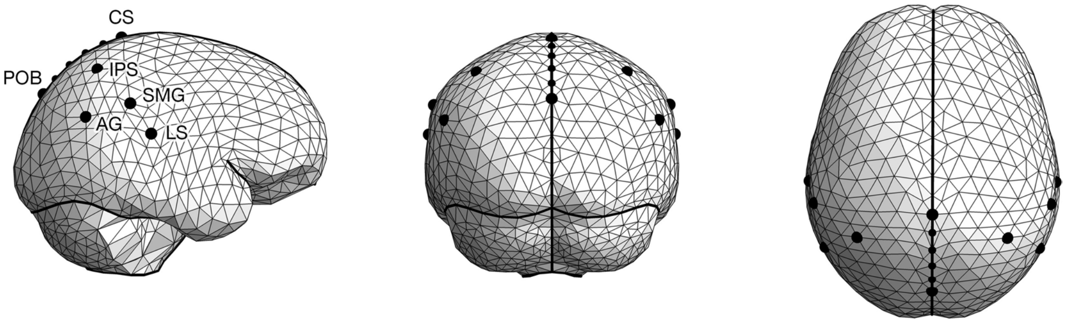

Fig. 3.1. Endocranial landmarks and semilandmarks (shown as triangulated surface and black curves) that capture overall brain shape have been combined with endocranial landmarks (shown as black spheres) that capture the shape of cortical impressions of the parietal brain lobe; from left to right: right, occipital, and superior views. Abbreviations: CS= central sulcus; POB= parietal-occipital boundary; LS= lateral sulcus distal termination; SMG= supramarginal gyrus boss; AG= angular gyrus boss; IPS= intraparietal sulcus meeting Jensen sulcus.

Error assessment

In order to evaluate uncertainty in locating the parietal landmarks, we measured four individuals four times, two modern humans and two Neanderthals (La Chapelle-aux-Saints and Feldhofer). Error in locating each landmark was calculated as the standard deviation of the four repeated measurements for each specimen. Figure **3.2** shows the distribution of landmark discrepancy.

Geometric morphometric analyses

Landmarks were symmetrized via reflected relabeling (Bookstein, 1991; Mardia et al., 2000) and superimposed through generalized Procrustes analysis by removing variation in size, location and orientation (Gower, 1975; Rohlf and Slice, 1990). We present three analyses

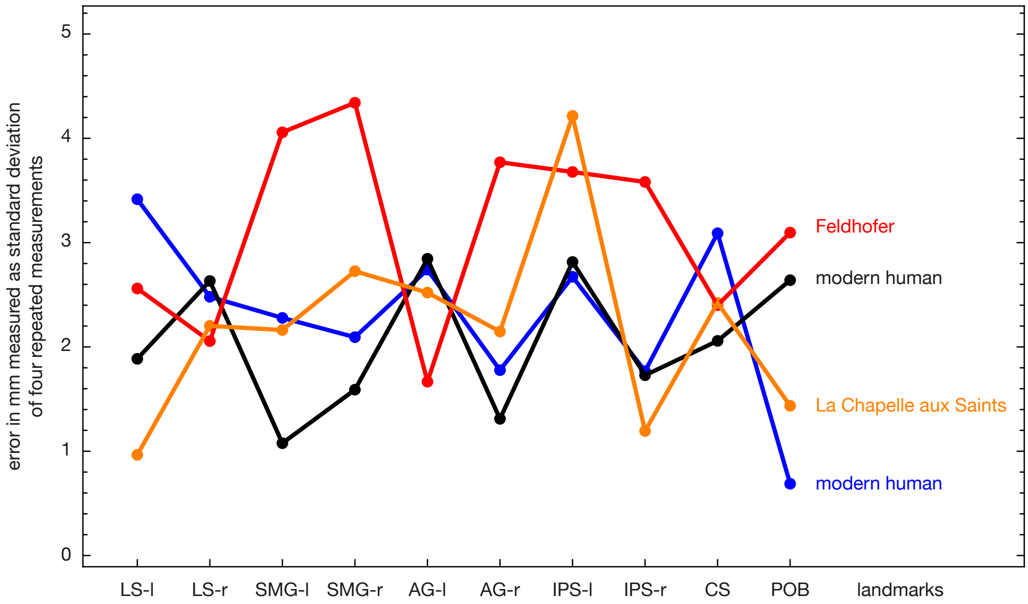

Fig. 3.2. Measurement error for each endocranial landmark across four specimens. Error is calculated as standard deviation of four repeated measurements, in mm. Abbreviations: for the lateral landmarks -l= left and -r= right; LS= lateral sulcus distal termination; SMG= supramarginal gyrus boss; AG= angular gyrus boss; IPS= intraparietal sulcus meeting Jensen sulcus; CS= central sulcus; POB= parietal-occipital boundary.

based on different kinds of data: (A) endocranial set; (B) relative parietal set; (C) parietal set (see **Fig. 3.3**a-c). The endocranial set includes the endocranial landmarks and semilandmarks as well as the parietal landmarks based on cortical features, providing information on the parietal lobe boundaries to the overall shape variation. The relative parietal set focuses on the parietal variation using only the subset of parietal landmarks and semilandmarks but after a Procrustes fit of the full endocranial configuration, thus additionally informing on the relative parietal position and proportions within the brain. The analysis of the parietal set includes only the parietal lobe landmarks and semilandmarks, hence being informative on within-parietal spatial relationships excluding the relationships of the parietal lobe to the rest of the brain.

For each of the three kinds of data we performed a principal component analysis (PCA) to ordinate the multidimensional data and thereby to investigate the pattern of largest variation in the sample. Because we are mainly interested in the species differences between modern humans and Neanderthals, we furthermore computed the difference vector between the average shapes of the two groups and projected each individual on this vector to compute mean difference scores. These scores are comparable to the 'globularity score' as presented in Gunz et al. (2019) and describe how Neanderthal-like or how modern human-like each individual of the sample is. Using a mesh generated from the landmarks and semilandmarks, we visualized the average shapes of Neanderthals and modern humans for comparisons. While group *shape* differences can be interpreted by comparison of the two averages, we additionally color-coded differences in surface area of each triangle of the mesh that is built by triangulation of the dense landmark set (Neubauer and Gunz, 2018). This allowed interpretation of local surface area

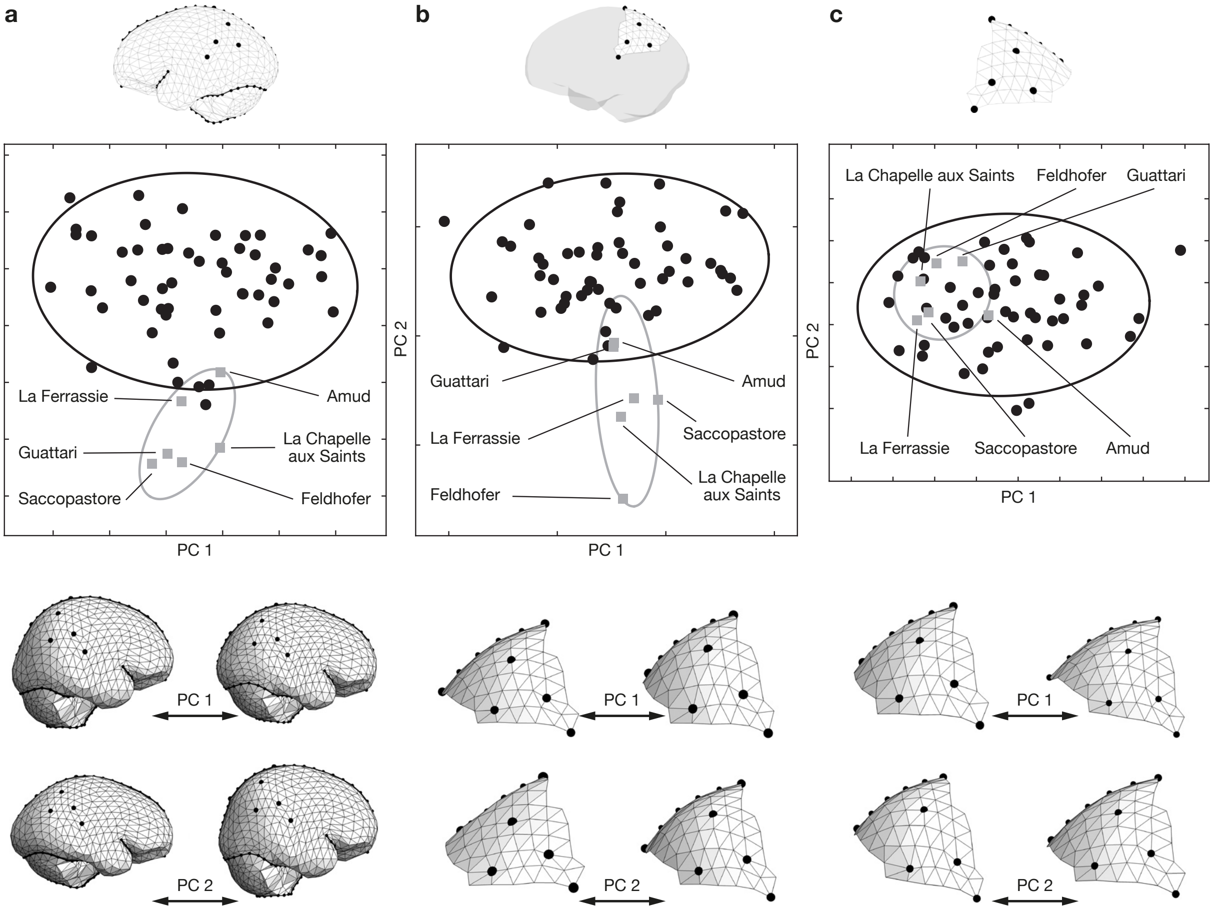

Fig. 3.3. Analysis of shape variation between Neanderthals and modern humans according to (a) the full endocranial landmark set, (b) the relative parietal landmark set (parietal subset after Procrustes fit of the full landmark set), (c) the parietal landmark set. The landmark set used for each of the three analyses is illustrated in the upper panel. The results from the principal component analyses in shape space are shown on the middle panel, with the groups shown with 95% confidence ellipses. (a): PC1 (22.8%) vs. PC2 (20.7%); (b) PC1 (35.4%) vs. PC2 (27.8%); (c): PC1 (41.0%) vs. PC2 (15.0%). The lower panel illustrates negative and positive extremes of PC 1 and PC2. Groups are: Neanderthals (squares), recent humans (circles).

differences as captured by the landmark set. In our figures, areas that were larger in modern humans are shown in warm colors and areas that were smaller are shown in cold colors.

Parietal traditional metrics and surface area

We also obtained the area of the total parietal surface and of a partial parietal surface enclosed between the landmarks SMG, AG, and IPS. Surface areas were calculated by summing up the areas of the triangles of the mesh contained within the region limited by the anatomical landmarks. Furthermore, we measured parietal chord and arc lengths in each individual. The parietal chord length was computed as the distance between the landmarks CS and POB. Parietal arc length was computed as the sum of distances of segments between the midsagittal curve semilandmarks from CS to POB. Given overall size variation among individuals, we adjusted these measurements for size differences. Parietal surfaces were considered relative to cerebral surface (i.e., the sum of triangle areas of the whole landmark set excluding the triangles of the cerebellar surface), and parietal arc and chord lengths relative to the cubic root of endocranial volume. We compared the variation in these measurements in modern humans and Neanderthals using box-and-whisker plots. Group mean differences were tested using permutation tests (10,000 permutations, original group sizes, $\alpha = 0.05$).

Results

Landmark discrepancy

The results from the repeated measurements are presented in figure 2. The smallest value was obtained for POB in one modern human, and the largest for the right SMG in one Neanderthal. Most of the landmarks show discrepancy values ranging between about 1.5 and 3 mm. Landmark discrepancy values vary across specimens with no landmark point consistently showing the largest values for all individuals. Similarly, the pattern of discrepancy distribution across the landmark set differs among the specimens.

Geometric morphometric analyses

Figure **3.3** shows the results from the PCAs based on the three different kinds of data. According to a PCA based on the full endocranial set (analysis A), 43.5% of the variation in shape is explained by the first two PCs, each describing a similar proportion of variation (**Fig. 3.3**a). PC1 (22.8%) describes variation within modern humans, distinguishing between short, brachycephalic and tall, dolichocephalic endocrania. Along this axis, Neanderthals group close to the average of the modern human distribution. PC2 (20.7%) separates the two human groups, with the modern humans displaying rounder and taller endocasts and Neanderthals having shorter, wider on the posterior region, and antero-posteriorly elongated endocrania.

When considering the parietal region after a Procrustes superimposition of the full endocranial set (analysis B: relative parietal set), the first two PCs describe 63.2% of the variation in shape (**Fig. 3.3**b). PC1 (35.4%) is again driven by the modern human variation, ranging from taller, longitudinally extended to shorter, longitudinally reduced, and slightly laterally rounder parietal regions. Neanderthals cluster on the modern human average values. PC2 (27.8%) separates Neanderthals, which display shorter, longitudinally reduced parietal regions, from modern humans, which tend to have taller and longitudinally stretched and curved parietal regions.

Regarding the PCA based only on the parietal region (analysis C), the first two PCs describe 56.0% of the variation in shape (**Fig. 3.3**c). Most of the variation is explained by PC1 (41.0%), which separates shorter, longitudinally reduced from taller, longitudinally elongated parietal regions. PC2 (15.0%) describes changes on the lower parietal lobule, mainly separating vertically stretched from antero-posteriorly stretched. The Neanderthals fall within the modern human range, clustering towards the negative values of PC1, and positive to central values of PC2; and thus display shorter and longitudinally reduced parietal lobes.

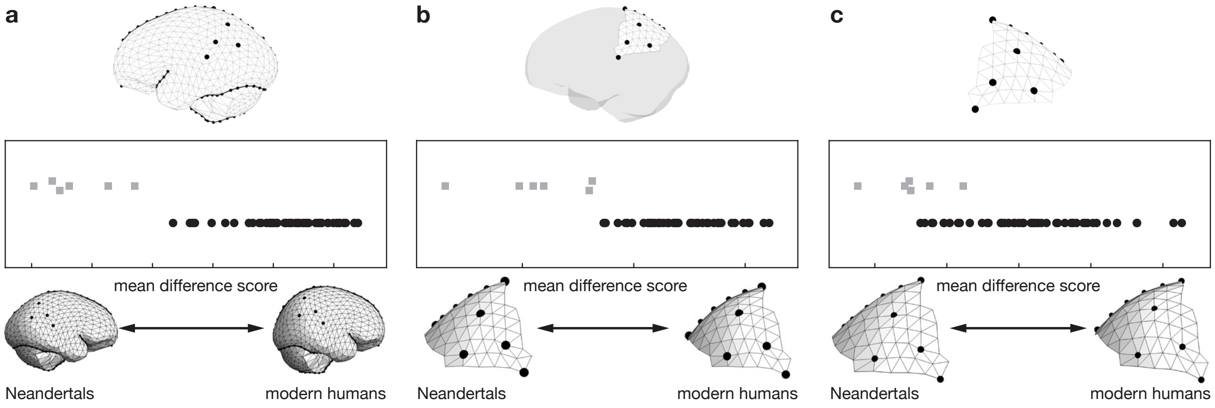

Fig. 3.4. Mean group differences scores for Neanderthals and modern humans according to (a) the full endocranial landmark set, (b) the relative parietal landmark set, (c) the parietal landmark. The landmark set used for each of the three analyses is illustrated in the upper panel. Mean shapes of Neanderthals and modern humans are illustrated below (for more detailed views see Figures 3.5-3.7). Individuals to the left look more Neanderthal-like, individuals to the right are more modern human-like.

Figure **3.4** shows the results from the mean difference scores based on the three different landmark sets. When using the full endocranial set (analysis A), modern humans and Neanderthals are completely separated, with the former displaying taller and globular endocrania, and the latter shorter and more elongated endocasts (**Fig. 3.4**a). When considering the parietal lobes after superimposition of the full endocranial set, there is also separation between the two groups, with modern humans displaying slightly rounder vaults and somewhat extended lower regions, compared to Neanderthals (**Fig. 3.4**b). Similar shape differences can be observed when considering the parietal-only variation, although in this case there is some overlap of the variation in the two groups (**Fig. 3.4**c).

Mean shape differences can be further observed in figures **3.5** to **3.7**. On average, compared to those of the Neanderthals, the parietal regions of modern humans are dorsally rounder and elongated, more superiorly positioned, and laterally inflated. As illustrated in figure 5, the more globular braincase of modern humans is due to vertical stretching, lateral narrowing, and anteroposterior shortening of the whole structure.

Regarding differences in absolute surface area, modern humans show expansion of the posterior cerebellar surface, the region around the temporal poles, and two regions within the parietal lobes, while having overall reduced areas along the frontal and posterior occipital regions (**Fig. 3.5**). With respect to the parietal surface, modern humans exhibit larger absolute areas on a small region at the midsagittal boundary with the occipital lobe (landmark POB), and another one delimited by the landmarks IPS, SMG, and AG (**Figs. 3.5, 3.6** and **3.7**). The first region roughly corresponds to the posterior portion of the superior parietal lobule. The second region comprises the superior portion of the inferior parietal lobule, in the transition between the supramarginal and angular gyri. As this corresponds to the region around the common location of the intermediate sulcus of Jensen (Wild et al., 2017) it will henceforth be referred to as ‘Jensen region’.

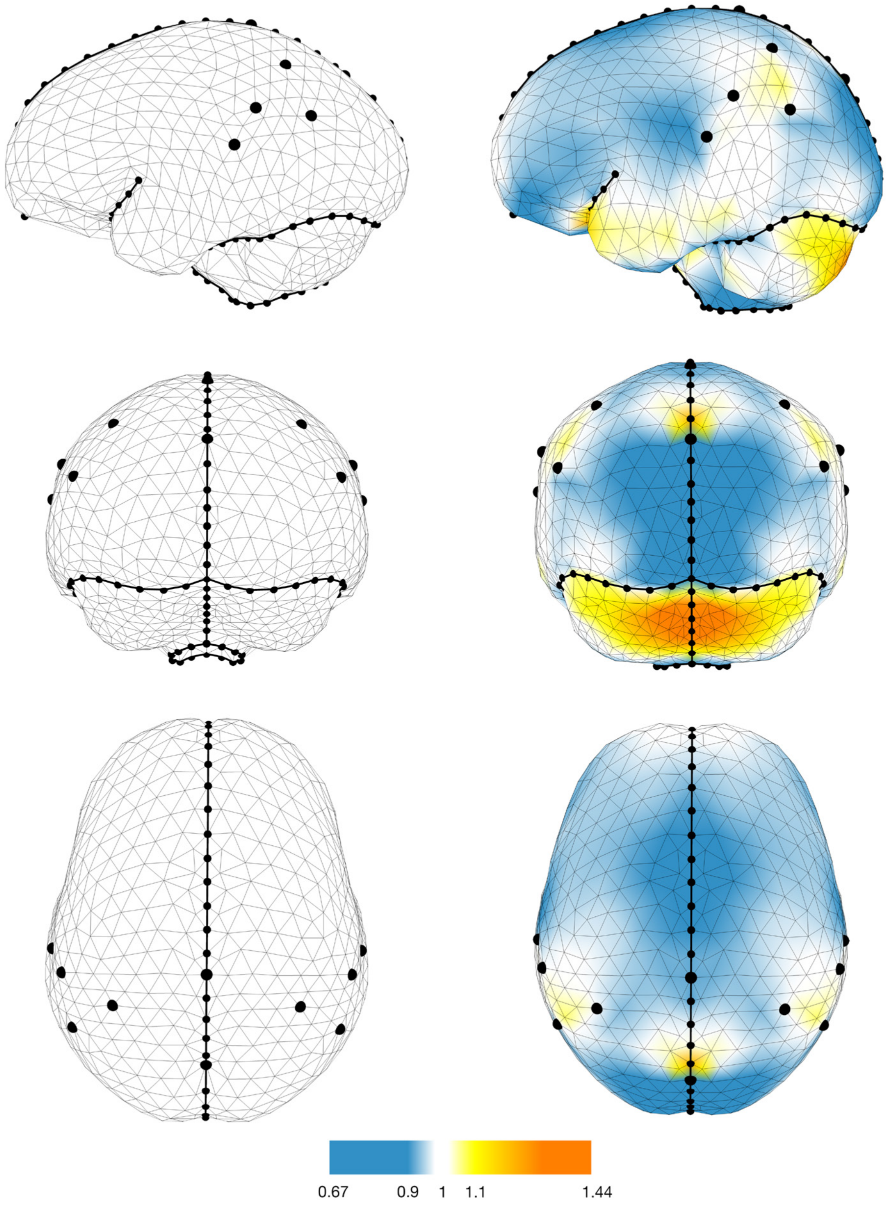

Fig. 3.5. Mean group difference between Neanderthals and modern humans, according to the full endocranial landmark set. From top to bottom: left, occipital, and superior views of the Neanderthal (left) and modern human (right) mean shapes. The modern human mean includes color coding that illustrates local absolute surface area difference to Neanderthals. Warm colored regions are larger in modern humans, cold colored regions are smaller according to the color code at the bottom.

Chords, arcs and surface

Table 1 shows the modern human and Neanderthal mean absolute values for the parietal chord and arc lengths, as well as for total parietal and Jensen region surface areas. Variation of all measurements overlaps between modern humans and Neanderthals. However, given overall size variation among individuals, and the known mean brain size difference between modern humans and Neanderthals, it is more meaningful to analyze relative area and length values (**Fig. 3.8**). For all four relative measurements, the two groups totally overlap but the variation of Neanderthals is smaller than that of modern humans and all Neanderthal individuals group

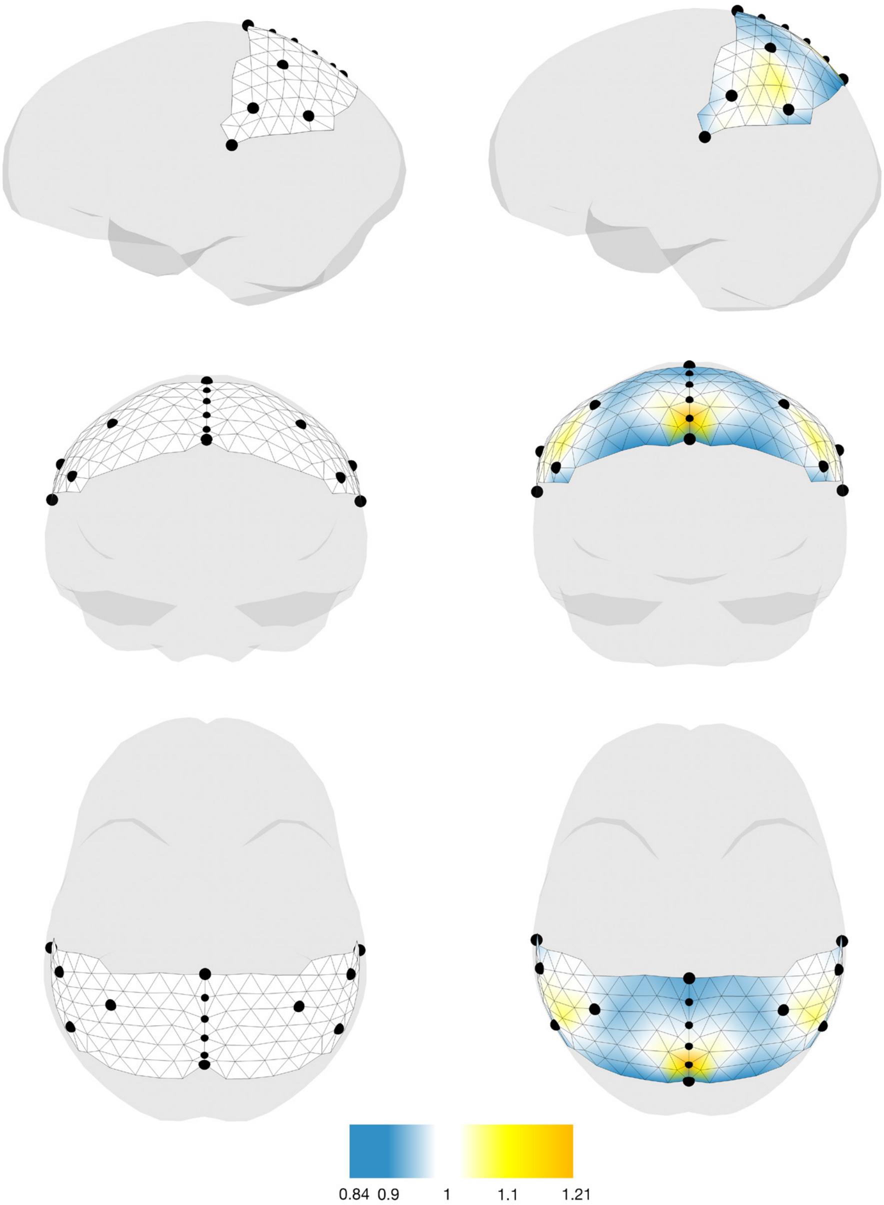

Fig. 3.6. Mean group difference between Neanderthals and modern humans, according to the relative parietal landmark set (parietal subset after Procrustes fit of the full endocranial landmark set). From top to bottom: left, occipital, and superior views of the Neanderthal (left) and modern human (right) mean shapes. The modern human mean includes color coding as in figure **3.5**.

in the lower half or even lower third of the modern human range resulting in lower group means. Although there is no clear difference among modern humans from different regions, it is interesting to note that individuals with the lowest values are from Europe. In spite of the overlap, mean differences are statistically significant (relative parietal chord: $p = 0.0030$; relative parietal arc: $p = 0.0087$; relative Jensen region surface: $p = 0.0053$) or at least tend to be (relative total parietal area: $p = 0.0625$).

Discussion

Bulging of the parietal region has been usually deemed one of the features contributing

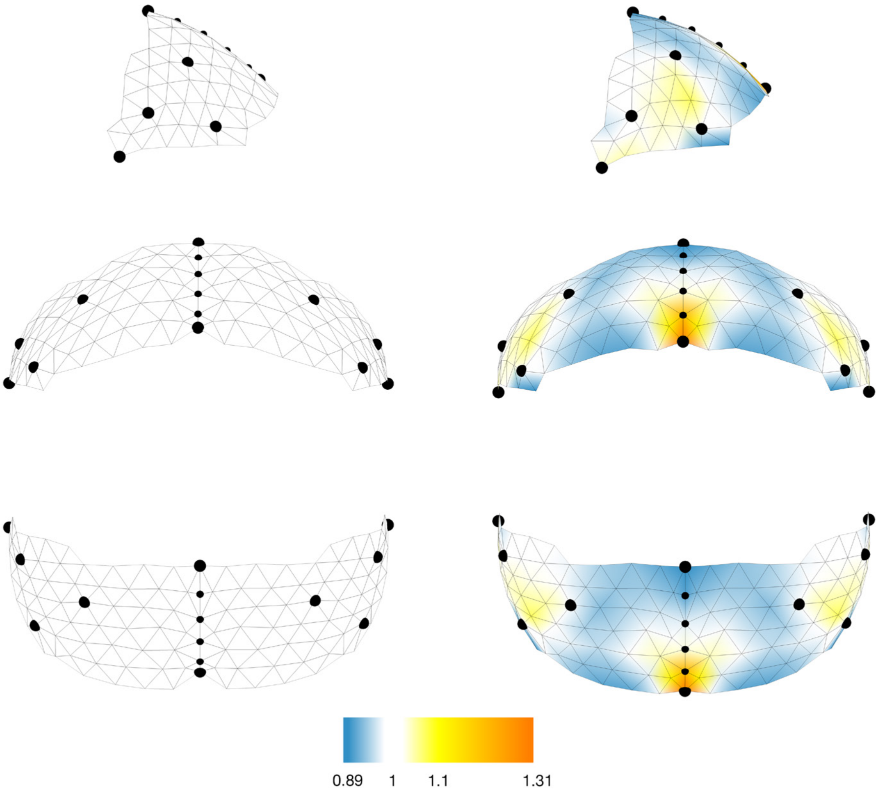

Fig. 3.7. Mean group difference between Neanderthals and modern humans, according to the parietal landmark set. From top to bottom: left, occipital, and superior views of the Neanderthal (left) and modern human (right) mean shapes. The modern human mean includes color coding as in figure **3.5**.

to the endocranial globularity of modern humans (Bruner, 2008, 2010; Gunz et al., 2010; 2012; Neubauer et al., 2009; 2010; 2018; Bruner et al., 2017a). While the form of the parietal bone might be influenced by other functional and structural factors, impressions of cortical details on the endocranial surface of the parietal bone result primarily from the parietal cortex itself (Bruner et al., 2019). To learn more about how the parietal region differs between modern humans and Neanderthals, we combined endocranial landmarks and semilandmarks that capture overall brain shape with endocranial landmarks defined on impressions of brain convolutions that capture the macroscopic boundaries of the parietal lobe. The inclusion of the parietal lobe boundaries into the dense endocranial landmarks and semilandmarks configuration allowed investigating the spatial relationships between the parietal region and the whole endocranial form. In this sense, the analysis of the combined set (analysis A) gives insight on the contributions of the parietal lobe to the endocranial differences between modern humans and Neanderthals, while analysis B informs on the influence of the whole endocranium on the parietal differences between the two human species. Besides, by using parietal lobe references, we were able to isolate parietal lobe morphology and analyze its variation in terms of within-lobe proportions, without influence from the rest of the endocranium.

When considering the parietal region within the whole endocranium the morphological differences between modern humans and Neanderthals are associated with the known globular

Table 1. Mean parietal absolute values of parietal chord and arc (mm) and total parietal and Jensen region surface areas (mm2) in Neanderthals and modern humans.

Metrics	total parietal area	Jensen area	parietal arc	parietal chord
Neanderthal (mean ± SD)	4013 ± 409.3	696.8 ± 105.8	78.7 ± 8.5	46.2 ± 4.8
Modern human (mean ± SD)	4078.5 ± 475.4	726.1 ± 84.6	88.1 ± 10.8	52.3 ± 6.3

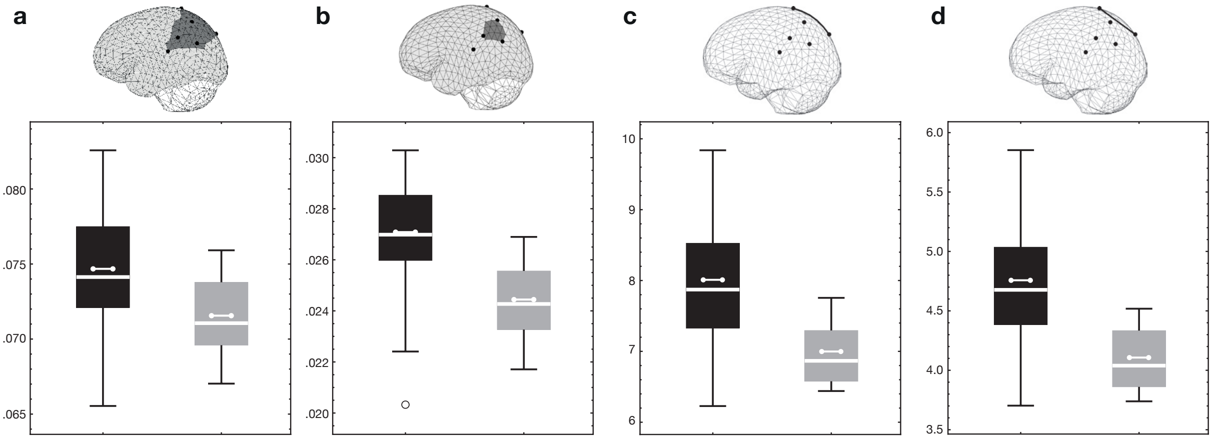

Fig. 3.8. Differences of relative parietal arc, chord, and surface areas between Neanderthals and modern humans. Box-and-whisker plots of modern human data (black) and Neanderthal data (gray) with range (whiskers), 25% to 75% quartile box, median (white line) and mean (white barbell) for, as visualized on top: a) total parietal area; b) Jensen region area enclosed by landmarks SMG, AG, and IPS; c) parietal arc; d) parietal chord. To take overall brain size variation into account, distance measurements are shown relative to the cube root of endocranial volume, surface areas are shown relative to cerebral surface area.

shape of the former species. Compared to those of the Neanderthals, the parietal lobes of modern humans are located in a more superior position, are slightly anteroposteriorly and vertically stretched, and display rounder and more bulging superior regions. Investigation of the within-parietal proportions further evidenced the vertical stretching, and upper bulging in modern humans. Hence, in general, the parietal lobes of modern humans are dorsally rounder, vertically more stretched, and antero-posteriorly more extended compared to those of the Neanderthals, which is in line with previous analyses (Bruner et al., 2003; Bruner, 2004, 2008, 2010; Gunz et al., 2010, 2012; Neubauer et al., 2010, 2018).

Regarding variation in absolute surface area, modern humans display expansion of the cerebellar surface, especially on the posterior region, on the temporal poles, and on discrete parietal regions, while exhibiting reduction along the frontal and occipital surfaces. Enlargement of the temporal poles is in line with previous findings indicating anterior projection of temporal tips in modern humans compared to Neanderthals (Bastir et al., 2008). Increased cerebellar surface in *H. sapiens* has been previously evidenced, with bulging of the cerebellum contributing to endocranial globularity, characteristic of present-day humans (Neubauer et al., 2018). In fact, cerebellar expansion seems to be a trend in primate evolution, as extant humans and apes have larger cerebellum relative to neocortex than other anthropoid primates, with our species representing an extreme in the allometric trajectory (Barton and Venditi, 2014). Moreover, modern humans display larger absolute and relative cerebellar volumes than Middle and Late Pleistocene humans, including Neanderthals (Weaver, 2005). Expansion of the cerebellum has been suggested to be related to its involvement in higher cognitive functions (Ramnani et al., 2006; Balsters et al., 2010).

Although the increase in surface area is greater on the cerebellar and temporal regions, the inclusion of parietal lobe boundaries allowed our model to detect expansion within the parietal surface as well. Results indicate that the parietal lobes of modern humans are expanded on the posterior dorsal region, towards the parieto-occipital boundary and around the region between the intraparietal sulcus and the supramarginal and angular gyri, i.e., the Jensen region. In modern humans, therefore, parietal lobes are dorsally longer and laterally inflated.

A preliminary comparison of modern human vs. Neanderthal parietal morphology based on cortical references previously indicated that the larger parietal lobe of modern humans was more prominent towards the intraparietal sulcus (Bruner, 2010). While Bruner (2010) located the IPS landmark on the anterior termination of the intraparietal sulcus, in this study it was placed on the intersection with the sulcus of Jensen, conferring a more central position that might have allowed for a more detailed location of the region that has enlarged in modern humans. Indeed, our results indicate significant surface expansion in modern humans relative to Neanderthals on the superior portion of the inferior parietal lobule, between the intraparietal sulcus and the supramarginal and angular gyri ('Jensen region'). Caspers et al. (2006, 2008) identified up to seven different cytoarchitectonic areas within the supramarginal and angular gyri. Two large subareas were identified in the transition between the two gyri, both reaching up to the intraparietal sulcus (Caspers et al., 2006, 2008). Similar subdivisions were obtained by Mars et al. (2011) using diffusion-weighted magnetic resonance imaging (MRI) based tractography. These areas seem to be activated in decision-making and redirection of visuospatial attention between locations (Mars et al., 2011). In general, the eye-hand system is largely involved in action simulation and decision-making, according to the available relationships between body and environment (Tunik et al., 2007). Nonetheless, it is worth noting that the correspondence between cytoarchitectonic areas and macroanatomical cortical reference is variable, and hence such association can be interpreted only very tentatively (Caspers et al., 2006, 2008). Moreover, our model cannot disclose whether it is the posterior portion of the supramarginal gyrus, or the anterior portion of the angular gyrus, or both regions, that have a larger surface area in modern humans than in Neanderthals. Besides, increase in surface area could also be caused by an expansion and 'outfolding' of the intraparietal sulcus.

Modern humans also display significant expansion on the medial parietal outline, towards the posterior region close to the boundary with the occipital lobe. A study of the midsagittal brain variation among humans and chimpanzees evidenced that the main geometrical difference between the two species is a forward longitudinal extension of the precuneus in modern humans (Bruner et al., 2017a). However, according to the model used to compare humans and chimpanzee brains (Bruner et al., 2017a), the expansion observed in humans mainly involves the anterior region of the dorsal (medial) parietal cortex. In contrast, the model used in the present study to compare modern human and Neanderthal endocasts suggests expansion in the posterior region. Despite the distinct sample types and composition within the two studies, the differences in the location of expansion merit further investigation, since the anterior and posterior regions of the superior parietal lobule seem to diverge in cytoarchitecture and functions. In terms of cytoarchitecture, two main anterior-to-posterior subdivisions can be identified on the superior parietal lobule, extending both on the lateral surface and the precuneus (Scheperjans et al., 2008). In their review of the precuneus, Cavanna and Trimble (2006) suggested functional division, with anterior portions more involved with mental imagery and the posterior with episodic memory retrieval. Later, Margulies et al. (2009) showed that the anterior region, along the marginal ramus of the cingulate sulcus is connected to sensorimotor regions, while the posterior portion, close to the parieto-occipital sulcus is connected to visual cortex. In this sense, expansion of the anterior portion might indicate changes in sensorimotor processing capacity, while expansion of the posterior regions might indicate changes related to visual processing capacity.

It is important to be cautious when interpreting interspecific differences in cortical areas. Homology is hardly straightforward, since some cortical regions are larger and more diversified in humans compared to other primates, and the locations do not correspond completely (Culham and Kanwisher, 2001; Vanduffel et al., 2002; Grefkes and Fink, 2005; Choi et al., 2006; Culham and Valyear, 2006). Nonetheless, these lateral parietal regions that are larger in modern humans are generally involved in visuospatial processing and hand-tool coordination (Caminiti et al., 2010; Bruner and Iriki, 2016; Catani et al., 2017; Kastner et al., 2017; Valyear et al., 2017). Interestingly, archaeological evidence suggests that, when compared with modern humans, Neanderthals relied more extensively on the mouth for tool manipulation (Bruner and Lozano, 2014) and on close-range hunting strategies (e.g., Gaudzinski-Windheuser et al., 2018). Taking also into account the limitations in their visual and graphic behaviors (even only by grade; Wynn et al., 2016; see also Hoffmann et al., 2018), it has been suggested that they lacked a specialized spatial processing capacity—at least, when compared with *H. sapiens* (see Bruner et al., 2018).

The emergence of brain globularity within *H. sapiens* seems to have occurred in parallel with the manifestation of modern behavior (Neubauer er al., 2018). Indeed, a MRI brain study of the degree of globularity within a large European sample of living people found links with some parietal cortical areas, being negatively associated with gray matter volume of left supramarginal gyrus, and positively associated with gray matter volume of right precuneus and right angular gyrus (Gunz et al., 2019). It would be interesting to investigate the association between shape and more specific cellular components (for example, connections).

Some methodological considerations

Landmark uncertainty is a main issue when dealing with endocasts, as these exhibit rather smooth surfaces, with few cortical features to use for guidance. Hence, the location of landmarks cannot rely only on local features but must consider the whole structure (Bruner, 2018b). In this study, the location of landmarks was conducted after detailed examination of the spatial relationship among the parietal cortical regions in reconstructions of brain lateral surface published in Wild et al. (2017). It must be taken into account that most of the parietal landmarks used in the present analysis would have represented approximate locations even if we were analyzing brains instead of endocasts (Goméz-Robles, 2018). Of course the estimation is more difficult on endocasts, and larger discrepancy might be introduced when placing landmarks with reference to each other. Our landmark uncertainty values range from less than 1 mm to more than 4 mm, with most of the landmarks falling between 1.5 and 3 mm. Large error values have been obtained when placing landmarks on 3D brain reconstructions: Maudgil et al. (1998) reported values that ranged from 2.8 – 5.0 mm (mean = 3.27 mm) and Chollet et al. (2014) from 1.0 - 5.6 mm (mean = 1.9 mm), though these authors computed the error as the distance of each measurement to a mean position. Regarding endocasts, Pereira-Pedro and Bruner (2018) obtained errors ranging between 0.15 and 3.44 mm, measured as standard deviation, using landmarks that represented cortical boundaries. According to their results, the landmarks displaying largest error were those located on the parietal region, representing the supramarginal and angular gyri (Pereira-Pedro and Bruner, 2018). Indeed, the parietal region on endocasts is particularly poor in cortical features and the placement of landmarks within this region largely relies on the surrounding structures for reference. Since the present study mainly includes parietal landmarks, large error was expected. In fact, the larger error associated with Feldhofer might be due to this specimen being incomplete, which reduces the points of reference for placing the landmarks. Nonetheless, there is no systematic error pattern, with different specimens having specific landmarks that display the largest deviations. In line with results from Pereira-Pedro and Bruner (2018), this seems to indicate that landmarking error might be idiosyncratic, influenced by the topographic characteristics of each endocast, such as the presence of determined anatomical features, like vessels or sutures, as well as the degree of localized smoothness or curvature. Overall, these error values can be considered acceptable (Maudgil et al., 1998; Chollet et al., 2014), at least when comparing different species (Pereira-Pedro and Bruner, 2018). However, the results must be interpreted with these limitations in mind. In any case, localizing landmarks representing cortical elements is the only approach for defining parietal lobe boundaries, and it seems to be sufficient to detect differences between modern humans and Neanderthals in the parietal surface.

Principal component analyses (Fig. **3.3**) revealed that the first two PCs accounted for similar amounts of variance. The first PC was mostly driven by the variation within modern humans, while interspecific differences were captured by PC2. Indeed, great variability in cortical organization has been repeatedly proved in adult modern humans, and associated with brain plasticity (Gomez-Robles et al., 2013, 2015), especially regarding the association cortex (Croxson et al., 2018; Reardon et al., 2018). Furthermore, the sample of modern humans is far larger than that of Neanderthals and therefore PC1 tends to be more affected by modern humans. However, it is interesting to note that Neanderthals are quite restricted in their range of variation along this PC. Since we have been mainly interested in the difference between modern humans and Neanderthals, we additionally computed difference scores between the two groups (Fig. **3.4**). While PCA analyses are informative about the variance within and between groups, these difference scores emphasize the variation concerning the difference between modern humans and Neanderthals. And indeed, differences in parietal shape were far more apparent in this analysis as compared to PCA.

Overall, landmarking uncertainty and differences in sample size warrant caution when considering the distribution of the specimens. Nonetheless, it is worth noting that the clustering of the Neanderthals within one end of the modern human distribution – both in terms of shape and metrics – seems to indicate that the differences between the two species in the form of the parietal lobe might be primarily in terms of degree. Interestingly, parietal bone size seems to influence the head functional axis in modern humans, at intraspecific level (Bruner et al. 2017b). Considering the differences between the cranial architecture in modern humans and Neanderthals, more detailed intraspecific differences in parietal cortical anatomy between globular and elongated brains should be further investigated in order to understand what structural factors or functional outcomes might be involved.

Conclusions

This study combined cortical-based anatomical landmarks with endocranial landmarks and semilandmarks to compare parietal lobe morphology between modern humans and Neanderthals. The inclusion of parietal landmarks allowed comparing the parietal region in combination with overall brain shape, as well as the shape of the parietal region in isolation. To our knowledge, this is the first study addressing differences in 3D morphology of the parietal region between modern humans and Neanderthals, especially regarding the inferior parietal lobule. Our results confirm that, on average, modern humans have more bulging and dorsally and laterally expanded parietal lobes than Neanderthals. These differences in shape also translate into differences in absolute size, with more pronounced enlargement on the posterior part of the superior parietal lobule, towards the parietooccipital sulcus, and on the lateral inferior parietal lobule around the sulcus of Jensen that separates the supramarginal and angular gyri. Particular differences in cortical areas need to be addressed through analyses of actual brains, both intra- and inter-specifically, and considering the contribution of subcortical structures as well. Namely, it should be solved whether the parietal lobes expand anteriorly or posteriorly. In addition, cortical and volumetric variation of the parietal lobe within modern humans should give insight on the differences between globular vs. Neanderthal-like braincase morphologies.

References

Ardesch, D.J., Scholtens, L.H., Li, L., Preuss, T.M., Rilling, J.K., van den Heuvel, M.P., 2019. Evolutionary expansion of connectivity between multimodal association areas in the human brain compared with chimpanzees. Proceedings of the National Academy of Sciences 116, 7101–7106.

Balsters, J.H., Cussans, E., Diedrichsen, J., Phillips, K.A., Preuss, T.M., Rilling, J.K., Ramnani, N., 2010. Evolution of the cerebellar cortex: the selective expansion of prefrontal-projecting cerebellar lobules. NeuroImage 49, 2045-2052.

Barton, R.A., Venditi, C., 2014. Rapid evolution of the cerebellum in humans and other great apes. Current Biology 24, 2440-2444.

Bastir, M., Rosas, A., Lieberman, D.E., O'Higgins, P., 2008. Middle cranial fossa anatomy and the origin of modern humans. Anatomical Record 291, 130–140.

Bookstein, F.L., 1991. Morphometric Tools for Landmark Data: Geometry and Biology, Cambridge University Press, New York.

Bookstein, F.L., 1997. Landmark methods for forms without landmarks: morphometrics of group differences in outline shape. Medical Image Analysis 1, 225–243.

Bruner, E., 2004. Geometric morphometrics and paleoneurology: brain shape evolution in the genus *Homo*. Journal of Human Evolution 47, 279–303.

Bruner, E., 2008. Comparing endocranial form and shape differences in modern humans and Neandertals: a geometric approach. PaleoAnthropology 2008, 93-106.

Bruner, E., 2010. Morphological differences in the parietal lobes within the human genus: a neurofunctional perspective. Current Anthropology 51, S77–S88.

Bruner, E., 2017. The fossil evidence of human brain evolution. In: Kaas, J.H. (Ed.), Evolution of Nervous Systems, 2nd ed. Academic Press, Oxford, pp. 63–92.

Bruner, E., 2018a. Human paleoneurology and the evolution of the parietal cortex. Brain, Behavior and Evolution 91, 136–147.

Bruner, E., 2018b. The brain, the braincase, and the morphospace. In: Bruner, E., Ogihara, N., Tanabe, H.C. (Eds.), Digital Endocasts: From Skulls to Brains. Springer Japan, Tokyo, pp. 93–114.

Bruner, E., 2019. Human paleoneurology: shaping cortical evolution in fossil hominids. Journal of Comparative Neurology. https://doi.org/10.1002/cne.24591.

Bruner, E., Iriki, A., 2015. Extending mind, visuospatial integration, and the evolution of the parietal lobes in the human genus. Quaternary International 405, 98–110.

Bruner, E., Lozano, M., 2014. Extended mind and visuo-spatial integration: three hands for the Neandertal lineage. Journal of Anthropological Sciences 92, 273–280.

Bruner, E., Pearson, O., 2013. Neurocranial evolution in modern humans: the case of Jebel Irhoud 1. Anthropological Science 121, 31–41.

Bruner, E., Manzi, G., Arsuaga, J.L., 2003. Encephalization and allometric trajectories in the genus *Homo*: Evidence from the Neandertal and modern lineages. Proceedings of the National Academy of Sciences USA 100, 15335–15340.

Bruner, E., De La Cuétara, J.M., Holloway, R., 2011. A bivariate approach to the variation of the parietal curvature in the genus *Homo*. Anatomical Record 294, 1548–1556.

Bruner, E., Amano, H., de la Cuétara, J.M., Ogihara, N., 2015. The brain and the braincase: a spatial analysis on the midsagittal profile in adult humans. Journal of Anatomy 227, 268-276.

Bruner, E., Preuss, T.M., Chen, X., Rilling, J.K., 2017a. Evidence for expansion of the precuneus in human evolution. Brain Structure and Function 222, 1053–1060.

Bruner, E., Pereira-Pedro, A.S., Bastir, M., 2017b. Patterns of morphological integration between parietal and temporal areas in the human skull. Journal of Morphology 278, 1312-1320.

Bruner, E., Spinapolice, E., Burke, A., Overmann, K.A., 2018. Visuospatial integration: Paleoanthropological and archaeological perspectives. In: Di Paolo, L.D., Di Vincenzo, F., De Petrillo, F. (Eds.), Evolution of Primate Social Cognition. Springer International Publishing, Cham, pp. 299–326.

Bruner, E., Esteve-Altava, B., Rasskin-Gutman, D., 2019. A network approach to brain form, cortical topology and human evolution. Brain Structure and Function 224, 2231-2245.

Bzdok, D., Hartwigsen, G., Reid, A., Laird, A.R., Fox, P.T., Eickhoff, S.B., 2016. Left inferior parietal lobe engagement in social cognition and language. Neuroscience & Biobehavioral Reviews 68, 319–334.

Caminiti, R., Chafee, M.V., Battaglia-Mayer, A., Averbeck, B.B., Crowe, D.A., Georgopoulos, A.P., 2010. Understanding the parietal lobe syndrome from a neurophysiological and evolutionary perspective. European Journal of Neuroscience 31, 2320–2340.

Caspers, S., Geyer, S., Schleicher, A., Mohlberg, H., Amunts, K., Zilles, K., 2006. The human inferior parietal cortex: cytoarchitectonic parcellation and interindividual variability. NeuroImage 33, 430–448.

Caspers, S., Eickhoff, S.B., Geyer, S., Scheperjans, F., Mohlberg, H., Zilles, K., Amunts, K., 2008. The human inferior parietal lobule in stereotaxic space. Brain Structure and Function 212, 481–495.

Catani, M., Robertsson, N., Beyh, A., Huynh, V., de Santiago Requejo, F., Howells, H., Barrett, R.L.C., Aiello, M., Cavaliere, C., Dyrby, T.B., Krug, K., Ptito, M., D'Arceuil, H., Forkel, S.J., Dell'Acqua, F., 2017. Short parietal lobe connections of the human and monkey brain. Cortex 97, 339–357.

Cavanna, A.E., Trimble, M.R., 2006. The precuneus: a review of its functional anatomy and behavioural correlates. Brain: A Journal of Neurology 129, 564–583.

Choi, H.-J., Zilles, K., Mohlberg, H., Schleicher, A., Fink, G.R., Armstrong, E., Amunts, K., 2006. Cytoarchitectonic identification and probabilistic mapping of two distinct areas within the anterior ventral bank of the human intraparietal sulcus. The Journal of

Comparative Neurology 495, 53–69.

Chollet, M.B., Aldridge, K., Pangborn, N., Weinberg, S.M., DeLeon, V.B., 2014. Landmarking the brain for geometric morphometric analysis: an error study. PLoS One 9(1), e86005.

Connolly, C.J., 1950. External Morphology of the Primate Brain. Charles C. Thomas, Springfield Illinois.

Croxson, P.L., Forkel, S.J., Cerliani, L., Thiebaut de Schotten, M., 2018. Structural variability across the primate brain: a cross-species comparison. Cerebral Cortex 28(11), 3829–3841.

Culham, J.C., Kanwisher, N.G., 2001. Neuroimaging of cognitive functions in human parietal cortex. Current Opinion in Neurobiology 11, 157–163.

Culham, J.C., Valyear, K.F., 2006. Human parietal cortex in action. Current Opinion in Neurobiology 16, 205–212.

Donahue, C.J., Glasser, M.F., Preuss, T.M., Rilling, J.K., Van Essen, D.C., 2018. Quantitative assessment of prefrontal cortex in humans relative to nonhuman primates. Proceedings of the National Academy of Sciences USA 115(22), E5183-E5192.

Flaherty, K., Richtsmeier, J.T., 2013. Hand in glove: brain and skull in development and dysmorphogenesis. Acta Neuropathologica 125(4), 469-489.

Gaudzinski-Windheuser, S., Noack, E.S., Pop, E., Herbst, C., Pfleging, J., Buchli, J., Jacob, A., Enzmann, F., Kindler, L., Iovita, R., Street, M., Roebroeks, W., 2018. Evidence for close-range hunting by last interglacial Neanderthals. Nature Ecology & Evolution 2, 1087.

Goldring, A.B., Krubitzer, L.A., 2017. Evolution of parietal cortex in mammals: from manipulation to tool use. In: Krubitzer, L., Kaas, J.H. (Eds.), Evolution of Nervous Systems. 2nd ed. Academic Press, Oxford, pp. 259–286.

Gómez-Robles, A., Reyes, L., Sherwood, C., 2018. Landmarking brains. In: Bruner E., Ogihara N., Tanabe H. (Eds), Digital Endocasts: From Skulls to Brains. Springer Japan, Tokyo. pp. 115–126.

Gómez-Robles, A., Hopkins, W.D., Schapiro, S.J., Sherwood, C.C., 2015. Relaxed genetic control of cortical organization in human brains compared with chimpanzees. Proceedings of the National Academy of Sciences USA 112, 14799 – 14804.

Gómez-Robles, A., Hopkins, W.D., Sherwood, C.C., 2013. Increased morphological asymmetry, evolvability and plasticity in human brain evolution. Proceedings of the Royal Society B. 280, 20130575.

Gower, J.C., 1975. Generalized Procrustes analysis. Psychometrika 40, 33–51.

Grefkes, C., Fink, G.R., 2005. The functional organization of the intraparietal sulcus in humans and monkeys. Journal of Anatomy 207, 3–17.

Gunz, P., Mitterœcker, P., 2013. Semilandmarks: a method for quantifying curves and surfaces. Hystrix 24, 103–109.

Gunz, P., Mitteroecker, P., Bookstein, F.L., 2005. Semilandmarks in three dimensions. In: Slice, D.E. (Ed.), Modern Morphometrics in Physical Anthropology. Kluwer Academic/

Plenum publishers, New York, pp. 73–98.

Gunz, P., Neubauer, S., Maureille, B., Hublin, J.-J., 2010. Brain development after birth differs between Neanderthals and modern humans. Current Biology 20, R921–R922.

Gunz, P., Neubauer, S., Golovanova, L., Doronichev, V., Maureille, B., Hublin, J.-J., 2012. A uniquely modern human pattern of endocranial development. Insights from a new cranial reconstruction of the Neandertal newborn from Mezmaiskaya. Journal of Human Evolution 62, 300–313.

Gunz, P., Tilot, A.K., Wittfeld, K., Teumer, A., Shapland, C.Y., van Erp, T.G.M., Dannemann, M., Vernot, B., Neubauer, S., Guadalupe, T., Fernández, G., Brunner, H.G., Enard, W., Fallon, J., Hosten, N., Völker, U., Profico, A., Di Vincenzo, F., Manzi, G., Kelso, J., St. Pourcain, B., Hublin, J.-J., Franke, B., Pääbo, S., Macciardi, F., Grabe, H.J., Fisher, S.E., 2019. Neandertal introgression sheds light on modern human endocranial globularity. Current Biology 29, 120-127.

Hoffmann, D.L., Standish, C.D., Garcia-Diez, M., Pettitt, P.B., Milton, J.A., Zilhao, J., Alcolea-Gonzalez, J.J., Cantalejo-Duarte, P., Collado, H., de Balbin, R., Lorblanchet, M., Ramos-Munoz, J., Weniger, G.C., Pike, A.W.G., 2018. U-Th dating of carbonate crusts reveals Neandertal origin of Iberian cave art. Science 359, 912-915.

Holloway, R.L., Broadfield, D.C., Yuan, M.S., 2004. Brain Endocasts: The Paleoneurological Evidence. John Wiley & Sons, Hoboken.

Hublin, J.-J., Ben-Ncer, A., Bailey, S.E., Freidline, S.E., Neubauer, S., Skinner, M.M., Bergmann, I., Le Cabec, A., Benazzi, S., Harvati, K., Gunz, P., 2017. New fossils from Jebel Irhoud, Morocco and the pan-African origin of Homo sapiens. Nature 546, 289-292.

Kastner, S., Chen, Q., Jeong, S.K., Mruczek, R.E.B., 2017. A brief comparative review of primate posterior parietal cortex: A novel hypothesis on the human toolmaker. Neuropsychologia 105, 123–134.

Kochiyama, T., Ogihara, N., Tanabe, H.C., Kondo, O., Amano, H., Hasegawa, K., Suzuki, H., León, M.S.P. de, Zollikofer, C.P.E., Bastir, M., Stringer, C., Sadato, N., Akazawa, T., 2018. Reconstructing the Neanderthal brain using computational anatomy. Scientific Reports 8, 6296.

Krienen, F.M., Buckner, R.L., 2017. Human association cortex: expanded, untethered, neotenous, and plastic. In: Kaas, J.H. (Ed.), Evolution of Nervous Systems, 2nd ed. Academic Press, Oxford, pp. 169–183.

Mardia, K.V., Bookstein, F.L., Moreton, I.J., 2000. Statistical assessment of bilateral symmetry of shapes. Biometrika 87, 285–300.

Margulies, D.S., Vincent, J.L., Kelly, C., Lohmann, G., Uddin, L.Q., Biswal, B.B., Villringer, A., Castellanos, F.X., Milham, M.P., Petrides, M., 2009. Precuneus shares intrinsic functional architecture in humans and monkeys. Proceedings of the National Academy of Sciences USA 106, 20069–20074.

Mars, R.B., Jbabdi, S., Sallet, J., O'Reilly, J.X., Croxson, P.L., Olivier, E., Noonan, M.P., Bergmann, C., Mitchell, A.S., Baxter, M.G., Behrens, T.E.J., Johansen-Berg, H., Tomassini, V., Miller, K.L., Rushworth, M.F.S., 2011. Diffusion-weighted imaging tractography-based parcellation of the human parietal cortex and comparison with human and macaque resting-state functional connectivity. The Journal of Neuroscience 31, 4087–4100.

Mars, R.B., Passingham, R.E., Neubert, F.-X., Verhagen, L., Sallet, J., 2017. Evolutionary specializations of human association cortex. In: Kaas, J.H. (Ed.), Evolution of Nervous Systems, 2nd ed. Academic Press, Oxford, pp. 185–205.

Maudgil, D.D., Free, S.L., Sisodiya, S.M., Lemieux, L., Woermann, F.G., Fish, D.R., Shorvon, S.D., 1998. Identifying homologous anatomical landmarks on reconstructed magnetic resonance images of the human cerebral cortical surface. Journal of Anatomy 193, 559–571.

Neubauer, S., 2014. Endocasts: possibilities and limitations for the interpretation of human brain evolution. Brain, Behavior and Evolution 84, 117–134.

Neubauer, S., Gunz, P., 2018. Endocasts and the evo-devo approach to study human brain evolution. In: Bruner, E., Ogihara, N., Tanabe, H.C. (Eds.), Digital Endocasts: From Skulls to Brains. Springer Japan, Tokyo, pp. 173–190.

Neubauer, S., Gunz, P., Hublin, J.-J., 2009. The pattern of endocranial ontogenetic shape changes in humans. Journal of Anatomy 215, 240–255.

Neubauer, S., Gunz, P., Hublin, J.-J., 2010. Endocranial shape changes during growth in chimpanzees and humans: A morphometric analysis of unique and shared aspects. Journal of Human Evolution 59, 555–566.

Neubauer, S., Hublin, J.-J., Gunz, P., 2018. The evolution of modern human brain shape. Science Advances 4, eaao5961.

Pearce, E., Stringer, C., Dunbar, R.I.M., 2013. New insights into differences in brain organization between Neanderthals and anatomically modern humans. Proceedings of the Royal Society B 280, 20130168.

Pereira-Pedro, A.S., Bruner, E., 2016. Sulcal pattern, extension, and morphology of the precuneus in adult humans. Annals of Anatomy 208, 85–93.

Pereira-Pedro, A.S., Bruner, E., 2018. Landmarking endocasts. In: Bruner, E., Ogihara, N., Tanabe, H.C. (Eds.), Digital Endocasts: From Skulls to Brains. Springer Japan, Tokyo, pp. 127–142.

Ponce de León, M.S., Bienvenu, T., Akazawa, T., Zollikofer, C.P.E., 2016. Brain development is similar in Neanderthals and modern humans. Current Biology 26, R665–R666.

Preuss, T.M., 2017. The human brain: evolution and distinctive features. In: Tibayrenc, M., Ayala, F.J. (Eds.), On Human Nature. Academic Press, San Diego, pp. 125–149.

Radinsky, L., 1974. The fossil evidence of anthropoid brain evolution. American Journal of Physical Anthropology 41, 15–27.

Ramnani, N., 2006. The primate cortico-cerebellar system: anatomy and function. Nature

Reviews Neuroscience 7, 511-522.

Reardon, P.K., Seidlitz, J., Vandekar, S., Liu, S., Patel, R., Park, M.T.M., Alexander-Bloch, A., Clasen, L.S., Blumenthal, J.D., Lalonde, F.M., Giedd, J.N., Gur, R.C., Gur, R.E., Lerch, J.P., Chakravarty, M.M., Satterthwaite, T.D., Shinohara, R.T., Raznahan, A., 2018. Normative brain size variation and brain shape diversity in humans. Science 360, 1222–1227.

Ribas, G.C., 2010. The cerebral sulci and gyri. Neurosurgical Focus 28 (2):E2.

Rilling, J.K., Seligman, R.A., 2002. A quantitative morphometric comparative analysis of the primate temporal lobe. Journal of Human Evolution 42, 505–533.

Rohlf, F.J., Slice, D.E., 1990. Extensions of the Procrustes method for the optimal superimposition of landmarks. Systematic Zoology 39, 40–59.

Scheperjans, F., Eickhoff, S.B., Hömke, L., Mohlberg, H., Hermann, K., Amunts, K., Zilles, K., 2008. Probabilistic maps, morphometry, and variability of cytoarchitectonic areas in the human superior parietal cortex. Cerebral Cortex 18, 2141–2157.

Schoenemann, P.T., Sheehan, M.J., Glotzer, L.D., 2005. Prefrontal white matter volume is disproportionately larger in humans than in other primates. Nature Neuroscience 8, 242–252.

Scott, N.A., Strauss, A., Hublin, J.-J., Gunz, P., Neubauer, S., 2018. Covariation of the endocranium and splanchnocranium during great ape ontogeny. PLoS One 13, e0208999.

Smaers, J.B., Schleicher, A., Zilles, K., Vinicius, L., 2010. Frontal white matter volume is associated with brain enlargement and higher structural connectivity in anthropoid primates. PLoS One 5, e9123.

Tunik, E., Rice, N.J., Hamilton, A., Grafton, S.T., 2007. Beyond grasping: Representation of action in human anterior intraparietal sulcus. NeuroImage 36, T77–T86.

Valyear, K.F., Fitzpatrick, A.M., McManus, E.F., 2017. The neuroscience of human tool use. In: Kaas, J.H. (Ed.), Evolution of Nervous Systems, 2nd ed. Academic Press, Oxford, pp. 341–353.

Vanduffel, W., Fize, D., Peuskens, H., Denys, K., Sunaert, S., Todd, J.T., Orban, G.A., 2002. Extracting 3D from motion: differences in human and monkey intraparietal cortex. Science 298, 413–415.

Weaver, A.H., 2005. Reciprocal evolution of the cerebellum and neocortex in fossil humans. Proceedings of the National Academy of Sciences 102(10), 3576-3580.

Wild, H.M., Heckemann, R.A., Studholme, C., Hammers, A., 2017. Gyri of the human parietal lobe: Volumes, spatial extents, automatic labelling, and probabilistic atlases. PLoS One 12, e0180866.

Wynn, T., Overmann, K.A., Coolidge, F.L., 2016. The false dichotomy: a refutation of the Neandertal indistinguishability claim. Journal of Anthropological Sciences 94, 201–221.

Zollikofer, C.P.E., Bienvenu, T., Ponce de León, M.S., 2017. Effects of cranial integration on hominid endocranial shape. Journal of Anatomy 230, 85–105.

Chapter 4

PARIETAL LOBE VARIATION IN THE MIDSAGITTAL BRAIN SURFACE: THE PRECUNEUS

4. PARIETAL LOBE VARIATION IN THE MIDSAGITTAL BRAIN SURFACE: THE PRECUNEUS

The longitudinal proportions of the precuneus comprise the main source of variation within adult humans and distinguishing humans from chimpanzees. Yet, the causes and consequences of this outstanding variability are still to be determined. Accordingly, we further explore the anatomical variation of the precuneus among humans and across non-human primates. The three studies are include geometric morphometrics analysis of 2D images extracted from MRI data.

In 4.1, we describe the variability of the human precuneus in terms of folding patterns observed on the midsagittal brain surface, and then consider the dimensions and geometry according to coronal sections. In this second part, the height and inner extension of the precuneus are measured through traditional methods, and the geometry is explored through geometric morphometrics analysis of 2D landmarks representing the main boundaries of the precuneus and the lateral curvature of the parietal lobe, on the coronal section cutting through the centre of the precuneus.

In 4.2, the variation in precuneus proportions on the midsagittal surface of the human brain is revisited considering a larger sample with diverse ancestry, and evaluating the association between anatomical variation of the precuneus with area and volume measurements, as well as with specific sulcal patterns.

In 4.3, we investigate midsagittal shape variation in a sample of non-human primates, including apes and New and Old World monkeys, in order to evaluate whether the precuneus enlargement in humans is due to allometry or whether it represents a species-specific trait.

4.1. SULCAL PATTERN, EXTENSION, AND MORPHOLOGY OF THE PRECUNEUS IN ADULT HUMANS

Authors: Ana Sofia Pereira Pedro, Emiliano Bruner

Journal: Annals of Anatomy, 208: 85-93

Status: Published in 2016

Annals of Anatomy 208 (2016) 85–93

Contents lists available at ScienceDirect

Annals of Anatomy

journal homepage: www.elsevier.com/locate/aanat

Research article

Sulcal pattern, extension, and morphology of the precuneus in adult humans

Ana Sofia Pereira-Pedro, Emiliano Bruner*

Centro Nacional de Investigación sobre la Evolución Humana, Spain

ARTICLE INFO

Article history:
Received 3 December 2015
Received in revised form 5 May 2016
Accepted 9 May 2016

Keywords:
Brain anatomy
Parietal lobes
Subparietal sulcus
Cortical folding
Shape analysis

ABSTRACT

The precuneus represents a relevant cortical component of the parietal lobes. It is involved in visuospatial integration, imagery and simulation, self-awareness, and it is a main node of the Default Mode Network. Its morphology is extremely variable among adult humans, and it has been hypothesized to have undergone major morphological changes in the evolution of *Homo sapiens*. Recent studies have evidenced a marked variation also associated with its sulcal patterns. The present survey contributes to add further information on this topic, investigating the extension of its main folds, their geometrical influence on the lateral parietal areas, and the relationships with the sulcal schemes. The subparietal sulcus, on average, extends 14 mm in its anterior and middle regions and 11 mm in its posterior area. The precuneal area extends 36 mm above this sulcus. The subparietal sulcus is generally wider on the right hemisphere. Males have larger values than females, but differences are not significant. Sulcal pattern is not correlated with the size of the subparietal sulcus extension. There is a lack of consistent correspondence between hemispheres in the sulcal patterns, pointing further towards a notable individual variability and random asymmetries. The vertical extension of the precuneus influences the height and proportions of the upper parietal profile, but the lateral parietal outline is not sensitive to precuneal variation. There is no correlation between external cortical shape and the size of the subparietal sulcus. Morphological analyses of the precuneus must be integrated with studies on histological factors involved in its variability and, ultimately, with analyses on possible relationships with functional factors.

1. Introduction

The precuneus is a cortical element positioned in the medial parietal surface, folded in the midsagittal plane and in contact with the falx cerebri (Fig. 1a). Its area is delimited by three sulci: the *ramus marginalis* of the cingulate sulcus (RC), the parieto-occipital sulcus (PO), and the subparietal sulcus (SS). This area corresponds to the Brodmann area (BA) 7 (Cavanna and Trimble, 2006), which is further divided into three different cytoarchitectonic regions (Mars et al., 2011; Scheperjans et al., 2008). Research on the precuneus has been increasing in the last decade, firstly due to improvements in imaging techniques which have facilitated access to this deep brain area, and secondly because many studies in independent fields have revealed its central role in brain organization and evolution. The precuneus is a centre for widespread neural connectivity (Cavanna and Trimble, 2006; Fransson and Marrelec, 2008; Hagmann et al., 2008; Khalsa et al., 2014). According to the cytoarchitectonic subdivisions by Scheperjans et al. (2008), the precuneus can be subdivided into three regions according to its connectivity: (1) a dorsal anterior region along the RC with a role in controlling spatially guided behaviour; (2) a dorsal posterior region connected to the visual cortex that is involved in visual/motor imagery; (3) a ventral central region, adjacent to the subparietal sulcus, which supplies a cortical integration between sensorial and superior cognitive functions (Cavanna and Trimble, 2006; Margulies et al., 2009; Zhang and Li, 2012). The precuneus is part of the Default Mode Network, responsible for baseline brain activity, and it participates in intrinsic ongoing mental processes involved in exploring and interpreting stored information (Greicius et al., 2003; Raichle et al., 2001; Raichle and Snyder, 2007). It is also involved in fundamental cognitive social functions, such as autobiographical memory and theory of mind (Spreng et al., 2009), recognition of familiar faces (Gobbini and Haxby, 2007), memory recall and reconstruction of imaginary scenes from an egocentric perspective (Freton et al., 2014; Hassabis and Maguire, 2009; Lou et al., 2004). According to Bruner and Iriki (2016), the precuneus, mediating the integration between the environment, the body, and the neural system, is probably a crucial node for embodiment and cognitive extension.

---

* Corresponding author at: Centro Nacional de Investigación sobre la Evolución Humana, Paseo Sierra de Atapuerca 3, 09002 Burgos, Spain.
E-mail address: emiliano.bruner@cenieh.es (E. Bruner).

http://dx.doi.org/10.1016/j.aanat.2016.05.001
0940-9602/

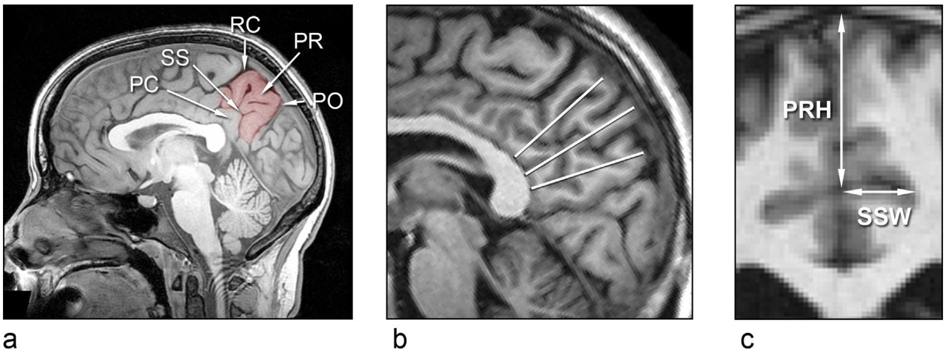

Fig. 1. (a) The precuneus (PR) is positioned between the marginal ramus of the cingulate sulcus (RC) and the parieto-occipital fissure (PO). Its main intrinsic fold is the subparietal sulcus (SS). The area below this sulcus is a meeting point between the posterior cingulate cortex, precuneus, and retrosplenial cortex (PC). (b) In this study, we analyzed three coronal sections (anterior, middle, posterior) approximately orthogonal to the curvature of the upper parietal lobule, in order to describe and quantify the inner extension of the precuneus. (c) For the three sections, we measured the lateral extension (width) of the subparietal sulcus (SSW), and for the middle section also the vertical extension (height) of the precuneal area, from the subparietal sulcus to the endocranial wall (PRH).

Recent morphometric analyses have shown that the longitudinal proportions of the precuneus are extremely variable among adult humans (Bruner et al., 2014, 2015a), and this variation parallels evolutionary changes associated with the origin of *Homo sapiens* (Bruner et al., 2004; Gunz et al., 2010). A larger precuneus also represents a major difference between human and chimpanzee midsagittal brain morphology (Bruner et al., 2016). The similarity between intra-specific brain changes and inter-specific cranial changes suggests that the precuneus may have undergone important morphological modifications in our phylogenetic lineage. The activation patterns, function and structure of this deep parietal region are similar in human and non-human primates such as chimpanzees (Barks et al., 2015; Rilling et al., 2007) and macaques (Margulies et al., 2009), and apparently they differ only in their degree of complexity. Because inter-specific differences in this area cannot be found, it was hypothesized that such evolutionary differences may be more a matter of grade and neural reuse than of newly evolved functions or structures (Caminiti et al., 2015). Interestingly, increased activity and high fluctuations can make cortical regions more vulnerable to pathologies like Alzheimer's disease (Buckner et al., 2009). Indeed, the early metabolic changes in this disease seem to influence the medial parietal cortex (Jacobs et al., 2012). Following this evidence, vulnerability to neurodegenerative processes was hypothesized to be a drawback of recent parietal complexity (Bruner and Jacobs, 2013). Attention deficit/hyperactivity disorder (Castellanos et al., 2008) and schizophrenia (Swanson et al., 2011) are other pathological conditions which have been associated with precuneus dysfunction.

Delays in studying this deep cortical region were probably due to its position, with consequent difficulties in planning anatomical survey or evaluating functional impairments. Also, neurosurgery in these areas is hampered by its spatial accessibility (Tokunaga et al., 2006). In general, sulcal patterns are used as a reference for neurosurgical guidance (Ribas et al., 2006). Morphometric evaluations, in this case, may largely depend on the variable nature of the subparietal sulcus (Spasojević et al., 2004). The patterns and connections of this sulcus were addressed recently in two different studies: Gürer et al. (2013) analyzed a small sample of 28 post-mortem brains and Kacar et al. (2015) studied the MRIs of 200 individuals. Both teams analyzed three parameters (patterns, connections to the cingulate and parieto-occipital sulci, and the number of branches that reached the external surface of the precuneus) obtaining similar results. They observed an H-like sulcal pattern in roughly half of their samples. Regarding connectivity, the subparietal sulcus was more frequently linked to the cingulate sulcus or to none of the sulci, and usually had at least one branch which reached the top of the precuneus. Kacar and colleagues report a significant asymmetry, with a subparietal sulcus connected to the cingulate and two branches reaching the top of the precuneus which appear more frequently on the left hemisphere. However, none of these studies consider other precuneus sulci that are unconnected to the subparietal sulcus.

The current article represents an additional study of the precuneus morphology. After the analyses of its longitudinal and midsagittal variation in adult humans (Bruner et al., 2014, 2015b), this survey supplies a quantitative evaluation of its lateral and vertical proportions, taking into consideration the extension of its main folds and the morphology of the sulcal patterns.

2. Materials and methods

2.1. Fold size

We used a sample of 50 specimens (25 males and 25 females) from the Magnetic Resonance (MR) OASIS collection, with a 1 mm isometric voxel (Marcus et al., 2007). Individuals are all young adults, aged between 20 and 40 years (mean age 25 ± 4.9 years). MR images were processed with ImageJ 1.48v (Schneider et al., 2012). Visualizing the precuneus on its most sagittal plane, we reformatted the stacks according to three coronal planes showing the precuneus in its anterior, middle, and posterior longitudinal sections (Fig. 1b). The planes were chosen in order to optimize the longitudinal curvature of the precuneus, and to approximate the orthogonal sections of the cortical layers. The precuneal surface is positioned within the interhemispheric fissure, juxtaposed on the midsagittal plane and in contact with the falx cerebri. Its main fold is the subparietal sulcus, which extends parasagittally from the midline towards the centre of the hemisphere. We measured the extension of the subparietal sulcus in the three coronal sections, from the surface of the precuneus to the innermost grey matter point of the subparietal fold (subparietal sulcus width; Fig. 1c). Ten individuals were measured three times each to calculate measurement error, computed as the mean value of the differences between the three trials for each variable. The overall error was obtained as the mean difference for all individuals and for the three sections. Additionally, for the middle section, we measured the vertical dimension of the mid-parietal area, from the

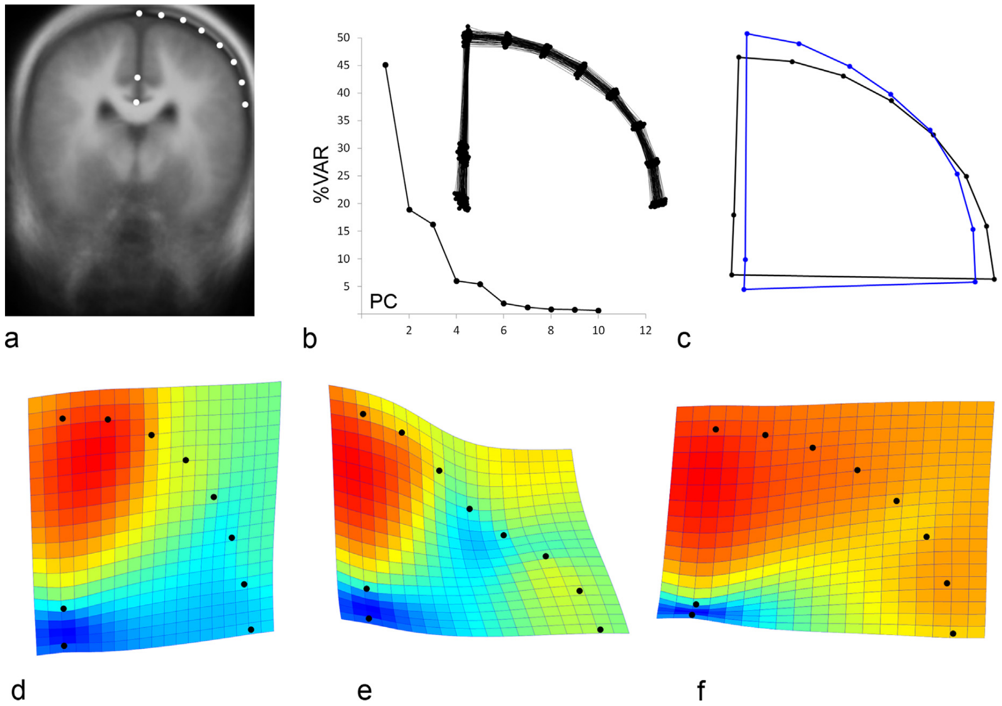

Fig. 2. In the middle section, we analyzed a configuration of 10 bidimensional landmarks (see text) to evaluate the influence of the precuneal extension on the outer parietal profile (a). Coordinates were superimposed by Procrustes superimposition and analyzed with a Principal Component Analysis, revealing one dominant vector and two secondary axes (b). A regression of shape variables (superimposed coordinates) on precuneus height was found to be significant, and associated with a vertical stretching of the whole parietal section. PC1 is associated with the same pattern (d). PC2 deals with vertical stretching of the precuneus and bulging of the midsagittal profile (e), and PC3 is associated with vertical stretching of the whole parietal section due to variation in the height of the posterior cingulate area (f).

subparietal sulcus to the endocranial wall (precuneus height). All metrics were sampled by the same observer (ASPP). The statistical analysis was performed with Statistica 12 (StatSoft Inc). All variables were tested for normality through Kolmogorov–Smirnov and Shapiro–Wilk tests. Normality could not be rejected for any variable, and therefore parametric tests were used to compare groups and distributions. *T*-test for dependent samples (within the same individual) and Pearson's correlation were used to compare the three precuneus sections, and to compare right and left hemispheres for each section. No correction for multiple comparisons was applied when dealing with the three sections. *T*-test for independent samples was used to compare males and females values. Results are considered significant for $p < 0.05$.

2.2. Precuneal folds and parietal outline

We computed a shape analysis to evaluate the relationships between fold extension and outer brain morphology (Fig. 2). On the middle section, we sampled 10 landmarks in 2 dimensions, using the deepest point of the inter-hemispheric fissure, the superficial point of the subparietal sulcus, and 8 equally-spaced semi-landmarks along the endocranial surface from the superior sagittal sinus to the same level of the inter-hemispheric fissure. Landmarks were superimposed by Procrustes registration to a common centroid, scaled to unitary size, and rotated in order to minimize the residual between corresponding landmarks (Bookstein, 1991). Residuals were analyzed by multivariate approaches according to the principles of geometric morphometrics (Zelditch et al., 2004). Shape coordinates were analyzed through Principal Component Analysis to evaluate the underlying patterns of variation, and correlated with precuneus height and subparietal sulcus width in order to consider the effect of lateral precuneus variation on the outer parietal profile. The analysis was computed pooling all the hemispheres from all the individuals. Geometric morphometrics analyses were computed with PAST 2.17c (Hammer et al., 2001) and MorphoJ 1.06a (Klingenberg, 2011).

2.3. Sulcal patterns and connections

The left and right hemispheres were separated, and then visualized in lateral view projecting the MR greyscale values on two dimensions by averaging the intensity values. Each projection was generated by using the five most sagittal sections. Accordingly, the morphological projection synthesizes the information of the most medial 5 mm of cortex. The sulcal pattern is visible from the medial view of the hemispheres, and its morphology does not change along the cortical thickness. Therefore, the first 5 mm are sufficient to reveal most of the information necessary to visualize the sulcal scheme, limiting the noise due to the superimposition with other cortical elements.

The analysis of the sulcal pattern was organized in three categorization systems (Table 1; Fig. 3). The first two systems are based on the sulcal connections: (A) connections of the subparietal sulcus and (B) connections of the other precuneal sulci. The third system (C) considers the overall sulcal patterns. Although the term *precuneal sulcus* is sometimes limited to the anterior fold only (e.g. Margulies et al., 2009), in this paper we refer to the *precuneal sulci* as all the additional precuneal folds beyond the subparietal one.

Table 1
Classification systems (variables) and correspondent categories.

(A) Connections of subparietal sulcus (SS)	
A1	Connected only to the ramus marginalis of the cingulate sulcus (RC)
A2	Connected only to the parieto-occipital sulcus (PO)
A3	Connected to both
A4	Connected to neither
(B) Connections of the precuneal sulci (PS)	
B1	At least 1 connected to the SS and none reaching the edge of the precuneus
B2	At least 1 connected to the SS and also reaching the edge of the precuneus
B3	At least 1 connected to the SS and not reaching the edge of the precuneus; and another reaching the edge of precuneus
B4	No precuneal sulcus connected to the SS but at least 1 reaching the edge of the precuneus
B5	No precuneal sulcus connected to the SS nor reaching the edge of the precuneus
(C) Sulcal patterns in the precuneus	
C1	H shape, or similar (X, π or K) large and full expressed
C2	Deformed H, X, or M, only partially expressed or incomplete
C3	Inverted T, or other mainly vertical shape that is not an H (SS with only one precuneal sulcus linked)
C4	Mainly horizontal shape (e.g. a laid Y, or simply one line (_) or two lines (=); or even a SS with no PS attached)
C5	Irregular: none of the anterior “categories” can be attributed

All individuals were classified three times by the same observer (ASPP), at intervals of 4 days between each trial, and in random order to prevent memorization. The intra-observer reliability was calculated as the percentage agreement for each of the classification systems; i.e. the percentage the rater attributed each specimen to the same category, in all trials. The specimens for which classification was not the same on all trials were reviewed in order to have a final classification for further analysis. Using the final classification, the proportions of the different groups for each categorization system were obtained, for the whole sample and then separated by hemisphere and sex. Association between the sulcal connection of A and B groups, and between the sulcal connections and pattern of the right and left hemispheres, was evaluated with cross tabulation and chi-square. Differences in the precuneus parasagittal extension among the categories in each group were tested with one-way ANOVA.

3. Results

3.1. Sulcal extension

The mean value for all hemispheres for the width of the subparietal sulcus at the central section is 14.3 ± 1.8 mm (range 10.3–18.3). The mean value for all the specimens for the height of the precuneal surface from the subparietal sulcus to the endocranial wall is 35.8 ± 3.5 mm (range 29.4–44.5). There is no significant correlation between subparietal width and precuneus height.

In all sections, a normal distribution of the subparietal sulcus width cannot be rejected (K–S $p > 0.20$, S–W $p > 0.20$ for all cases) (Fig. 4a). The overall mean extension is 13.1 ± 2.3 mm, with an average error of 0.6 mm. The figures are different for the three sections of the precuneus, as the anterior (14.1 ± 1.8 mm) and middle (14.3 ± 1.8 mm) sections have larger values than the posterior section (11.1 ± 1.9 mm) (Fig. 4). The anterior and middle sections are not significantly different from each other, but both differ significantly from the posterior section ($p < 0.001$ for both). The subparietal sulcus tends to be wider on the right hemisphere in both the anterior and middle parts, but on the posterior part the values overlap (Fig. 4b). On the anterior section, the extension in the right hemisphere (14.4 ± 1.8 mm) is wider than on the left (13.7 ± 1.7 mm; $p = 0.009$). Similarly, on the middle part, the subparietal sulcus has a significantly larger inner extension on the right (14.7 ± 1.7 mm) than on the left (13.9 ± 1.7 mm) hemisphere ($p = 0.005$). Conversely, on the posterior part, the precuneus is thicker on the left (11.2 ± 2.0 mm) hemisphere than on the right (11.0 ± 1.7 mm), although the difference in this case is not significant. The subparietal sulcus meets the inter-hemispheric fissure at the same level in the right and left hemispheres. Nonetheless, the widths of the left and right side show only a modest correlation in all sections (Pearson's correlation: anterior: $r = 0.42$, $p = 0.003$; middle: $r = 0.38$, $p = 0.007$; posterior: $r = 0.64$, $p < 0.001$). Males always have a wider subparietal sulcus than females in all sections, but differences are not significant. When testing differences between hemispheres for each sex separately, only males confirm statistically significant differences for the anterior ($p = 0.027$) and middle ($p = 0.004$) sections.

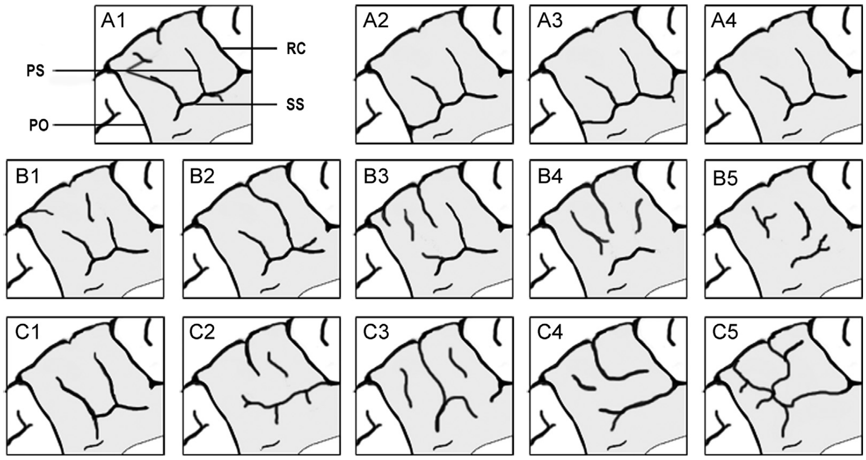

Fig. 3. Illustration of the precuneus sulci connections (A and B) and patterns (C). Categories are described in Table 1. PS: precuneal sulci; PO: parieto-occipital sulcus; RC: *ramus marginalis* of the cingulate sulcus; SS: subparietal sulcus.

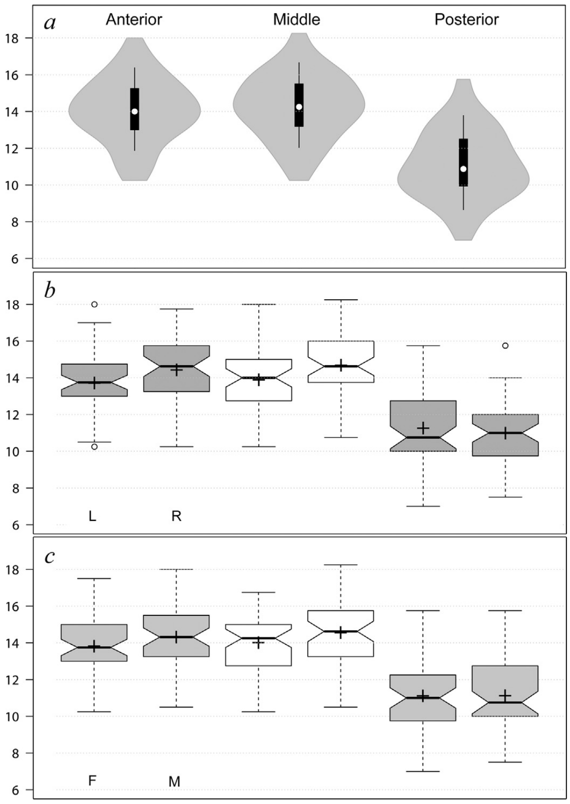

Fig. 4. Distribution of the inner extension values in the three precuneus sections for the whole sample (a) and for hemispheres (b) and sex (c) separately. Graphics is computed with BoxPlotR (Spitzer et al., 2014).

3.2. Precuneal measurements and parietal outline

The principal component analysis of the parietal coronal section reveals three main covariation patterns, one dominant component and two secondary axes (Fig. 2b–f). Successive vectors explain less than 6% of the variance, and are below the standard thresholds of statistical reliability. PC1 (45% of the variance) is associated with precuneus height and vertical stretching of the parietal curve. PC2 (19%) is associated with precuneus height and midsagittal vertical bulging of the profile. This bulging is associated with a parasagittal depression of the upper parietal outline. PC3 (16%) is associated with vertical shortening of the parietal outline due to a decrease in the area below the subparietal sulcus, namely the posterior cingulate cortex. Shape differences are not significant between males and females. Shape variation is not correlated with the width of the subparietal sulcus, but it is statistically correlated to the height of the precuneus ($R^2 = 0.23$; $p < 0.0001$). The pattern associated with precuneal height increase (Fig. 2c) is similar to the pattern associated with PC1, involving a general vertical stretching of the parietal section. Precuneal height increase is not correlated to PC2 ($p = 0.17$), and hence this second vector is not associated with an absolute variation of the precuneal height, but with an absolute increase/decrease of the lateral parasagittal volume.

Therefore, we can conclude that precuneal width (subparietal sulcus) is not associated with morphological changes of the parietal outline, while precuneal height influences the vertical stretching of the upper parietal morphology, but not its parasagittal bulging/depression.

3.3. Sulcal patterns and connections

Categories based on sulcal connections are more reliable than categories based on sulcal patterns, as A (96.0%) and B (92.7%) reveal larger percentage agreement than C (72.3%). Fig. 5 shows the frequencies of the three categorical variables for the whole sample and per hemisphere and sex separately. The subparietal sulcus (groups A) is generally associated with two main patterns: it is connected only to RC (A1: 46%) or it is isolated from both RC and PO (A4: 52%). Connection only to PO was found in only two specimens (A2: 2%), and connections to both RC and PO was not observed. A connection with the cingulate sulcus is more frequent on the right side, but differences are not significant. Regarding the precuneal sulci (groups B), we observed mainly three arrangements, in which at least one sulcus is connected to the subparietal sulcus (B1–B3). In most cases, the sulci reach the edge of the precuneus (B2 and B3). The main difference in this category is based on whether the sulcus reaching the edge of the precuneus is linked to the subparietal sulcus (B2: 37%) or not (B3: 51%). The remaining configurations (where the subparietal sulcus is unlinked to other precuneal sulci) are residual (B4: 1%) or not represented (B5). There are no differences between sexes, but there are significant differences between hemispheres, with the left side displaying a marked increase in the B2 pattern, doubling its prevalence (Chi-square test for difference in distribution $p = 0.024$).

Concerning the overall sulcal pattern (groups C), the most frequent morphology is represented by the inverted T scheme (C3). This pattern is frequently observed in the entire sample (44%), in each hemisphere (left: 40%; right: 48%), and both in females (46%) and males (42%). The H (C1) and deformed H (C2) patterns represent approximately 40% of the cases, with hemispheric differences which are nonetheless not significant. The frequency of the horizontal patterns is rare (C4: 7%). In 10% of the cases, we were not able to recognize any specific pattern (C5).

There is a significant association between A1 and B3 and between A4 and B2 (Cross-tabulation Chi-square $p = 0.017$). However, the correlation is weak, these patterns being associated in only 60–65% of the cases. There is no significant correspondence between hemispheres for the sulcal categories. There is no significant difference for the extension of the subparietal sulcus among the different sulcal pattern groups in any category.

4. Discussion

4.1. The extension of the precuneal folds

Most of the anatomical studies on the precuneus concern its longitudinal and sagittal dimensions. Although the coronal plane can be very informative in MRI studies and although it is largely used in clinical surveys (Salamon et al., 2005), the lateral morphology of this deep parietal element is hardly known. In the present work, we measured the lateral extension of the precuneus, namely the width of the subparietal sulcus, and the length of its main vertical surface.

Metric data on the precuneus based on anatomical (physical) preparations are rare. A survey on fixed brains suggested that males have larger surface area than females, and that the right side is larger than the left one (Spasojević et al., 2004). A recent MRI analysis evidenced that sexual differences may be due to cortical thickness more than to surface, and that the right side has larger cortical surface but smaller cortical thickness (Bruner et al., 2015a). It is worth noting that, in general, the whole parietal lobes are larger

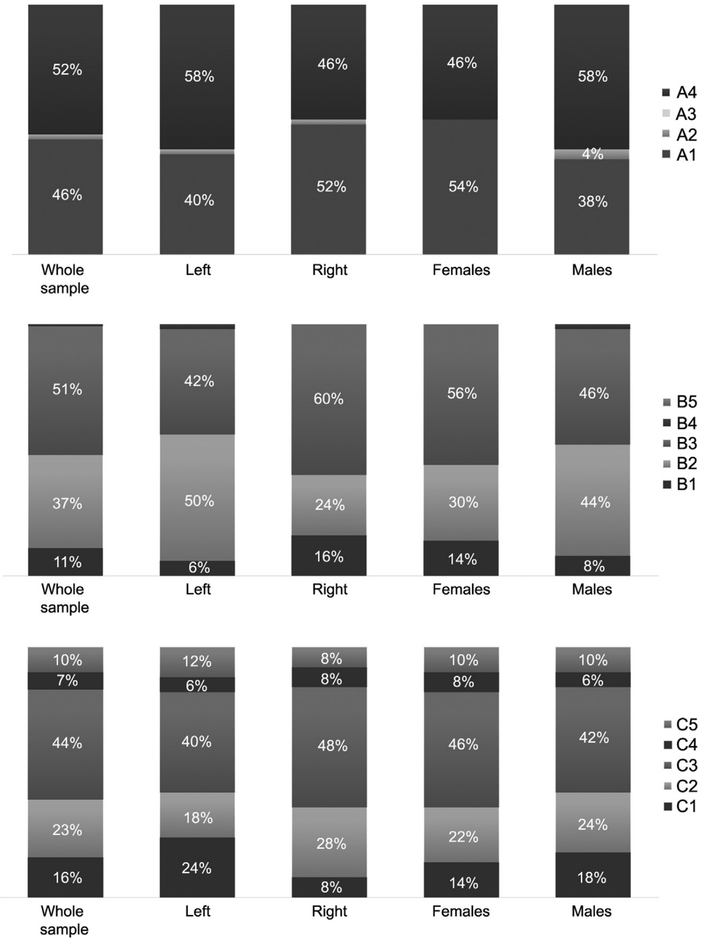

Fig. 5. Proportion of the categories in each variable (A, B and C), considering the whole sample, separate hemispheres and separate sexes.

in males than in females, but only in females is there a recognized hemispheric asymmetry (Allen et al., 2002). In all cases, the correlations between metric variables are generally modest, suggesting a marked individual variation that may obscure shared trends and patterns.

According to the current MRI survey, in its central portion the precuneus on average is 36 mm tall, and the width of its main lateral fold is 14 mm. The posterior area is slightly thinner, and it also shows a lesser complexity of sulcal morphology. Males tend to have a wider precuneus than females in all sections, but differences do not reach significance. The fact that subparietal sulcal size and precuneal surface area are generally larger in males but without reaching significance may be the result of limits in statistical power, due to subtle differences, large individual variability, and small samples. The subparietal sulcus is wider on the right hemisphere, at least for the anterior and middle portions, and most visibly for males. Other areas have been hypothesized to be more asymmetric in males (Kovalev et al., 2003; Luders et al., 2006). Studies on cortical thickness failed to reveal any consistent hemispheric differences for the precuneus region, mostly because of the large individual variation (Bruner et al., 2015a; Koelkebeck et al., 2014; Luders et al., 2006; Zhou et al., 2013). It is therefore likely that the asymmetry we found is due to the length of the fold (surface area) and not to the thickness of the cortex.

The variation of the subparietal sulcus does not influence the outer morphology of the parietal lobes, at least in their coronal plane and lateral profile. In contrast, the vertical extension of the precuneus involves a change in the parietal proportions, stretching the outline vertically. Also, the height of the posterior cingulate cortex can be associated with these vertical changes, but to a minor extent. The influence of these deep cortical changes in the outer brain morphology is relevant for those fields which analyze brain form variation from cranial remains, like paleoneurology (Bruner, 2015). If there is a correspondence between inner and outer changes, the former can be used to investigate the latter in extinct species. In this case, these results suggest that a vertical stretching of the upper parietal profile can indicate an increase in the precuneal height. Conversely, the parasagittal bulging/flattening of the upper parietal surface, although associated with midline bulging, is not a result of changes in midline elements but instead a change of the lateral volumes. Such morphology can be the result of volumetric variation of the lateral surface of the upper and lower parietal areas. In the first case, the intraparietal sulcus is the best candidate, being positioned between the surface and the subparietal sulcus. In the second case, the supramarginal gyrus can be responsible for the parietal curvature. This is particularly interesting taking into account that archaic humans were characterized by a visible parasagittal flattening of the upper parietal areas, Neanderthals by the lateral bulging of these same areas, and modern humans by longitudinal expansion of the whole upper parietal morphology (Bruner, 2004, 2014; Bruner et al., 2003, 2015c). The results of the present analysis suggest that in the case of Neanderthals, the morphological changes may be due to variation in the intraparietal cortex, more than in the precuneal areas, while in modern humans both districts are likely to be involved. In all cases, at least in adult humans, changes in the subparietal sulcus cannot be evidenced by an indirect evaluation of the outer geometry.

In terms of asymmetries, it is worth noting that, in general, the surface area of the right parietal lobes is larger and more bulging on the right side (Balzeau et al., 2012), and this pattern can be observed in all extinct human species (see Bruner, 2015). Taking into account the lack of evidence for the role of the precuneus in this kind of morphological variation, also in this case, the intraparietal sulcus could be the element involved.

4.2. *Sulcal patterns and connections*

The subparietal sulcus is generally connected with the marginal ramus of the cingulate sulcus (46%) or it is isolated (52%). These figures are similar to the ones published by Kacar et al. (2015) (40% and 42%, respectively) and Gürer et al. (2013) (41% and 38%, respectively). However, both teams observed more cases with connections with the parieto-occipital sulcus (Gürer et al.: 13%; Kacar et al.: 6%) and with both parieto-occipital and cingulate sulci (Gürer et al.: 6%; Kacar et al.: 12%), which were rarely or not observed in our sample. Kacar and colleagues also found significant differences between hemispheres, with the subparietal sulcus being connected to the cingulate sulcus more frequently in the left hemisphere. In our study, differences were not significant, and the proportions are even inverted; i.e. the subparietal sulcus is more frequently linked to the cingulate in the right hemisphere.

In the case of the connections of the precuneal sulci with the subparietal sulcus and to the edge of the precuneus, we cannot directly compare our results to the studies by Gürer's and Kacar's teams. They considered only the branches of the subparietal sulcus that reached the edge of the precuneus, while we provide a more comprehensive analysis including all of the precuneus sulci (namely all the sulci inside the precuneus) that reached the edge of the precuneus whether linked to the subparietal sulcus or not. Our pivotal finding here is that in a large percentage of cases, the sulci that reach the external surface of the precuneus are not linked to the subparietal sulcus (52%), a feature that has not been considered before. This finding is important as neurosurgeons rely on sulci as a reference during surgery.

In 99% of the cases, the subparietal sulcus has at least one more sulcus connected, and in 62% of the cases, this secondary sulcus reaches the external (dorsal) cortical surface. This figure was more frequent on the left hemisphere, while on the right hemisphere the secondary sulcus connected to the subparietal sulcus reached the external cortical surface less frequently. Gürer's and Kacar's teams described a more general situation, interpreting every additional sulcus as an extension of the subparietal sulcus. Nonetheless, Kacar et al. (2015) found a significantly larger frequency of two extensions of the subparietal sulcus reaching the external surface of the precuneus on the left hemisphere. Furthermore, they observed a larger number of subparietal sulcus extensions reaching the external cortical surface on the left (74%) than on the right (64%) hemispheres. We also found that the left hemisphere shows a larger prevalence of sulci reaching the external cortical surface.

Considering the general sulcal pattern, the most frequent was the inverted T pattern, followed by the H-like patterns. The remaining patterns appeared less frequently, and in 10% of the cases, we were not able to classify the morphology of the sulcal pattern according to any conventional group. The nomenclature we use here is somewhat distinct from that applied by Gürer et al. (2013) and Kacar et al. (2015). In both studies, the H-like patterns appeared more frequently (Gürer et al. – H: 50%, split – H: 4%; Kacar et al. – H: 45%, split – H: 13%). The double horizontal patterns have a similar low prevalence in all studies (Gürer et al.: 5%; Kacar et al.: 4%) and irregular patterns were only found by Gürer and colleagues, who classified only one hemisphere (2%) with an unidentified pattern. Our mainly vertical pattern probably includes three of the patterns in the cited works (oblique, single upward, and three upward branches), the summed proportions of which (39% for Gürer et al. and 38% for Kacar et al.) still remain lower than those of H shapes. H-like patterns were observed more frequently (61%) by Bruner et al. (2014) as well. It remains to be evaluated whether the differences in prevalence between studies may result from the observer's experience and perception of the sulcal patterns, or from random effects of the samples associated with marked individual variability. It is worth noting, however, that in the present study, the classification of the sulcal patterns displayed lower intra-observer reliability, compared to the grouping based on sulcal connections. Indeed, attributing a shape to the patterns of the precuneus sulci was challenging due to their geometrical diversity. In fact, similarly to the other analyses (Bruner et al., 2015a; Kacar et al., 2015), this study also evidences a marked variation, at both inter-individual and inter-hemispheric levels.

4.3. *Sulcal pattern and sulcal extension*

Mechanical forces exerted by the neural elements may play a relevant role in shaping the cortical morphology and the sulcal pattern, influencing the cortical curvature and thickness (Hilgetag and Barbas, 2005, 2006). Namely, the folding pattern may be a structural consequence of the biomechanical properties of the cortex, and not associated with functional organization or specific genetic regulation (Toro and Burnod, 2005; Bayly et al., 2014). A recent simulation based on both digital and physical models strongly suggests that the sulcal morphology may be a passive mechanical result of allometric constraints associated with the volume-surface relationships (Tallinen et al., 2016). In this case, the cerebral folds must be interpreted not as functional units, but in term of geometrical properties of the cortical morphogenesis.

In this study, we found no significant correlation between the depth of the subparietal sulcus and the sulcal pattern of the precuneus. Therefore, the depth of the fold seems not to be associated with the folding scheme. Complexity of the sulcal patterns seems to be larger on the right hemisphere (Liu et al., 2010; Luders et al., 2004; Sowell et al., 2002) and complexity of gyrification seems to be greater in females (Liu et al., 2010; Luders et al., 2004). As in previous studies (Kacar et al., 2015; Nopoulos et al., 2000), we found no sex differences in sulcal pattern or in sulcal extension. Although genetics plays a role in sulcal morphology, it remains to be established to what extent genes and environment contribute to the general cortical morphology, most of all in areas sensitive to external influences like the parietal ones (Bruner and Iriki, 2016). Heritability was demonstrated for the length and depth of the central sulcus in baboons (Kochunov et al., 2010) and humans (McKay et al., 2013), but in our species the sulcal schemes are apparently less constrained by the genetic background when compared with non-human primates (Gómez-Robles et al., 2015). Nonetheless, even single genes can change the folding schemes (Rakic, 2004), and recently the general cortical morphology was shown to have a correlation with genetic ancestry (Fan et al., 2015). A genetic component may be hypothesized when considering that the precuneus is actually associated with a precise genetic context (Chen et al., 2013). Of course, we can integrate genetic and biomechanical hypotheses taking into account that the genetic programme can influence the time and rate of cortical growth and, consequently, the biomechanical folding sequence. In either case, we cannot exclude that these morphological variations can be simply a matter of genetic/morphogenetic patterning without any major functional consequences. In fact, as demonstrated for other brain areas, also in the precuneus the sulcal morphology shows only a feeble correspondence with the cytoarchitectonic regions (Scheperjans et al., 2008).

We found some weak asymmetric patterning: the left hemisphere tends to have more sulci reaching the external surface of the brain, while the right hemisphere tends to display deeper folding. We also found a minor association between the frequency of sulcal connections with the cingulate sulcus and frequency of sulcal connections with the external surface: when the sulcal pattern contacts the cingulate sulcus, the sulcal connections with the external surface are less frequent, and vice versa. Because of the large morphological variation and modest association, this result should be confirmed with larger samples. Nonetheless, such inverse frequency between sulci merits attention, being directly related to the folding mechanisms.

It is worth noting that if folding is a passive consequence of the geometrical properties of the cortex (e.g., Tallinen et al., 2016), then some traditional functional inferences may no longer be substantiated but, nonetheless, a different kind of information can be obtained related to the sulcal morphology. In fact, in this case the folding pattern can be used as an indirect indication of the underlying processes of cortical growth. That is, in the future, folding patterns should be investigated in terms of relative proportions and sequence of differential growth, hopefully giving information on time and rate of cortical development.

A major limit when comparing brain morphology and anatomy is due to differences in methods, definitions, and samples (Chee et al., 2011; Koelkebeck et al., 2014; Luders et al., 2006). Individual variability may be considerable, and this can influence sample-specific results (Bruner et al., 2014, 2015a; Koelkebeck et al., 2014; Kovalev et al., 2003). Therefore, in neuroanatomy, consistent conclusions need multiple verifications using different samples and different approaches, and, for the precuneus, several publications have supplied complementary data. An ontogenetic series can further add to this topic, as well as results from distinct human populations. In terms of morphogenesis, further studies are needed to consider the structural factors that generate different cortical arrangements. Namely, the histological mechanisms and cytological elements behind the observed morphological variability must be investigated to evaluate the anatomical source of these differences.

Conflict of interest

The authors declare no conflict of interest.

Acknowledgements

This paper is supported by the Italian Institute of Anthropology. ASPP is funded by a grant of the Atapuerca Foundation, Spain. EB is funded by the Spanish Government (CGL2012-38434-C03-02). We would like to thank Gizéh Rangel de Lázaro, José Manuel de la Cuétara, Jim Rilling, Todd Preuss, Heidi Jacobs, Manuel Martín-Loeches, Roberto Colom, Slobodan Malobabić and Atsushi Iriki for their comments and collaboration on the topics introduced in this article.

References

Allen, J.S., Damasio, H., Grabowski, T.J., 2002. Normal neuroanatomical variation in the human brain: an MRI-Volumetric Study. Am. J. Phys. Anthropol. 118, 341–358.

Balzeau, A., Holloway, R.L., Grimaud-Hervé, D., 2012. Variations and asymmetries in regional brain surface in the genus *Homo*. J. Hum. Evol. 62, 696–706.

Barks, S.K., Parr, L.A., Rilling, J.K., 2015. The default mode network in chimpanzees (*Pan troglodytes*) is similar to that of humans. Cereb. Cortex 25, 538–544.

Bayly, P.V., Taber, L.A., Kroenke, C.D., 2014. Mechanical forces in cerebral cortical folding: a review of measurements and models. J. Mech. Behav. Biomed. Mater. 29, 568–581.

Bookstein, F.L., 1991. Morphometric Tools for Landmark Data: Geometry and Biology. Cambridge University Press, Cambridge.

Bruner, E., 2004. Geometric morphometrics and paleoneurology: brain shape evolution in the genus *Homo*. J. Hum. Evol. 47, 279–303.

Bruner, E., 2014. Functional craniology, human evolution, and anatomical constraints in the neanderthal braincase. In: Akazawa, T., Ogihara, N., Tanabe, H.C., Terashima, H. (Eds.), Dynamics of Learning in Neanderthals and Modern Humans. Springer, Japan, pp. 121–129.

Bruner, E., 2015. Functional craniology and brain evolution. In: Bruner, E. (Ed.), Human Paleoneurology. Springer, Switzerland, pp. 57–94.

Bruner, E., Iriki, A., 2016. Extending mind, visuospatial integration, and the evolution of the parietal lobes in the human genus. Quat. Int., http://dx.doi.org/10.1016/j.quaint.2015.05.019.

Bruner, E., Jacobs, H.I.L., 2013. Alzheimer's disease: the downside of a highly evolved parietal lobe? J. Alzheimers Dis. 35, 227–240.

Bruner, E., Manzi, G., Arsuaga, J.L., 2003. Encephalization and allometric trajectories in the genus *Homo*: evidence from the Neandertal and modern lineages. Proc. Natl. Acad. Sci. U.S.A. 100, 15335–15340.

Bruner, E., Saracino, B., Ricci, F., Tafuri, M., Passarello, P., Manzi, G., 2004. Midsagittal cranial shape variation in the genus *Homo* by geometric morphometrics. Coll. Antropol. 28, 99–112.

Bruner, E., Rangel de Lázaro, G., de la Cuétara, J.M., Martín-Loeches, M., Colom, R., Jacobs, H.I.L., 2014. Midsagittal brain variation and MRI shape analysis of the precuneus in adult individuals. J. Anat. 224, 367–376.

Bruner, E., Román, F.J., de la Cuétara, J.M., Martín-Loeches, M., Colom, R., 2015a. Cortical surface area and cortical thickness in the precuneus of adult humans. Neuroscience 286, 345–352.

Bruner, E., Amano, H., de la Cuétara, J.M., Ogihara, N., 2015b. The brain and the braincase: a spatial analysis on the midsagittal profile in adult humans. J. Anat. 227, 268–276.

Bruner, E., Grimaud-Hervé, D., Wu, X., de la Cuétara, J.M., Holloway, R., 2015c. A paleoneurological survey of *Homo erectus* endocranial metrics. Quat. Int. 368, 80–87.

Bruner, E., Preuss, T., Chen, X., Rilling, J., 2016. Evidence for expansion of the precuneus in human evolution. Brain Struct. Funct., http://dx.doi.org/10.1007/s00429-015-1172-y.

Buckner, R.L., Sepulcre, J., Talukdar, T., Krienen, F.M., Liu, H., Hedden, T., Andrews-Hanna, J., Sperling, R.A., Johnson, K.A., 2009. Cortical hubs revealed by intrinsic functional connectivity: mapping, assessment of stability, and relation to Alzheimer's disease. J. Neurosci. 29, 1860–1873.

Caminiti, R., Innocenti, G.M., Battaglia-Mayer, A., 2015. Organization and evolution of parieto-frontal processing streams in macaque monkeys and humans. Neurosci. Biobehav. Rev. 56, 73–96.

Castellanos, F.X., Margulies, D.S., Kelly, C., Uddin, L.Q., Ghaffari, M., Kirsch, A., Shaw, D., Shehzad, Z., Di Martino, A., Biswal, B., Sonuga-Barke, E., Rotrosen, J., Adler, L.A., Milham, M.P., 2008. Cingulate–precuneus interactions: a new locus of dysfunction in adult attention-deficit/hyperactivity disorder. Biol. Psychiatry 63, 332–337.

Cavanna, A.E., Trimble, M.R., 2006. The precuneus: a review of its functional anatomy and behavioural correlates. Brain 129, 564–583.

Chee, M.W.L., Zheng, H., Goh, J.O.S., Park, D., Sutton, B.P., 2011. Brain structure in young and old East Asians and westerners: comparisons of structural volume and cortical thickness. J. Cogn. Neurosci. 23, 1065–1079.

Chen, C.-H., Fiecas, M., Gutiérrez, E.D., Panizzon, M.S., Eyler, L.T., Vuoksimaa, E., Thompson, W.K., Fennema-Notestine, C., Hagler, D.J., Jernigan, T.L., Neale, M.C., Franz, C.E., Lyons, M.J., Fischl, B., Tsuang, M.T., Dale, A.M., Kremen, W.S., 2013. Genetic topography of brain morphology. Proc. Natl. Acad. Sci. U.S.A. 110, 17089–17094.

Fan, C.C., Bartsch, H., Schork, A.J., Chen, C-H., Wang, Y., Lo, M-T., Brown, T.T., Kuperman, J.M., Hagler, D.J., Schork, N.J., Jernigan, T.L., Dale, A.M., 2015. Modeling the 3d geometry of the cortical surface with genetic ancestry. Curr. Biol. 25, 1988–1992.

Fransson, P., Marrelec, G., 2008. The precuneus/posterior cingulate cortex plays a pivotal role in the default mode network: evidence from a partial correlation network analysis. NeuroImage 42, 1178–1184.

Freton, M., Lemogne, C., Bergouignan, L., Delaveau, P., Lahéricy, S., Fossati, P., 2014. The eye of the self: precuneus volume and visual perspective during autobiographical memory retrieval. Brain Struct. Funct. 219, 959–968.

Gobbini, M.I., Haxby, J.V., 2007. Neural systems for recognition of familiar faces. Neuropsychologia 45, 32–41.

Gómez-Robles, A., Hopkins, W.D., Schapiro, S.J., Sherwood, C.C., 2015. Relaxed genetic control of cortical organization in human brains compared with chimpanzees. Proc. Natl. Acad. Sci. U.S.A. 112, 14799–14804.

Greicius, M.D., Krasnow, B., Reiss, A.L., Menon, V., 2003. Functional connectivity in the resting brain: a network analysis of the default mode hypothesis. Proc. Natl. Acad. Sci. U.S.A. 100, 253–258.

Gunz, P., Neubauer, S., Maureille, B., Hublin, J.-J., 2010. Brain development after birth differs between Neanderthals and modern humans. Curr. Biol. 20, R921–R922.

Gürer, B., Bozkurt, M., Neves, G., Cikla, U., Hananya, T., Antar, V., Salamat, S., Başkaya, M.K., 2013. The subparietal and parietooccipital sulci: an anatomical study. Clin. Anat. 26, 667–674.

Hagmann, P., Cammoun, L., Gigandet, X., Meuli, R., Honey, C.J., Wedeen, V.J., Sporns, O., 2008. Mapping the structural core of human cerebral cortex. PLoS Biol. 6, e159.

Hammer, Ø., Ryan, P., Harper, D., 2001. PAST: Paleontological statistics software package for education and data analysis. Palaeontol. Electron. 4, 1–9.

Hassabis, D., Maguire, E.A., 2009. The construction system of the brain. Phil. Trans. R. Soc. B 364, 1263–1271.

Hilgetag, C.C., Barbas, H., 2005. Developmental mechanics of the primate cerebral cortex. Anat. Embryol. 210, 411–417.

Hilgetag, C.C., Barbas, H., 2006. Role of mechanical factors in the morphology of the primate cerebral cortex. PLoS Comput. Biol. 2 (3), e22.

Jacobs, H.I.L., Van Boxtel, M.P.J., Jolles, J., Verhey, F.R.J., Uylings, H.B.M., 2012. Parietal cortex matters in Alzheimer's disease: an overview of structural, functional and metabolic findings. Neurosci. Biobehav. Rev. 36, 297–309.

Kacar, E., Nas, O.F., Okeer, E., Hakyemez, B., 2015. Pattern, variability, and hemispheric differences of the subparietal sulcus on multiplanar reconstructed MR images. Surg. Radiol. Anat., http://dx.doi.org/10.1007/s00276-015-1525-5.

Khalsa, S., Mayhew, S.D., Chechlacz, M., Bagary, M., Bagshaw, A.P., 2014. The structural and functional connectivity of the posterior cingulate cortex: comparison between deterministic and probabilistic tractography for the investigation of structure–function relationships. NeuroImage 102 (1), 118–127.

Klingenberg, C.P., 2011. Morphoj: an integrated software package for geometric morphometrics. Mol. Ecol. Resour. 11, 353–357.

Kochunov, P., Glahn, D.C., Fox, P.T., Lancaster, J.L., Saleem, K., Shelledy, W., Zilles, K., Thompson, P.M., Coulon, O., Mangin, J.F., Blangero, J., Rogers, J., 2010. Genetics of primary cerebral gyrification: heritability of length, depth and area of primary sulci in an extended pedigree of Papio baboons. NeuroImage 53, 1126–1134.

Koelkebeck, K., Miyata, J., Kubota, M., Kohl, W., Son, S., Fukuyaman, H., Sawamoto, N., Takahashi, H., Murai, T., 2014. The contribution of cortical thickness and surface area to gray matter asymmetries in the healthy human brain. Hum. Brain. Mapp. 35, 6011–6022.

Kovalev, V.A., Kruggel, F., von Cramon, D.Y., 2003. Gender and age effects in structural brain asymmetry as measured by MRI texture analysis. NeuroImage 19, 895–905.

Liu, T., Wen, W., Zhu, W., Trollor, J., Reppermund, S., Crawford, J., Jin, J.S., Luo, S., Brodaty, H., Sachdev, P., 2010. The effects of age and sex on cortical sulci in the elderly. NeuroImage 51, 19–27.

Lou, H.C., Luber, B., Crupain, M., Keenan, J.P., Nowak, M., Kjaer, T.W:, Sackeim, H.A., Lisanby, S.H., 2004. Parietal cortex and representation of the mental self. Proc. Natl. Acad. Sci. U.S.A. 101, 6827–6832.

Luders, E., Narr, K.L., Thompson, P.M., Rex, D.E., Jancke, I., Steinmetz, H., Toga, A.W., 2004. Gender differences in cortical complexity. Nat. Neurosci. 7, 799–800.

Luders, E., Narr, K.I., Thompson, P.M., Rex, D.E., Jancke, I., Toga, A.W., 2006. Hemispheric asymmetries in cortical thickness. Cereb. Cortex 16, 1232–1238.

Marcus, D.S., Wang, T.H., Parker, J., Csernansky, J.G., Morris, J.C., Buckner, R.L., 2007. Open Access Series of Imaging Studies (OASIS): cross-sectional MRI data in young, middle aged, nondemented, and demented older adults. J. Cognitive Neurosci. 19, 1498–1507.

Margulies, D.S., Vincent, J.L., Kelly, C., Lohmann, G., Uddin, L.Q., Biswal, B.B., Villringer, A., Castellanos, F.X., Milham, M.P., Petrides, M., 2009. Precuneus shares intrinsic functional architecture in humans and monkeys. Proc. Natl. Acad. Sci. U.S.A. 106, 20069–20074.

Mars, R.B., Jbabdi, S., Sallet, J., O'Reilly, J.X., Croxson, P.L., Olivier, E., Noonan, M., Bergmann, C., Mitchell, A.S., Baxter, M.G., Behrens, T., Johansen-Berg, H., Tomassini, V., Miller, K.L., Rushworth, M., 2011. Diffusion-weighted imaging tractography-based parcellation of the human parietal cortex and comparison with human and macaque resting-state functional connectivity. J. Neurosci. 31, 4087–4100.

McKay, D.R., Kochunov, P., Cykowski, M.D., Kent, J.W., Laird, A.R:, Lancaster, J.L., Blangero, J., Glahn, D.C., Rex, P.T., 2013. Sulcal depth-position profile is a genetically mediated neuroscientific trait: description and characterization in the central sulcus. J. Neurosci. 33, 15618–15625.

Nopoulos, P., Flaum, M., O'Leary, D., Andreasen, N.C., 2000. Sexual dimorphism in the human brain: evaluation of tissue volume, tissue composition and surface anatomy using magnetic resonance imaging. Psychiatry Res. Neuroimaging 98, 1–13.

Raichle, M.E., Snyder, A.Z., 2007. A default mode of brain function: a brief history of an evolving idea. NeuroImage 37, 1083–1090.

Raichle, M.E., MacLeod, A.M., Snyder, A.Z., Powers, W.J., Gusnard, D.A., Shulman, G.L., 2001. A default mode of brain function. Proc. Natl. Acad. Sci. U.S.A. 98, 676–682.

Rakic, P., 2004. Neuroscience: genetic control of cortical convolutions. Science 303, 1983–1984.

Ribas, G.C., Yasuda, A., Ribas, E.C., Nishikuni, K., Rodrigues Jr., A.J., 2006. Surgical anatomy of microneurosurgical sulcal key points. Neurosurgery 59, 177–210.

Rilling, J.K., Barks, S.K., Parr, L.A., Preuss, T.M., Faber, T.L., Pagnoni, G., Bremner, J.D., Votaw, J.R., 2007. A comparison of resting-state brain activity in humans and chimpanzees. Proc. Natl. Acad. Sci. U.S.A. 104, 17146–17151.

Salamon, N., Sicotte, N., Mongkolwat, P., Shattuck, D., Salamon, G., 2005. The human cerebral cortex on MRI: value of the coronal plane. Surg. Radiol. Anat. 27, 431–443.

Scheperjans, F., Hermann, K., Eickhoff, S.B., Amunts, K., Schleicher, A., Zilles, K., 2008. Observer-independent cytoarchitectonic mapping of the human superior parietal cortex. Cereb. Cortex 18, 846–867.

Schneider, C.A., Rasband, W.S., Eliceiri, K.W., 2012. Nih image to imagej: 25 years of image analysis. Nat. Methods 9, 671–675.

Sowell, E.R., Thompson, P.M., Rex, D., Kornsand, D., Tessner, K.D., Jernigan, T.L:, Toga, A.W., 2002. Mapping sulcal pattern asymmetry and local cortical surface gray matter distribution in vivo: maturation in perisylvian cortices. Cereb. Cortex 12, 17–26.

Spasojević, G., Malobabic, S., Suscevic, D., Milijovic, Z., 2004. Morphometric variability of precuneus in relation to gender and the hemisphere of human brain. Vojnosanit. Pregl. 61, 365–370.

Spitzer, M., Wildenhain, J., Rappsilber, J., Tyers, M., 2014. Boxplotr: a web tool for generation of box plots. Nat. Methods 11, 121–122.

Spreng, R.N., Mar, R.A., Kim, A.S.N., 2009. The common neural basis of autobiographical memory, prospection, navigation, theory of mind, and the default mode: a quantitative meta-analysis. J. Cogn. Neurosci. 21, 489–510.

Swanson, N., Eichele, T., Pearlson, G., Kiehl, K., Yu, Q., Calhoun, V.D., 2011. Lateral differences in the default mode network in healthy controls and patients with schizophrenia. Hum. Brain Mapp. 32, 654–664.

Tallinen, T., Chung, J.Y., Rousseau, F., Girard, N., Lefèvre, J., Mahadevan, L., 2016. On the growth and form of cortical convolutions. Nat. Phys., http://dx.doi.org/10.1038/nphys3632.

Tokunaga, K., Tamiya, T., Date, I., 2006. Transient memory disturbance after removal of an intraventricular trigonal meningioma by a parieto-occipital interhemispheric precuneus approach. Case report. Surg. Neurol. 65, 167–169.

Toro, R., Burnod, Y., 2005. A morphogenetic model for the development of cortical convolutions. Cereb. Cortex 15, 1900–1913.

Zhang, S., Li, C.S.R., 2012. Functional connectivity mapping of the human precuneus by resting state fMRI. Neuroimage 59, 3548–3562.

Zelditch, M.L., Swiderski, D.L., Sheets, H.D., 2004. Geometric Morphometrics for Biologists: A Primer. Elsevier, New York, London.

Zhou, D., Lebel, C., Evans, A., Beaulieu, C., 2013. Cortical thickness asymmetry from childhood to older adulthood. NeuroImage 83, 66–74.

4.2. PRECUNEUS PROPORTIONS AND CORTICAL FOLDING: A MORPHOMETRIC EVALUATION ON A RACIALLY DIVERSE HUMAN SAMPLE

Authors: Emiliano Bruner, Ana Sofia Pereira Pedro, Xu Chen, James K. Rilling

Journal: Annals of Anatomy, 211: 120-128

Status: Published in 2017

Annals of Anatomy 211 (2017) 120–128

Contents lists available at ScienceDirect

Annals of Anatomy

journal homepage: www.elsevier.com/locate/aanat

RESEARCH ARTICLE

Precuneus proportions and cortical folding: A morphometric evaluation on a racially diverse human sample

Emiliano Bruner[a,*], Ana Sofia Pereira-Pedro[a], Xu Chen[b,c], James K. Rilling[b,c,d,e,f]

[a] Grupo de Paleobiología, Centro Nacional de Investigación sobre la Evolución Humana, Burgos, Spain
[b] Department of Anthropology, Emory University, Atlanta, GA, USA
[c] Department of Psychiatry and Behavioral Sciences, Emory University, Atlanta, GA, USA
[d] Center for Translational Social Neuroscience, Atlanta, GA, USA
[e] Center for Behavioral Neuroscience, Emory University, Atlanta, GA, USA
[f] Yerkes National Primate Research Center, Emory University, Atlanta, GA, USA

ARTICLE INFO

Article history:
Received 5 December 2016
Received in revised form 30 January 2017
Accepted 21 February 2017

Keywords:
Parietal lobes
Geometric morphometrics
Brain morphology
Brain shape
Sulcal patterns
Subparietal sulcus

ABSTRACT

Recent analyses have suggested that the size and proportions of the precuneus are remarkably variable among adult humans, representing a major source of geometrical difference in midsagittal brain morphology. The same area also represents the main midsagittal brain difference between humans and chimpanzees, being more expanded in our species. Enlargement of the upper parietal surface is a specific feature of *Homo sapiens*, when compared with other fossil hominids, suggesting the involvement of these cortical areas in recent modern human evolution. Here, we provide a survey on midsagittal brain morphology by investigating whether precuneus size represents the largest component of variance within a larger and racially diverse sample of 265 adult humans. Additionally, we investigate the relationship between precuneus shape variation and folding patterns. Precuneus proportions are confirmed to be a major source of human brain variation even when racial variability is considered. Larger precuneus size is associated with additional precuneal gyri, generally in its anterior district. Spatial variation is most pronounced in the dorsal areas, with no apparent differences between hemispheres, between sexes, or among different racial groups. These dorsal areas integrate somatic and visual information together with the lateral elements of the parietal cortex, representing a crucial node for self-centered mental imagery. The histological basis and functional significance of this intra-specific variation in the upper precuneus remains to be evaluated.

1. Introduction

Precuneus proportions represent a major source of brain morphological variability among adult humans (Bruner et al., 2014a), with spatial changes associated with increase/decrease in its cortical surface area (Bruner et al., 2015a). Precuneus dimensions are also the main difference between human and chimpanzee midsagittal brain morphology, with humans exhibiting marked expansion of this medial parietal element (Bruner et al., 2017). The precuneus is part of the superior parietal lobules, and it is positioned medially between the somatosensory cortex and the occipital cortex, corresponding to Brodmann area 7 (see Spasojevic et al., 2004; Cavanna and Trimble, 2006; Margulies et al., 2009). In adult humans its sagittal aspect has an average height of 36 mm and average length of 37 mm, and it is delimitated inferiorly by a parasagittal fold, the subparietal sulcus, with an average width of 14 mm (Bruner et al., 2015b; Pereira-Pedro and Bruner, 2016). The right precuneus is generally larger than the left one, and the morphological correlation between the two hemispheres is generally modest, in terms of size, shape, and sulcal patterns. Its upper areas are involved in visuo-spatial integration, imagery, autonoesis, egocentric memory, and many different tasks integrating spatial, chronological, and social relationships, while the lower areas are contiguous with a crucial node in the Default Mode Network (Cavanna and Trimble, 2006; Margulies et al., 2009; Zhang and Li, 2012; Utevsky et al., 2014). Parietal cortex is sensitive to both genetic (Chen et al., 2012) and environmental (Quallo et al., 2009) effects, and the origin of this morphological variation among adult humans is not known. Furthermore, there is no apparent correlation with basic standard psychometric scores (Bruner et al., 2015a),

---

[*] Corresponding author at: Centro Nacional de Investigación sobre la Evolución Humana, Paseo Sierra de Atapuerca 3, 09002 Burgos, Spain.
E-mail address: emiliano.bruner@cenieh.es (E. Bruner).

http://dx.doi.org/10.1016/j.aanat.2017.02.003

Table 1
Sample.

	N
Sex	
Males	126
Females	139
Ancestry	
Africa	57
Europe	94
Asia	84
Hispanic	16
Mixed	12
Native American	1
Unknown	1
Tot	265

although precuneus variations have been related to creative thinking (Chen et al., 2015).

Although it has traditionally been interpreted as a single cortical element, modern mapping of the precuneus shows a parcellation into many distinct sub-areas (Zilles and Palomero-Gallagher, 2001; Scheperjans et al., 2008; Glasser et al., 2016). In terms of anatomy, information is lacking on the histological basis and functional significance of precuneus variation. In terms of morphology, it remains to be established to what extent variability in precuneus shape is associated with anatomical factors (volume and sulcal patterns) and with genetic variability. In this study, we extend the previous morphological analyses on precuneus morphology in humans (Bruner et al., 2014a,b, 2015a,b; Pereira-Pedro and Bruner, 2016) in two directions. First, we test midsagittal brain variation in a wider human sample including different racial groups. Second, we evaluate whether precuneus shape is associated with variations of its folding scheme.

2. Materials and methods

2.1. Sample and digital imaging

We analyzed MRI data from 265 adults (126 men and 139 women) with diverse ancestral backgrounds (self-reported race; Table 1). All subjects were healthy adults from the Emory University community between the ages of 18 and 22 (mean and standard deviation = 20.7 ± 2.2 years for men, and 20.5 ± 1.3 years for women). Subjects underwent MRI scanning at Emory University on a 3 Tesla Siemens Trio MRI scanner (Siemens Medical System, Malvern, PA, USA) with a 12-channel parallel imaging phase-array coil. Foam cushions were used to minimize head motion. All procedures were carried out in accordance with protocols approved by the Emory University Institutional Review Board (IRB# 000007905). Our current study uses only the T1-weighted structural MRI images, which were acquired using a 3D magnetization-prepared rapid gradient-echo (MPRAGE) sequence with a GRAPPA (Generalized Autocalibrating Partially Parallel Acquisitions) factor of 2. The T1 scan protocol, optimized for 3 Tesla, used the following imaging parameters: a repetition time/inversion time/echo time (TR/TI/TE) of 2600/900/3.02 ms, a flip angle of 8°, a volume of view of 256 × 256 × 176 mm3, a matrix of 256 × 256 × 176, and isotropic spatial resolution of 1.0 × 1.0 × 1.0 mm^3, one average. Total T1 scan time was approximately 5 min.

For each subject, brain volume and precuneus volume were estimated. Brain volume includes the whole brain mass, while precuneus volume includes only the cortical gray matter. Cortical reconstruction and volumetric segmentation were automatically performed with Freesurfer v5.3.0 (Dale et al., 1999; Fischl and Dale, 2000; Fischl et al., 1999, 2002, 2004). Parcellation of the cerebral cortex into units (including the precuneus) was performed with respect to gyral and sulcal structure, based on the Desikan–Killiany cortical atlas (Desikan et al., 2006; Fischl et al., 2004). Brain volume was estimated in FMRIB Software Library (Smith et al., 2004) after removing the skull using Brain Extraction Tool (Smith, 2002). The functional and architectural boundaries between the precuneus, posterior cingulate cortex and retrosplenial cortex are generally blurred, and the current Freesurfer parcellation, based on the Desikan–Killiany cortical atlas (Desikan et al., 2006), includes areas below the subparietal sulcus (Fig. 1a). Precuneus relative volume was computed as the ratio between precuneus cortical volume (summed hemispheres) and brain volume. Shape comparison between humans and chimpanzees pointed to the anterior-superior parietal area as the possible localization of spatial differences (Bruner et al., 2017). Therefore, we also calculated the geometrical area included between the margin of the cingulate gyrus and the upper border of the perpendicular scissure (ASPA, Anterior-Superior Precuneus Area) to evaluate the contribution of this specific district (Fig. 1b).

2.2. Shape analysis

MRI images of all subjects were first aligned to a human brain template (MNI-152) using rigid body linear registration with 6 degree of freedom (DoF) so that all individual brains had a standard orientation and the sagittal plane was parallel to the interhemispheric fissure of the brain. Each individual brain was then visualized in FSLVIEW and snapshots were taken of the sagittal slice that is 6.0 mm lateral from the mid-sagittal slice in both hemispheres. This specific slice was chosen to cut through the middle thickness of the medial parietal cortex. We sampled 16 two-dimensional landmarks from the same sagittal slice for each hemisphere, as to consider the geometry of the midsagittal brain elements (Fig. 1c). The landmark configuration includes the center of the genu, the center of the splenium, the center of the thalamus, the center of the quadrigeminal lamina, the anterior border of the optic chiasm, the central sulcus, the marginal ramus of the cingulate sulcus, the marginal/precuneal notch, the midpoint of the subparietal sulcus, the external and internal extremes of the perpendicular sulcus, and the occipito-cerebellar fissure (internal occipital protuberance). Four semi-landmarks were sampled as equally distant points along the frontal (3 landmarks) and occipital (1 landmark) profiles. The configuration was similar to that used in the previous study (Bruner et al., 2014a), with some minor differences like the addition of the central sulcus and of the middle point of the subparietal sulcus. The central sulcus is useful to separate the conventional territories of the frontal and parietal lobes. This landmark is useful to delimitate the posterior area of the paracentral lobule, which is regarded as part of the superior parietal cortex (Scheperjans et al., 2008). The subparietal sulcus is a highly variable fold of the precuneus, which may be connected with the outer surface, with the marginal ramus of the cingulate surface, or even with the parieto-occipital fissure (Pereira-Pedro and Bruner, 2016). Although its morphology is highly variable between individuals and between hemispheres, the localization of a middle point is easy and practical, because it establishes an inferior boundary for the precuneus. The marginal notch is a minor flexion of the marginal ramus, generally identifiable through additional short folding elements which can be in some cases associated with longer precuneal sulci.

Coordinates were registered through Procrustes superimposition (Fig. 1d). This registration translates all the specimens to a common centroid (average coordinate value), scales the coordinate systems to unitary size by normalizing the centroid size value (square root of the sum of squared distances of a set of landmarks from their centroid) and rotates the configurations as to minimize

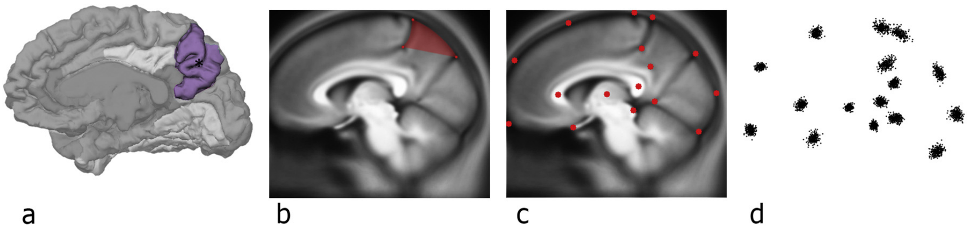

Fig. 1. Precuneus volume was calculated according to the Freesurfer parcellation template (a), and its anterior-posterior area was calculated between the marginal ramus of the cingulate sulcus and the perpendicular scissure (b). Midsagittal shape was analyzed with a configuration of 16 bi-dimensional landmarks (c), superimposed by Procrustes registration (d).

the distance between corresponding landmarks (Bookstein, 1991). Coordinates were used to compute a principal component analysis following the principles and methods of geometric morphometrics (Zelditch et al., 2004). Coordinates were also used to analyze the distribution of all the interlandmark distances (Euclidean Distance Matrix Analysis; Lele and Richtsmeier, 1991) as to calculate their coefficients of variation.

We also evaluated the morphological modularity of the precuneus, that is to what extent the landmarks forming the precuneal geometry (see Fig. 4d) display an internal correlation which is stronger than the rest of the coordinates. Integration and modularity are hierarchical concepts based on different degree of reciprocal or shared influences among biological processes and traits, aimed at localizing functional, structural, genetic, and morphogenetic units within a given anatomical system (Cheverud, 1996 Mitteroecker and Bookstein, 2007). Integrated anatomical areas display high covariance and shared patterns of variation, while non-integrated anatomical systems are formed by independent elements influenced by distinct factors (Klingenberg, 2009). A module is a group of elements which show a higher degree of reciprocal variation when compared with other elements or with other groups. Modularity within the current configuration of landmarks was tested taking into consideration the relative degree of correlation between adjacent partitions by using the Escouffier coefficients, comparing the value of multiple correlations of the medial parietal geometry (from the retrosplenial cortex to the upper parietal profile) with the distribution of the values obtained for all the other possible combinations with similar parameters (Klingenberg, 2009, 2013).

2.3. Sulcal pattern

The precuneus displays a highly variable sulcal pattern, which is apparently not associated with the thickness of the cortical folding (Pereira-Pedro and Bruner, 2016). Additional sulci (precuneal sulci) can increase the sulcal complexity, being connected or not to the main central fold (subparietal sulcus). Precuneal sulci, and associated additional precuneal gyri, are more frequent anteriorly, although in some cases they can be found toward the posterior (occipital) boundary. Here, we evaluate whether the presence of additional gyri are associated with variation of the precuneus geometry, considering three morphotypes (Fig. 2): absence of additional gyri (type I), partial additional gyrus (type II), and complete additional gyrus (type III).

2.4. Statistics

The study was performed on the whole sample of 530 hemispheres as well as on 265 mean values obtained after averaging the left and right hemisphere for each individual. Left and right sides display a high correlation of their covariance matrices ($p < 0.0001$; $R = 0.98$), and the only asymmetry, as evidenced by the current configuration, is a very minor difference in the retrosplenial space, smaller in the right hemisphere because of relatively larger occipital length. However, the two analyses gave the same multivariate results, so here we present only the study on averaged shapes, except the sulcal analysis which was performed on all hemispheres independently. Because of small sample size for some ancestry groups, inferential statistics were only computed for the three largest groups, namely African, European, and Asian ancestry. Morphometrics were computed by using PAST 2.17c (Hammer et al., 2001) and MorphoJ 1.06a (Klingenberg, 2011). Differences have been tested through permutation tests.

3. Results

3.1. Volumes and metrics

Precuneus cortical volume averages 10.4 ± 1.2 cc (interquartile 9.6–11.2; coefficient of variation 12%), and represents 1.4 ± 0.1% of the whole brain volume (Table 2). Brain volume is correlated with precuneus volume ($p < 0.0001$; $r = 0.74$) and with ASPA ($p < 0.0001$; $r = 0.40$) but not precuneus relative volume ($p = 0.49$). ASPA is also correlated to precuneus volume ($p < 0.0001$; $r = 0.48$) and modestly to precuneus relative volume ($p < 0.0002$; $r = 0.23$). Precuneus volume is correlated to precuneus relative volume ($p < 0.0001$; $r = 0.61$). Males have larger values than females for all absolute variables ($p < 0.0001$), but there is no difference between sexes for relative precuneus volume ($p = 0.72$). Analyzing sex differences by analysis of covariances, there are no differences in means ($p = 0.74$) or slopes ($p = 0.39$) when comparing precuneus volume with brain volume. In contrast, males have larger ASPA at a given brain size ($p = 0.04$), despite no difference in slope ($p = 0.64$). This result suggests that males have relatively larger upper precuneal extension when compared with females, when brain size variation is taken into account. Comparisons between ancestry groups reveals differences in precuneus volume (Europe > Asia > Africa; $p < 0.0001$), and precuneus relative volume (Asia = Europe > Africa; $p < 0.001$). A similar situation is found when comparing precuneus volume and brain size covariance, with the three groups showing the same slopes ($p = 0.99$) but with African sample showing smaller mean ($p = 0.001$). However, average differences are minimal, overlap is extensive, and mean group-wise values for the relative volume only differ by between 1.4% and 1.5%. Differences for ASPA are significant when comparing European and African ancestry (smaller in the second group; $p = 0.04$), but neither differed from the Asian sample. The proportion of the upper precuneus area (ASPA divided for brain volume) did not differ among ancestry groups and, taking into account brain size, analysis of covariance reveal same slopes ($p = 0.77$) and means ($p = 0.91$) for the anterior-superior precuneus extension.

Analyzing the mean and standard deviation of all the interlandmark distances and computing their coefficients of variation,

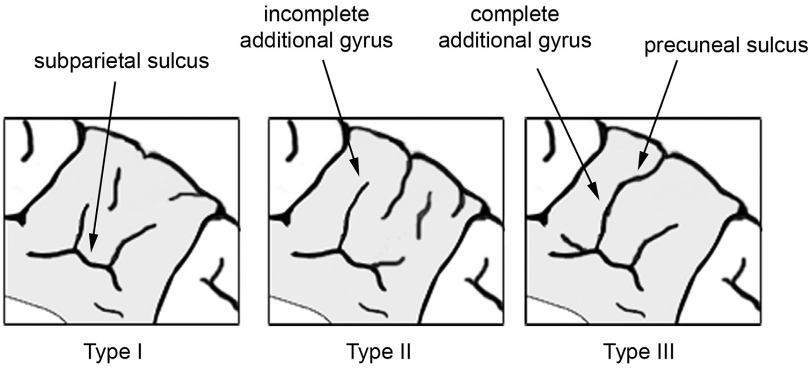

Fig. 2. Three sulcal patterns were considered: with no additional gyrus (Type I), with incomplete additional gyrus (Type II) and with complete additional gyrus (Type III).

Table 2
Precuneus volume per group.

	Precuneus volume (cc)					Precuneus volume (%)				
	Males	Females	Europe	Africa	Asia	Males	Females	Europe	Africa	Asia
Mean	11.0	9.9	10.9	9.7	10.5	1.43%	1.44%	1.44%	1.39%	1.46%
St. dev	1.1	1.1	1.2	1.1	1.2	0.12%	0.12%	0.10%	0.11%	0.13%
25th	10.1	9.2	10.0	8.9	9.7	1.40%	1.40%	1.40%	1.30%	1.40%
Median	10.9	9.8	10.8	9.7	10.5	1.40%	1.40%	1.40%	1.40%	1.50%
75th	11.8	10.7	11.8	10.5	11.2	1.50%	1.50%	1.50%	1.50%	1.50%

most diameters display values between 4% and 11%, except five distances associated with precuneus and with the deep posterior (retrosplenial and cerebro-cerebellar) districts, showing values of 13–21% (see Fig. 4f).

3.2. *Shape variation*

The overall midsagittal shape variation is correlated with midsagittal centroid size ($p < 0.0001$), although the correlation explains only 2.9% of the variance, through a pattern characterized by precuneus dilation and occipital bulging (Fig. 3a). A discriminant analysis between males and females on the whole shape coordinates is significant ($p = 0.002$) and associated with a more dolichocephalic (flattened) braincase in the former group (Fig. 3b). This pattern is able to correctly classify 75–78% of the specimens after cross-validation. Comparing the three main ancestry groups, Asians display a morphological difference from the other two groups which is significant according to Mahalanobis distance ($p < 0.001$ and $p = 0.001$ for African and European ancestry, respectively) and significant/marginal according to Procrustes distance ($p = 0.003$ and $p = 0.07$ for African and European ancestry, respectively). The difference mainly separates Asian from African ancestry because of the brachycephalic proportions of the former group (Fig. 3c). As for sex variation, differences are apparently due to the form of the braincase rather than local changes of specific brain areas. Although the separation is significant, a cross validation shows that differences are subtle, with large overlap between the two groups, and a discrimination function based on coordinates is able to classify correctly only 56% of the individuals with African ancestry and 60% of the individuals with Asian ancestry.

The principal component analysis shows a morphospace which is not characterized by few distinct patterns, but instead by a set of components with a smooth and gradual decrease of explained variance (Fig. 4a). Only the first vector displays a marked separation in terms of variance (24%), and after the fifth vector the eigenvalues are not even above a threshold of random variation. Such structure of the multivariate space reflects scarce integration of the overall geometrical system, due to many local and independent factors influencing the global spatial distribution of the midsagittal brain elements (Bruner et al., 2010). Therefore, we only consider the first component here, which is supposed to represent a reliable biological vector of variation. This first axis of variation is strictly associated with the relative proportion and shape of the precuneus (Fig. 4b,c). The upper part of the precuneus undergoes a longitudinal dilation/compression, without any patent shape change in the other districts, except a spatial shift of the frontal and occipital volumes due to the lengthening of the parietal space.

This principal component is not correlated with brain volume ($p = 0.29$), is slightly correlated with precuneus volume ($p = 0.01$; $R = 0.15$) and relative precuneus volume ($p = 0.02$; $r = 0.14$), and moderately correlated with ASPA ($p < 0.0001$; $r = 0.40$). There are neither sexual ($p = 0.50$) nor racial ($p = 0.38$) differences for PC1 values.

The modularity analysis shows that the landmarks forming the medial parietal geometry (Fig. 4d) do not show a higher correlation when compared with the rest of the coordinates ($p = 0.55$), suggesting that it does not represent a separate morphological module. In contrast, its lower parts and the posterior subcortical areas represent the most integrated module that is, using the same modularity parameters, the group of landmarks showing the higher internal cohesion (Fig. 4e).

3.3. *Sulcal analysis*

The analysis of all 530 hemispheres shows that in 54% of the cases there is an incomplete additional gyrus, in 43% of the cases there is a complete additional gyrus, and only on 3% of the cases there is no additional folding. There is no difference in sulcal patterns between males and females according to a Chi-square test. In contrast, the right hemisphere shows more incomplete

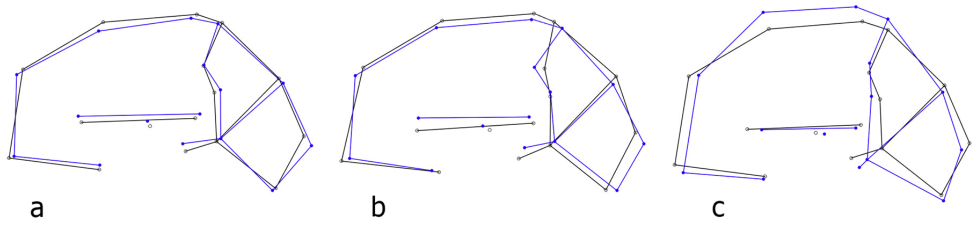

Fig. 3. Shape variation includes a minor allometric component (a; blue wireframe: larger brain sections), sexual differences (b; blue wireframe: males), and racial differences, mostly between African ancestry and Asian ancestry (c; blue wireframe: Asian group). (For interpretation of the references to color in this figure legend, the reader is referred to the web version of this article.)

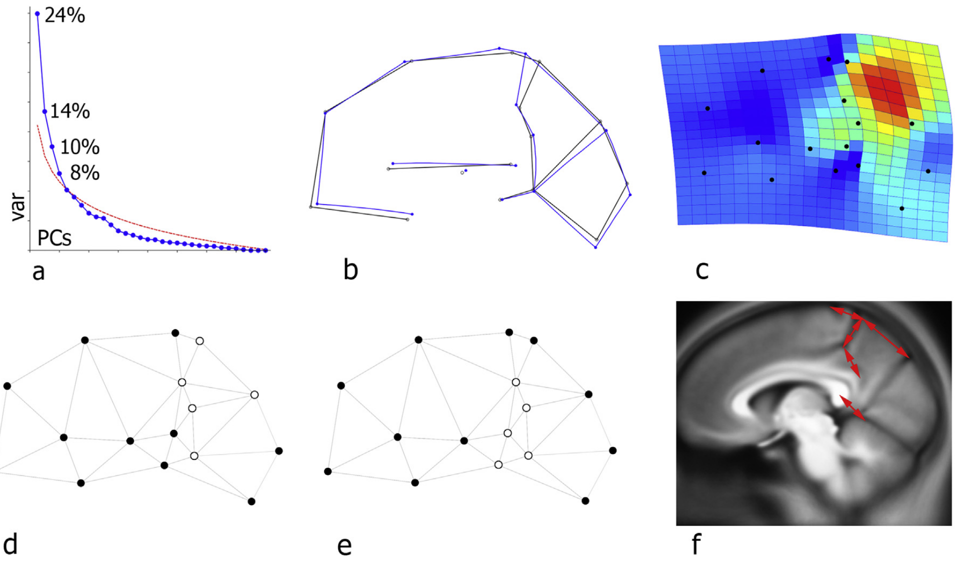

Fig. 4. Principal Component Analysis shows four vectors above the threshold of random eigenvalue (red line), with the first component explaining 24% of the variance (a). This component is strictly associated with increase/decrease of the upper precuneus proportions, here showed though wireframe (b) and thin-plate spline deformation grid with deformation map (c; red: geometric dilation). The landmarks forming the parietal medial districts, from the retrosplenial cortex to the upper parietal profile (d; white dots) do not display a modular correlation. Instead, its lower areas and the posterior subcortical areas represent a more integrated unit (e). Taking into account all the raw interlandmark distances, the ones showing the larger coefficient of variation (13-21%) are associated with the upper parietal and restrosplenial districts (f). (For interpretation of the references to color in this figure legend, the reader is referred to the web version of this article.)

gyri (61%) and the left hemisphere shows more complete gyri (50%). Racial differences are significant ($p = 0.05$): individuals with African ancestry show more absence of additional gyri, more complete additional gyri, and less frequent incomplete gyri. Individuals with European ancestry display the opposite patterns, showing an increase of the frequency of incomplete gyri (62%). The presence of additional gyrus is not associated with brain volume ($p = 0.18$), but both ASPA ($p = 0.00004$) and PC1 (toward larger precuneus; $p = 0.0004$) increase from no additional gyrus, to incomplete additional gyrus, to complete additional gyrus (Fig. 5). The difference is more marked between no additional gyrus and incomplete additional gyrus, while it is less pronounced between the latter and complete additional gyrus ($p = 0.01$). Shape analysis discriminates between absence and presence of gyrus ($p = 0.0001$ for both Procrustes distance and Hotelling T), but is less decisive to discriminate between complete and incomplete gyrus ($p = 0.01$ and 0.15 for Procrustes distance and Hotelling T). In this case cross-validation is able to classify only 54% of the specimens. In all comparisons, the shape difference among sulcal types is associated with precuneus expansion.

4. Discussion

4.1. Morphometrics and precuneus variation

The size of the precuneus is highly variable among adult humans, representing the main source of shape variation in midsagittal brain geometry, largely because of its longitudinal extension (Bruner et al., 2014a,b, 2015a). Past morphological analyses on these cortical districts were based on samples including about one hundred specimens with homogeneous ancestry. In this study we extend the analysis to a larger sample, including individuals from various racial groups. We also use a configuration of landmarks able to separate the areas above the subparietal sulcus, and the posterior district of the paracentral lobule. Finally, we also evaluate to what extent this morphological variation is associated with specific sulcal patterns.

As for earlier analyses, variation in midsagittal brain shape is not characterized by few global morphological patterns, probably because it is influenced by many local and independent factors (Bruner et al., 2010; Gómez-Robles et al., 2014). The

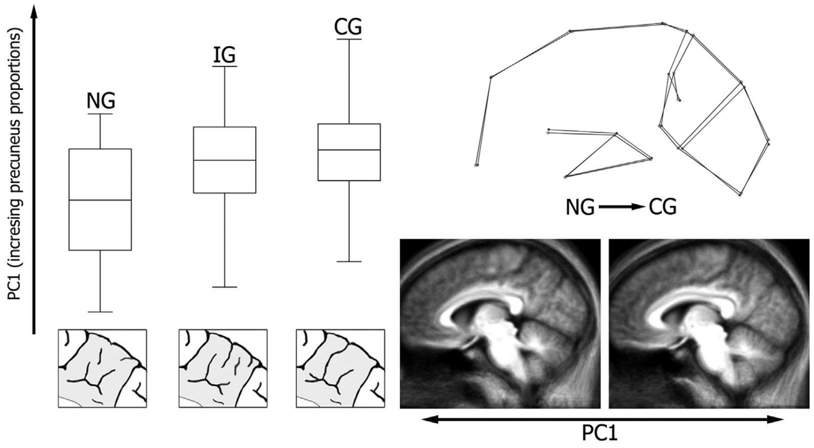

Fig. 5. Boxplots show the distribution of the three sulcal types along the first Principal Component (PC1): no additional gyrus (NG), incomplete additional gyrus (IG), and complete additional gyrus (CG). Wireframe shows shape difference after discriminant analysis from specimens without additional gyrus to specimens with complete additional gyrus. The two MRI images are computed as the densitometric superimpositions of the 20 specimens with highest and lowest PC1 values, showing the actual extent of the precuneus variation associated with this shape vector. Note that larger precuneus is associated with an additional precuneal sulcus. No other morphological change is apparently associated with this vector.

allometric effect is minor, at least when dealing with adult phenotype. Nonetheless, the shape of the precuneus represents a consistent trait influencing individual variability and generating a consistent vector of variation (24% of the variance), as described in previous studies. Because of the difficulties associated with MRI imaging and brain landmarking, reproducibility of these results is crucial. To date, precuneus form has been confirmed to be the main source of midsagittal brain variation among adult humans in a local European sample (Bruner et al., 2014a), in a biomedical sample (Bruner et al., 2015b), and in an anthropological sample with distinct racial groups (this study), three studies in which landmarking was performed by independent observers. This shape variation is not due to brain size differences. It is weakly correlated ($r = 0.15$) with absolute and relative precuneus volume as calculated according to traditional neuroanatomical templates, which include lower areas fading into the posterior cingulate and retrosplenial cortex. On the other hand, this shape component is moderately correlated with the size of the superior and anterior precuneus areas ($r = 0.40$). Brain volume and precuneus relative volume are not correlated, confirming that changes in the precuneus proportions in general do not depend upon brain size. The size of its superior areas is only modestly correlated to the whole precuneus absolute and relative size, suggesting that other parts of the segmented volumes (the posterior and inferior areas) may vary independently. In this study, in addition to *shape* analysis we also computed a *form* analysis based on Euclidean Distance Matrix, showing that all the superior and anterior boundaries of the precuneus include the most variable inter-landmark distances. This result, based on absolute values and not on registered/normalized coordinates, further substantiates marked individual variability of this district. Indeed, the current geometrical models points at these areas as the origin of the spatial differences. At the same time, the configuration of landmarks used in this study stresses further that the inferior and posterior areas are not involved in the dominant spatial pattern of variation, as also observed for the human-chimpanzee comparison (Bruner et al., 2017). The modularity analysis further suggests independence between superior and inferior medial geometry. The posterior part of the paracentral lobule is not implicated in the main pattern of shape differences, although it too is highly variable.

Sex differences in the precuneus are largely due to general brain size differences. The relative precuneus volume is similar in males and females, and the scaling between brain volume and precuneus volume shows a shared allometric trajectory. Males have slightly larger anterior-superior precuneus extension when brain size is considered, although the individual variation is remarkable and group differences are subtle. Current psychometric evidence suggests that males perform better than females on visuospatial cognitive tasks (e.g., Gur et al., 2000; Sacher et al., 2013), however the anatomical group-difference found in this study is minimal and with extensive overlap. The distribution of males and females along the main shape pattern (precuneus expansion/reduction) is similar, and the overall midsagittal brain differences are due to brachycephalic-dolichocephalic neurocranial variation, more than to actual differences in brain proportions. A similar situation can be described for the ancestry groups: there is no difference among racial groups for the distribution along the main shape vector (precuneus expansion/reduction), and global shape differences are due to brachycephalic (Asian ancestry) and dolichocephalic (African ancestry) cranial architectures, without apparent localized changes of specific brain areas. Dolichocephalic-brachycephalic neurocranial variations (i.e., relatively longer and narrow skulls vs relatively shorter and wider skulls), can probably result from distinct morphogenetic processes (Zollikofer and Ponce de León, 2002) but, in any case, they are likely to be influenced by cranial constraints (Lieberman et al., 2000; Bastir and Rosas, 2016) and not by specific patterns of brain growth and development. The African group displays smaller precuneus volume when brain size is taken into account, but the proportional difference is very minor, and overlap among racial groups is extensive. The fact that the same group does not show differences in the extension of the dorsal proportions suggests that this variation of the precuneus, if confirmed, should be associated with differences in the other precuneus areas, approaching the subparietal sulcus or the retrosplenial/cingulate cortex. As a cautionary note, it must be observed that these results are based on self-reported race rather than genealogic or genetic data.

The analysis of the sulcal patterns add to the current knowledge on precuneus anatomical variation. The folding patterns associated with the subparietal sulcus are highly variable, without a clear association with fold size, sex, or hemispheric asymmetry (Pereira-Pedro and Bruner, 2016). Although the height of the precuneus can influence the outer brain form, the variations of the folding scheme likely have no effects on the external brain outline (Pereira-Pedro and Bruner, 2016). According to the results presented in this study, most individuals (97%) display at least one additional folding branch, associated with complete or incomplete precuneal sulci. Such additional gyri are slightly associated with longer precuneus, and with the main pattern of shape variation described for the midsagittal brain morphology. The difference is more marked between specimens with or without additional gyri, but there is also a minor difference between specimens with incomplete and complete additional gyrus. Therefore, although the relationship is not stringent, larger precuneus size is partially associated with additional longitudinal folding. Of course, the polarity of this relationship cannot be evaluated with the current data, and additional folding can be the cause or else the consequence of cortical area expansion. Recent empirical and experimental models suggest that folding is largely due to geometrical mechanical adjustments between volume and surface growth (Tallinen et al., 2016). Therefore, an additional gyrus can be the cause of the cortical expansion, or else a mechanical consequence passively induced by the growth of a larger surface.

There are no sex differences in the folding pattern, but the left side seems to show more frequently complete additional gyri. This is counterintuitive when considering that the right side is generally larger, but a similar result was found in a different sample, showing more precuneal sulci in the left hemisphere (Pereira-Pedro and Bruner, 2016). Nonetheless, sex and asymmetry patterns for these areas are still not clear, and there are still contrasting results which require further investigation (Zhang and Li, 2013; Bruner et al., 2015a). Similarly, the racial trend, which associates African ancestry with increasing frequency of absent and complete additional folds, cannot be easily interpreted. Critically, the minor sex and racial differences reported here could be due to either genetic or environmental factors.

It is worth noting that all these relationships reveal modest ($R \approx 0.15$), or moderate ($R \approx 0.40$) correlations. The large individual variability makes trends weak and, even in the most consistent cases, minimally predictive. Such large individual variation may be due to multiple factors influencing the final phenotype and idiosyncratic features. It is nonetheless suggestive that, as trends and patterns, these relationships can be found even when considering adult individuals of the same species. The same rules are likely to be stronger when dealing with ontogenetic or inter-specific variation.

4.2. *Precuneus variation and cortical areas*

This study further suggests that the dorsal areas of the precuneus may represent a relevant source of individual variability. The width of the precuneus is extremely small when compared with its length and height (Pereira-Pedro and Bruner 2016), and its variation largely deals with its longitudinal extension, in particular with the extension of its dorsal parts. The fact that sex, race, and size do not exert a major influence on these differences suggests that individual factors contribute to this pattern of midsagittal brain variability. Cranial architecture (in particular the dolichocephalic-brachycephalic axis) displays sexual and racial trends, which are not associated with the main pattern of variation and precuneus proportions. Therefore, precuneus expansion/reduction seems not affected by the general cranial proportions. Increase/decrease of a cortical surface is unlikely to be a passive consequence of “space filling” after cranial adjustments, and hence we must assume that it is associated with expansion/reduction of specific histological components. These areas display a remarkable cytoarchitectonic individual variation (Scheperjans et al., 2008). Although we know that precuneus variation is associated with surface extension, we ignore the exact anatomical nature of these changes, or the functional and morphogenetic process involved. The parietal areas mature very early during ontogeny (Gogtay et al., 2004), but they are also exceptionally sensitive to later influences of training (Quallo et al., 2009). Despite shared genetic factors (Chen et al., 2012), we currently ignore to what extent the precuneus variation is the result of innate or environmentally shaped differences. We also ignore whether precuneus morphological variation is due to difference in neuron size or density, connections, or non-neuronal cerebral components (e.g., glia, vascular elements, etc.).

The precuneus is generally labeled as Brodmann area 7, but its cytoarchitectonic parcellation is currently under investigation, revealing a finer degree of complexity (Scheperjans et al., 2008). Although our geometrical model cannot discriminate among specific sub-areas of the precuneus, it suggest that the morphological variation is associated with a district which, according to the cytoarchitectonic probabilistic map of Scheperjans et al. (2008), spatially matches areas 7A and 7P. Area 7A is the largest among those described for the superior parietal cortex, it is the most variable between individuals, and extends from the medial (interhemispheric) fold to the outer superior parietal lobule. Therefore, it is a good candidate for further anatomical surveys. Interestingly, while the medial part of the precuneus represents a connection hub in most primates, the external part may have hub properties only in humans (Li et al., 2013).

In terms of functions, it remains to be established whether these morphological changes are actually associated with cognitive or metabolic variations. Area 7A is particularly associated with functions dealing with self-centered mental imagery and attentional processes (Scheperjans et al., 2008). In general, the dorsal areas of the precuneus are more connected with somatosensory and motor cortex (dorsal anterior) and visual cortex (dorsal posterior), representing a crucial node for visuospatial integration, while the ventral areas are more connected with the frontal and cingulate cortex, acknowledging functions associated with episodic memory and self-representation (Lou et al., 2004; Zhang and Li, 2012; Bzdok et al., 2015). A preliminary survey with traditional psychometric tests failed to reveal any apparent difference associated with precuneus size (Bruner et al., 2015a). Nonetheless, due to the several functional and cognitive processes in which the precuneus is involved (Cavanna and Trimble 2006; Margulies et al., 2009; Zhang and Li, 2012), assessments must be based on more extensive and specialized approaches. Grey matter increase and functional homogeneity of the right precuneus is positively correlated with verbal creative thinking ability (Chen et al., 2015). It is worth noting that visuospatial functions, body perception and self-awareness are crucial also for social relationships (Hills et al., 2015; Maister et al., 2015; Peer et al., 2015), and precuneus cortical reduction is one of the few grey matter alterations associated with autism (Via et al., 2011).

Our shape analysis also confirms that the dorsal areas of the precuneus and the inferior ones should be considered separately when dealing with individual variation. The analysis of modularity adds further evidence to the hypothesis of a morphological integration between lower precuneus, retrosplenial and posterior cingulate areas, splenium, and posterior subcortical elements, as described in another sample (Bruner et al., 2014a). Also functional mapping suggests a distinction between dorsal and ventral precuneus, with the ventral areas more connected with those same regions evidenced by a shared modular structure (Zhang and Li, 2012). This ventral part is also the one possibly more involved in the Default Mode Network and connected with the angular gyrus, while the dorsal areas are less involved in the default mode and more connected with the rest of the parietal cortex, namely with parasagittal elements (not included in this study) like the intraparietal sulcus and the supramarginal gyrus. The spatial correlation between lower precuneal landmarks, retrosplenial cortex and posterior subcortical areas, provides therefore an interesting convergence between geometrical patterns and connectivity schemes.

A final issue concerns metabolism. The precuneus represent a highly metabolically active area, which is positioned close to the thermal core of the brain (the geometric area of maximum heat accumulation according to the spatial pattern of heat dissipation) and in a crucial vascular district (Sotero and Iturria-Medina, 2011; Bruner et al., 2014b). Its involvement in metabolic dysfunctions and Alzheimer's disease therefore raises questions about possible functional consequences (Zhang and Li, 2012; Bruner and Jacobs 2013). It is worth noting that the inferior areas of the precuneus is part of (Utevsky et al., 2014) or is contiguous with (Bzdok et al., 2015) crucial connection hubs, including relevant nodes of the Default Mode Network which are shared among primates, introducing issues bridging functional and structural levels of brain organization (Raichle et al., 2001; Hagmann et al., 2008; Meunier et al., 2010; Van den Heuvel et al., 2016). As mentioned, the superior parietal lobules may present some human specific connection nodes (Li et al., 2013) and might represent an outer extension of the area 7A of the precuneus (Scheperjans et al., 2008).

5. Conclusions

For many years, information on human parietal cortex was limited, and we still lack many details of its neuroanatomical organization (Zilles and Palomero-Gallagher, 2001). Its areas are currently under investigation based on functional and structural properties, but there is much disagreement on its parcellation, homology, functions, and boundaries. The current study further points to the precuneus as a main factor of intra-specific human brain variation. Its relative extension is not dependent on size, sex, or race, suggesting individual factors associated with shared genetic or environmental effects. It remains to be investigated what structural and histological elements are involved in generating this spatial change, and if these are associated with specific functional issues. A rounded braincase is a specific trait of *Homo sapiens* (Lieberman et al., 2002; Gómez-Robles et al., 2017), mostly due to enlarged parietal bones and lobes (Bruner et al., 2014b). A globular braincase in *H. sapiens* is due to a morphogenetic endocranial stage which is specific of our species, occurring either before (Ponce de León et al., 2016) or after (Gunz et al., 2010) birth. This stage is absent in chimpanzees and other living apes (Neubauer et al., 2009; Scott et al., 2014), and enlargement of the precuneus is also a major difference distinguishing human from chimpanzee midsagittal brain morphology (Bruner et al., 2017). Both intra-specific and inter-specific geometrical models point to the same anterior and dorsal areas of the precuneus, roughly corresponding to area 7A, associated with visuospatial integration and self-centered mental imagery (Scheperjans et al., 2008). Visuospatial integration combines egocentric representations with spatial, chronological, and social abilities (Land, 2014; Peer et al., 2015). Taking into account the importance of technology and visual imagery in our species, we should evaluate whether visuospatial capacity and extended cognitive abilities may have been enhanced along our evolutionary lineage (Iriki 2006; Iriki and Taoka 2012; Bruner and Iriki, 2016). Area-specific analyses will be necessary to evaluate further the neuroanatomical changes associated with both intra- and interspecific variation of the parietal districts, taking into account parcellation schemes which include both functional and structural territories (Glasser et al., 2016).

Acknowledgments

We thank Dr. JiuQuan Zhang (MD/PhD) for help in landmark sampling. EB is funded by the Spanish Government (CGL2015-65387-C3-3-P) and by the Italian Institute of Anthropology. ASPP is funded by the Atapuerca Foundation. This study was supported by National Institute of Mental Health (R01 MH084068-01A1).

Appendix A. Supplementary data

Supplementary data associated with this article can be found, in the online version, at http://dx.doi.org/10.1016/j.aanat.2017.02.003.

References

Bastir, M., Rosas, A., 2016. Cranial base topology and basic trends in the facial evolution of *Homo*. J. Hum. Evol. 91, 26–35.

Bookstein, F.L., 1991. Morphometric Tools for Landmark Data: Geometry and Biology. Cambridge University Press, New York.

Bruner, E., Iriki, A., 2016. Extending mind, visuospatial integration, and the evolution of the parietal lobes in the human genus. Quat. Int. 405 (A), 98–110.

Bruner, E., Jacobs, H.I.L., 2013. Alzheimer's disease: the downside of a highly evolved parietal lobe? J. Alzheimers Dis. 35, 227–240.

Bruner, E., Martin-Loeches, M., Colom, R., 2010. Human midsagittal brain shape variation: patterns, allometry and integration. J. Anat. 216, 589–599.

Bruner, E., Rangel de Lázaro, G., de la Cuétara, J.M., Martín-Loeches, M., Colom, R., Jacobs, H.I.L., 2014a. Midsagittal brain variation and MRI shape analysis of the precuneus in adult individuals. J. Anat. 224, 367–376.

Bruner, E., De la Cuétara, J.M., Masters, M., Amano, H., Ogihara, N., 2014b. Functional craniology and brain evolution: from paleontology to biomedicine. Front. Neuroanat. 8, 19.

Bruner, E., Román, F.J., de la Cuétara, J.M., Martin-Loeches, M., Colom, R., 2015a. Cortical surface area and cortical thickness in the precuneus of adult humans. Neuroscience 286, 345–352.

Bruner, E., Amano, H., de la Cuétara, J.M., Ogihara, N., 2015b. The brain and the braincase: a spatial analysis on the midsagittal profile in adult humans. J. Anat. 227, 268–276.

Bruner, E., Preuss, T.M., Chen, X., Rilling, J.K., 2017. Evidence for expansion of the precuneus in human evolution. Brain Struct. Funct. 222, 1053–1060.

Bzdok, D., Heeger, A., Langner, R., Laird, A.R., Fox, P.T., Palomero-Gallagher, N., Vogt, B.A., Zilles, K., Eickhoff, S.B., 2015. Subspecialization in the human posterior medial cortex. Neuroimage 106, 55–71.

Cavanna, A.E., Trimble, M.R., 2006. The precuneus: a review of its functional anatomy and behavioural correlates. Brain 129, 564–583.

Chen, C.-H., Gutierrez, E.D., Thompson, W., Panizzon, M.S., Jernigan, T.L., Eyler, L.T., Fennema-Notestine, C., Jak, A.J., Neale, M.C., Franz, C.E., Lyons, M.J., Grant, M.D., Fischl, B., Seidman, L.J., Tsuang, M.T., Kremen, W.S., Dale, A.M., 2012. Hierarchical genetic organization of human cortical surface area. Science 335, 1634–1636.

Chen, Q.-L., Xu, T., Yang, W.-J., Li, Y.-D., Sun, J.-Z., Wang, K.-C., Beaty, R.E., Zhang, Q.-L., Zuo, X.-N., Qiu, J., 2015. Individual differences in verbal creative thinking are reflected in the precuneus. Neuropsychologia 75, 441–449.

Cheverud, J.M., 1996. Developmental integration and the evolution of pleiotropy. Am. Zool. 36, 44–50.

Dale, A.M., Fischl, B., Sereno, M.I., 1999. Cortical surface-based analysis: I. segmentation and surface reconstruction. Neuroimage 9, 179–194.

Desikan, R.S., Ségonne, F., Fischl, B., Quinn, B.T., Dickerson, B.C., Blacker, D., Buckner, R.L., Dale, A.M., Maguire, R.P., Hyman, B.T., Albert, M.S., Killiany, R.J., 2006. An automated labeling system for subdividing the human cerebral cortex on MRI scans into gyral based regions of interest. Neuroimage 31, 968–980.

Fischl, B., Dale, A.M., 2000. Measuring the thickness of the human cerebral cortex from magnetic resonance images. Proc. Natl. Acad. Sci. U. S. A. 97, 11050–11055.

Fischl, B., Sereno, M.I., Dale, A.M., 1999. Cortical surface-based analysis: II: inflation, flattening, and a surface-based coordinate system. Neuroimage 9, 195–207.

Fischl, B., Salat, D.H., Busa, E., Albert, M., Dieterich, M., Haselgrove, C., van der Kouwe, A., Killiany, R., Kennedy, D., Klaveness, S., Montillo, A., Makris, N., Rosen, B., Dale, A.M., 2002. Whole brain segmentation: automated labeling of neuroanatomical structures in the human brain. Neuron 33, 341–355.

Fischl, B., van der, Kouwe A., Destrieux, C., Halgren, E., Ségonne, F., Salat, D.H., Busa, E., Seidman, L.J., Goldstein, J., Kennedy, D., Caviness, V., Makris, N., Rosen, B., Dale, A.M., 2004. Automatically parcellating the human cerebral cortex. Cereb. Cortex 14, 11–22.

Gómez-Robles, A., Hopkins, W.D., Sherwood, C.C., 2014. Modular structure facilitates mosaic evolution of the brain in chimpanzees and humans. Nat. Commun. 5.

Gómez-Robles, A., Smaers, J.B., Holloway, R.L., Polly, P.D., Wood, B.A., 2017. Brain enlargement and dental reduction were not linked in hominin evolution. Proc. Natl. Acad. Sci. U. S. A. 114, 468–473.

Glasser, M.F., Coalson, T.S., Robinson, E.C., Hacker, C.D., Harwell, J., Yacoub, E., Ugurbil, K., Andersson, J., Beckmann, C.F., Jenkinson, M., Smith, S.M., Van Essen, D.C., 2016. A multi-modal parcellation of human cerebral cortex. Nature 536, 171–178.

Gogtay, N., Giedd, J.N., Lusk, L., Hayashi, K.M., Greenstein, D., Vaituzis, A.C., Nugent, T.F., Herman, D.H., Clasen, L.S., Toga, A.W., Rapoport, J.L., Thompson, P.M., 2004. Dynamic mapping of human cortical development during childhood through early adulthood. Proc. Natl. Acad. Sci. U. S. A. 101, 8174–8179.

Gunz, P., Neubauer, S., Maureille, B., Hublin, J.-J., 2010. Brain development after birth differs between Neanderthals and modern humans. Curr. Biol. 20, R921–R922.

Gur, R.C., Alsop, D., Glahn, D., Petty, R., Swanson, C.L., Maldjian, J.A., Turetsky, B.I., Detre, J.A., Gee, J., Gur, R.E., 2000. An fMRI study of sex differences in regional activation to a verbal and a spatial task. Brain Lang. 74, 157–170.

Hagmann, P., Cammoun, L., Gigandet, X., Meuli, R., Honey, C.J., Wedeen, V.J., Sporns, O., 2008. Mapping the structural core of human cerebral cortex. PLoS Biol. 6, e159.

Hammer, Ø., Ryan, P., Harper, D., 2001. PAST: paleontological statistics software package for education and data analysis. Palaeontol. Electron. 4, 9.

Hills, T.T., Todd, P.M., Lazer, D., Redish, A.D., Couzin, I.D., 2015. Exploration versus exploitation in space, mind, and society. Trends Cogn. Sci. 19, 46–54.

Iriki, A., Taoka, M., 2012. Triadic (ecological, neural, cognitive) niche construction: a scenario of human brain evolution extrapolating tool use and language from the control of reaching actions. Phil. Trans. R. Soc. B 367, 10–23.

Iriki, A., 2006. The neural origins and implications of imitation, mirror neurons and tool use. Curr. Opin. Neurobiol. Motor Syst./Neurobiol. Behav. 16, 660–667.

Klingenberg, C.P., 2009. Morphometric integration and modularity in configurations of landmarks: tools for evaluating a-priori hypotheses. Evol. Dev. 11, 405–421.

Klingenberg, C.P., 2011. MorphoJ: an integrated software package for geometric morphometrics. Mol. Ecol. Resour. 11, 353–357.

Klingenberg, C.P., 2013. Cranial integration and modularity: insights into evolution and development from morphometric data. Hystrix 24, 43–58.

Land, M.F., 2014. Do we have an internal model of the outside world? Phil. Trans. R. Soc. B 369, 20130045–20130045.

Lele, S., Richtsmeier, J.T., 1991. Euclidean distance matrix analysis: a coordinate-free approach for comparing biological shapes using landmark data. Am. J. Phys. Anthropol. 86, 415–427.

Li, L., Hu, X., Preuss, T.M., Glasser, M.F., Damen, F.W., Qiu, Y., Rilling, J., 2013. Mapping putative hubs in human, chimpanzee and rhesus macaque connectomes via diffusion tractography. Neuroimage 80, 462–474.

Lieberman, D.E., Pearson, O.M., Mowbray, K.M., 2000. Basicranial influence on overall cranial shape. J. Hum. Evol. 38, 291–315.

Lieberman, D.E., McBratney, B.M., Krovitz, G., 2002. The evolution and development of cranial form in *Homo* sapiens. Proc. Natl. Acad. Sci. U. S. A. 99, 1134–1139.

Lou, H.C., Luber, B., Crupain, M., Keenan, J.P., Nowak, M., Kjaer, T.W., Sackeim, H.A., Lisanby, S.H., 2004. Parietal cortex and representation of the mental Self. Proc. Natl. Acad. Sci. U. S. A. 101, 6827–6832.

Maister, L., Slater, M., Sanchez-Vives, M.V., Tsakiris, M., 2015. Changing bodies changes minds: owning another body affects social cognition. Trends Cogn. Sci. 19, 6–12.

Margulies, D.S., Vincent, J.L., Kelly, C., Lohmann, G., Uddin, L.Q., Biswal, B.B., Villringer, A., Castellanos, F.X., Milham, M.P., Petrides, M., 2009. Precuneus shares intrinsic functional architecture in humans and monkeys. Proc. Natl. Acad. Sci. U. S. A. 106, 20069–20074.

Meunier, D., Lambiotte, R., Bullmore, E.T., 2010. Modular and hierarchically modular organization of brain networks. Front. Neurosci. 4 (200).

Mitteroecker, P., Bookstein, F.L., 2007. The conceptual and statistical relationship between modularity and morphological integration. Syst. Biol. 56, 818–836.

Neubauer, S., Gunz, P., Hublin, J.-J., 2009. The pattern of endocranial ontogenetic shape changes in humans. J. Anat. 215, 240–255.

Peer, M., Salomon, R., Goldberg, I., Blanke, O., Arzy, S., 2015. Brain system for mental orientation in space, time, and person. Proc. Natl. Acad. Sci. U. S. A. 112, 11072–11077.

Pereira-Pedro, A.S., Bruner, E., 2016. Sulcal pattern, extension, and morphology of the precuneus in adult humans. Ann. Anat. 208, 85–93.

Ponce de León, M.S., Bienvenu, T., Akazawa, T., Zollikofer, C.P.E., 2016. Brain development is similar in Neanderthals and modern humans. Curr. Biol. 26, R665–R666.

Quallo, M.M., Price, C.J., Ueno, K., Asamizuya, T., Cheng, K., Lemon, R.N., Iriki, A., 2009. Gray and white matter changes associated with tool-use learning in macaque monkeys. Proc. Natl. Acad. Sci. U. S. A. 106, 18379–18384.

Raichle, M.E., MacLeod, A.M., Snyder, A.Z., Powers, W.J., Gusnard, D.A., Shulman, G.L., 2001. A default mode of brain function. Proc. Natl. Acad. Sci. U. S. A. 98, 676–682.

Sacher, J., Neumann, J., Okon-Singer, H., Gotowiec, S., Villringer, A., 2013. Sexual dimorphism in the human brain: evidence from neuroimaging. J. Magn. Reson. Imaging 31, 366–375.

Scheperjans, F., Eickhoff, S.B., Hömke, L., Mohlberg, H., Hermann, K., Amunts, K., Zilles, K., 2008. Probabilistic maps, morphometry, and variability of cytoarchitectonic areas in the human superior parietal cortex. Cereb. Cortex 18, 2141–2157.

Scott, N., Neubauer, S., Hublin, J.-J., Gunz, P., 2014. A shared pattern of postnatal endocranial development in extant hominoids. Evol. Biol. 41, 572–594.

Smith, S.M., 2002. Fast robust automated brain extraction. Hum. Brain Mapp. 17, 143–155.

Smith, S.M., Jenkinson, M., Woolrich, M.W., Beckmann, C.F., Behrens, T.E.J., Johansen-Berg, H., Bannister, P.R., De Luca, M., Drobnjak, I., Flitney, D.E., Niazy, R.K., Saunders, J., Vickers, J., Zhang, Y., De Stefano, N., Brady, J.M., Matthews, P.M., 2004. Advances in functional and structural MR image analysis and implementation as FSL. NeuroImage 23 (Supplement 1), S208–S219.

Sotero, R.C., Iturria-Medina, Y., 2011. From blood oxygenation level dependent (BOLD) signals to brain temperature maps. Bull. Math. Biol. 73, 2731–2747.

Spasojevic, G., Malobabic, S., Suscevic, D., Miljkovic, Z., 2004. Morphometric variability of precuneus in relation to gender and the hemisphere of human brain. Vojnosanit. Pregl. 61, 365–370.

Tallinen, T., Chung, J.Y., Rousseau, F., Girard, N., Lefèvre, J., Mahadevan, L., 2016. On the growth and form of cortical convolutions. Nat. Phys. 12, 588–593.

Utevsky, A.V., Smith, D.V., Huettel, S.A., 2014. Precuneus is a functional core of the default-mode network. J. Neurosci. 34, 932–940.

Van den Heuvel, M.P., Bullmore, E.T., Sporns, O., 2016. Comparative connectomics. Trends Cogn. Sci. 20, 345–361.

Via, E., Radua, J., Cardoner, N., Happé, F., Mataix-Cols, D., 2011. Meta-analysis of gray matter abnormalities in Autism Spectrum Disorder: should Asperger disorder be subsumed under a broader umbrella of autistic spectrum disorder? Arch. Gen. Psychiatry 68, 409–418.

Zelditch, M.L., Swiderski, D.L., Sheets, H.D., Fink, W.L., 2004. Geometric Morphometrics for Biologists. Elsevier Academic Press, New York and London.

Zhang, S., Li, C.R., 2012. Functional connectivity mapping of the human precuneus by resting state fMRI. Neuroimage 59, 3548–3562.

Zilles, K., Palomero-Gallagher, N., 2001. Cyto-, myelo-, and receptor architectonics of the human parietal cortex. Neuroimage 14, S8–S20.

Zollikofer, C.P.E., Ponce de León, M., 2002. Visualizing patterns of craniofacial shape variation in *Homo sapiens*. Proc. R. Soc. B 269, 801–807.

4.3. MIDSAGITTAL BRAIN VARIATION AMONG NON-HUMAN PRIMATES: INSIGHTS INTO EVOLUTIONARY EXPANSION OF THE HUMAN PRECUNEUS

Authors: Ana Sofia Pereira Pedro, James K. Rilling, Xu Chen, Todd M. Preuss, Emiliano Bruner

Journal: Brain, Behavior and Evolution, 90:255-263

Status: Published in 2017

Original Paper

Brain, Behavior and Evolution

Brain Behav Evol 2017;90:255–263
DOI: 10.1159/000481085

Received: April 11, 2017
Returned for revision: May 29, 2017
Accepted after revision: August 29, 2017

Midsagittal Brain Variation among Non-Human Primates: Insights into Evolutionary Expansion of the Human Precuneus

Ana Sofia Pereira-Pedro[a] James K. Rilling[b–f] Xu Chen[b, c] Todd M. Preuss[d, e, g]
Emiliano Bruner[a]

[a]Grupo de Paleoneurología, Centro Nacional de Investigación sobre la Evolución Humana, Burgos, Spain;
Departments of [b]Anthropology and [c]Psychiatry and Behavioral Sciences, [d]Center for Translational Social Neuroscience, [e]Center for Behavioral Neuroscience, [f]Yerkes National Primate Research Center, and [g]Division of Neuropharmacology and Neurologic Diseases, Yerkes National Primate Research Center, Emory University, Atlanta, GA, USA

Keywords
Precuneus · Geometric morphometrics · Brain morphology · Macaques · Apes

Abstract
The precuneus is a major element of the superior parietal lobule, positioned on the medial side of the hemisphere and reaching the dorsal surface of the brain. It is a crucial functional region for visuospatial integration, visual imagery, and body coordination. Previously, we argued that the precuneus expanded in recent human evolution, based on a combination of paleontological, comparative, and intraspecific evidence from fossil and modern human endocasts as well as from human and chimpanzee brains. The longitudinal proportions of this region are a major source of anatomical variation among adult humans and, being much larger in *Homo sapiens*, is the main characteristic differentiating human midsagittal brain morphology from that of our closest living primate relative, the chimpanzee. In the current shape analysis, we examine precuneus variation in non-human primates through landmark-based models, to evaluate the general pattern of variability in non-human primates, and to test whether precuneus proportions are influenced by allometric effects of brain size. Results show that precuneus proportions do not covary with brain size, and that the main difference between monkeys and apes involves a vertical expansion of the frontal and occipital regions in apes. Such differences might reflect differences in brain proportions or differences in cranial architecture. In this sample, precuneus variation is apparently not influenced by phylogenetic or allometric factors, but does vary consistently within species, at least in chimpanzees and macaques. This result further supports the hypothesis that precuneus expansion in modern humans is not merely a consequence of increasing brain size or of allometric scaling, but rather represents a species-specific morphological change in our lineage.

KARGER

E-Mail karger@karger.com
www.karger.com/bbe

Emiliano Bruner
Centro Nacional de Investigación sobre la Evolución Humana
Paseo Sierra de Atapuerca 3
ES–09002 Burgos (Spain)
E-Mail emiliano.bruner@cenieh.es

Introduction

Positioned at the medial cortical surface, the precuneus constitutes the medial portion of the parietal lobe, juxtaposed to the falx cerebri and extending onto the dorsal surface of the upper parietal lobule. In primates, it is delimited anteriorly by the marginal ramus of the cingulate sulcus, posteriorly by the parieto-occipital sulcus, and inferiorly by the subparietal sulcus [Cavanna and Trimble, 2006; Margulies et al., 2009]. Research on the precuneus has accelerated in the past decade due to the development of noninvasive medical imaging techniques, namely MRI, fMRI, and PET. Functional studies have revealed that the precuneus is involved in a variety of functions associated with self-perception and visual imagery [Lou et al., 2004; Land, 2014], processing of spatial working memory [Wallentin et al., 2006, 2008], and memory retrieval (recognition of familiar faces [Gobbini and Haxby, 2007; Lee et al., 2013]; episodic memory [Vannini et al., 2011]; recognition memory [Hassabis and Maguire, 2009], and autobiographical memory [Freton et al., 2014]). Moreover, the precuneus is a functional core of the default mode network, a set of interconnected cortical areas that is active at rest [Raichle et al., 2001; Tomasi and Volkow, 2010; Utevsky et al., 2014], and it is a crucial hub of large-scale brain connectivity [Hagmann et al., 2008; Li et al., 2013; de Reus et al., 2014]. Therefore, the precuneus is a region that is both structurally and functionally central for integrating multiple neural systems, and is comprised of different subregions involved in distinct cognitive functions [Margulies et al., 2009; Zhang and Li, 2012].

Adult humans display marked intraspecific variability in precuneus anatomy and morphology. When dealing with midsagittal brain geometry, the longitudinal proportions of the precuneus represent the main factor of variation among adult humans [Bruner et al., 2014b] by virtue of differences in cortical surface area [Bruner et al., 2015]. In adult humans, having a larger precuneus is partially associated with additional sulci and with an expansion of its anterior-dorsal region [Bruner et al., 2017a], corresponding in location to parietal area 7a [Scheperjans et al., 2008].

The histological and functional bases of this variation are not known, and changes in precuneus proportions are apparently not correlated with broad standard psychometric scores [Bruner et al., 2015]. Recent comparisons of humans and non-human primates using task-based and resting-state functional neuroimaging, as well as functional-connectivity MRI, indicate that these species share many features of precuneus organization [Rilling et al., 2007; Vincent et al., 2007; Kojima et al., 2009; Margulies et al., 2009; Barks et al., 2015; Caminiti et al., 2015].

Table 1. Sample included in the analysis

Species	*n*	Average brain volume, cc	Average spatial resolution, mm^2
Capuchin (*Cebus apella*)	3	66.5	0.57
Rhesus monkey (*Macaca mulatta*)	7	79.1	0.56
Mangabey (*Cercocebus atys*)	3	98.8	0.50
Baboon (*Papio cynocephalus*)	2	143.3	0.50
Gorilla (*Gorilla gorilla*)	2	397.3	0.70
Gibbon (*Hylobates lar*)	4	83	0.52
Orangutan (*Pongo pygmaeus*)	3	406.9	0.73
Bonobo (*Pan paniscus*)	3	311.2	0.73
Chimpanzee (*Pan troglodytes*)	15	337.3	0.75

Nevertheless, in addition to the marked intraspecific variation in humans, two observations suggest possibly significant evolutionary changes in humans. First, when comparing midsagittal brain morphology in humans and chimpanzees, the main difference is that *Homo sapiens* has a much larger precuneus in terms of absolute and relative size [Bruner et al., 2017b]. Second, when comparing brain morphology in modern and extinct human species, such as Neanderthals, the main difference is a patent enlargement in *H. sapiens* of the dorsal parietal surface, in a position that matches the precuneus longitudinal expansion [Bruner et al., 2003, 2014a; Bruner, 2004].

The precuneus morphology of non-human primates has not yet been analyzed quantitatively, and taking into account the large size of the human brain, it remains to be determined whether human precuneus enlargement is due to allometric patterns and scaling rules associated with the encephalization process. In this study, we analyze the shape variation of the precuneus in monkeys and apes, with the dual goals of investigating this cortical element in non-human primates, and of testing possible allometric patterns driving its morphological variability.

Materials and Methods

The sample was composed of 42 non-human primate MRI scans from 4 monkey species and 5 ape species (Table 1). The specimens are all adults, and sex was not considered in the current survey. For this study, we used existing MRI databases described previously [Rilling and Insel, 1998, 1999; Rilling and Seligman, 2002; Chen et al., 2013] (available at http://www.chimpanzeebrain.org),

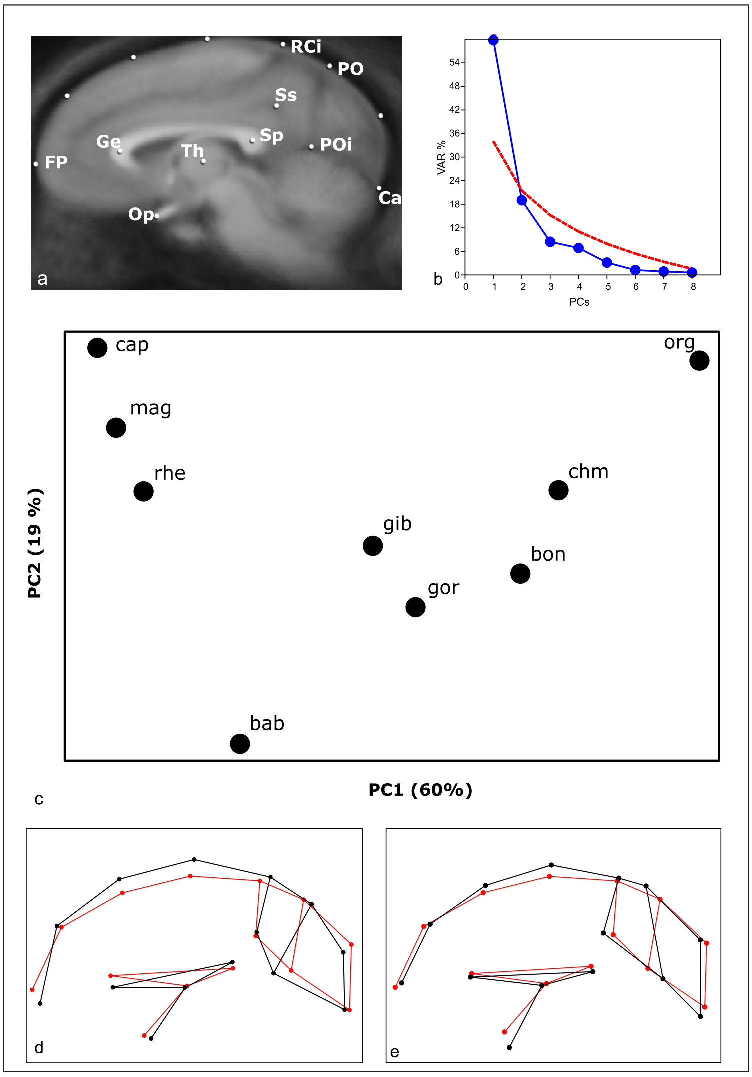

Color version available online

Fig. 1. a Landmark set used in the analysis. **b**, **c** Only the first principal component is above the threshold of random variation, although the second component can also be considered, mostly taking into account that multiple-species samples are not expected to be normally distributed. **d** PC1 separates monkeys and apes and it is associated, in the latter group, with a pronounced vertical stretching of the frontal profile and with longitudinal stretching of the occipital lobe. **e** The second principal component separates baboons from capuchins and orangutans, because of shortening of the precuneus dorsal length and stretching of the retrosplenial cortex (black and red wireframes show positive and negative shape values for each component). Cap, capuchins; mag, mangabeys; rhe, rhesus monkeys; bab, baboons; gib, gibbons; gor, gorillas; bon, bonobos; chm, chimpanzees; org, orangutans.

scanned at 1.5 T, except for 10 chimpanzees which were scanned at 3 T. MRI images were first reoriented using Nudge in FSL (https://fsl.fmrib.ox.ac.uk) so that the most anterior and the most posterior points were oriented in the horizontal plane, and the sagittal plane was parallel to the interhemispheric fissure of the brain. For 10 chimpanzees scanned separately at 3 T, brain images were aligned to a chimpanzee brain template [Bruner et al., 2017b] using rigid body linear registration with 6 degrees of freedom, so that the sagittal plane was parallel to the interhemispheric fissure of the brain. The reoriented images were then resampled to a consistent isotropic spatial resolution of 0.8 mm (for all apes except gibbons) or 0.5 mm (for all monkeys and gibbons). Each individual brain was then visualized in FSLVIEW and snapshots were taken for the first 3 sagittal slices in both hemispheres. These 3 slices were then joined in a single scout view by averaging the grayscale values into a single 2-dimensional image, to effectively display the midsagittal brain gross morphology while limiting local noise [Pereira-Pedro and Bruner, 2016]. Shape variation of the midsagittal morphology was analyzed following the principles of geometric morphometrics [Zelditch et al., 2004]. We chose a set of 14 landmarks and semilandmarks (Fig. 1a) in accordance with previous studies [Bruner et al., 2014b, 2017b]: optic chiasm (Op), thalamus center (Th), center of the genu (Ge) and splenium (Sp) of the corpus callosum, frontal pole (FP; anterior-most point), marginal ramus of the cin-

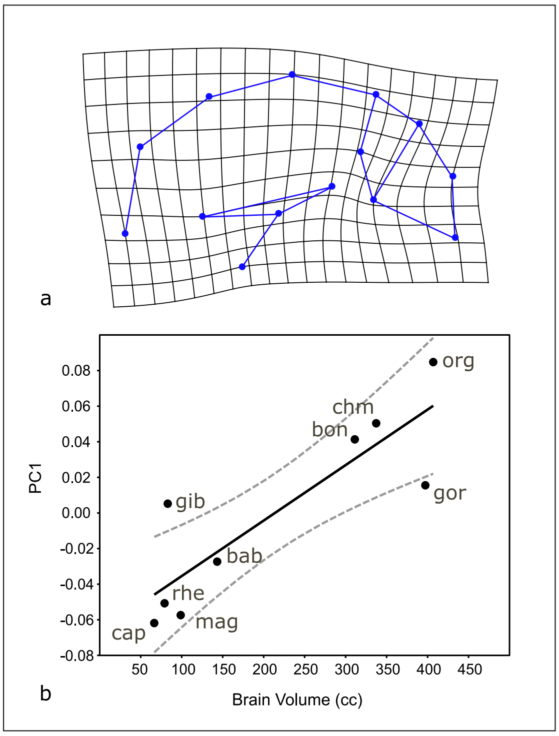

Fig. 2. a Shape variation associated with brain size increase is similar to the pattern observed in PC1. **b** There is a positive correlation between brain volume and PC1 scores. Species abbreviations are as in Figure 1.

gulate sulcus (RCi), central point of the subparietal sulcus (Ss), external (PO) and internal (POi) extremes of the parieto-occipital sulcus, and occipito-cerebellar boundary (Oc). According to the current knowledge on these anatomical areas, all these points are considered to be homologous in monkeys and apes. The frontal curvature was sampled by 3 equally distant semi-landmarks from the frontal pole to the precuneus. A semi-landmark was also sampled at 50% of the occipital curvature. Both hemispheres were digitized and then averaged. Landmark sets were scaled to the unitary size, translated to the same centroid, and rotated through Procrustes registration, minimizing the distance between corresponding landmarks [Bookstein, 1991]. The resulting shape coordinates were used for multivariate analyses. A first analysis considered species-average shapes, to provide a general perspective on the morphological variation in primates. Shape patterns of variation were analyzed through principal component analysis. Allometry was tested by multivariate regression of shape variables versus brain volume, so as to identify possible correlations between midsagittal morphology and whole brain size. For this survey we used species average values of brain volume published in Rilling and Seligman [2002]. A second analysis considered only chimpanzees and macaques, which are the only 2 groups in our sample with a number of specimens that allows intraspecific considerations. This second analysis is useful to compare 2 species with marked brain size differences. Geometric morphometrics were computed with PAST [Hammer et al., 2001] and Morpho J [Klingenberg, 2011].

Results

Following principal component analysis of the species average shapes, there was only 1 component above a threshold of random variation (Fig. 1b, c). This principal component explained 60% of the total variance, distributing species along a vector from capuchins to orangutans, associated with a generalized vertical stretching of the whole brain, which becomes rounder (Fig. 1d). This vector separates monkeys and apes, with gibbons and gorillas in an intermediate position. PC2 was roughly at the border with the threshold of normal random variation, explaining 19% of the variance (Fig. 1b, c), and is worth mentioning. It mainly separated orangutans and capuchins from baboons: the former displayed a relatively shorter length of the dorsal precuneus and a relatively greater length at the retrosplenial cortex (Fig. 1e), while the latter showed the opposite features. When all specimens were analyzed together (data not shown), PC1 remained the same as in the previous analysis computed on species' means, but PC2 was strictly associated with precuneus dorsal length. However, most of the species analyzed in this survey include too few specimens, and hence the information on intraspecific variation was not sufficiently stable or reliable to merit robust conclusions.

Brain volume explained 45.5% of the whole shape variation (p = 0.008). The shape pattern associated with increasing brain size was the same as PC1 (Fig. 2a), and brain size was highly correlated with this vector (Fig. 2b; $R = 0.87$; $R^2 = 0.75$; p value for permutation test = 0.007). According to this allometric pattern, there was a tendency for smaller-brained monkeys to have flatter brains, and for the larger-brained great apes to have rounder brains. Gibbons and gorillas departed from this general trend, falling outside the 95% confidence interval, with the former showing a rounder brain relative to the small-brained monkeys, and the latter showing a more elongated brain compared with other apes.

When analyzing only chimpanzee and macaque specimens, PC1 explained 54% of the shape variation, and it separated the 2 species by a discrete morphological gap (Fig. 3a, b). This component was similar to the previous one, being associated with an increasing rounder shape

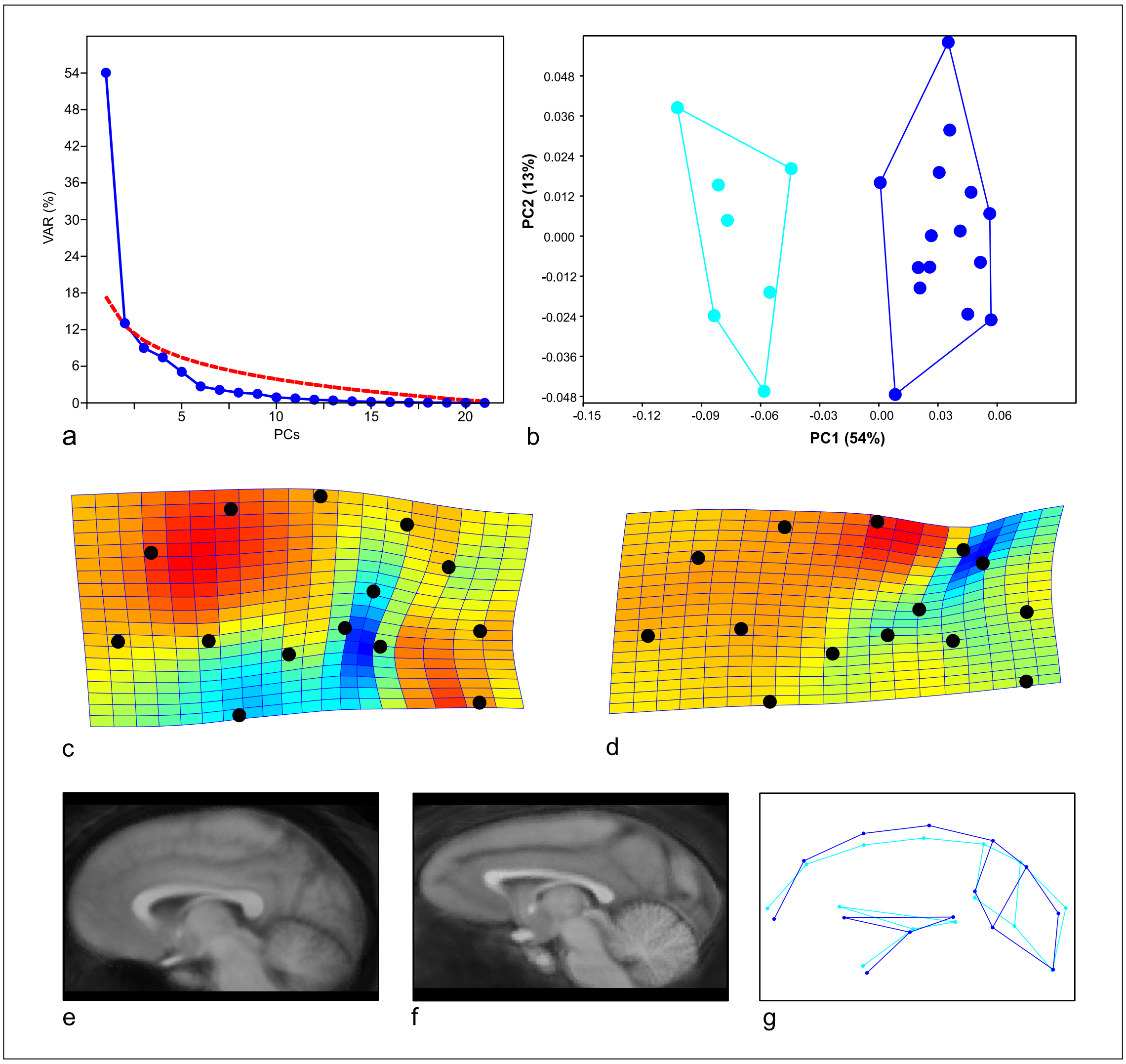

Color version available online

Fig. 3. Comparison between chimpanzees and macaques: variation explained by each principal component (**a**); plot of the first 2 principal components (**b**); deformation grids displaying shape variation along PC1 (**c**) and PC2 (**d**); average shape of chimpanzees (**e**) and of rhesus monkeys (**f**); and difference between the 2 species according to a discriminant function (**g**). In **b** and **g** rhesus monkeys are light blue and chimpanzees are dark blue. On the transformation grids red represents expansion and blue is reduction.

(from macaques to chimpanzees) because of bulging of the frontal curve and vertical stretching of the occipital morphology (Fig. 3c). PC2 (13%) was borderline relative to the threshold of random variation, and hence it was less consistent in terms of stability. Nonetheless, it is worth noting that PC2 was related to intraspecific (individual) variation associated with precuneus dorsal expansion/reduction (Fig. 3d). That is, this second component suggested that precuneus variation is a relevant factor within both species, and to a similar extent. A discriminant function between the two groups (Fig. 3e, f) showed that chimpanzees displayed a more curved frontal profile and relatively larger occipital lobes ($p < 0.0001$; Fig. 3g).

Discussion

In humans, the longitudinal extent of the precuneus represents a major source of individual variation in brain anatomy [Bruner et al., 2014b, 2015]. The precuneus is also proportionally much larger in humans than in chimpanzees, not only in terms of absolute size but also in its proportions relative to other cortical regions [Bruner et al., 2017b], and the corresponding dorsal parietal areas are expanded in modern human endocasts when compared with those of extinct human species [Bruner et al., 2014a]. Precuneus proportions among adult humans are unrelated to brain size, excluding allometric factors as an explanation for intraspecific variation. Fossil evidence similarly suggests that allometry cannot explain differential parietal enlargement in *H. sapiens* since Neanderthals had similar brain volumes but flatter and shorter parietal surfaces compared with modern humans [Bruner et al., 2003]. However, it is not known if allometric factors can explain differences in precuneus relative size between humans and chimpanzees. To evaluate this possibility, in this survey we tested whether the brain size increase in non-human primates is associated with an increase of precuneus proportions. We analyzed midsagittal brain shape in a sample of apes and monkeys that includes diverse genera with distinct adaptations and a wide range of brain sizes, to investigate precuneus morphological variation in living non-human anthropoid primates, and to test whether interspecific variability can be explained by allometric effects.

Our shape analysis showed that the main pattern of midsagittal brain variation among primates involves the general shape of the braincase, distinguishing rounded versus elongated brains, with no apparent change of local brain proportions. This morphological factor separated monkeys from apes, ranging from cebids (the flattest) to orangutans (the roundest). This pattern was associated with brain size, except in gibbons, which have a small brain size (83 cm^3) but a rounder brain shape, and in gorillas, who have a large brain size (397 cm^3) but a more elongated brain shape. Bienvenu et al. [2011] obtained similar results in great apes based on the 3D morphology of endocasts: gorillas displayed long and narrow endocrania, and orangutans exhibited short and wide brains, while chimpanzees and bonobos (and humans) were intermediate. In our study, gorillas and gibbons, despite their brain size differences, displayed a similar brain shape, at least according to this main pattern of variation. Similarity between these 2 species was also observed by McNulty [2004] in a craniofacial analysis of extant apes. He found that, when adjusting for size, gorillas and gibbons were closest among extant apes, and equally distant from chimpanzees, and suggested this similarity in shape might be due to the retention of ancestral hominoid cranial morphology. Gibbons also display a subcortical brain shape which is similar to apes and departs from a possible allometric trend, suggesting that beyond size-related effects there are some probable phylogenetic effects [Bruner and Jeffery, 2007].

The fact that the main pattern of variation, which is partially size related, involves the general form of the braincase without localized changes of brain proportions, suggests that this component is probably due to cranial constraints rather than changes in the relative size of different brain regions. The cranial form in monkeys and apes is influenced by posture and muscle attachments, cranial base constraints, and facial integration, influencing the general proportions of the braincase [Moss and Young, 1960; Shea, 1985; Lieberman et al., 2000; Bastir et al., 2010]. In this sense, the main neurocranial difference between and within species is represented by the ratio between length and width, ranging from long, narrow, and more elongated (dolichocephalic), to short, wide, and more rounded braincases (brachycephalic), a variation which is due to distinct morphogenetic and phenotypic factors [Zollikofer and Ponce de León, 2002]. Therefore, at least for the features analyzed through this shape model, allometric variation in brain shape is apparently attributable to changes in cranial form rather than the local expansion or contraction of brain regions. A recent analysis has demonstrated an important association between cranial and endocranial variation in hominoids, further stressing the role of skull constraints on brain shape evolution [Zollikofer et al., 2017], as already suggested according to the principles of functional craniology [Enlow, 1990; Bastir et al., 2006; Bruner and Ripani, 2008]. Nonetheless, most constraints have been identified in the cranial base and face, not in the dorsal cranium, and most shape analyses of the ape brain have been put forward only in terms of overall geometry, without taking into consideration the contribution of different brain districts. Therefore, we cannot exclude that part of our shape variation could also be due to real changes of brain proportions, although this is difficult to assess when dealing with the midsagittal morphology alone. For example, there is evidence suggesting that apes evolved relatively and absolutely larger frontal lobes when compared with other primates [Semendeferi et al., 1997, 2002; Semendeferi and Damasio, 2000; Smaers and Soligo, 2013], and we therefore cannot exclude that the pattern of frontal bulging described in this study could also be associated, at least in part, with an actual enlargement of the frontal cortex. Our results also suggest that, at least when compared with macaques, chimpanzees display a relatively larger occipital region.

The case of gorillas merits further discussion. Gorillas and chimpanzees share a large allometric component, although gorillas display a marked projection of the facial block which longitudinally stretches the braincase [Shea, 1983; Bruner and Manzi, 2001; Mitteroecker et al., 2004]. In contrast, orangutans have a specialized cranial architecture, with a pronounced airorhynchy (dorsal flexion on the facial block) leading to a globular braincase [Shea, 1985; Bruner et al., 2004]. In this study, however, gorilla, and not orangutan, departs from the allometric trend. It is therefore probable that this general trend can hide multiple independent trajectories. A finer regression analysis distinguishing subgroups was, however, not feasible in this study because of the small number of species included and consequent lack of statistical power.

Beyond any species-specific assessment, it is important to emphasize that the precuneus does not display any apparent variation in its proportions across this sample of non-human primate genera, which varies greatly in brain size. Apart from a change in its orientation due to the brachycephalic versus dolichocephalic condition, there is no evidence of a relative enlargement or reduction. The comparison between chimpanzee and macaques further highlights this result: chimpanzees have a brain size about 4 times that of macaques, but there is no evidence of changes in the general proportions of the precuneus.

Therefore, all the current evidence suggests that parietal expansion in modern humans is a specific feature of our evolutionary lineage, and not a secondary allometric consequence of large brain size. In adult modern humans, precuneus variation is not correlated with brain size [Bruner et al., 2014b, 2017a]. Within the genus *Homo*, Neanderthals had a similar brain size as modern humans, but they did not display any parietal longitudinal enlargement [Bruner et al., 2003]. Finally, taking into account variation across primate species, the larger precuneus in modern humans, when compared with chimpanzees [Bruner et al., 2017b], cannot be explained by allometric variation associated with brain size (this study).

It is interesting to note that, as in humans, we found marked within-species (individual) variation in relative precuneus size in our small macaque and chimpanzee samples, a result that deserves additional investigation with larger samples. Thus, precuneus plasticity may be a major feature shared among primates. The further increase in modern humans could be interpreted as the expression of an intrinsic potential of the primate brain. Evolutionary changes often occur in the same direction of the greatest genotypic/phenotypic variance, because the latter constrains the former, or because both patterns undergo the same selective pressure, generating evolutionary "lines of least resistance" [Schluter, 1996]. Therefore, we must evaluate whether the precuneus has some intrinsic property, because of genetic or environmental factors, which makes it particularly sensitive to individual variation. Surely, the fact that it is positioned between the frontal and occipital blocks makes it susceptible to spatial limitations and morphogenetic constraints. Nonetheless, it is worth noting that our study, like previous studies on the same topic, relies on anatomical landmarks associated with specific boundaries of brain regions. Therefore, the relative expansion or reduction of a specific brain region cannot be explained simply as a passive consequence of spatial adjustments, but must be associated with the proportional increase or decrease of some histological component (number or size of neurons, connections, glia, etc.).

As a cautionary note, we must stress that this general survey is based on a limited number of primate species, each represented by only a few specimens. Taxon-specific analyses on larger collections would provide additional evidence on other species or genera. In particular, grade shifts between genera are expected and must be investigated with robust statistical samples, properly representing intraspecific variability and correlations. Also, we recognize that the precuneus is formed by distinct areas or subareas [Scheperjans et al., 2008], and variations within and between taxa have yet to be investigated at this level of organization. It will therefore be essential to investigate the different contributions of these areas to the overall morphological variability. Unfortunately, most parcellation schemes are based on parameters (cells, connections, functions, or physiological properties) that are not identifiable through macroscopic analyses.

The precuneus is crucial for the integration of the body and environment, in terms of spatial coordination but also in terms of simulation and visual imagery [Cavanna and Trimble, 2006; Margulies et al., 2009; Land, 2014]. It is also crucial for the perception and interpretation of social structure [Peer et al., 2015]. It has a notable metabolic load and thermal load, and is associated with metabolic impairments and vulnerability to neurodegenerative processes like Alzheimer disease [Zhang and Li, 2012; Bruner and Jacobs, 2013; Bruner et al., 2014a]. The evidence presented in this study further suggests that its enlargement in modern humans is not likely to be a consequence of brain size increase, and may represent a localized and specific characteristic of *H. sapiens*. We should now evaluate the precise histological components involved, and the possible functional significance of this distinctive human brain morphology.

Acknowledgments

This work was supported by grants from the National Institutes of Health (P01AG026423 and R24NS092988) and the National Center for Research Resources (P51RR165; superseded by the Office of Research Infrastructure Programs/OD P51OD11132). A.S.P.-P. is funded by the Atapuerca Foundation. E.B. is funded by the Spanish Government (CGL2015-65387-C3-3-P) and by the Italian Institute of Anthropology.

Disclosure Statement

The authors declare no conflicts of interest.

References

Barks SK, Parr LA, Rilling JK (2015): The default mode network in chimpanzees (*Pan troglodytes*) is similar to that of humans. Cereb Cortex 25:538–544.

Bastir M, Rosas A, O'Higgins P (2006): Craniofacial levels and the morphological maturation of the human skull: spatiotemporal pattern of cranial ontogeny. J Anat 209:637–654.

Bastir M, Rosas A, Stringer C, Cuétara JM, Kruszynski R, Weber GW, Ross CF, Ravosa M (2010): Effects of brain and facial size on basicranial form in human and primate evolution. J Hum Evol 58:424–431.

Bienvenu T, Guy F, Coudyzer W, Gilissen E, Roualdès G, Vignaud P, Brunet M (2011): Assessing endocranial variations in great apes and humans using 3D data from virtual endocasts. Am J Phys Anthropol 145:231–246.

Bookstein FL (1991): Morphometric Tools for Landmark Data: Geometry and Biology. New York, Cambridge University Press.

Bruner E (2004): Geometric morphometrics and paleoneurology: brain shape evolution in the genus *Homo*. J Hum Evol 47:279–303.

Bruner E, De la Cuétara JM, Masters M, Amano H, Ogihara N (2014a): Functional craniology and brain evolution: from paleontology to biomedicine. Front Neuroanat 8:19.

Bruner E, Jacobs HIL (2013): Alzheimer's disease: the downside of a highly evolved parietal lobe? J Alzheimers Dis 35:227–240.

Bruner E, Jeffery N (2007): Extracting functional, phylogenetic and structural data from the subcortical brain: an exploratory geometric morphometric survey. J Anthropol Sci 85: 125–138.

Bruner E, Manzi G (2001): Allometric analysis of the skull in Pan and Gorilla by geometric morphometrics. Riv Antropol 79:45–52.

Bruner E, Manzi G, Arsuaga JL (2003): Encephalization and allometric trajectories in the genus *Homo*: evidence from the Neandertal and modern lineages. Proc Natl Acad Sci USA 100:15335–15340.

Bruner E, Pereira-Pedro AS, Chen X, Rilling JK (2017a): Precuneus proportions and cortical folding: a morphometric evaluation on a racially diverse human sample. Ann Anat 211: 120–128.

Bruner E, Preuss TM, Chen X, Rilling JK (2017b): Evidence for expansion of the precuneus in human evolution. Brain Struct Funct 222: 1053–1060.

Bruner E, Román FJ, de la Cuétara JM, Martin-Loeches M, Colom R (2015): Cortical surface area and cortical thickness in the precuneus of adult humans. Neuroscience 286:345–352.

Bruner E, Rangel de Lázaro G, de la Cuétara JM, Martín-Loeches M, Colom R, Jacobs HIL (2014b): Midsagittal brain variation and MRI shape analysis of the precuneus in adult individuals. J Anat 224:367–376.

Bruner E, Ripani M (2008): A quantitative and descriptive approach to morphological variation of the endocranial base in modern humans. Am J Phys Anthropol 137:30–40.

Bruner E, Saracino B, Ricci F, Tafuri M, Passarello P, Manzi G (2004): Midsagittal cranial shape variation in the genus *Homo* by geometric morphometrics. Coll Antropol 28:99–112.

Caminiti R, Innocenti GM, Battaglia-Mayer A (2015): Organization and evolution of parieto-frontal processing streams in macaque monkeys and humans. Neurosci Biobehav Rev 56:73–96.

Cavanna AE, Trimble MR (2006): The precuneus: a review of its functional anatomy and behavioural correlates. Brain 129:564–583.

Chen X, Errangi B, Li L, Glasser MF, Westlye LT, Fjell AM, Walh K, Hu X, Herndon J, Preuss T, Rilling J (2013): Brain aging in humans, chimpanzees (*Pan troglodytes*), and rhesus macaques (*Macaca mulatta*): magnetic resonance imaging studies of macro- and microstructural changes. Neurobiol Aging 34: 2248–2260.

de Reus MA, Saenger VM, Kahn RS, van den Heuvel MP (2014): An edge-centric perspective on the human connectome: link communities in the brain. Philos Trans R Soc Lond B Biol Sci 2014;369:20130527.

Enlow DH (1990): Facial Growth. Philadelphia, WB Saunders.

Freton M, Lemogne C, Bergouignan L, Delaveau P, Lehéricy S, Fossati P (2014): The eye of the self: precuneus volume and visual perspective during autobiographical memory retrieval. Brain Struct Funct 219:959–968.

Gobbini MI, Haxby JV (2007): Neural systems for recognition of familiar faces. Neuropsychologia 45:32–41.

Hagmann P, Cammoun L, Gigandet X, Meuli R, Honey CJ, Wedeen VJ, Sporns O (2008): Mapping the structural core of human cerebral cortex. PLoS Biol 6:e159.

Hammer Ø, Ryan P, Harper D (2001): PAST: Paleontological Statistics software package for education and data analysis. Palaeontol Electronica 4:9.

Hassabis D, Maguire EA (2009): The construction system of the brain. Philos Trans R Soc Lond B Biol Sci 364:1263–1271.

Klingenberg CP (2011): MorphoJ: an integrated software package for geometric morphometrics. Mol Ecol Resour 11:353–357.

Kojima T, Onoe H, Hikosaka K, Tsutsui K, Tsukada H, Watanabe M (2009): Default mode of brain activity demonstrated by positron emission tomography imaging in awake monkeys: higher rest-related than working memory-related activity in medial cortical areas. J Neurosci 29:14463–14471.

Land MF (2014): Do we have an internal model of the outside world? Philos Trans R Soc Lond B Biol Sci 369:20130045–20130045.

Lee TMC, Leung M, Lee TMY, Raine A, Chan CCH (2013): I want to lie about not knowing you, but my precuneus refuses to cooperate. Sci Rep 3:1636.

Li L, Hu X, Preuss TM, Glasser MF, Damen FW, Qiu Y, Rilling J (2013): Mapping putative hubs in human, chimpanzee and rhesus macaque connectomes via diffusion tractography. NeuroImage 80:462–474.

Lieberman DE, Ross CF, Ravosa MJ (2000): The primate cranial base: ontogeny, function, and integration. Am J Phys Anthropol 43:117–169.

Lou HC, Luber B, Crupain M, Keenan JP, Nowak M, Kjaer TW, Sackeim HA, Lisanby SH (2004): Parietal cortex and representation of the mental Self. Proc Natl Acad Sci USA 101: 6827–6832.

Margulies DS, Vincent JL, Kelly C, Lohmann G, Uddin LQ, Biswal BB, Villringer A, Castellanos FX, Milham MP, Petrides M (2009): Precuneus shares intrinsic functional architecture in humans and monkeys. Proc Natl Acad Sci USA 106:20069–20074.

McNulty KP (2004): A geometric morphometric assessment of hominoid crania: conservative African apes and their liberal implications. Ann Anat 186:429–433.

Mitteroecker P, Gunz P, Bernhard M, Schaefer K, Bookstein FL (2004): Comparison of cranial ontogenetic trajectories among great apes and humans. J Hum Evol 46:679–698.

Moss ML, Young RW (1960): A functional approach to craniology. Am J Phys Anthropol 18:281–292.

Peer M, Salomon R, Goldberg I, Blanke O, Arzy S (2015): Brain system for mental orientation in space, time, and person. Proc Natl Acad Sci USA 112:11072–11077.

Pereira-Pedro AS, Bruner E (2016): Sulcal pattern, extension, and morphology of the precuneus in adult humans. Ann Anat 208:85–93.

Raichle ME, MacLeod AM, Snyder AZ, Powers WJ, Gusnard DA, Shulman GL (2001): A default mode of brain function. Proc Natl Acad Sci USA 98:676–682.

Rilling JK, Barks SK, Parr LA, Preuss TM, Faber TL, Pagnoni G, Bremner JD, Votaw JR (2007): A comparison of resting-state brain activity in humans and chimpanzees. Proc Natl Acad Sci USA 104:17146–17151.

Rilling JK, Insel TR (1998): Evolution of the cerebellum in primates: differences in relative volume among monkeys, apes and humans. Brain Behav Evol 52:308–314.

Rilling, JK, Insel TR (1999): The primate neocortex in comparative perspective using magnetic resonance imaging. J Hum Evol 37:191–223.

Rilling JK, Seligman RA (2002): A quantitative morphometric comparative analysis of the primate temporal lobe. J Hum Evol 42:505–533.

Scheperjans F, Hermann K, Eickhoff SB, Amunts K, Schleicher A, Zilles K (2008): Observer-independent cytoarchitectonic mapping of the human superior parietal cortex. Cereb Cortex 18:846–867.

Schluter D (1996): Adaptive radiation along genetic lines of least resistance. Evolution 50: 1766–1774.

Semendeferi K, Damasio H (2000): The brain and its main anatomical subdivisions in living hominoids using magnetic resonance imaging. J Hum Evol 38:317–332.

Semendeferi K, Damasio H, Frank R, van Hoesen GW (1997): The evolution of the frontal lobes: a volumetric analysis based on three-dimensional reconstructions of magnetic resonance scans of human and ape brains. J Hum Evol 32:375–388.

Semendeferi K, Lu A, Schenker N, Damasio H (2002): Humans and great apes share a large frontal cortex. Nat Neurosci 5:272–276.

Shea BT (1983): Allometry and heterochrony in the African apes. Am J Phys Anthropol 62: 275–289.

Shea BT (1985): The ontogeny of sexual dimorphism in the African apes. Am J Primatol 8: 183–188.

Smaers JB, Soligo C (2013): Brain reorganization, not relative brain size, primarily characterizes anthropoid brain evolution. Proc R Soc Lond B Biol Sci 280:20130269.

Tomasi D, Volkow ND (2010): Functional connectivity density mapping. Proc Natl Acad Sci USA 107:9885–9890.

Utevsky AV, Smith DV, Huettel SA (2014): Precuneus is a functional core of the default-mode network. J Neurosci 34:932–940.

Vannini P, O'Brien J, O'Keefe K, Pihlajamäki M, Laviolette P, Sperling RA (2011): What goes down must come up: role of the posteromedial cortices in encoding and retrieval. Cereb Cortex 21:22–34.

Vincent JL, Patel GH, Fox MD, Snyder AZ, Baker JT, van Essen DC, Zempel JM, Snyder LH, Corbetta M, Raichle ME (2007): Intrinsic functional architecture in the anaesthetized monkey brain. Nature 447:83–86.

Wallentin M, Roepstorff A, Glover R, Burgess N (2006): Parallel memory systems for talking about location and age in precuneus, caudate and Broca's region. Neuroimage 32:1850–1864.

Wallentin M, Weed E, Østergaard L, Mouridsen K, Roepstorff A (2008): Accessing the mental space: spatial working memory processes for language and vision overlap in precuneus. Hum Brain Mapp 29:524–532.

Zelditch ML, Swiderski DL, Sheets HD, Fink WL (2004): Geometric Morphometrics for Biologists. New York, Elsevier Academic Press.

Zhang S, Li CR (2012): Functional connectivity mapping of the human precuneus by resting state fMRI. Neuroimage 59:3548–3562.

Zollikofer CPE, Bienvenu T, Ponce de León M (2017): Effects of integration on hominoid endocranial shape. J Anat 230:85–105.

Zollikofer CPE, Ponce de León M (2002): Visualizing patterns of craniofacial shape variation in *Homo sapiens*. Proc R Soc Lond B Biol Sci 269:801–807.

Chapter 5

GENERAL DISCUSSION

5. GENERAL DISCUSSION

5.1. STRUCTURAL RELATIONSHIPS INVOLVING THE FRONTAL AND PARIETAL REGIONS

Modern *Homo sapiens* is characterized by unique craniofacial features, including a globular neurocranium, a retracted face, and a flexed cranial base, and it is generally accepted that encephalization plays a role in the development of these cranial traits (Ross & Henneberg, 1995; McCarthy, 2001; Lieberman et al., 2002, 2004; Bruner, 2007; Bastir et al., 2010). The cranial vault is considered to be mainly shaped by the underlying neural tissue, and, in fact, the increase in cranial capacity in modern humans is associated with vertical and lateral development of the frontal and parietal vault regions (Bruner et al., 2003, 2004). However, the parietal and frontal bones depend on distinct structural and functional matrices (Moss & Young, 1960). In the first chapter of this thesis, we focused on the spatial relationships between the anterior cerebro-cranial and orbito-ocular structures, and between the parietal bone and middle cranial fossa.

5.1.1. Spatial relationships among orbito-ocular structures and fronto-temporal regions within adult modern humans

Our first study (chapter 2.1.) comprises the first description of anatomical variation between the eye and the brain and between the orbit and the anterior neurocranium within adult modern humans. With respect to the eye-brain spatial relationship, our results show that the major pattern of variation is associated with changes in horizontal position of the eyeball, that is, in the distance to the temporal lobes, while variation in the distance from the frontal lobe is secondary. We suggest this could be due to less strict spatial constraints on the horizontal direction, with the eyeball position being only limited by the middle cranial fossa/temporal lobes behind. In contrast, the vertical position is probably more strongly restricted by the frontal lobes above, and the midfacial structures below. However, since the midface was not included in our geometrical model we were unable to provide insight on the constraints exerted by the underlying facial structures on eye position.

Variation in eyeball position seems to be coupled with slight changes in its geometry, although changes in shape are difficult to discern, and appear to be generally minor. For instance, more posteriorly located eyeballs, closer to the temporal lobes, seem to be slightly antero-posteriorly shorter. This morphology is associated with bulging frontal profile. In contrast, more anteriorly located eyeballs, further from the temporal lobes, display a rounder geometry in association with flatter frontal profile. More precisely, anteriorly located eye seems to be associated with antero-posteriorly elongated, dolichocephalic cranial architecture, while more posteriorly placed eyeball are associated with rounder, brachycephalic morphology. Thus, these opposite morphological patterns might indicate a relationship between eyeball shape and position with overall variation in cranial architecture. It stands to reason that the position of the eyeball relative to the cerebro-cranial structures should be related to the proportions and dimensions of the orbit. As a matter of fact, taller faces have been shown to be associated with antero-posteriorly shorter anterior cranial floor/orbital roof (Bastir & Rosas, 2006).

When considering the cranial structures, the greatest variation involved the orientation of the orbit relative to frontal profile, while secondary variation was associated with orbital anteroposterior and vertical dimensions. The variation in orbit orientation and proportions could influence the spatial relationship between the eye and the temporal and frontal regions. More specifically, if the eyeball usually occupies the anterior portion of the orbit (Detorakis et al., 2010), a reduction in the antero-posterior dimensions of the face, and consequently of the orbit, would result in closer proximity between the eye and the temporal pole. In order to specifically explore the influence of the facial and orbital dimensions, as well as dolichocephalic vs. brachycephalic architectures, on the spatial conflict between the eye and neural tissues, MRI and CT scans from the same individuals should be included.

5.1.2. Eye-brain relationship and considerations for myopia

Masters (2012) hypothesized that juvenile-onset myopia could result from changes in the structural relationship between the soft tissues of the eye and the bony orbit during ontogeny in association with evolutionary changes in craniofacial morphology in modern humans. It follows that an increase in brain volume would affect eyeball size and shape. Our results only partially support this hypothesis. We observed a relationship between lobe volume and eyeball position and size, but not between lobe volume and eyeball shape. This suggests that brain size alone cannot induce ocular deformation, and other factors, such as extra-ocular fat, should be taken into account as well. Alternatively, it could be that our geometrical model was insufficient to detect minor shape changes in the eyeball outline.

While the shape of the myopic eye is usually associated with axial elongation, spherical and oblate (wide) shapes have also been described (Stone & Flitcroft, 2004). But different eye shapes are not always observed, particularly when refractive error is reduced as in the case of our sample, and size seems to be the main factor distinguishing myopic from non-myopic eyes (Cheng et al., 1992; Palmowski-Wolfe et al., 2009). Nonetheless, it must be considered that the eyeball is a complex structure, and different components may affect visual acuity (Pennie et al., 2001; González-Blanco et al., 2008; Bhatti et al., 2016). Besides, critical vision abilities such as fixation, focusing, control of eye movement, and hand-eye coordination develop during the first four years of life (van Cruchten et al., 2017). Hence, alterations in factors affecting the normal development of the eye and vision could occur in any developmental stage, stressing that the structural interaction between ocular, cerebral, and craniofacial structures should be assessed during ontogeny.

5.1.3. Orbit-braincase spatial relationship in a comparative perspective

In the third part of our first study (chapter 2.1.), a comparative analysis of the geometry or the orbit and anterior braincase across modern humans, chimpanzees, and Middle Pleistocene hominins (Bodo and Broken Hill 1) separated these species according to the distance between the orbital margin and the frontal profile. Chimpanzees have relatively larger orbits, with wide vertical apertures, that are forwardly projected beyond the flat frontal profile. Modern humans display the opposite morphology, with relatively smaller orbits that are vertically aligned with the bulging frontal profile. The two fossil specimens assigned to *H. heidelbergensis*, as well as the Neanderthal specimen (Gibraltar 1), at least in terms of orbital structure, seem to display intermediate morphotypes. These results illustrate the evolutionary reduction and retraction of the face associated with increased curvature of the frontal profile in modern humans, with the extinct human species exhibiting intermediate morphologies between modern humans and extant apes (Bruner et al., 2013; Beaudet & Bruner, 2017). Furthermore, we also observed the more anteriorly projected temporal tip of modern humans compared to other human species, and also to chimpanzees (Bastir et al., 2008; Bastir & Rosas, 2016). The temporal poles of modern humans seem to be located in a more superior position, aligned with the orbits, and this proximity between the posterior portion of the orbit and the anterior portion of the middle cranial fossa and temporal lobes could impose structural limits for both anatomical parts.

Among these specimens the increase in neuro-orbital proximity is associated with increase in relative brain size and decrease in facial prognathism and browridge development. This seems to be an interspecific pattern of craniofacial variation, since it has been shown that within modern humans browridge morphology is unrelated to neurocranial size or neuro-orbital disjunction (Nowaczewska et al., 2015). Interestingly, it seems that the supraorbital structures differ between extant great apes and fossil hominins, with the former having a distinctive bony arch separating the face from the neurocranium, while in the latter the browridge does not constitute such a clear topographic separation (Lacruz et al., 2019). It has been suggested that browridge morphology could be associated with social display and communication (Godinho et al., 2018). Browridge reduction in modern humans could be a result of craniofacial feminization associated with the evolution of prosocial behavior (Cieri et al., 2014).

5.1.4. Parietal bone dimensions and base orientation within modern humans

Expansion of the parietal region and anterior projection of the middle cranial fossae are unique in modern human cranial architecture. Our second study (chapter 2.2.) showed that the curvature of the parietal bone has no effect on the displacement of the temporal tip, supporting the absence of morphological integration between the cranial vault and base. It is worth noting that this lack of morphological integration could result from combining midline vault and lateral base elements, as it has been shown that lateral and midline elements are rather independent, at least regarding the cranial base structures (Bastir & Rosas, 2005; Bruner & Ripani, 2008). While there seems to be no morphological integration, variation in the proportions of one of the modules seems to be associated with changes in the orientation of the other. We observed that bulging of the parietal bone is associated with a forward rotation of the base as a block, and taller skulls are associated with a backward rotation of the parietal lobe. These interactions could indicate structural adjustments to maintain the head functional axis. The natural position of the head is that in which the visual axis is parallel to the floor, with the eyes focusing on the horizon (Broca, 1862 cited in Moorrees & Kean, 1958). In this sense, it would be important to study whether the patterns of variation observed in the different studies correspond to the same process, as it would clarify if variation in the proportions of the parietal bone is associated with changes in the functional orientation of the face and orbits.

5.1.5. Craniofacial architecture and functional axis of the orbits

Overall, the two studies within chapter 2 add to the knowledge on the structural relationship between face and neurocranium, further stressing the role of the anterior and middle cranial bases as interfaces (Lieberman et al., 2008; Bastir et al., 2006; Bastir & Rosas, 2006; Bruner & Ripani, 2008; Esteve-Altava et al., 2013). Both studies evidenced that the main patterns of morphological variation within modern humans were associated with the orientation of the orbits (2.1.) and of the base and face as a block (2.2.). The cranial base angle is differently affected by facial and neurocranial size across non-human primates and hominins, decreasing with increasing brain size and increasing with increase in the size of the face (Bastir et al., 2010). Changes in orientation of the orbits also comprised an intra-specific pattern of shape variation in chimpanzees and fossil hominin species (2.1.), further stressing the importance of morphological adjustments to maintain function. A recent study has evidenced that sagittal craniosynostosis and intentional cranial deformations, though comprising different changes in braincase morphology induced similar orbital modification, suggesting a standardized response of the orbital cavity to external mechanical forces (Sandy et al., 2018). In this sense, future investigations the influence of neurocranial morphology on the form and position of the orbit should be taken from a developmental perspective (Marcucio et al., 2011).

In addition, we only considered variation on the sagittal plane, and combined sagittal and parasagittal structures, averaging the position of left and right elements. This approach allowed analyzing lateral and midsagittal structures in two dimensions and reducing the influence of asymmetrical variation. However, it must be acknowledged that these structures are in different planes, and that variation in lateral dimensions also contributes to increase or reduce structural constraint. In fact, the spatial relationship between the orbits and the temporal tips should be further investigated considering the variation in the lateral proportions, in a three-dimensional approach.

5.2. LATERAL PARIETAL LOBE VARIATION ASSESSED THROUGH ENDOCASTS

While the morphology of the parietal bones could be influenced by structural integration with the cranial base and surrounding cranial vault bones, it is generally accepted that, as part of the vault, these are largely moulded by the underlying neural tissues (Moss & Young, 1960; Richtsmeier et al., 2006; Richtsmeier & Flaherty, 2013; Lesciotto & Richtsmeier, 2019; Bruner et al., 2019). This is important considering that parietal bulging is a distinctive feature of modern humans, contributing to the classic neurocranial globular shape that separates modern humans from Neanderthals (Bruner et al., 2003; Neubauer et al., 2009; Gunz et al., 2010). In the absence of the brain, endocasts constitute the only insight on brain architecture from fossil taxa. However, the frequency and clarity of imprints of cortical features on the internal bony tables limits what can be inferred about brain anatomy from endocasts. In chapter 3 we showed parietal lobe morphology can be isolated and assessed on endocasts.

5.2.1. Opposite proportions of parietal and occipital lobes in Cercopithecidae

The degree of expression of cortical sulcal patterns in macaque monkey endocasts is close to that observed in the actual brains (*Macaca fascicularis*; Kobayashi et al., 2014). Hence, brain anatomy can be inferred from monkey endocasts with reasonable reliability. Pioneer studies describing sulcal patterns of Old World monkeys (Cercopithecidae), evidenced differences in the position of the lunate sulcus between the two subfamilies, Colobinae and Cercopithecinae, with the former displaying relatively larger parietal lobes and the latter larger occipital lobes (Connolly, 1950; Radinsky, 1974; Falk, 1978). Our geometrical model, based on the main sulci that define the lobes, was able to separate the Cercopithecid groups according to the previously described opposite parietal and occipital lobe proportions (chapter 3.1.). In fact, we observed that this pattern of morphological variation mainly distinguished between the Colobini and Cercopithecini tribes. Papionini showed a larger range of variation, with geladas and baboons displaying colobin-like proportions, while macaques, mangabeys, and mandrills have intermediate schemes. In addition, we observed size-related shape variations, with the larger-sized baboons exhibiting higher vaults and medio-lateraly inflated parietals, and smaller-sized colobines having flatter cranial vaults.

In sum, larger parietal proportions were displayed by the two colobine genera analyzed, *Colobus* and *Piliocolobus*, and also by *Theropithecus* and *Papio*. Given the distinct ecological and social strategies among these taxa, the larger parietal lobes likely reflect independent traits, not necessarily associated with analogous morphogenetic processes or functions. Nonetheless, it is yet to be determined whether the differences in lobe proportions are due to evolutionary expansion of the occipital cortex in cercopithecini or of the parietal cortex in colobini, *Theropithecus* and *Papio*. Radinsky (1974) identified the colobine sulcal pattern on the 9 million-year-old Mesopithecus, the oldest undoubted cercopithecid, and, based on the fact that prosimians have relatively smaller occipital lobes, he suggested the cercopithecine pattern to be the derived one. Falk (1978) added that cercopithecines seem to have undergone also expansion of prefrontal and inferior temporal association areas.

Considering that the role of the posterior parietal cortex in visuospatial processing, visually guided behavior, and hand dexterity (Grefkes & Fink, 2005; Ross & Martin, 2007; Kravitz et al., 2011), it is intriguing that larger parietal proportions are observed in *Colobus*, which do not show hand dexterity (van Schaik et al., 1999). While hand dexterity is an important topic in primate evolution, since it provides a base-ground for tool use and making, it cannot be directly associated with macroscopic parietal anatomy. Indeed, both cercopithecini and papionini tribes include genera that show high dexterity and tool use for feeding (van Schaik et al., 1999). Interestingly, both *Theropithecus* and *Cebus* seem to have convergently evolved hand proportions similar to those of humans, compatible with opposable thumbs (Almécija et al., 2015; Heldstab et al., 2016). Because evolutionary changes in hand morphology must involve modification to the parietal cortex involved in somatosensory representation of the hand as well as in skilled hand use (Padberg et al., 2007; Almécija & Sherwood, 2017), it would be interesting to compare cortical morphology between taxa with rudimentary thumbs, such as colobines, and dexterous genera with opposable thumbs, like *Theropithecus* and *Cebus*. Although differences probably can only be detected through analyses of cytoarchitecture or functional parcellation, cortical differences between dexterous and non-dexterous species could shed light on parietal changes associated with tool use.

5.2.2. Parietal lobe differences between modern humans and Neanderthals

Due to the rather blurred and smooth surface of human endocasts (Neubauer, 2014), analyses of endocranial shape variation have been based either on cranial references (Bienvenu et al., 2011), or considered the geometry of the endocast as a whole (e.g. Neubauer et al., 2009, 2010; Gunz et al., 2010, 2012). However, these approaches do not allow the delimitation of the parietal lobe, which is essential for determining the contribution of this region to overall endocranial morphology. Our approach, combining landmarks representing cortical impressions that define parietal lobe boundaries with endocranial landmarks and semilandmarks that capture overall brain shape, constitutes the first study addressing the three dimensional morphology of the parietal lobes in modern humans and Neanderthals (chapter 3.2.).

In terms of shape, our results mostly confirm previous studies indicating that the parietal regions of modern humans are dorsally rounder, anteroposteriorly more extended, and vertically more stretched compared to those of Neanderthals (Bruner et al., 2003, 2011; Bruner, 2004, 2010; Gunz et al., 2010, 2012; Neubauer et al., 2010, 2018). In terms of surface area, we observed two main regions within the parietal lobe boundaries that have expanded in modern humans: the posterior dorsal region, towards the parieto-occipital boundary, and the region between the intraparietal sulcus and the supramarginal and angular gyri. The inclusion of parietal cortical references allowed the exposure of changes in parietal surface area, which previous comparisons of general endocranial form were unable to detect (Neubauer et al., 2018). Overall, on average, modern humans display laterally and dorsally stretched, more bulging parietal lobes, that are absolutely larger on the posterior part of the superior parietal lobule and on the interior parietal lobule around the boundary between the supramarginal and angular bosses.

It is worth noting, however, that Neanderthals consistently cluster within one extreme of the modern human distribution, both in terms of shape and size, which could indicate that the observed differences in parietal form may be a matter of degree. In fact, the characteristic modern human globular shape was not displayed by early *Homo sapiens*, but emerged gradually, being established approximately between 100 and 35 thousand years ago (Neubauer et al., 2018). Moreover, it seems that Neanderthal variants of genes involved in neurogenesis and myelination are associated with an elongated neurocranial shape among living European modern humans (Gunz et al., 2019). Because these Neanderthal alleles regulate the expression of other genes involved in neurogenesis and myelination, in the putamen (basal ganglia) and cerebellum, respectively, Gunz and colleagues (2019) suggested these could alter neuroanatomy of some subcortical structures and cerebellum, resulting in lower overall globularity. Interestingly, the patterns of endocranial shape changes observed during the evolution of modern human globularity mimic those previously described during the developmental globularization phase; initial globularization being driven by brain changes and later by integration with facial skeleton (Neubauer et al., 2009, 2018). Our results also point to an expansion in parietal lobe surface area in association with modern human morphotype (chapter 3.2.).

It is clear that globularity is a complex feature, which might result from a combination of changes to different cortical and subcortical components of the brain (Bruner, 2019; Gunz et al., 2019), as well as by structural integration between neurocranium and splanchnocranium (Zollikofer et al., 2017; Scott et al., 2018). The parallel emergence of modern human globularity and archaeological evidence for modern behaviour (Mcbrearty & Brooks, 2000; Neubauer et al., 2018) suggests fundamental cognitive functions must be associated with this neurocranial morphology. The involvement of the parietal cortex in social cognition, language, tool use, and technological extension (Bzdok et al., 2016; Bruner & Iriki, 2016; Goldring & Krubitzer, 2017; Valyear et al., 2017), as well as its implication in general intelligence among humans (Jung & Haier, 2007), make it a region of interest in the context of human brain evolution. The intra-specific variation from globular to Neanderthal-like neurocranial morphology observed within modern humans provides an interesting stage to understand the contribution of different brain components to globularity, particularly, how the parietal lobes differ between these two extremes, and what this might mean in terms of cognition.

5.2.3. On the use of landmarks based on cortical features to quantify parietal lobe variation on endocasts and what can be inferred on brain anatomy

Collectively, the two studies presented in chapter 3 evaluate the use of landmarks based on cortical features to quantify parietal lobe variation on endocasts in order to infer on the evolution of this cortical district. Certainly, it depends on the degree of expression of the cortical features in endocasts. In this sense, the clarity of sulcal imprints observed on macaque endocasts largely facilitates the location of the major lobe boundaries, providing also more reliable results. Indeed, while we were able to isolate the parietal lobe in both studies, the definition of parietal lobe boundaries on cercopithecid endocasts (chapter 3.1.) was more straightforward, since the traces of the sulci were visible, with more or less clarity. Besides, we were able to extract and investigate the surface topology of the parietal lobe separately. There is no question that cortical anatomy of monkeys (Old and New World) can be reliably inferred from their endocasts (Radinksy, 1974; Falk, 1978; Kobayashi et al., 2014; Beaudet et al., 2016). Visibility and identification of the sulci is also simplified by the lower complexity of the sulcal patterns (Connolly, 1950). It must be stressed that the patterns of variation observed in the two studies cannot be compared to each other since parietal lobe homology between human and non-human primates is still largely unknown. First of all, the posterior boundary of the parietal lobe is defined by the lunate sulcus in cercopithecids and by the parieto-occipital sulcus in humans. Moreover, various studies have been investigating the homology of cortical areas defined in macaque and human brains based on cytoarchitecture and function. While homology has already been demonstrated for some cortical areas, even though some of these show a completely different location in humans and macaques, for others homology is yet to be defined (e.g. Impieri et al., 2019).

In contrast to the macaques, humans display a much more complex folding pattern, but the surface of the endocast is rather smooth. This largely hampers a clear-cut location of the parietal lobe boundaries, which can only be estimated based on the surface relieve and surrounding elements, and with respect to the whole structure (Bruner, 2018; Pereira-Pedro & Bruner, 2018). In our comparison of modern human and Neanderthal endocasts (chapter 3.2.), the location of parietal landmarks was performed after detailed analysis of the spatial relationship among the parietal elements and boundaries as observed on the lateral human brain surface. While the placement of these landmarks can only be estimated, even in actual brains (Goméz-Robles, 2018) and the parietal region is especially prone to landmarking uncertainty (Pereira-Pedro & Bruner, 2018), this use of cortical references is the only approach for the definition of parietal lobe boundaries on endocasts. With our combined dataset we were able to detect differences between the two species, although the results must be interpreted within the limitations of endocasts and landmark uncertainty, and should be further confirmed through analysis of parietal variation in form and proportions across extant taxa, based on actual brain morphology.

Large individual variability and low correlation in the spatial relationships between the boundaries of bones and lobes suggest external brain morphology is independent from braincase structural organization, which hampers inferring brain anatomy from endocranial bone subdivisions (Bruner et al., 2015b; Warren et al., 2019). It has even been suggested that neurocranial morphology cannot provide insight on cortical morphology (Warren et al., 2019). Independence between skull and brain development has been previously demonstrated. For example, computational approaches based on network analysis indicate that bone growth and architecture of bone network are sufficient to explain the location of sutures and boundaries between bones on the cranial vault (Esteve-Altava & Rasskin-Gutman, 2014; Esteve-Altava et al., 2017). Similarly, differences in neural tissue densities and mechanical forces at the cellular level seem to be sufficient to explain the location of major cortical convolutions (Tallinen et al., 2016; Kroenke & Bayly, 2018).

Nonetheless, there is still evidence supporting the tight integration between brain and skull during ontogeny, especially provided by studies on craniosynostosis (Aldridge et al., 2002; Richtsmeier et al., 2006). Moreover, in terms of topological and spatial contact, the frontal cortex is less influenced by changes to the posterior cortical districts, probably being more sensitive to intrinsic factors and the surrounding cranial structures (Bruner et al., 2019). Since many genetic networks controlling the development of neural and skeletal tissues are the same, changes in the developmental programs possibly result in concerted changes to both tissues (Richtsmeier & Flaherty, 2013; Lesciotto & Richtsmeier, 2018). Interestingly, the topographic relationship between primary cortical areas and the vault bones that protect them is largely conserved across mammals. The primary motor areas, part of the frontal cortex, are covered by the frontal bone, the primary somatosensory areas of the parietal cortex by the parietal bone, and the primary visual areas of the occipital cortex lie below the occipital bone (O'Leary et al., 2007). While it is not clear whether this arrangement is purely anatomical or if there are developmental or functional implications (Lesciotto & Richtsmeier, 2018), it demonstrates that there is some correspondence in the structural organization of the brain and skull. Besides, variation in spatial relationships does not necessarily falsify general morphological integration (Bruner et al., 2015b).

5.3. ANATOMICAL VARIATION OF THE PRECUNEUS IN HUMANS AND NON-HUMAN PRIMATES

Chapter 4.1 comprises the first analysis of the precuneus as observed on the coronal section. We showed that the subparietal sulcus, which is the inferior boundary of the precuneus, extends more deeply on the anterior and middle portions, being more superficial on the posterior portion. On average, the central portion of the precuneus is about 14 mm deep (infolding of the subparital sulcus) and about 36 mm tall (measured from the subparietal sulcus to the superior surface). In a morphological analysis comprising the precuneus limits and the parietal outer profile as observed on the coronal section we evidenced that vertical extension of the precuneus (increase in height) is associated with changes in the dorsal parietal morphology, which is vertically stretched. This correspondence between inner and outer morphology is relevant for paleoneurology, as morphology of the parietal endocranial surface can give insight on precuneus vertical dimensions in fossil human species.

In addition, our detailed analysis of the folding schemes observed for the subparietal sulcus on the medial brain surface (sagittal plane) showed that this sulcus usually displays additional branches, which tend to reach to the marginal ramus of the cingulate sulcus (anterior limit of the precuneus) or the superior edge of the precuneus. Classification of the sulcal patterns evidenced the complex and irregular nature of the cortical folds, which displayed marked inter-individual and inter-hemispheric variability. We observed that the left hemisphere tends to have more additional sulci reaching the external brain surface and the right hemisphere tends to display deeper folds. Moreover, there seems to be a trade-off in sulcal connections, since sulcal connections with the external surface are less frequent when the subparietal sulcus is linked to the marginal ramus of the cingulate sulcus, and vice versa. While this is only a modest association, such inverse frequency merits further investigation as it could be related to folding mechanisms (see below).

The second study on the precuneus (chapter 4.2.) further signaled the precuneus as the source of midsagittal brain variation among humans, independently of brain size, sex, or ancestry. The results point to the anterior portion of the precuneus as the origin of the anatomical variation, as the changes in precuneus proportions are moderately associated with the size of the anterior and superior areas. This suggests that further studies should consider the contribution of different portions of the precuneus for anatomical variation, especially discriminating between the superior and inferior regions. In fact, the dorsal portion of the precuneus is functionally linked to the primary somatosensory and motor cortices and to the primary visual areas, being involved in visuospatial integration, while the ventral portion is functionally connected to the frontal and cingulate cortices, being enrolled in episodic memory and self representation (Zhang & Li, 2012). In this sense, failure of previous traditional psychometric tests in detecting cognitive differences associated with precuneus proportions (Bruner et al., 2015a), might be due to this segregation of precuneus function. Comparing more specific cognitive capacities, such as those related to visuospatial integration could provide valuable information (Land, 2014; Peer et al., 2015; Bruner & Iriki, 2016). For example, enhanced precuneus connectivity has been reported in professionals of visual arts and musicians compared to controls (de Pisapia et al., 2016; Tanaka & Kirino, 2018).

Our results also showed that larger precuneus proportions tend to have additional folds. Yet, we could not determine whether these are the cause or the consequence of precuneus enlargement. Understanding how folding patterns relate to function is one of the main challenges in neuroanatomy, and requires a multidisciplinary approach combining biology, mathematics, physics, physiology, and histology (Welker, 1990; Goriely et al., 2015). The association between the location of primary folds and the primary cortices and the similarity in folding patterns among closely related species (Zilles et al., 2013), suggest that some aspects of folding might be related to cortical differentiation (Kroenke & Bayly, 2018). While mechanical models have successfully reproduced the location of the primary folds, based on adjustments between volume and surface growth (Tallinen et al., 2016), refinement of the folding mechanisms requires considering interactions at the cellular level (Kroenke & Bayly, 2018).

Our last study (chapter 4.3.), on the midsagittal brain variation among non-human primates indicated that the main pattern involved the general shape of the brain, without apparent changes to precuneus proportions. This main pattern of variation is associated with size, and separated monkeys, which display more elongated shapes, from apes, which have rounder brains. The absence of a patent variation in the precuneus proportions across non-human primates suggests the precuneus expansion in humans does not result from allometric factors, and thus must be a species-specific trait. Nonetheless, although variation in precuneus proportions might not be an interspecific feature, intra-specific variation in relative size was observed within macaques and within chimpanzees, which could indicate precuneus plasticity to be a shared primate trait, becoming more expressed in humans.

5.4. FUTURE DIRECTIONS

One key finding of this work that needs to be further investigated is the seeming mismatch between medial and dorsolateral parietal patterns of variation. In the case of non-human primates, while the dorsolateral proportions of the parietal lobe vary among cercopithecids, especially when comparing the cercopithecini and colobini tribes (chapter 3.1.), there seems to be no inter-specific variation in the precuneus longitudinal proportions across monkeys and apes (chapter 4.3.). In any case, this could be due inter-specific variation since the two studies included different species. However, differences in patterns of parietal lobe extension between dorsolateral and medial surfaces were also observed in modern humans compared to chimpanzees (Bruner et al., 2017) and to Neanderthals (chapter 3.2.). Our comparison of modern human and Neanderthal parietal lobe morphology on endocasts (chapter 3.2.) indicated an expansion of the modern human parietal lobes on the posterior region, towards the parieto-occipital boundary. In contrast, morphological variation of the precuneus in the medial brain surface, within humans as well as between humans and chimpanzees, indicated longitudinal extension on the anterior portion of the precuneus, towards the marginal ramus of the cingulate sulcus (Bruner et al., 2014b; 2015a, 2017; chapter 4.2.). In addition, the anterior and central portions of the precuneus display deeper folding of the subparietal sulcus (chapter 4.1.), which could introduce a further source of plasticity. While the above-mentioned studies compared distinct species and are based on different sample types, it is important to clarify this seemingly opposite directions of parietal lobes expansion, since this might involve changes to distinct integrative functions (Cavanna & Trimble, 2006; Huang et al., 2019). Following Margulies and colleagues (2009), expansion of the anterior region could involve changes to the sensorimotor processing capacity, while expansion of the posterior portion could be associated with changes to visual processing capacity. In this sense, a study of human brain anatomy including both medial and lateral parietal cortices should solve the discrepancy in parietal lobe longitudinal expansion. We have shown that variation in precuneus vertical dimensions is associated with morphological changes to the lateral profile (chapter 4.1.). A three-dimensional analysis of the spatial relationships among the main parietal cortical elements could provide further insight on the patterns of parietal lobe variability and plasticity within humans.

Another aspect that merits further investigation is the outstanding anatomical and morphological variability within modern humans, which has been consistently observed throughout the present work. In this context, one of the most variable structures is the precuneus, both in terms of its longitudinal proportions and sulcal patterns. While this thesis provided more information on anatomical variation within adult humans, we still ignore the causes and consequences of the folding patterns and cortical thickness, as well as their functional significance. Future studies should investigate how the macroanatomical parameters of the precuneus relate to each other and to microanatomical variation as to shed some light on the mechanisms behind neuroanatomical variability and plasticity.

Chapter 6

CONCLUSIONS / CONCLUSIONES

6. CONCLUSIONS

Throughout the research works presented in this PhD dissertation, we investigated morphological relationships and anatomical variation among cranial and cerebral structures in modern humans, fossil hominids, and non-human primates, through the geometric morphometrics analysis of CT and MRI data. The most relevant conclusion obtained in the present thesis are detailed below:

1. The **position of the eye in adult modern humans varies primarily in the horizontal distance from the temporal lobe**/middle cranial fossa. Brain size affects the size and position of the eyeball: **with larger frontal and temporal lobe volumes, the frontal profile is more bulging and the eye is located closer to the temporal lobe**. Since there are no apparent influences of brain size in eyeball shape, our results provide only partial support for the hypothesis that proximity between neurocranium and face in modern humans could constrain development of the eye and orbit and lead to deformation of the eye.

2. The patterns of spatial relationship between orbit and braincase differ within and between species. The main **variation within modern humans concerns the orientation of the orbit relative to the frontal profile**, while the interspecific pattern is driven by the spatial distance between the orbit and the braincase. Chimpanzees display larger, anteriorly projected orbits detached from the braincase, while modern humans have smaller orbits, placed much closer to the braincase, and the fossil humans (Bodo, Broken Hill 1, Gibraltar 1) display intermediate architectures. Compared to chimpanzees and to the fossil human species, **the temporal tips in modern humans are more anteriorly projected, beyond the posterior portion of the orbit**, indicating possible spatial conflict.

3. Within adult modern humans, longitudinal expansion of the parietal bone influences the orientation of the cranial base, with **larger parietal bones being associated with forward rotation of the cranial base as a block**. This pattern of variation also includes facial rotation, suggesting that the dimensions of the parietal bone could influence the **functional orientation of the head**.

4. The main pattern of variation among Old World monkeys (Cercopithecidae) concerns the relative proportions of the parietal and occipital lobes. Cercopithecini display proportionally larger occipital lobes, while Colobini have proportionally larger parietal

lobes. Papionini exhibit a larger range of variation, with *Papio* and *Theropithecus* having enlarged parietal lobes while the remaining taxa display intermediate proportions. While proportionally larger parietal lobes are observed in colobines, *Theropithecus*, and *Papio*, differences in social and ecological strategies among these taxa suggest independent evolution of the lobe proportions.

5. By incorporating landmarks representing parietal lobe boundaries into a dense geometric model, it was possible to **identify previously undetected differences between modern humans and Neanderthals**. Compared to Neanderthals, modern humans display **larger parietal surface areas on the posterior dorsal region**, close to the boundary with the occipital lobe, and on the lateral surface corresponding to a region of the **inferior parietal lobule, between the intraparietal sulcus and the supramarginal and angular gyri**. While the two species differ in the average shape and size, it is noteworthy that **Neanderthals consistently cluster on the lower extreme of the modern human distribution**, suggesting the differences could be in degree.

6. Using landmarks based on cortical elements could provide a new approach to investigate brain anatomy from endocasts, since this constitutes the only way in which the brain districts could be defined. In the case of cercopithecids, isolation of the parietal lobe surface in endocasts is feasible and can be useful to investigate topographical variation. In humans, however, given the lack of cortical references in the surface of endocasts, the **results should be interpreted with caution, keeping in mind that the cortical landmarks only constitute estimations of the location of the elements they represent**.

7. On average, **the central portion of the precuneus in humans is about 14 mm deep** (inward extension of the subparietal sulcus) and about **36 mm tall** (measured from the subparietal sulcus to the superior surface). There is a morphological relationship between the precuneus vertical dimension and the lateral parietal outline, as assessed on a coronal section cutting through the central portion of the precuneus, with **increase in precuneus height being associated with vertical stretching of the upper parietal profile**. This is fundamental for paleoneurology in the sense that morphology of the outer structures can be used for assessing changes to the internal elements.

8. The subparietal sulcus, which constitutes the inferior limit of the precuneus, **extends more inwards on the anterior and central portions of the precuneus**, constituting a more superficial fold on the posterior part. This sulcus usually reaches the marginal ramus of the cingulate sulcus (anterior precuneus limit) and commonly displays additional branches that frequently reach the dorsal brain surface. The left hemisphere

seems to display more additional sulci reaching the external brain surface and the right hemisphere has deeper folds.

9. Changes in the longitudinal proportions of the precuneus within adult modern humans are associated with corresponding **variation in its supero-anterior portion**. This suggests that different subdivisions of the precuneus should be considered separately. Longitudinally more extended precuneus tend to have additional folds.

10. Dilation of the precuneus is not a consequence of interspecific variation across non-human primates, suggesting **human antero-posterior expansion is not due to allometry and must be a species-specific characteristic**. Nonetheless, intra-specific variation in precuneus size within chimpanzees and Rhesus monkeys suggests precuneus plasticity could be an intra-specific trait shared among primates.

6. CONCLUSIONES

Mediante los trabajos de investigación presentados en esta tesis doctoral, investigamos las relaciones morfológicas y la variación anatómica entre las estructuras craneales y cerebrales en humanos modernos, homínidos fósiles y primates no humanos, a través del análisis de morfometria geométrica de muestras de tomografía computarizada y resonancia magnética. A continuación se detallan las conclusiones más relevantes obtenidas en la presente tesis doctoral:

1. La **posición del ojo en humanos modernos adultos varía principalmente en la distancia horizontal al lóbulo temporal** / fosa craneal media. El tamaño del cerebro afecta al tamaño y a la posición del globo ocular: **con el aumento de los volúmenes de los lóbulos frontal y temporal, el perfil frontal es más abultado y el ojo se encuentra más cerca del lóbulo temporal**. Dado que no hay influencias aparentes del tamaño del cerebro en la forma del globo ocular, nuestros resultados proporcionan un apoyo parcial a la hipótesis de que la proximidad entre cara y neurocráneo en humanos modernos podría restringir el desarrollo del ojo y de la órbita y conducir a la deformación del ojo.

2. Los patrones de relación espacial entre la órbita y el cráneo difieren a nivel intra- e inter-específico. **El principal patrón de variación dentro de los humanos modernos está relacionado con la orientación de la órbita en relación al perfil frontal**, mientras que el patrón inter-específico describe la distancia espacial entre la órbita y el endocráneo. Los chimpancés tienen órbitas más grandes y proyectadas anteriormente, separadas del endocráneo. Los humanos modernos, por su parte, tienen órbitas más pequeñas y encajadas bajo el endocráneo, mientras que especies humanas extintas (Bodo, Broken Hill 1, Gibraltar 1) tienen morfologías intermedias. En comparación con los chimpancés y las especies humanas fósiles, **los polos temporales en los humanos modernos tienen una proyección más anterior, más allá de la parte posterior de la órbita**, lo que indica un posible conflicto espacial.

3. Entre los humanos modernos adultos, la expansión longitudinal del hueso parietal influye en la orientación de la base craneal, de forma que **huesos parietales más grandes están asociados a una rotación en bloque de la base craneal hacia adelante**. Este patrón de variación también incluye rotación facial, lo que sugiere que las dimensiones del hueso parietal podrían influir en la **orientación funcional de la cabeza**.

4. El principal patrón de variación entre monos del Viejo Mundo (Cercopithecidae), que

describe las **proporciones relativas de los lóbulos parietales y occipitales**. Cercopithecini muestra lóbulos occipitales proporcionalmente más grandes, Colobini presenta lóbulos parietales proporcionalmente más grandes. Papionini muestra un mayor rango de variación, con *Papio* y *Theropithecus* mostrando proporciones semejantes a las de colobines y los taxones restantes proporciones intermedias. Aunque lóbulos parietales proporcionalmente más grandes se observan en colobines, *Theropithecus* y *Papio*, las diferencias en las estrategias sociales y ecológicas entre estos taxones sugieren una evolución independiente de las proporciones de los lóbulos.

5. Al incorporar puntos de referencia que representan los límites del lóbulo parietal en un modelo geométrico denso, fue posible **identificar diferencias previamente no detectadas entre humanos modernos y neandertales**. En comparación con los neandertales, los humanos modernos muestran **un aumento del área de la superficie parietal en la región dorsal posterior**, próxima al límite con el lóbulo occipital, así como un aumento en la superficie lateral correspondiente a una región del **lóbulo parietal inferior, entre el surco intraparietal y las convoluciones supramarginal y angular**. Aunque las dos especies difieren en los valores promedios, **los neandertales se agrupan de forma consistente en el extremo inferior de la distribución humana** moderna, tanto en tamaño como en forma, lo que sugiere que las diferencias podrían ser una cuestión de grado.

6. El uso de puntos de referencia basados en elementos corticales podría proporcionar un nuevo enfoque para investigar la anatomía del cerebro a partir de moldes endocraneales, ya que es la única forma en que se pueden definir los distritos cerebrales en el endocráneo. En el caso de los cercopitécidos, el aislamiento de la superficie del lóbulo parietal en moldes endocraneales de es factible y puede ser útil para investigar la variación topográfica. En humanos, sin embargo, dada la falta de referencias corticales en la superficie de los moldes endocraneales, **los resultados deben interpretarse con precaución, teniendo en cuenta que los puntos de referencia corticales solo constituyen estimaciones de la posición de los elementos que representan**.

7. En promedio, la porción central del precúneo en humanos tiene aproximadamente **14 mm de profundidad** (extensión interna del surco subparietal) y aproximadamente **36 mm de altura** (medida desde el surco subparietal hasta la superficie superior). Existe una relación morfológica entre la dimensión vertical del precúneo y el contorno dorsal del parietal, según se evalúa en una sección coronal que corta a través de la porción central del precúneo. Asimismo, **un aumento en la altura del precúneo está asociado a un estiramiento vertical del perfil dorsal del parietal**. Esta relación es fundamental para la paleoneurología en el sentido de que la morfología de las estructuras externas se puede utilizar para evaluar los cambios en los elementos internos.

8. El surco subparietal, que constituye el límite inferior del precúneo, **se extiende más hacia el interior en las porciones anterior y central de este elemento parietal**, constituyendo un pliegue más superficial en la parte posterior. Este surco generalmente alcanza la rama marginal del surco cingulado (límite anterior del precúneo) y normalmente tiene ramas adicionales que con frecuencia alcanzan la superficie dorsal del cerebro. El hemisferio izquierdo tiene más surcos adicionales que alcancen la superficie externa del cerebro y el derecho pliegues más profundos.

9. Los cambios en la proporción longitudinal del precúneo en humanos adultos están asociados a **variaciones correspondientes en su porción superior y anterior.** Esto sugiere que diferentes subdivisiones del precúneo deben ser consideradas por separado. La extensión longitudinal del precúneo está asociada a la existencia de pliegues adicionales.

10. La dilatación del precúneo no constituye una variación inter-específica entre primates no humanos. Esto sugiere que **la expansión anteroposterior en humanos no se debe a efectos alométricos, sino que debe ser una característica específica de la especie**. Sin embargo, la variación intra-específica en el tamaño del precúneo observada en chimpancés y macacos Rhesus sugiere que la plasticidad del precúneo podría ser un rasgo intra-específico compartido entre los primates.

Chapter 7

REFERENCES

7. REFERENCES

Adams, D.C., Rohlf, F.J., Slice, D.E., 2004. Geometric morphometrics: ten years of progress following the 'revolution.' *Italian Journal of Zoology,* 71, 5–16.

Aldridge, K., 2011. Patterns of differences in brain morphology in humans as compared to extant apes. *Journal of Human Evolution*, 60, 94–105.

Aldridge, K., Marsh, J.L., Govier, D., Richtsmeier, J.T., 2002. Central nervous system phenotypes in craniosynostosis. *Journal of Anatomy*, 201, 31–39.

Almécija, S., Sherwood, C.C., 2017. Hands, brains, and precision grips: origins of tool use behaviors. In: Kaas, J.H. (Ed.), *Evolution of nervous systems* (pp. 299–315) Oxford, UK: Elsevier.

Almécija, S., Smaers, J.B., Jungers, W.L., 2015. The evolution of human and ape hand proportions. *Nature Communications*, 6, 7717.

Atchison, D.A., Jones, C.E., Schmid, K.L., Pritchard, N., Pope, J.M., Strugnell, W.E., Riley, R.A., 2004. Eye shape in emmetropia and myopia. *Investigative Ophthalmology & Visual Science*, 45, 3380.

Barton, R.A., Harvey, P.H., 2000. Mosaic evolution of brain structure in mammals. *Nature*, 405, 1055–1058.

Barton, R.A., Venditti, C., 2013. Human frontal lobes are not relatively large. *Proceedings of the National Academy of Sciences of the United States of America*, 110, 9001–9006.

Bastir, M., Rosas, A., 2005. Hierarchical nature of morphological integration and modularity in the human posterior face. *American Journal of Physical Anthropology*, 128, 26–34.

Bastir, M., Rosas, A., 2006. Correlated variation between the lateral basicranium and the face: a geometric morphometric study in different human groups. *Archives of Oral Biology*, 51, 814–824.

Bastir, M., Rosas, A., 2009. Mosaic evolution of the basicranium in *Homo* and its relation to modular development. *Evolutionary Biology*, 36, 57–70.

Bastir, M., Rosas, A., 2016. Cranial base topology and basic trends in the facial evolution of *Homo*. *Journal of Human Evolution*, 91, 26–35.

Bastir, M., Rosas, A., Kuroe, K., 2004. Petrosal orientation and mandibular ramus breadth: evidence for an integrated petroso-mandibular developmental unit. *American Journal of Physical Anthropology*, 123, 340–350.

Bastir, M., Rosas, A., O'Higgins, P., 2006. Craniofacial levels and the morphological maturation of the human skull: Spatiotemporal pattern of cranial ontogeny. *Journal of Anatomy*, 209, 637–654.

Bastir, M., Rosas, A., Lieberman, D.E., O'Higgins, P., 2008. Middle cranial fossa anatomy and the origin of modern humans. *Anatomical Record*, 291, 130–140.

Bastir, M., Rosas, A., Stringer, C., Cuétara, J.M., Kruszynski, R., Weber, G.W., Ross, C.F., Ravosa, M.J., 2010. Effects of brain and facial size on basicranial form in human and primate evolution. *Journal of Human Evolution*, 58, 424–431.

Beaudet, A., Bruner, E., 2017. A frontal lobe surface analysis in three African human fossils: OH 9, Buia, and Bodo. *Comptes Rendus Palevol*, 16, 499–507.

Beaudet, A., Dumoncel, J., de Beer, F., Duployer, B., Durrleman, S., Gilissen, E., Hoffman, J., Tenailleau, C., Thackeray, J.F., Braga, J., 2016. Morphoarchitectural variation in South African fossil cercopithecoid endocasts. *Journal of Human Evolution*, 101, 65–78.

Bhatti, S., Paysse, E.A., Weikert, M.P., Kong, L., 2016. Evaluation of structural contributors in myopic eyes of preterm and full-term children. *Graefe's Archive for Clinical and Experimental Ophthalmology*, 254, 957–962.

Bienvenu, T., Guy, F., Coudyzer, W., Gilissen, E., Roualdès, G., Vignaud, P., Brunet, M., 2011. Assessing endocranial variations in great apes and humans using 3D data from virtual endocasts. *American Journal of Physical Anthropology*, 145, 231–246.

Bookstein, F.L., 1996. Biometrics, Biomathematics and the Morphometric synthesis. *Bulletin of Mathematical Biology*, 58, 313–365.

Bookstein, F.L., 1997. Landmark methods for forms without landmarks: morphometrics of group differences in outline shape. *Medical Image Analysis*, 1, 225–243.

Bookstein, F.L., Gunz, P., Mitterœcker, P., Prossinger, H., Schæfer, K., Seidler, H., 2003. Cranial integration in *Homo*: singular warps analysis of the midsagittal plane in ontogeny and evolution. *Journal of Human Evolution*, 44, 167–187.

Brown, P., Maeda, T., 2004. Post-Pleistocene diachronic change in East Asian facial skeletons: the size, shape and volume of the orbits. *Journal of Anthropological Sciences*, 112, 29–40.

Bruner, E., 2003. Fossil traces of the human thought: paleoneurology and the evolution of the genus *Homo*. *Journal of Anthropological Sciences*, 81, 29–56.

Bruner, E., 2004. Geometric morphometrics and paleoneurology: brain shape evolution in the genus *Homo*. Journal of Human Evolution 47, 279–303.

Bruner, E., 2007. Cranial shape and size variation in human evolution: structural and functional perspectives. *Child's Nervous System*, 23, 1357–1365.

Bruner, E., 2010. Morphological differences in the parietal lobes within the human genus: a neurofunctional perspective. *Current Anthropology*, 51, S77–S88.

Bruner, E., 2018. The brain, the braincase, and the morphospace. In: Bruner, E., Ogihara, N., Tanabe, H.C. (Eds.), *Digital endocasts: from skulls to brains* (pp. 93–114). Tokyo, Japan: Springer.

Bruner, E., 2019. Human paleoneurology: shaping cortical evolution in fossil hominids. *Journal of Comparative Neurology*, 527, 1753-1765.

Bruner, E., Holloway, R.L., 2010. A bivariate approach to the widening of the frontal lobes in the genus *Homo*. *Journal of Human Evolution*, 58, 138–146.

Bruner, E., Iriki, A., 2016. Extending mind, visuospatial integration, and the evolution of the parietal lobes in the human genus. *Quaternary International*, 405, 98–110.

Bruner, E., Jacobs, H.I.L., 2013. Alzheimer's disease: the downside of a highly evolved parietal lobe? *Journal of Alzheimer's Disease*, 35, 227–240.

Bruner, E., Ripani, M., 2008. A quantitative and descriptive approach to morphological variation of the endocranial base in modern humans. *American Journal of Physical Anthropology*, 137, 30–40.

Bruner, E., Sherkat, S., 2008. The middle meningeal artery: from clinics to fossils. *Child's Nervous System*, 24, 1289–1298.

Bruner, E., Manzi, G., Arsuaga, J.L., 2003. Encephalization and allometric trajectories in the genus *Homo*: evidence from the Neandertal and modern lineages. *Proceedings of the National Academy of Sciences of the United States of America*, 100, 15335–15340.

Bruner, E., Saracino, B., Ricci, F., Tafuri, M., Passarello, P., Manzi, G., 2004. Midsagittal cranial shape variation in the genus *Homo* by geometric morphometrics. Coll Antropol 28, 99–112.

Bruner, E., Mantini, S., Perna, A., Maffei, C., Manzi, G., 2005. Fractal dimension of the middle meningeal vessels: variation and evolution in *Homo erectus*, Neanderthals, and modern humans. *European Journal of Morphology*, 42, 217–224.

Bruner, E., Mantini, S., Ripani, M., 2009. Landmark-based analysis of the morphological relationship between endocranial shape and traces of the middle meningeal vessels. *Anatomical Record*, 292, 518–527.

Bruner, E., Martin-Loeches, M., Colom, R., 2010. Human midsagittal brain shape variation: patterns, allometry and integration. *Journal of Anatomy*, 216, 589–599.

Bruner, E., De La Cuétara, J.M., Holloway, R., 2011. A bivariate approach to the variation of the parietal curvature in the genus *Homo*. *Anatomical Record*, 294, 1548–1556.

Bruner, E., De La Cuétara, J.M., Musso, F., 2012. Quantifying patterns of endocranial heat distribution: brain geometry and thermoregulation. *American Journal of Human Biology*, 24, 753–762.

Bruner, E., Athreya, S., de la Cuétara, J.M., Marks, T., 2013. Geometric variation of the frontal squama in the genus *Homo*: frontal bulging and the origin of modern human morphology. *American Journal of Physical Anthropology*, 150, 313–323.

Bruner, E., De la Cuétara, J.M., Masters, M., Amano, H., Ogihara, N., 2014a. Functional craniology and brain evolution: from paleontology to biomedicine. *Frontiers in Neuroanatomy*, 8, 19.

Bruner, E., Rangel de Lázaro, G., de la Cuétara, J.M., Martín-Loeches, M., Colom, R., Jacobs, H.I.L., 2014b. Midsagittal brain variation and MRI shape analysis of the precuneus in adult individuals. *Journal of Anatomy*, 224, 367–376.

Bruner, E., Román, F.J., de la Cuétara, J.M., Martin-Loeches, M., Colom, R., 2015a. Cortical surface area and cortical thickness in the precuneus of adult humans. *Neuroscience*, 286, 345–352.

Bruner, E., Amano, H., de la Cuétara, J.M., Ogihara, N., 2015b. The brain and the braincase: a spatial analysis on the midsagittal profile in adult humans. *Journal of Anatomy*, 227, 268–276.

Bruner, E., Preuss, T.M., Chen, X., Rilling, J.K., 2017. Evidence for expansion of the precuneus in human evolution. *Brain Structure & Function*, 222, 1053–1060.

Bruner, E., Esteve-Altava, B., Rasskin-Gutman, D., 2019. A network approach to brain form, cortical topology and human evolution. *Brain Structure & Function*, 224, 2231.

Buckner, R.L., Sepulcre, J., Talukdar, T., Krienen, F.M., Liu, H., Hedden, T., Andrews-Hanna, J.R., Sperling, R.A., Johnson, K.A., 2009. Cortical hubs revealed by intrinsic functional connectivity: mapping, assessment of stability, and relation to Alzheimer's disease. *Journal of Neuroscience*, 29, 1860–1873.

Bzdok, D., Hartwigsen, G., Reid, A., Laird, A.R., Fox, P.T., Eickhoff, S.B., 2016. Left inferior parietal lobe engagement in social cognition and language. *Neuroscience & Biobehavioral Reviews*, 68, 319–334.

Caldemeyer, K.S., Buckwalter, K.A., 1999. The basic principles of computed tomography and magnetic resonance imaging. *Journal of the American Academy of Dermatology*, 41, 768–771.

Caminiti, R., Chafee, M.V., Battaglia-Mayer, A., Averbeck, B.B., Crowe, D.A., Georgopoulos, A.P., 2010. Understanding the parietal lobe syndrome from a neurophysiological and evolutionary perspective. *European Journal of Neuroscience*, 31, 2320–2340.

Campero, A., Ajler, P., Emmerich, J., Goldschmidt, E., Martins, C., Rhoton, A., 2014. Brain sulci and gyri: A practical anatomical review. Journal of Clinical Neuroscience 21, 2219–2225.

Cartmill, M., 1980. Morphology, function, and evolution of the anthropoid postorbital septum. In: Ciochon, R.L., Chiarelli, A.B. (Eds.), *Evolutionary biology of the New World monkeys and continental drift, advances in primatology* (pp. 243–274). Boston, MA: Springer.

Caspers, S., Zilles, K. 2018. Microarchitecture and connectivity of the parietal lobe. In: Vallar, H., Coslett, H.B., (Eds), *The parietal lobe, handbook of clinical neurology*, (pp. 53-72). Amsterdam, The Netherlands: Elsevier.

Caspers, S., Zilles, K., Laird, A.R., Eickhoff, S.B., 2010. ALE meta-analysis of action observation and imitation in the human brain. *NeuroImage*, 50, 1148–1167.

Cavanna, A.E., Trimble, M.R., 2006. The precuneus: a review of its functional anatomy and behavioural correlates. *Brain*, 129, 564–583.

Cheng, H.M., Singh, O.S., Kwong, K.K., Xiong, J., Woods, B.T., Brady, T.J., 1992. Shape of the myopic eye as seen with high-resolution magnetic resonance imaging. *Optometry and Vision Science*, 69, 698–701.

Chervenak, F.A., Jeanty, P., Cantraine, F., Chitkara, U., Venus, I., Berkowitz, R.L., Hobbins, J.C., 1984. The diagnosis of fetal microcephaly. *American Journal of Obstetrics and Gynecology*, 149, 512–517.

Cheverud, J.M., 1996. Developmental integration and the evolution of pleiotropy. *American Zoologist*, 36, 44–50.

Chi, J.G., Dooling, E.C., Gilles, F.H., 1977. Gyral development of the human brain. *Annals of Neurology*, 1, 86–93.

Cieri, R.L., Churchill, S.E., Franciscus, R.G., Tan, J., Hare, B., 2014. Craniofacial feminization, social tolerance, and the origins of behavioral modernity. *Current Anthropology*, 55, 419–443.

Cole, M.W., Pathak, S., Schneider, W., 2010. Identifying the brain's most globally connected regions. *NeuroImage*, 49, 3132–3148.

Connolly, C.J., 1950. *External morphology of the primate brain*. Springfield, IL, USA: Charles C. Thomas.

De Pisapia, N., Bacci, F., Parrott, D., Melcher, D., 2016. Brain networks for visual creativity: a functional connectivity study of planning a visual artwork. *Scientific Reports*, 6, 39185.

de Sousa, A.A., Sherwood, C.C., Mohlberg, H., Amunts, K., Schleicher, A., MacLeod, C.E., Hof, P.R., Frahm, H., Zilles, K., 2010. Hominoid visual brain structure volumes and the position of the lunate sulcus. *Journal of Human Evolution*, 58, 281–292.

Deschamps, I., Baum, S.R., Gracco, V.L., 2014. On the role of the supramarginal gyrus in phonological processing and verbal working memory: evidence from rTMS studies. *Neuropsychologia*, 53, 39–46.

Detorakis, E.T., Drakonaki, E., Papadaki, E., Pallikaris, I.G., Tsilimbaris, M.K., 2010. Effective orbital volume and eyeball position: an MRI study. *Orbit*, 29, 244–249.

Eidelberg D, Galaburda AM, 1984. Inferior parietal lobule: divergent architectonic asymmetries in the human brain. *Archives of Neurology*, 41, 843–852.

Enlow, D.H. 1968. *The human face: an account of the postnatal growth and development of the craniofacial skeleton*. New York, USA: Harper & Row, Publishers.

Enlow, D.H. 1990. *Facial growth*. Philadelphia, USA: Sounders.

Esteve-Altava, B., Rasskin-Gutman, D., 2014. Beyond the functional matrix hypothesis: a network null model of human skull growth for the formation of bone articulations. *Journal of Anatomy*, 225, 306–316.

Esteve-Altava, B., Marugán-Lobón, J., Botella, H., Bastir, M., Rasskin-Gutman, D., 2013. Grist for Riedl's mill: a network model perspective on the integration and modularity of the human skull. *Journal of Experimental Zoology Part B: Molecular and Developmental Evolution*, 320, 489–500.

Esteve-Altava, B., Vallès-Català, T., Guimerà, R., Sales-Pardo, M., Rasskin-Gutman, D., 2017. Bone fusion in normal and pathological development is constrained by the network architecture of the human skull. *Scientific Reports*, 7, 1–7.

Falk, D., 1978. Brain evolution in Old World monkeys. *American Journal of Physical*

Anthropology, 48, 315–319.

Falk, D., 2015. Evolution of the primate brain. In: Henke W., Tattersall I. (Eds), *Handbook of Paleoanthropology* (pp. 1495-1525). Berlin, Germany: Springer.

Finlay, B.L., Darlington, R.B., 1995. Linked regularities in the development and evolution of mammalian brains. *Science*, 268, 1578–1584.

Fox, M.D., Snyder, A.Z., Vincent, J.L., Corbetta, M., Essen, D.C.V., Raichle, M.E., 2005. The human brain is intrinsically organized into dynamic, anticorrelated functional networks. *Proceedings of the National Academy of Sciences of the United States of America*, 102, 9673–9678.

Flaherty, K., Singh, N., Richtsmeier, J.T., 2016. Understanding craniosynostosis as a growth disorder. *Wiley Interdisciplinary Reviews: Developmental Biology*, 5, 429–459.

Fredrick, D.R., 2002. Myopia. *The BMJ*, 324, 1195–1199.

Friede, H., 1981. Normal Development and growth of the human neurocranium and cranial base. *Scandinavian Journal of Plastic and Reconstructive Surgery*, 15, 163–169.

Fuster, J.M., 2014. The prefrontal cortex makes the brain a preadaptive system. *Proceedings of the IEEE*, 102, 417–426.

Godinho, R.M., Spikins, P., O'Higgins, P., 2018. Supraorbital morphology and social dynamics in human evolution. *Nature Ecology & Evolution*, 2, 956–961.

Goldman-Rakic, P.S., 1988. Topography of cognition: parallel distributed networks in primate association cortex. *Annual Review of Neuroscience*, 11, 137-156.

Goldring, A.B., Krubitzer, L.A., 2017. Evolution of parietal cortex in mammals: from manipulation to tool use. In: Kaas, J.H. (Ed.), *Evolution of nervous systems* (pp. 259–286). Oxford, UK: Elsevier.

Goldschmidt, E., Fledelius, H.C., 2011. Clinical features in high myopia: a Danish cohort study of high myopia cases followed from age 14 to age 60. *Acta Ophthalmologica*, 89, 97–98.

Gómez-Robles, A., Reyes, L., Sherwood, C.C. 2018. Landmarking brains. In: Bruner, E., Ogihara, N., Tanabe, H.C. (Eds.), *Digital endocasts: from skulls to brains* (pp. 115-126). Tokyo, Japan: Springer.

González Blanco, F., Sanz Ferńandez, J.C., Muńoz Sanz, M.A., 2008. Axial length, corneal radius, and age of myopia onset. *Optometry and Vision Science*, 85, 89–96.

Goriely, A., Geers, M.G.D., Holzapfel, G.A., Jayamohan, J., Jérusalem, A., Sivaloganathan, S., Squier, W., van Dommelen, J.A.W., Waters, S., Kuhl, E., 2015. Mechanics of the brain: perspectives, challenges, and opportunities. *Biomechanics and Modeling in Mechanobiology*, 14, 931–965.

Goss, D.A., Cox, V.D., Herrin-Lawson, G.A., Nielsen, E.D., Dolton, W.A., 1990. Refractive error, axial length, and height as a function of age in young myopes. *Optometry and Vision Science*, 67, 332–338.

Gould, S.J., 1977. *Ontogeny and Phylogeny*. Cambridge, Massachusetts: Belknap Press of Harvard University Press.

Gower, J.C., 1975. Generalized Procrustes analysis. *Psychometrika*, 40, 33–51.

Grefkes, C., Fink, G.R., 2005. The functional organization of the intraparietal sulcus in humans and monkeys. *Journal of Anatomy*, 207, 3–17.

Gunz, P., Harvati, K., 2007. The Neanderthal "chignon": variation, integration, and homology. *Journal of Human Evolution*, 52, 262–274.

Gunz, P., Mitterœcker, P., 2013. Semilandmarks: a method for quantifying curves and surfaces. *Hystrix, the Italian Journal of Mammalogy*, 24, 103–109.

Gunz, P., Mitteroecker, P., Bookstein, F.L., 2005. Semilandmarks in three dimensions. In: Slice, D.E. (Ed.), *Modern morphometrics in physical Anthropology* (pp. 73–98). New York, NY: Springer.

Gunz, P., Neubauer, S., Maureille, B., Hublin, J.-J., 2010. Brain development after birth differs between Neanderthals and modern humans. *Current Biology*, 20, R921–R922.

Gunz, P., Neubauer, S., Golovanova, L., Doronichev, V., Maureille, B., Hublin, J.-J., 2012. A uniquely modern human pattern of endocranial development. Insights from a new cranial reconstruction of the Neandertal newborn from Mezmaiskaya. *Journal of Human Evolution*, 62, 300–313.

Gunz, P., Tilot, A.K., Wittfeld, K., Teumer, A., Shapland, C.Y., van Erp, T.G.M., Dannemann, M., Vernot, B., Neubauer, S., Guadalupe, T., Fernández, G., Brunner, H.G., Enard, W., Fallon, J., Hosten, N., Völker, U., Profico, A., Di Vincenzo, F., Manzi, G., Kelso, J., St. Pourcain, B., Hublin, J.-J., Franke, B., Pääbo, S., Macciardi, F., Grabe, H.J., Fisher, S.E., 2019. Neandertal introgression sheds light on modern human endocranial globularity. *Current Biology*, 29, 120-127.e5.

Hagmann, P., Cammoun, L., Gigandet, X., Meuli, R., Honey, C.J., Wedeen, V.J., Sporns, O., 2008. Mapping the structural core of human cerebral cortex. *PLOS Biology*, 6, e159.

Hallgrímsson, B., Lieberman, D.E., Liu, W., Ford-Hutchinson, A.F., Jirik, F.R., 2007. Epigenetic interactions and the structure of phenotypic variation in the cranium: epigenetic interactions in the cranium. *Evolution & Development*, 9, 76–91.

Heldstab, S.A., Kosonen, Z.K., Koski, S.E., Burkart, J.M., van Schaik, C.P., Isler, K., 2016. Manipulation complexity in primates coevolved with brain size and terrestriality. *Scientific Reports*, 6, 24528.

Hofman, M.A., 2012. Design principles of the human brain. In: Falk, D., Hofman, M. A. (Eds.), *Evolution of the primate brain* (pp. 373–390). Oxford, UK: Elsevier.

Hofman, M.A., 2014. Evolution of the human brain: when bigger is better. *Frontiers in Neuroanatomy*, 8, 15.

Holloway, R.L., 1975. *The role of human social behavior in the evolution of the brain* (James Arthur lecture on the evolution of the human brain, no. 43, 1973), New York: The American Museum of Natural History.

Holloway, R.L., 2015. The evolution of the hominid brain. In: Henke W., Tattersall I. (Eds.) *Handbook of Paleoanthropology* (pp. 1961-1987). Berlin, Germany: Springer.

Holloway, R.L., Broadfield, D.C., Yuan, M.S., 2004. *The human fossil record: brain endocasts - the paleoneurological evidence*. John Wiley & Sons.

Holloway R.L., Sherwood C.C., Hof P.R., Rilling J.K. 2009. Evolution of the brain in humans: Paleoneurology. Binder M.D., Hirokawa N., Windhorst U. (Eds.), *Encyclopedia of Neuroscience* (pp. 1326-1334). Berlin, Germany: Springer.

Huang, Y., Hullfish, J., De Ridder, D., Vanneste, S., 2019. Meta-analysis of functional subdivisions within human posteromedial cortex. *Brain Structure & Function*, 224, 435–452.

Husain, M., Nachev, P., 2007. Space and the parietal cortex. *Trends in Cognitive Sciences*, 11, 30–36.

Impieri, D., Zilles, K., Niu, M., Rapan, L., Schubert, N., Galletti, C., Palomero-Gallagher, N., 2019. Receptor density pattern confirms and enhances the anatomic-functional features of the macaque superior parietal lobule areas. *Brain Structure & Function*, 224, 2733–2756.

Iriki, A., 2006. The neural origins and implications of imitation, mirror neurons and tool use. *Current Opinion in Neurobiology*, 16, 660–667.

Jiang, X., Iseki, S., Maxson, R.E., Sucov, H.M., Morriss-Kay, G.M., 2002. Tissue origins and interactions in the mammalian skull vault. *Developmental Biology*, 241, 106–116.

Jolliffe, I.T., 2002. *Principal Component Analysis*. New York: Springer.

Judas, M., Cepanec, M., Sedmak, G., 2012. Brodmann's map of the human cerebral cortex — or Brodmann's maps? *Translational Neuroscience*, 3, 67-74.

Jung, R.E., Haier, R.J., 2007. The Parieto-Frontal Integration Theory (P-FIT) of intelligence: converging neuroimaging evidence. *Behavioral and Brain Sciences*, 30, 135–154.

Kaas, J.H., 2000. Why is brain size so important: design problems and solutions as neocortex gets bigger or smaller. *Brain and Mind*, 1, 7-23.

Karbowski, J., 2001. Optimal wiring principle and plateaus in the degree of separation for cortical neurons. *Physical Review Letters*, 86, 3674–3677.

Karbowski, J., 2009. Thermodynamic constraints on neural dimensions, firing rates, brain temperature and size. *Journal of Computational Neuroscience*, 27, 415–436.

Kendall, D. G. 1977. The diffusion of shape. *Advances in Applied Probability*, 9, 428430.

Klingenberg, C.P., 1998. Heterochrony and allometry: the analysis of evolutionary change in ontogeny. *Biological Reviews*, 73, 79–123.

Klingenberg, C.P., 2008. Morphological integration and developmental modularity. *Annual Review of Ecology, Evolution, and Systematics*, 39, 115–132.

Klingenberg, C.P., 2009. Morphometric integration and modularity in configurations of landmarks: tools for evaluating a priori hypotheses. *Evolution & Development*, 11, 405–421.

Klingenberg, C.P., 2013. Cranial integration and modularity: insights into evolution and development from morphometric data. *Hystrix, the Italian Journal of Mammalogy*, 24, 43–58.

Klingenberg, C.P., 2014. Studying morphological integration and modularity at multiple levels: concepts and analysis. *Philosophical Transactions of the Royal Society B: Biological Sciences,* 369, 20130249.

Kobayashi, Y., Matsui, T., Haizuka, Y., Ogihara, N., Hirai, N., Matsumura, G., 2014. Cerebral sulci and gyri observed on macaque endocasts. In: Akazawa, T., Ogihara, N., Tanabe, H.C., Terashima, H. (Eds.), *Dynamics of Learning in Neanderthals and Modern Humans* (pp. 131–137). Tokyo, Japan: Springer.

Kornack, D.R., Rakic, P., 2001. Cell proliferation without neurogenesis in adult primate neocortex. *Science*, 294, 2127–2130.

Kravitz, D.J., Saleem, K.S., Baker, C.I., Mishkin, M., 2011. A new neural framework for visuospatial processing. *Nature Reviews Neuroscience*, 12, 217–230.

Kroenke, C.D., Bayly, P.V., 2018. How forces fold the cerebral cortex. *The Journal of Neuroscience*, 38, 767–775.

Lacruz, R.S., Stringer, C.B., Kimbel, W.H., Wood, B., Harvati, K., O'Higgins, P., Bromage, T.G., Arsuaga, J.-L., 2019. The evolutionary history of the human face. *Nature Ecology & Evolution*, 3, 726–736.

Land, M.F., 2014. Do we have an internal model of the outside world? *Philosophical Transactions of the Royal Society B: Biological Sciences,* 369, 20130045–20130045.

Lang, J., 2012. *Clinical anatomy of the head: neurocranium, orbit, craniocervical regions*. Berlin, Germany: Springer-Verlag.

Leonard, W.R., Snodgrass, J.J., Robertson, M.L., 2007. Effects of brain evolution on human nutrition and metabolism. *Annual Review of Nutrition*, 27, 311–327.

Lesciotto, K.M., Richtsmeier, J.T., 2019. Craniofacial skeletal response to encephalization: how do we know what we think we know? *Yearbook of Physical Anthropology*, 168, 27–46.

Lieberman, D.E., 2011. *The evolution of the human head.* Cambridge, USA: Harvard University Press.

Lieberman, D.E., McCarthy, R.C., 1999. The ontogeny of cranial base angulation in humans and chimpanzees and its implications for reconstructing pharyngeal dimensions. *Journal of Human Evolution*, 36, 487–517.

Lieberman, D.E., Pearson, O.M., Mowbray, K.M., 2000. Basicranial influence on overall cranial shape. Journal of Human Evolution 38, 291–315.

Lieberman, D.E., McBratney, B.M., Krovitz, G., 2002. The evolution and development of cranial form in *Homo sapiens*. *Proceedings of the National Academy of Sciences of the United States of America*, 99, 1134–1139.

Lieberman, D.E., Krovitz, G.E., McBratney-Owen, B., 2004. Testing hypotheses about tinkering in the fossil record: the case of the human skull. *Journal of Experimental Zoology Part B: Molecular and Developmental Evolution*, 302, 284–301.

Lieberman, D.E., Hallgrímsson, B., Liu, W., Parsons, T.E., Jamniczky, H.A., 2008. Spatial packing, cranial base angulation, and craniofacial shape variation in the mammalian skull: testing a new model using mice. *Journal of Anatomy*, 212, 720–735.

Mancall, E.L., Brock, D.G. 2010. *Gray's clinical neuroanatomy: the anatomic basis for clinical neuroscience*. Philadelphia: Elsevier Soundars.

Marcucio, R.S., Young, N.M., Hu, D., Hallgrimsson, B., 2011. Mechanisms that underlie co-variation of the brain and face. *Genesis*, 49, 177–189.

Margulies, D.S., Vincent, J.L., Kelly, C., Lohmann, G., Uddin, L.Q., Biswal, B.B., Villringer, A., Castellanos, F.X., Milham, M.P., Petrides, M., 2009. Precuneus shares intrinsic functional architecture in humans and monkeys. *Proceedings of the National Academy of Sciences of the United States of America*, 106, 20069–20074.

Masters, M.P., 2009. Modern variation and evolutionary change in the hominin eye orbit. PhD Thesis. OhioLINK digital resource commons. <http://www.drc.ohiolink.edu/handle/2374.OX/107528>.

Masters, M.P., 2012. Relative size of the eye and orbit: an evolutionary and craniofacial constraint model for examining the etiology and disparate incidence of juvenile-onset myopia in humans. *Medical Hypotheses*, 78, 649–656.

Masters, M., Bruner, E., Queer, S., Traynor, S., Senjem, J., 2015. Analysis of the volumetric relationship among human ocular, orbital and fronto-occipital cortical morphology. *Journal of Anatomy*, 227, 460–473.

Mcbrearty, S., Brooks, A.S., 2000. The revolution that wasn't: a new interpretation of the origin of modern human behavior. *Journal of Human Evolution*, 39, 453–563.

McCarthy, R.C., 2001. Anthropoid cranial base architecture and scaling relationships. *Journal of Human Evolution*, 40, 41–66.

Meunier, D., Lambiotte, R., Fornito, A., Ersche, K.D., Bullmore, E.T., 2009. Hierarchical modularity in human brain functional networks. *Frontiers in Neuroinformatics*, 3, 37.

Moorrees, C.F.A., Kean, M.R., 1958. Natural head position, a basic consideration in the interpretation of cephalometric radiographs. *American Journal of Physical Anthropology*, 16, 213–234.

Morimoto, K., Nishikuni, K., Hirano, S., Takemoto, O., Futagi, Y., 2003. Quantitative follow-up analysis by computed tomographic imaging in neonatal hydrocephalus. *Pediatric Neurology*, 29, 435–439.

Morriss-Kay, G.M., Wilkie, A.O.M., 2005. Growth of the normal skull vault and its alteration in craniosynostosis: insights from human genetics and experimental studies. *Journal of Anatomy*, 207, 637–653.

Moss, M.L., Young, R.W., 1960. A functional approach to craniology. *American Journal of Physical Anthropology*, 18, 281–292.

Naghavi, H.R., Nyberg, L., 2005. Common fronto-parietal activity in attention, memory, and consciousness: shared demands on integration? *Consciousness and Cognition*, 14, 390–425.

Neaux, D., Guy, F., Gilissen, E., Coudyzer, W., Ducrocq, S., 2013. Covariation between midline cranial base, lateral basicranium, and face in modern humans and chimpanzees: a 3D geometric morphometric analysis. *Anatomical Record*, 296, 568–579.

Nejad, K.K., Sugiura, M., Nozawa, T., Kotozaki, Y., Furusawa, Y., Nishino, K., Nukiwa, T., Kawashima, R., 2015. Supramarginal activity in interoceptive attention tasks. *Neuroscience Letters*, 589, 42–46.

Neubauer, S., 2014. Endocasts: possibilities and limitations for the interpretation of human brain evolution. *Brain, Behavior and Evolution*, 84, 117–134.

Neubauer, S., Hublin, J.-J., 2012. The Evolution of human brain development. *Evolutionary Biology*, 39, 568–586.

Neubauer, S., Gunz, P., Hublin, J.-J., 2009. The pattern of endocranial ontogenetic shape changes in humans. *Journal of Anatomy*, 215, 240–255.

Neubauer, S., Gunz, P., Hublin, J.-J., 2010. Endocranial shape changes during growth in chimpanzees and humans: a morphometric analysis of unique and shared aspects. *Journal of Human Evolution*, 59, 555–566.

Neubauer, S., Hublin, J.-J., Gunz, P., 2018. The evolution of modern human brain shape. *Science Advances*, 4, eaao5961.

Northcutt, R.G., Kaas, J.H., 1995. The emergence and evolution of mammalian neocortex. *Trends in Neurosciences*, 18, 373–379.

Nowaczewska, W., Kuźmiński, Ł., Biecek, P., 2015. Morphological relationship between the cranial and supraorbital regions in *Homo sapiens*. *American Journal of Physical Anthropology*, 156, 110–124.

O'Leary, D.D.M., Chou, S.-J., Sahara, S., 2007. Area patterning of the mammalian cortex. *Neuron*, 56, 252–269.

Olson, E.C., Miller, R.L., 1958. *Morphological Integration*. Chicago: University Chicago Press.

Opperman, L.A., 2000. Cranial sutures as intramembranous bone growth sites. *Developmental Dynamics*, 219, 472–485.

Padberg, J., Franca, J.G., Cooke, D.F., Soares, J.G.M., Rosa, M.G.P., Fiorani, M., Gattass, R., Krubitzer, L., 2007. Parallel evolution of cortical areas involved in skilled hand use. *Journal of Neuroscience*, 27, 10106–10115.

Palmowski-Wolfe, A.M., Kober, C., Berg, I., Kunz, C., Wetzel, S., Buitrago-Téllez, C., Radü, E.W., Scheffler, K., 2009. Globe restriction in a severely myopic patient visualized through oculodynamic magnetic resonance imaging (od-MRI). *Journal of American Association for Pediatric Ophthalmology and Strabismus,* 13, 322–324.

Pandya, D.N., Seltzer, B., 1982. Association areas of the cerebral cortex. *Trends in Neurosciences*, 5, 386–390.

Passingham, R.E. 1973. Anatomical differences between the neocortex of man and other primates. *Brain, Behavior and Evolution*, 7, 337-359.

Pearce, E., Bridge, H., 2013. Is orbital volume associated with eyeball and visual cortex volume in humans? *Annals of Human Biology*, 40, 531–540.

Peer, M., Salomon, R., Goldberg, I., Blanke, O., Arzy, S., 2015. Brain system for mental orientation in space, time, and person. *Proceedings of the National Academy of Sciences of the United States of America*, 112,11072–11077.

Peeters, R., Simone, L., Nelissen, K., Fabbri-Destro, M., Vanduffel, W., Rizzolatti, G., Orban, G.A., 2009. The representation of tool use in humans and monkeys: common and uniquely human features. *The Journal of Neuroscience*, 29, 11523–11539.

Pennie, F.C., Wood, I.C.J., Olsen, C., White, S., Charman, W.N., 2001. A longitudinal study of the biometric and refractive changes in full-term infants during the first year of life. *Vision Research*, 41, 2799–2810.

Pereira-Pedro, A.S., Bruner, E., 2018. Landmarking endocasts. In: Bruner, E., Ogihara, N., Tanabe, H.C. (Eds.), *Digital endocasts: from skulls to brains* (pp. 127–142). Tokyo, Japan: Springer.

Phillips, K.A., Subiaul, F., Sherwood, C.C., 2012. Curious monkeys have increased gray matter density in the precuneus. *Neuroscience Letters*, 518, 172–175.

Preuss, T.M., 2011. The human brain: rewired and running hot. *Annals of the New York Academy of Sciences*, 1225, E182–E191.

Price, C.J., 2000. The anatomy of language: contributions from functional neuroimaging. *Journal of Anatomy*, 197, 335–359.

Purves, D., Augustine, G.J., Fitzpatrick, D., Hall., W.C., LaMantia, A.-S., McNamara, J.O.n Williams, S.M. 2004. *Neuroscience*. Massachusetts, USA: Sinauer Associates.

Radinsky, L., 1974. The fossil evidence of anthropoid brain evolution. *American Journal of Physical Anthropology*, 41, 15–27.

Rangel de Lázaro, G., de la Cuétara, J.M., Píšová, H., Lorenzo, C., Bruner, E., 2016. Diploic vessels and computed tomography: segmentation and comparison in modern humans and fossil hominids. *American Journal of Physical Anthropology*, 159:313-24

Ravosa, M.J., 1991. Interspecific perspective on mechanical and nonmechanical models of primate circumorbital morphology. *American Journal of Physical Anthropology*, 86, 369–396.

Ribas, G.C., 2010. The cerebral sulci and gyri. *Neurosurgical Focus*, 28, E2.

Richtsmeier, J.T., Flaherty, K., 2013. Hand in glove: brain and skull in development and dysmorphogenesis. *Acta Neuropathologica*, 125, 469–489.

Richtsmeier, J.T., Aldridge, K., DeLeon, V.B., Panchal, J., Kane, A.A., Marsh, J.L., Yan, P., Cole, T.M., 2006. Phenotypic integration of neurocranium and brain. *Journal of Experimental Biology Part B, Molecular and Developmental Evolution*, 306, 360–378.

Rilling, J.K., 2006. Human and nonhuman primate brains: are they allometrically scaled versions of the same design? *Evolutionary Anthropology*, 15, 65–77.

Rilling, J.K., 2008. Neuroscientific approaches and applications within anthropology. *American Journal of Physical Anthropology*, 137, 2–32.

Rilling, J.K., Insel, T.R., 1999. The primate neocortex in comparative perspective using magnetic resonance imaging. *Journal of Human Evolution*, 37, 191–223.

Rilling, J.K., Seligman, R.A., 2002. A quantitative morphometric comparative analysis of the primate temporal lobe. *Journal of Human Evolution*, 42, 505–533.

Rohlf, F.J., 1999. Shape statistics: Procrustes superimpositions and tangent spaces. *Journal of Classification*, 16, 197–223.

Rohlf, F.J., Marcus, L.F., 1993. A revolution in morphometrics. *Trends in Ecology and Evolution*, 8, 129–132.

Rohlf, F.J., Slice, D.E., 1990. Extensions of the Procrustes method for the optimal superimposition of landmarks. *Systematic Zoology*, 39, 40–59.

Ross, C.F., 1995. Allometric and functional influences on primate orbit orientation and the origins of the Anthropoidea. *Journal of Human Evolution*, 29, 201–227.

Ross, C., Henneberg, M., 1995. Basicranial flexion, relative brain size, and facial kyphosis in *Homo sapiens* and some fossil hominids. *American Journal of Physical Anthropology*, 98, 575–593.

Ross, C.F., Martin, R.D., 2007. The role of vision in the origin and evolution of primates. In: Kaas, J.H. (Ed.), *Evolution of nervous systems* (pp. 59–78). Oxford, UK: Elsevier.

Ross, C.F., Ravosa, M.J., 1993. Basicranial flexion, relative brain size, and facial kyphosis in nonhuman primates. *American Journal of Physical Anthropology*, 91, 305–324.

Sandy, R., Hennocq, Q., Nysjö, J., Giran, G., Friess, M., Khonsari, R.H., 2018. Orbital shape in intentional skull deformations and adult sagittal craniosynostoses. *Journal of Anatomy*, 233, 302–310.

Saw, S.-M., Katz, J., Schein, O.D., Chew, S.-J., Chan, T.-K., 1996. Epidemiology of myopia. *Epidemiologic reviews*, 18, 175–187.

Scammon, R.E., Armstrong, E.L., 1925. On the growth of the human eyeball and optic nerve. *Journal of Comparative Neurology*, 38, 165–219.

Schoenemann, P.T., 2006. Evolution of the size and functional areas of the human brain. *Annual Review of Anthropology*, 35, 379–406.

Schoenemann, P.T., Sheehan, M.J., Glotzer, L.D., 2005. Prefrontal white matter volume is disproportionately larger in humans than in other primates. *Nature Neuroscience*, 8, 242–252.

Schultz, A.H., 1940. The size of the orbit and of the eye in primates. *American Journal of Physical Anthropology*, 26, 389–408.

Scott, N., Neubauer, S., Hublin, J.-J., Gunz, P., 2014. A shared pattern of postnatal endocranial development in extant hominoids. *Evolutionary Biology*, 41, 572–594.

Scott, N.A., Strauss, A., Hublin, J.-J., Gunz, P., Neubauer, S., 2018. Covariation of the endocranium and splanchnocranium during great ape ontogeny. *PLOS ONE*, 13, e0208999.

Seghier, M.L., 2013. The angular gyrus multiple functions and multiple subdivisions. *The*

Neuroscientist, 19, 43–61.

Semendeferi, K., Damasio, H., 2000. The brain and its main anatomical subdivisions in living hominoids using magnetic resonance imaging. *Journal of Human Evolution*, 38, 317–332.

Semendeferi, K., Damasio, H., Frank, R., Van Hoesen, G.W., 1997. The evolution of the frontal lobes: a volumetric analysis based on three-dimensional reconstructions of magnetic resonance scans of human and ape brains. *Journal of Human Evolution*, 32, 375–388.

Semendeferi, K., Lu, A., Schenker, N., Damasio, H., 2002. Humans and great apes share a large frontal cortex. *Nature Neuroscience*, 5, 272–276.

Simon, O., Kherif, F., Flandin, G., Poline, J.-B., Rivière, D., Mangin, J.-F., Le Bihan, D., Dehaene, S., 2004. Automatized clustering and functional geometry of human parietofrontal networks for language, space, and number. *NeuroImage*, 23, 1192–1202.

Smaers, J.B., Soligo, C., 2013. Brain reorganization, not relative brain size, primarily characterizes anthropoid brain evolution. *Proceedings of the Royal Society B Biological Sciences*, 280, 20130269.

Smaers, J.B., Steele, J., Case, C.R., Cowper, A., Amunts, K., Zilles, K., 2011. Primate prefrontal cortex evolution: human brains are the extreme of a lateralized ape trend. *Brain, Behavior and Evolution*, 77, 67–78.

Seeley, R., Stephens, T., Tate, P. 2003. *Anatomy and physiology*, 6th edition. Boston : McGraw-Hill.

Sperber, G.H., 2001. *Craniofacial development*. London: BC Decker Inc.

Spoor, F., Zonneveld, F., 1995. Morphometry of the primate bony labyrinth: a new method based on high-resolution computed tomography. *Journal of Anatomy*, 186, 271–286.

Spoor, F., Jeffrey, N., Zonneveld, F., 2000. Using diagnostic radiology in human evolutionary studies. *Journal of Anatomy*, 197, 61–76.

Stone, R.A., Flitcroft, D.I., 2004. Ocular shape and myopia. *Annals Academy of Medicine Singapore*, 33, 7–15.

Studer, B., Cen, D., Walsh, V., 2014. The angular gyrus and visuospatial attention in decision-making under risk. *NeuroImage*, 103, 75–80.

Tallinen, T., Chung, J.Y., Rousseau, F., Girard, N., Lefèvre, J., Mahadevan, L., 2016. On the growth and form of cortical convolutions. *Nature Physics*, 12, 588–593.

Tanaka, S., Kirino, E., 2018. The parietal opercular auditory-sensorimotor network in musicians: a resting-state fMRI study. *Brain and Cognition*, 120, 43–47.

Todd, T.W., Beecher, H., Williams, G.H., Todd, A.W., 1940. The weight and growth of the human eyeball. *Human Biology*, 12, 1–20.

Valyear, K.F., Fitzpatrick, A.M., McManus, E.F., 2017. The neuroscience of human tool use. In: Kaas, J.H. (Ed.), *Evolution of nervous systems* (pp. 341–353). Oxford, UK: Academic Press.

van Cruchten, S, Vrolyk, V., Perron Lepage, M.-F., Baudon, M., Voute, H., Schoofs, S., Haruna, J., Benoit-Biancamano, M.-O., Ruot, B., Allegaert, K., 2017. Pre- and postnatal development of the eye: a species comparison. *Birth Defects Research*, 109, 1540–1567.

van Essen, D.C., Lewis, J.W., Drury, H.A., Hadjikhani, N., Tootell, R.B.H., Bakircioglu, M., Miller, M.I., 2001. Mapping visual cortex in monkeys and humans using surface-based atlases. *Vision Research*, 41, 1359–1378.

van Schaik, C.P., Deaner, R.O., Merrill, M.Y., 1999. The conditions for tool use in primates: implications for the evolution of material culture. *Journal of Human Evolution*, 36, 719–741.

Vigneau, M., Beaucousin, V., Hervé, P.Y., Duffau, H., Crivello, F., Houdé, O., Mazoyer, B., Tzourio-Mazoyer, N., 2006. Meta-analyzing left hemisphere language areas: phonology, semantics, and sentence processing. *NeuroImage*, 30, 1414–1432.

Wagner, G.P., 1996. Homologues, natural kinds and the evolution of modularity. *Integrative and Comparative Biology*, 36, 36–43.

Waitzman, A.A., Posnick, J.C., Armstrong, D.C., Pron, G.E., 1992. Craniofacial skeletal measurements based on computed tomography: part II. Normal values and growth trends. *The Cleft Palate-Craniofacial Journal*, 29, 118–128.

Wallentin, M., Weed, E., Østergaard, L., Mouridsen, K., Roepstorff, A., 2008. Accessing the mental space—Spatial working memory processes for language and vision overlap in precuneus. *Human Brain Mapping*, 29, 524–532.

Warren, J.L.A., León, M.S.P. de, Hopkins, W.D., Zollikofer, C.P.E., 2019. Evidence for independent brain and neurocranial reorganization during hominin evolution. *Proceedings of the National Academy of Sciences of the United States of America,* 116, 22115-22121.

Weber, G.W., 2015. Virtual Anthropology. *American Journal of Physical Anthropology*, 156, 22–42.

Welker, W., 1990. Why does cerebral cortex fissure and fold? In: Jones, E.G., Peters, A. (Eds.), *Cerebral Cortex: comparative structure and evolution of cerebral cortex, part II* (pp. 3–136). Boston, MA: Springer.

Wu, X., Liu, W., Zhang, Q., Zhu, H., Norton, C.J., 2007. Craniofacial morphological microevolution of Holocene populations in northern China. *Chinese Science Bulletin*, 52, 1661–1668.

Yeo, B.T., Krienen, F.M., Sepulcre, J., Sabuncu, M.R., Lashkari, D., Hollinshead, M., Roffman, J.L., Smoller, J.W., Zöllei, L., Polimeni, J.R., Fischl, B., Liu, H., Buckner, R.L., 2011. The organization of the human cerebral cortex estimated by intrinsic functional connectivity. *Journal of Neurophysiology*, 106, 1125–1165.

Young, R.W., 1957. Postnatal growth of the frontal and parietal bones in white males. *American Journal of Physical Anthropology*, 15, 367–386.

Zelditch, M.L., Swiderski, D.L., Sheets, H.D., Fink, W.L., 2004. *Geometric morphometrics for biologists*. New York: Elsevier Academic Press.

Zhang, S., Li, C.R., 2012. Functional connectivity mapping of the human precuneus by resting state fMRI. *NeuroImage*, 59, 3548–3562.

Zilles, K., Amunts, K., 2010. Centenary of Brodmann's map: conception and fate. *Nature Reviews Neuroscience*, 11, 139–145.

Zilles, K., Armstrong, E., Schleicher, A., Kretschmann, H.-J., 1988. The human pattern of gyrification in the cerebral cortex. *Anatomy and Embryology*, 179, 173–179.

Zilles, K., Armstrong, E., Moser, K.H., Schleicher, A., Stephan, H., 1989. Gyrification in the cerebral cortex of primates. *Brain, Behavior and Evolution*, 34, 143–150.

Zilles, K., Palomero-Gallagher, N., Amunts, K., 2013. Development of cortical folding during evolution and ontogeny. *Trends in Neurosciences*, 36, 275–284.

Zollikofer, C.P.E., Ponce De León, M.S., Martin, R.D., 1998. Computer-assisted paleoanthropology. *Evolutionary Anthropology*, 6, 41–54.

Zollikofer, C.P.E., Ponce de León, M.S., 2013. Pandora's growing box: inferring the evolution and development of hominin brains from endocasts. *Evolutionary Anthropology*, 22, 20–33.

Zollikofer, C.P.E., Bienvenu, T., Ponce de León, M.S., 2017. Effects of cranial integration on hominid endocranial shape. *Journal of Anatomy*, 230, 85–105.

UNIVERSIDAD
DE BURGOS

CENIEH